5-2016

Dating Late Quaternary Alluvial Fills in the Platte River Valley using Optically Stimulated Luminescence Dating

Jacob C. Bruihler

University of Nebraska - Lincoln, jacob.bruihler@huskers.unl.edu

Dating Late Quaternary Alluvial Fills in the Platte River Valley

using Optically Stimulated Luminescence Dating

by

Jacob C. Bruihler

A THESIS

Presented to the Faculty of

The Graduate College at the University of Nebraska

In Partial Fulfillment of Requirements

For the Degree of Master of Arts

Major: Geography

Under the Supervision of Professor Paul R. Hanson

Lincoln, Nebraska

May, 2016

Dating Late Quaternary Alluvial Fills in the Platte River Valley
using Optically Stimulated Luminescence Dating

Jacob C. Bruihler, M.A.

University of Nebraska, 2016

Advisor: Paul R. Hanson

Alluvial fills underlying the Platte River Valley in Nebraska record the geologic history of the Platte River in the late Quaternary. This study investigated the alluvium underlying the valley near the cities of North Platte and Kearney, Nebraska. Data obtained from sediment cores drilled in the alluvial deposits was used to investigate the changes in Platte River dynamics on a glacial – interglacial timescale. Optically Stimulated Luminescence (OSL) dating was used to determine burial ages of recovered sediments and to quantify the thicknesses of the late Pleistocene and Holocene alluvial fills at each study area. Our geochronology depicts considerable differences in age with depth at the two study sites. Results from OSL dating indicate that the Platte River was aggrading during the late Pleistocene and into the early Holocene. Approximately 8 to 10 meters of sediment was deposited near North Platte, and 15 + meters of sediment was deposited near Kearney. Aggradation ended sometime in the early Holocene, most likely between 10 to 11.9 ka, and during the Holocene the Platte re-worked these older alluvial deposits. The total thickness of the Holocene fill ranged from 3 to 8 meters near North Platte, and 10 to 12 meters near Kearney. Locally, the Holocene alluvial fill is entrenched 3 to 4 meters into the underlying late Pleistocene alluvium. This fundamental change in river dynamics is attributed to long-term changes in the ratio of discharge to sediment supply in the basin.

Dedication

This thesis is dedicated to my parents, Carl and MaryKay Bruihler, who have encouraged, loved, and

supported me in this journey of life. Mom and Dad, thanks for introducing me to the great outdoors!

You taught me to embrace challenges, be curious, and learn everything I can about the world we live in.

Acknowledgements

Grant Information

Table of Contents

List of Figures and Tables

1 Introduction

water and sediments shed from the east central Rocky Mountains and the central Great Plains (Figure 1.1). The modern Platte River sits atop older deposits of its own alluvium, overlying Tertiary aged deposits including the Ogallala Group and Broadwater Formation. (Condon 2005). The Platte River occupies a valley cut into the underlying alluvium, with valley walls formed by the deposition of Quaternary eolian sediment (Lugn, 1935). These sediments form the uplands in both study areas, and contribute to the geomorphology of the valley. Some fraction of sediment transported through the Platte River system was deposited in the alluvial fills, recording the geologic history and geomorphic evolution of the largest, braided river system in North America (Miall 1978; Kammerer 1990).

The geomorphic evolution of the river system on a long timescale remains poorly understood, and little work has previously been done in regards to alluvial responses to climate change on a glacial-interglacial timescale in this system. Much of the modern research on fluvial response to climate change has focused on the past ~20,000 years of geologic history; it is important to study the fluvial responses to climate change on longer timescales. Relatively few investigations have examined fluvial responses throughout complete glacial-interglacial cycles, which occur on timescales of approximately 100,000 years (Blum & Tornqvist 2000). Many current studies only cover the most recent ~20% of the last glacial-interglacial timescale, and more information is needed to accurately interpret fluvial responses to the complete cycle (Blum & Tornqvist 2000). This study was designed to investigate the chronostratigraphic record of alluvial fills and corresponding surficial features in the Platte River Valley during the late Pleistocene and Holocene. Results from this study add significant detail to the fluvial response of this system to climate change in the Great Plains.
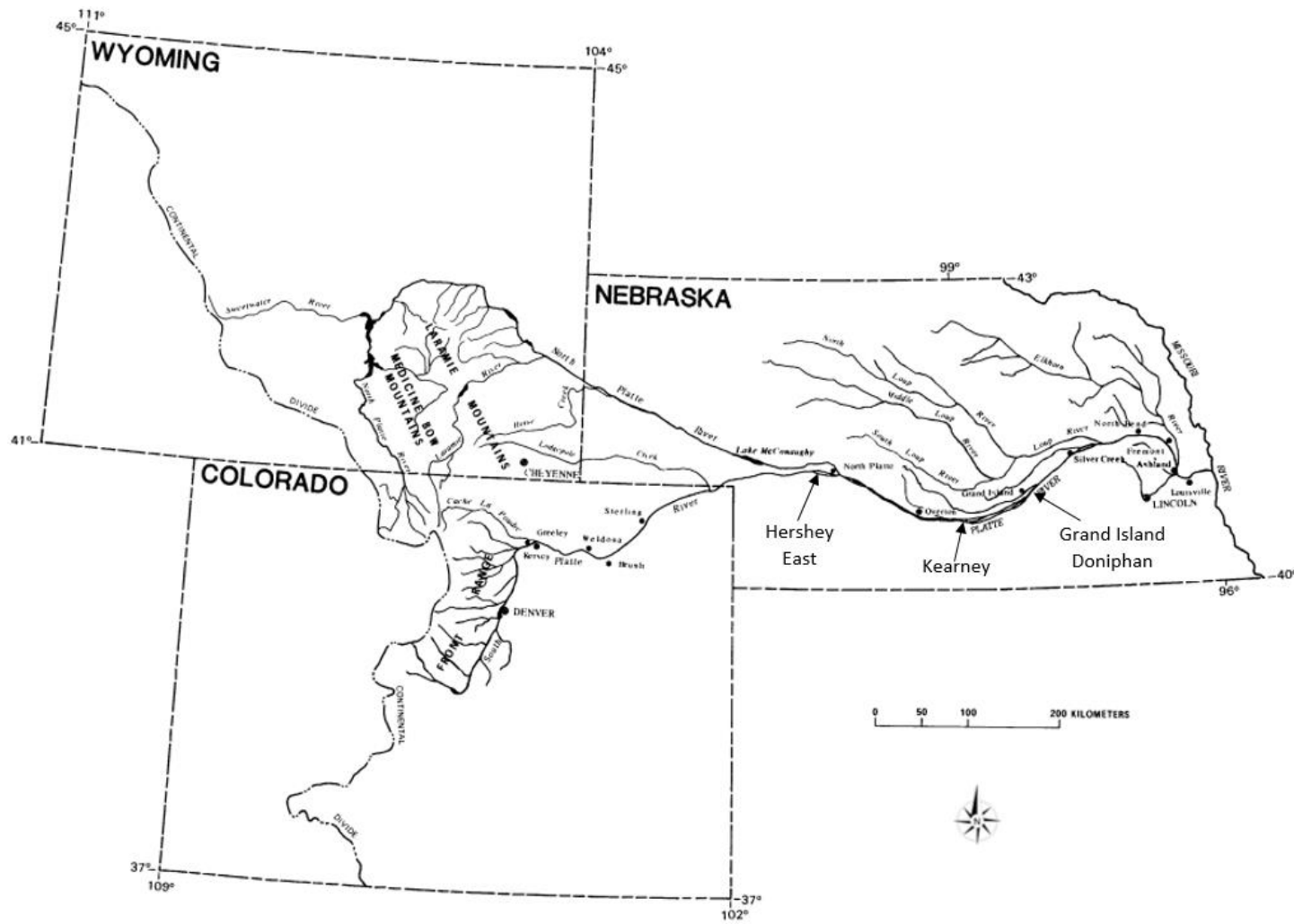
Figure 1.1 Regional Map of the Platte River watershed
The Platte River drains the east-central Rocky Mountains and High Plains of Colorado, and Wyoming, as well as much of central Nebraska. Study sites indicated by arrows. Hershey East and Kearney study areas will be compared to each other and to earlier work completed near Grand Island-Doniphan (Horn, 2010). Map adapted from Crowley et al. 1983.

The Platte River is one of the best examples of a braided river: wide, shallow, with a high sediment load (Smith 1971). These conditions favor multiple episodes of erosion, transport, and deposition of sediment following erosion from source rock (Bridge 1993, 2009). This study focuses on the alluvial fills deposited in two locations within the Platte River system, the Hershey East and Kearney 1:24,000 scale, 7.5 minute quadrangles, in western and central Nebraska (Figure 1.2).

The modern Platte River system drains approximately 220,000 km^2 of Colorado, Wyoming, and Nebraska. However, the Nebraska Sand Hills, which account for roughly 30% of the total watershed, are drained by tributaries entering the Platte River system downstream of the study sites. Thus, the effective area drained by tributaries relevant to the Platte River system in this study is only approximately 145,000 km^2. The source of most of the tributaries relevant to this study originating in the Rocky Mountains and high plains of Colorado and Wyoming (Figure 1.1). Additionally, no significant tributaries enter the Platte River system between the study sites.

1.1   Quaternary History of the Great Plains

There has been contemporary research investigating the eolian geologic record of the late Quaternary in Nebraska and the Great Plains (Bettis et al. 2003, Lu et al. 2011, Mason et al. 2008, Miao et al. 2005, Miao et al. 2007). These and other works examine surficial deposits of loess deposits, eolian sand dunes and paleosol development, and their record of climate and the geologic environments in Nebraska and the central Great Plains during the late Quaternary. These studies emphasize the importance of the eolian record in the late Quaternary, including the transition from glaciated to non-glaciated environments in Nebraska and the Great Plains. Beyond their importance to the geologic record of the Quaternary, these eolian deposits form upland features that act as valley walls at both the Hershey East and Kearney study sites.

Significant loess deposits are observed in the southern and eastern parts of Nebraska. These loess deposits have been the focus of several studies on Quaternary environments in the central Great Plains. Peoria Loess in Nebraska was transported by westerly to northerly winds from unglaciated landscapes to the northwest (Mason 2001). Roberts et al. (2003) used Optically Stimulated Luminescence (OSL) dating to study the relationships between timing and deposition rates of the Peoria Loess deposits in western Nebraska. Results from this study depict a loess accumulation thicker than any other location on earth from 25 to 14 ka, with the highest accumulation rates of up to 4 m kyr^{-1} between 18 to 14 ka. Subsequent research investigated the effects of the termination of the last glaciation in North America using the loess record in the northern and central Great Plains. In Nebraska, this termination is marked by the Brady Soil, which developed as Peoria Loess deposition subsided. The Brady soil represents an increase in effective moisture, as well as eolian stability following de-glaciation (Mason et al. 2008).

Vegetated eolian dunes of the Nebraska Sand Hills lie in north central Nebraska, with the southeastern most dunes encroaching into the loess deposits to the south and east. The Sand Hills have been the subject of many studies researching the Quaternary geology of Nebraska. Miao et al. (2007) found evidence supporting previous interpretations of landscape response to dry climate in central North America. OSL ages from this study indicate that the Sand Hills were episodically active, with the most recent eolian activity occurring at approximately 0.7, 2.5, and 3.8 ka. Results also showed significant loess deposition occurring between 9.4 to 6.5 ka. Muhs et al. (2000) show evidence for eolian activity in the Nebraska Sand Hills damming the North and South Platte Rivers near the Hershey East study site in the late Pleistocene prior to 11,000 ^{14}C years BP. This damming of the river likely added a significant amount of sediment to the river system, and also indicates that there were likely long periods of low discharge, allowing for dune migration across the North and South Platte River Valleys during the late Pleistocene.

Goble et al. (2004) used OSL to study the relationships between eolian dune activity and paleosol development during periods of eolian inactivity. Dune stratigraphy resulted in clustered

OSL ages, indicating that eolian activity was episodic, with intermittent low-activity periods during which paleosols developed in inter-dune wetlands. Paleosols were not observed in the dunefield during periods of eolian activity, reinforcing the interpretation of episodic eolian activity in the Nebraska Sand Hills. Hanson et al. (2009) completed a similar study of episodic activation in a small dunefield in the Platte River Valley near Duncan, NE, approximately 200 km east of the Nebraska Sand Hills. It was concluded that although the eolian dunes had been stabilized by vegetation for much of the Holocene, extended periods of megadrought allowed for episodic re-activation of the dunefield. These re-activation episodes occurred between 4.4 to 3.4 and 0.8 to 0.5 ka. Findings from this study were similar to results from Goble et al. (2004), showing episodic eolian activity with intermittent periods of little to no eolian activity.

1.2   Sedimentology of the Platte River

The Platte River was the subject of many studies in the 1970's and 80's, with most work focused on various aspects of sedimentary structures and the architecture of macroform features typically found in braided river systems (Crowley 1983, May 1989, Smith 1970). Other studies investigated the depositional environments typical of braided rivers (Miall 1977, 1978). These studies found relationships between discharge, flow velocity and grain size in forming transverse braid bars (Blodgett & Stanley 1980), as well as the planar-tabular cross stratification sets associated with transverse bars (Smith 1972). Results showed general architecture of transverse and longitudinal bars, with decreasing grain size and better sorting moving downstream (Smith 1970, 1971 and 1972). Significantly, Blodgett & Stanley (1980) noted the likelihood of incomplete sequences of the sedimentary record in braided river systems such as the Platte. Crowley (1983) completed a study of the controls on macroform bedforms in the Platte River near Grand Island, Nebraska, relating discharge to erosional and depositional processes transporting the macroform down the channel. Crowley observed significant narrowing of Platte

River channels in the recent past, due to the encroachment of vegetation, which resulted in decreased erosion. The decrease in erosion acted as an anchoring mechanism, holding macroforms in place and slowing their transport downstream.

These studies addressed poorly understood relationships between discharge, sediment loads, and the variations between macroforms in braided river systems. However, these studies could not address the relationships of sediment deposits of different ages. Contacts between different sedimentary units within the Platte River alluvial fill are essentially indistinguishable due to the gradational nature of boundaries between stratigraphic packages. Without accurate age control provided by geochronology, significant unconformities spanning tens of thousands of years were entirely unrecognizable. This lack of an effective chronology meant that very few conclusions could be made with any accuracy about the older stratigraphic relationships recorded in subsurface sediments.

More recently, the Platte River valley and its tributaries have been the renewed subject of studies investigating the sedimentology and surficial processes occurring in braided river systems (Condon 2005, Fotherby 2009, Horn 2012a, Horn 2012b, Joeckel & Henebry 2008), and provide further insights into the evolution of the Platte River. Anthropogenic alterations of the natural river system – e.g. dams, bridges, and canals have caused significant changes to river dynamics in the modern era (Fotherby 2009, Joeckel & Henebry, 2008).

Skelly et al. (2003) observed aggradation in the Niobrara River, a braided tributary to the Missouri River. Evidence from aerial photography and channel surveys indicate that aggradation has been occurring since the 1950's, transforming the previously deep, stable channel to shallow, braided channels. This aggradation in the historic period is likely related to damming on the Missouri River. Joeckel and Henebry (2008) used historical aerial photography from 1938 to 2005 to study the central Platte River between the cities of Grand Island and Plattesmouth, Nebraska. They observed large fluctuations in island size downstream of major confluences, and a decrease in channel size upstream of the Loup and Elkhorn Rivers, which are large tributaries to

the Platte. In stretches upstream of major confluences, accretion tended to stabilize islands and decrease channel size. Moving forward in time, it was shown that the rates of change were decreasing, and the river system was becoming more stable with a trend of prominent channel shrinkage in the time period of the study.

Fotherby (2009) studied the changes in planform of the Platte River from Lexington to Grand Island due to anthropogenic confinement of the Platte River Valley during the 20th century. Valley confinement is thought to be the primary determining factor in planform, as differences in braid belt width correlate with distances between confining features both man-made and natural. Additional work on channel size found an average decrease in mean channel area in the central Platte River of 46% between 1938 and 2006. This decrease in channel size coincides with increasing vegetation on channel banks and islands, which is thought to be the dominant factor in braid bar and channel morphology. Evidence suggests that these changes began occurring prior to European settlement.

1.3   OSL Dating in Fluvial Geomorphology

Rivers are highly dynamic systems that alter the surface of the land as they transport sediment downstream. The resulting deposits and landforms left behind contain the record of the changes in river dynamics in response to climatic and tectonic variations (Rittenour 2008). Using OSL dating, geologists can approximate the age of these alluvial features. Applying temporal data to spatial relationships of alluvial deposits allows for interpretations about changes in river dynamics on a geologic timescale. OSL is often a suitable method for studying the geologic history and geochronology of a variety of alluvial deposits, and variety of these deposits, including flood plain deposits (Rittenour et al. 2003) and terraces (Colls et al. 2001). In many such deposits, datable carbon for use in radiometric dating is often not available. When it is recovered, the re-working of old carbon by fluvial systems occasionally results in age-

overestimation (Gillespie et al. 1992, Stanley & Hait 2000, Blong & Gillispie 1978). However, radiocarbon dating can occasionally be used to provide independent confirmation of OSL ages (Rodnight et al. 2006). The primary datable materials for OSL – grains of quartz and feldspar sand, are abundant in alluvial deposits, making OSL a viable dating method for many such studies. Very little datable carbon is present in the Platte River alluvial fill, and none was recovered in core sediments obtained for this study.

OSL dating techniques are best suited to eolian sediments, where grains typically experience adequate exposure to sunlight at the time of deposition (Duller 2004, Olley et al. 1998, Rhodes 2011). However, recent advances in OSL dating have proven that OSL is a reliable dating method in deposits where sediments are less likely to have full exposure to sunlight (Rittenour et al 2005, Rodnight et al 2005, Tornqvist et al. 2000). Problems typically encountered with OSL dating in alluvial deposits are well understood, with a variety of effective solutions (Rittenour 2008, Rodnight 2006, Rhodes 2011).

One of the most common problems encountered while using OSL in alluvial deposits occurs when not all sand grains in a deposit are exposed to sunlight for long enough to bleach the grain and fully erase the luminescence signal. This problem is known as 'partial bleaching,' and means that the quartz grains hold a residual luminescence signal from a prior burial (Murray et al. 1995; Olley et al. 1998), leading to a wide, asymmetric distribution of dose (Olley et al. 1999). Partial bleaching results in an age over-estimation, as the paleodose contained in the quartz sand grain does not correspond to the true burial dose (Galbraith 1999). Re-setting of luminescence signals by sunlight is limited by the attenuation of light through the water column (Berger 1990), especially when suspended sediment loads are high (Berger & Lauterner 1987, Rittenour 2008). Other factors, including depth of water, sediment transport mode, and transport distance from the sediment source play a role in a quartz grain's exposure to sunlight (Rittenour 2008). Using coarser grain sizes for OSL dating decreases the risk of complications due to partial bleaching. Larger grains move more slowly through fluvial systems, and are potentially deposited on

channel bars more often, increasing exposure to sunlight and improving the probability of bleaching. Further, the cohesive nature of fine-grained sediments, means that smaller grains may be transported as an aggregate, impeding solar bleaching (Rittenour 2008, Olley et al 1998).

Alluvial deposits contain a mix of grains, some of which were well bleached at deposition, and others that were not (Olley et al. 1998). One technique used to minimize the effect of partial bleaching is to decrease the number of sand grains per aliquot, using either a small mask (2 mm) or single-grain technique to limit contribution from non-bleached grains to the measured signal (Galbraith et al.1999). Further, single-grain techniques allow non-bleached populations to be identified (Duller 2000, 2008), allowing users to run age models that can limit the impacts of these ages on the OSL age (Hanson 2006, Rittenour 2008).

A variety of statistical techniques have been developed to isolate grains representing the most appropriate burial dose (Olley et al. 1998). The central age model is used to provide an estimate of mean dose and uncertainty in well-bleached samples. Using the central age model, the algorithm places more weight on moderate D_e values and less weight on the outlying high and low D_e values. The minimum age model is used when aliquots show substantial variation in D_e, and places more weight on the lowest D_e values, resulting in an estimate of a statistically valid minimum age for a sample (Rhodes 2011). Another technique separates the different components of the OSL signal, isolating the most light-sensitive traps (Jain et al. 2005). This technique uses dose distributions from the fast component, as it is the most readily bleached, and is therefore less impacted by poor exposure to sunlight.

Evidence of partial bleaching is often discovered through graphical analysis of luminescence data. Radial plots display D_e values with associated precision for individual aliquots. Variation in D_e values for different aliquots indicates different doses of individual grains, and is an indicator of partial bleaching (Rhodes 2011). Frequency histograms are used to display the number of aliquots and their equivalent dose. Partially bleached samples typically show

distributions with high scatter or asymmetric or positively skewed distributions where a small number of aliquots skewed towards higher doses (Hanson 2006, Rittenour 2008).

2 Setting

Condon (2005) summarized the geology of the area, discussing the geologic history of the western Great Plains region from the Laramide Orogeny through the Holocene. The drainage basin of the Platte River is a very complex system that has undergone many changes since the Laramide Orogeny. Uplifting mountains provided a source for the sediment that filled the developing foreland basin. Over time, the foreland basin filled with clastic debris, as sediment supply and accommodation space were ample. Very little sediment was deposited to the east of the Rocky Mountains in Nebraska until the Eocene, during the deposition of the Chadron Formation, as well as volcaniclastic materials blown in from western source areas (Swinehart & Diffendal, 1989). During the Oligocene, the Brule Formation of the White River Group was deposited in much of western Nebraska, along with volcaniclastic sediments that form the lower Arikaree Group (Swinehart, 1985). This deposition continued into the Miocene, forming the upper section of the Arikaree Group in western Nebraska. Flowing water re-worked the uppermost sediments of the Arikaree Group and created an erosion surface prior to deposition of the Ogallala during the middle to late Miocene. The sand-dominated sediments of the Ogallala Group were deposited from South Dakota to Texas by rivers draining the eastern flank of the Rocky Mountains (Joeckel et al. 2014). In the Pliocene the Broadwater Formation alluvium was deposited in western and northern Nebraska, and consists of alluvial deposits of conglomerate, sandstone, siltstone, and mudstone (Swinehart & Diffendal 1997).

Following the last glacial maximum approximately 20 ka, the climate in Nebraska was relatively cold and dry (Bromwich et al. 2005, Muhs et al. 2008, Miao et al. 2005, Miao et al. 2007), as evidenced through geochemistry of loess deposits and dune records from the Sand Hills.

The Rocky Mountains in Colorado experienced phases of alpine glacier expansion during the last glacial cycle (Benedict, 1973). The Front Range area and tributaries flow east to the South Platte, while the Park and Medicine Bow Ranges flow from the North Park area north into Wyoming, and turn southeast near Cheyanne. These watersheds are the significant sources of Platte River sediments deposited in the Platte River Valley following de-glaciation of North America approximately 12,000 years ago (Condon 2005).

Quaternary-aged surficial geologic features found in the upper and central Platte River Valley differ with topographic position. Lowland floodplain deposits are dominantly alluvial sand and gravel forming braided bars, channels, and alluvial fills. The alluvial sediments are largely bed-load sediments sourced from the Rocky Mountains and high plains of Colorado and Wyoming (Condon 2005), as well as from the Nebraska Sand Hills near North Platte, Nebraska (Muhs et al. 2000). Surficial features found in the uplands typically consist of eolian deposits of sand dunes, sand sheets and loess deposits.

2.1 Geochronologic Framework of Platte River Sediments

Horn (2010) completed the first study creating a geochronology for the Platte River alluvial fills. This study investigated the Platte River near Grand Island, Nebraska, using OSL dating to create a geochronology of the alluvial fills in the Platte River. This geochronology allowed for the initial depiction of relationships between surficial features and the underlying stratigraphy in the Platte River. Findings from Horn (2010) include aggradation during the late Pleistocene, with approximately eight meters of entrenchment in the Platte River Valley during the Holocene.

The present study provides a more complete understanding of the dynamics of the Platte River by investigating locations upstream of Horn (2010), to improve understanding of the changes in the Platte River at a larger scale. Similarly to Horn (2010), this study investigates the

response of the Platte River to the last glacial-interglacial cycle. Further, this study will allow for interpretations to be made about river dynamics between upstream and downstream locations.
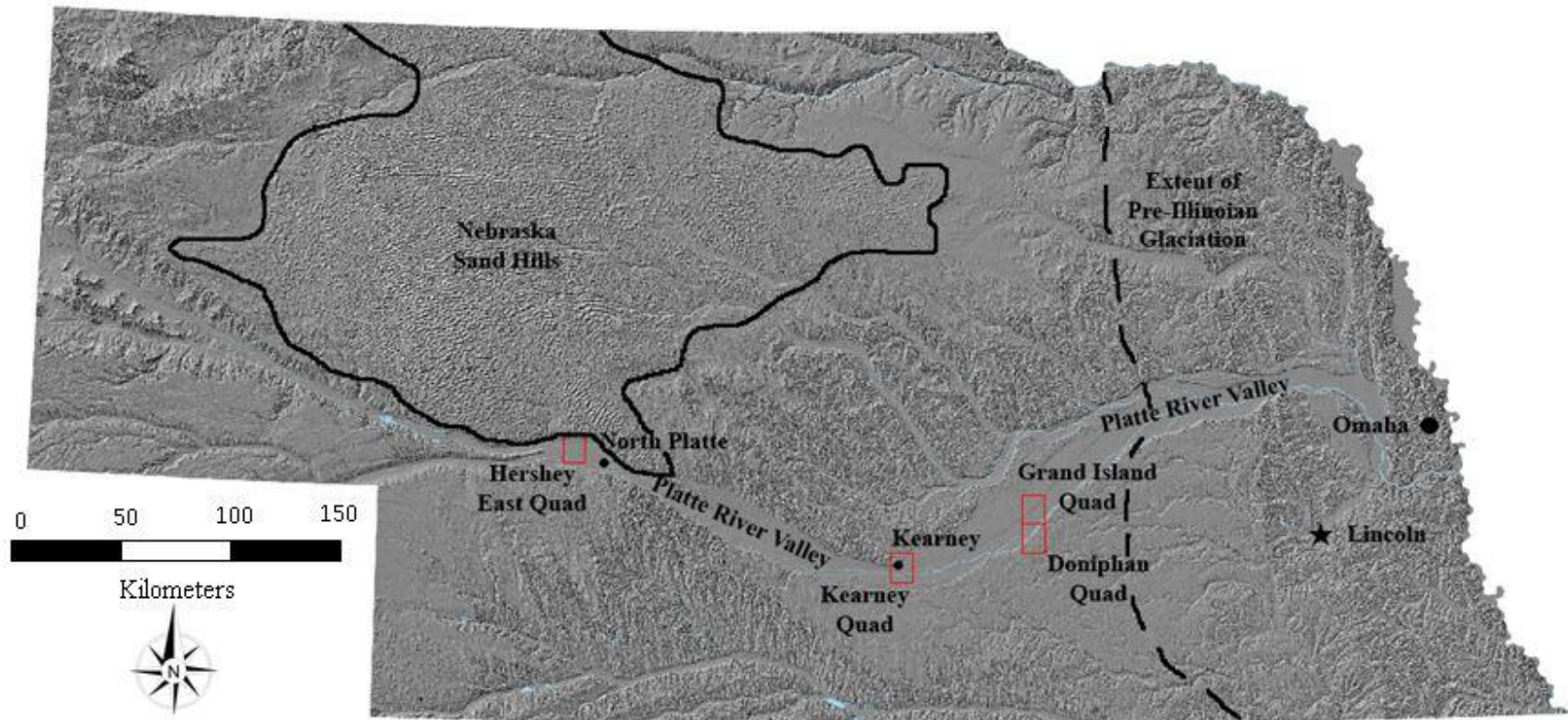
Figure 2.1 Hillshade generated from a 10 meter DEM of Nebraska
Results from this study, the Hershey East (Hanson et al. 2015) and Kearney (Hanson et al. 2014) Quadrangles, are compared to work at the Grand Island & Doniphan sites from Horn (2010). Note the Nebraska Sand Hills in the north-central portion of the map, and the dissected loess deposits to the southeast. The broad, flat Platte River Valley is clearly visible in center of Nebraska. The approximate extent of Pre-Illinoian glaciation is marked by the dashed line.
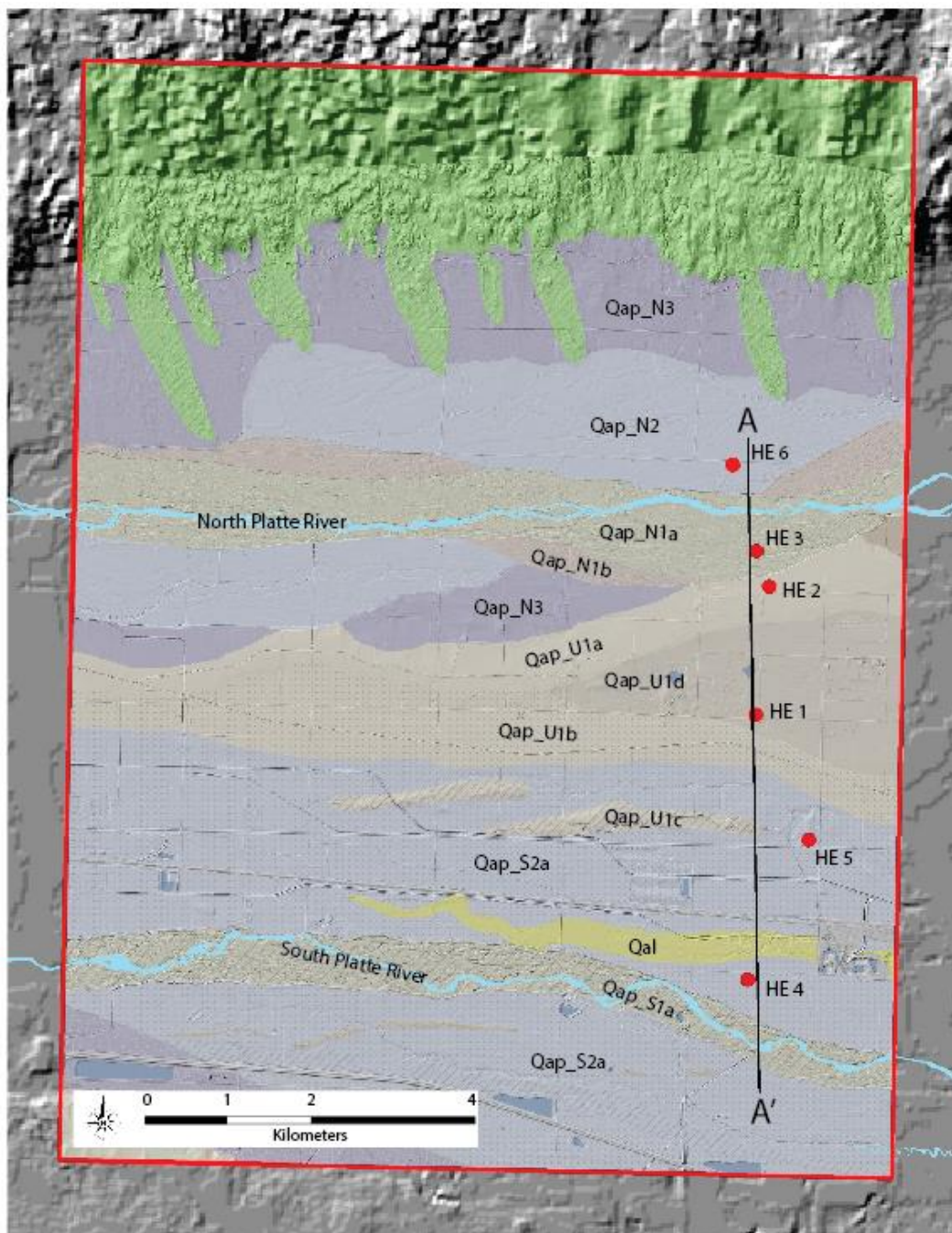
Figure 2.2 Hershey East 1:24,000 Quadrangle
The valley is ~10 km wide in this area. Note that this study area is upstream of the confluence of the North and South Platte Rivers. Eolian dunes form the northern valley wall and encroach on the floodplain; loess deposits form the southern valley wall, limiting southern migration of South Platte River. Alluvial deposits of varying age are deposited in the floodplain. Map adapted from Hanson et al. (2015)
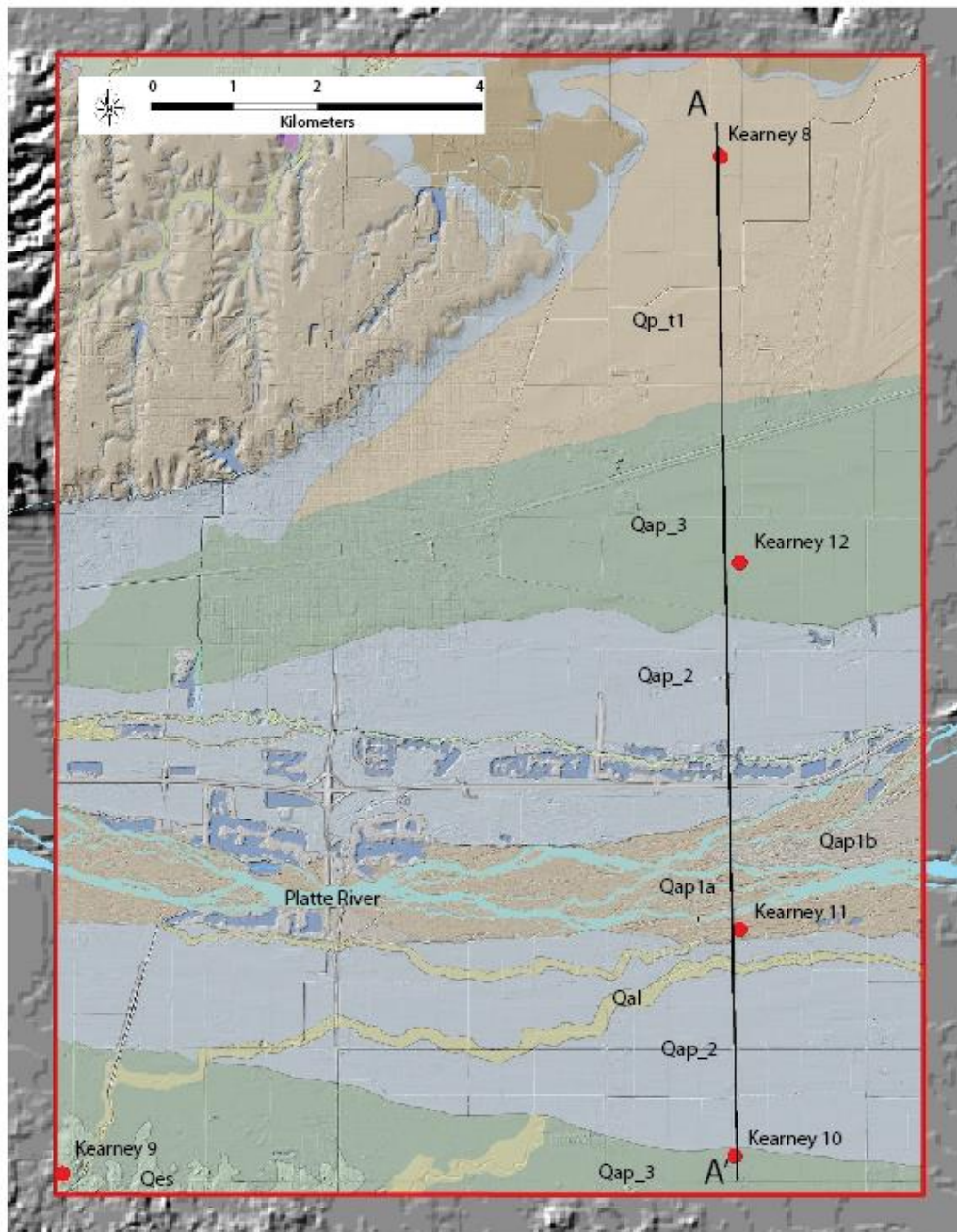
Figure 2.3 Kearney 1:24,000 Quadrangle
The valley is ~8 km wide in the east, and 15+ km wide in the west.
Note that this study area is downstream of the confluence of the
North and South Platte Rivers. Thick loess deposits are present in
the northwestern part of the quadrangle and forms the northern
valley wall, limiting northward migration of the Platte. Eolian
dunes are present in the southern part of the quadrangle, and form
the southern valley wall. Alluvial sediments of varying age are
deposited in the Platte River floodplain. Map adapted from Hanson
et al. (2014)

3   Materials and Methods

Six boreholes were drilled near Hershey, NE, and four boreholes were drilled approximately 180 km downstream near Kearney, NE. Study sites were located on the floodplain within the Platte River Valley. Ideally, cores were drilled on different surfaces within the valley, on both the active floodplain and abandoned alluvial surfaces. USGS topographic maps of the Hershey East and Kearney 7.5' quadrangles were referenced in choosing sites, as well as hillshade maps and Digital Elevation Models (DEM) created in ESRI ArcMAP® 10.1 using LiDAR data. Road access was necessary for drilling rigs and field vehicles to access the drill site, with drilling permission granted by the landowner. Cores were drilled by the Nebraska Conservation & Survey Division (CSD) using a GeoProbe© coring device, in rough transects across the Platte River Valley.

The GeoProbe© is a track-mounted, remote-controlled rig that drills 1.5 m length x 6.5 cm diameter cores, with a removable plastic sleeve that contains the recovered sediments. These core barrel sleeves are ideal for this application; they are wide enough to maintain existing sedimentary structures and are small enough for transportation and handling purposes. Cores were drilled to refusal; depth varied depending on factors such as lithology, grain size, and water content. Every other section of core barrel was fitted with a thin, opaque liner. The liner was necessary to prevent bleaching of the outermost sand grains recovered in the core barrel, allowing for recovered sediments to be used for the Optically Stimulated Luminescence (OSL) dating method.

3.1   Core Description & Logging

Sediment cores with opaque liners to be used for OSL samples were opened under amber and/or red light sources to preserve luminescence signals. Samples for OSL dating were taken

primarily in portions of the cores that showed alluvial sedimentary structures, to ensure sediments were alluvial deposits.   In some cases, no sedimentary structures were present. In these cases samples were collected in areas without any visible disturbance, typically greater than 30 cm from the top or bottom of recovered core.

Following OSL sampling, sediment cores were opened under normal lighting conditions, and the recovered sediments were visually described. Changes in sediment lithology, grain size, texture, and color were used to identify distinct sedimentary packages. In initial description, approximate mean grain size was determined visually. Presence of calcium carbonate in sedimentary packages was determined by the presence of an effervescent reaction caused by dripping 10% hydrochloric acid on core sediments at ~5 cm intervals. Core descriptions were logged, and stratigraphic columns were created using descriptive data in Adobe® Illustrator®.

3.2   Particle Size Analysis

Following the logging of the cores, samples were taken for particle size analysis to show changes in grain size through the core. Samples were taken throughout the cores to more accurately characterize the changes in grain size throughout sedimentary packages recovered in cores. The cores contained a variety of materials, ranging from very fine-grained silt and clay to packages of much coarser sand and gravel. Because of this disparity, two methods were needed for accurate particle size analysis. Fine-grained sediments less than 1000 μm were analyzed via laser diffraction using the Malvern® Mastersizer™ 2000, while coarser sediments were analyzed using sieves.

Data from particle size analysis was used to quantify the qualitative data used to create graphic logs and cross sections. Particle size graphs were completed for each core, comparing amounts of clay, silt, sand, and gravel through the full depth of each core. This analysis makes

apparent gradual changes in grain size through sediment packages that may not have been accounted for in initial core descriptions.

Sediments finer than 1000 μm (1 mm) were sampled on a 30 cm interval starting at a depth of 15 cm from the surface. Samples analyzed using laser diffraction required some preparation prior to analysis. Each sample was massed according to approximate grain size ranges to achieve the correct concentration of sample moving through the machine. Sediment samples analyzed by laser diffraction required very little material; ~10 g/sample was archived, and only 1-2 g was actually used for analysis. Samples for analysis were then placed in a 50 ml centrifuge tube with 10 ml sodium hexametaphosphate, a de-flocculent used to disperse cohesive fine-grained materials, and shaken horizontally for 12+ hours to ensure that the samples were disaggregated.

Laser diffraction sample analysis begins with ~800 ml of de-ionized water in a 1000 ml beaker. A pump with an attached propeller spins at 2000 rpm, keeping the sediment sample in suspension. Prior to adding the sample, the machine pumps de-ionized water through the measurement chamber, obtaining a background measurement. Once the background measurement is complete, the sample is added to the de-ionized water and exposed to sonication for 1 minute to break up any possible remaining aggregates of fine materials. After sonication, the pump pulls the sample through the machine, where it moves past two glass plates, which are spaced 2 mm apart. As the sediment moves between the plates, a laser is directed on to the fluid containing the sediment, and the detectors located on the other side of the plates measure the difference in the angle of the incoming light. The angle of diffraction is measured and correlated to grain size. Using laser diffraction, three individual measurements of the sample, and an average of the three samples is calculated to ensure quality control. The measurement process takes about five minutes, with another five minutes dedicated to cleaning the system to prepare for the next sample. The water is changed, rinsing the inside of the machine until no detectable sediment is present in the system.

Sediments coarser than 1000 µm could not be analyzed using laser analysis, so sieve analysis was used. While the sieving method is useful in analyzing coarse sediments, it is limited in being inherently less accurate than the laser diffraction method. Sieve samples were taken on a 50 cm interval, rather than the 30 cm interval used for laser diffraction, as significantly more material was required for sieve analysis. Each sample was massed prior to analysis; each sample required 300+ grams of material for statistical accuracy. No pre-treatment was necessary for sediments analyzed with a sieve stack; all sediments were dry and crumbled when sampled.

A sieve stack was prepared, with each sieve opening decreasing in size by half. Sieve opening sizes were: 16 mm, 8 mm, 4 mm, 2 mm, 1 mm, 0.5 mm, 0.25 mm, 0.125 mm, and 0.063 mm (-4φ to 4φ). A sieve pan was placed below the sieve stack to catch any silt and clay-sized sediment less than 63 µm (0.063 mm) dropping through the smallest sieve. Initial mass (approximately 300+ grams) of the sediment sample is measured and recorded prior to analysis. The sieve stack was vibrated for 10 minutes. Final mass of the sediment was totaled, and percent of total mass was calculated for each grain size. There was some inherent error (generally less than 0.5%) caused by minimal spillage and/or grains that were stuck in sieves. Sieves were carefully brushed out and inspected prior to the next sample run.

3.3 Optically Stimulated Luminescence (OSL) Dating

Optically Stimulated Luminescence (OSL) dating was used to determine the age of the last exposure to sunlight for quartz sand from the collected cores. OSL dating of quartz sand is well-suited to alluvial deposits, as quartz sand is abundant throughout the Platte River fills. OSL dating essentially uses quartz sand as a 'battery,' and uses the 'charge' to determine the depositional age for sediments (Rhodes 2011). When quartz grains are buried, they are exposed to naturally occurring radiation- Uranium, Thorium, Radon, Potassium emitted from sediments buried nearby. The effects of bombardment by radionuclides from cosmic rays also need to be

accounted for, as cosmogenic irradiation contributes to the accumulated luminescence signal in the sand grain. This contribution of the cosmogenic dose varies with burial depth, and is calculated using equations from Prescott and Hutton (1994). Exposure to radiation causes electrons within the quartz crystal lattice to 'jump' from their original space to a different 'electron trap' in the lattice, landing in point defects in the quartz grain. This process builds the luminescence signal within the grain, 'charging' the battery. Eventually, buried quartz sand grains will be eroded and potentially exposed to sunlight. If the grain is exposed to sunlight, or bleached, for as little as 30 – 60 seconds, the luminescence signal is removed, 'draining' the battery (Rhodes 2011). When the sand is re-deposited, the luminescence signal will again start to build, 'recharging' the battery. This 'charge' is measured in the lab, and used to calculate the time since last exposure to sunlight.

There have been many studies in which OSL dating was successfully used in similar alluvial settings, such as Colls et al. (2001), Duller et al. (2004), Rittenour et al. (2005), and Tornqvist et al. (2000). There have also been applications of OSL dating in the Platte River Valley: Hanson et al. (2009), Horn et al. (2012). No datable carbon was present in recovered cores for age comparison using radiocarbon dating techniques.

Twenty three samples- eleven from Kearney and twelve from Hershey East were processed and dated using the single-aliquot regenerative (SAR) method (Murray & Wintle 2000). Samples were opened in the luminescence laboratory darkroom at the University of Nebraska, under amber and red lighting conditions. Each sample was assigned a unique UNL sample number.

Samples for OSL analysis were wet-sieved to 90-150 μm; remaining sediment at larger grain sizes was archived for later use if necessary. Sediments falling in the 90-150 μm grain size range were treated with approximately 10 ml of 10% hydrochloric acid to dissolve any carbonates that were present. Samples were rinsed 7 times using de-ionized water to remove any remaining Hydrochloric acid, and dried at approximately 55° C.

Higher density portions of the sample were then separated from heavy minerals present using sodium polytungstate, a heavy liquid with a specific gravity of ~2.72 (Aitken, 1998). In this treatment, samples were placed in a centrifuge tube and filled with ~25 ml of sodium polytungstate.   Centrifuge tubes were placed in a water-filled sonication tank for five minutes, and then centrifuged for 10 minutes. This process leaves the quartz sand floating atop the polytungstate, while the heavy minerals sink to the bottom. Liquid nitrogen was then used to freeze the heavy minerals to the bottom of the centrifuge tubes. Quartz sand and polytungstate were then flushed into a clean beaker, and remaining polytungstate was removed and filtered to be re-used. The sand was then rinsed 5 times with de-ionized water to remove trace amounts of sodium polytungstate.   The quartz sand was transferred to a Teflon™ bottle, and ~10 ml of de-ionized water was added. An approximately 50 minute wash in 48% hydrofluoric acid was then used to dissolve feldspar minerals and etch the quartz grains. Following the hydrofluoric treatment samples were rinsed with de-ionized water and dried in the oven at approximately 55°C. Etched quartz grains were dry sieved, and grains that were either finer or coarser than 90 – 150 μm were removed from the sample.

All sample aliquots were created using a mask to cover all but the innermost 2 mm of the 10 mm diameter aluminum disks. After applying the mask, disks were sprayed with a medical-grade silicon spray, allowing sand grains to stick only to the center 2 mm of each disk. This technique results in approximately 250 grains or quartz sand per disk. Assuming that roughly 3-8% of grains are luminescing, this technique approaches the accuracy of single-grain techniques, but taking much less time to prepare and run.

Preheat plateau experiments were used to determine the optimal temperature for pre-heating samples. Preheat Plateau experiments were run using sediment from sample UNL-3932, with temperatures ranging from 180° C to 260° C in increments of 20° C. The preheat plateau experiments resulted in the use of 220° C as preheat and cut-heat temperature.   A Dose

Recovery test was performed on 10 aliquots of UNL-3932 to determine if samples could be precisely dated using OSL dating procedures (Murray and Wintle, 2006).

Samples were analyzed on DA-20 Risø TL/OSL readers in the luminescence lab at the University of Nebraska-Lincoln. Age estimations were determined using a minimum of 40 accepted aliquots. D_e values were calculated using the Central Age Model (Galbraith et al. 1999). Aliquots were rejected if their recycling ratios were greater than $\pm$ 10%, or if they had measurable signals when exposed to IR diodes. Further rejection of aliquots with D_e values greater than 3 σ from the mean D_e was necessary to limit problems related to age over-estimation.

Moisture content and environmental dose rates were calculated from sediments collected adjacent to OSL sample sites. Moisture content was initially determined by measuring water weight by mass in each sample (wet weight - dry weight / dry weight). However, some cores had higher measured water contents near the ground surface than at depth, which is a likely scenario in a short time frame, but is not likely over geologic time frames. In some cases these cores had age estimates that were stratigraphically inverted, perhaps a result of using these measured moisture contents. Given the proximity to the Platte River and approximate elevation of the water table (Hershey East 1:24,000 Quadrangle, Kearney 1:24,000 Quadrangle), samples that should have been saturated weren't, and other samples that were nearly saturated shouldn't have been. Water contents were adjusted by determining approximate depth to groundwater using LiDAR elevations and depth of boreholes. Samples collected from less than 3 m depth were assigned water contents of 15%, while samples collected from deeper than 3 m were assigned 25% water contents. This revision brought all but one sample with inverted ages into the 1 σ error range of the other sample.

Concentration of radioactive materials in sediment surrounding OSL samples was determined using high resolution gamma spectrometry. Dose rate samples were taken from directly above and below the OSL sample, and dried in an oven at 55° C. Approximately 20 g of dried sediment was milled to silt/clay sized particles, and compressed into a petri dish. The petri

dish was sealed using hot glue and was analyzed using the gamma spectrometer at the UNL

Luminescence Laboratory to calculate the concentrations of K, U, and Th. The gamma

spectrometer takes a 20 hour (72,000 second) measurement of each sample. Using equations

from Aitken (1998), these concentrations were used to calculate the environmental dose rate

values. Cosmic irradiation also contributes to the environmental dose rate, and varies with burial

depth. Equations from Prescott & Hutton (1994) were used to estimate the dose rate contributed

by cosmic rays.

3.4   Surficial Geological Mapping & Cross Sections

Geomorphic features of the central Platte River Valley were mapped using GIS in ESRI

ArcMAP® 10.1 and edited using the graphics capabilities of Adobe® Illustrator®. A variety of

data was used- sediment cores, OSL dating, and stratigraphic relations of landforms. LiDAR data

was used to create a digital elevation model (DEM) of the study area, which was used to create a

base map of study areas. 1:24,000 Digital Raster Graphics (DRGs) of the Hershey East and

Kearney USGS topographic quadrangles overlain on the DEM to illustrate both geologic and

man-made surficial features. Borehole coordinates from drilling operations were added to the

map, displayed as XY data.

Various techniques were used in ArcMAP® to improve understanding of surficial

features. The hillshade tool was used to enhance the visualization of study area surfaces for

analysis. Hillshade analysis allowed the two-dimensional DEM to appear three-dimensional by

creating a false illumination of the surface. The effects of the hillshade tool help small-scale

features- braid bars, paleo channels, and dunes, to 'pop' out of the background.

Using ArcGIS®, 3D analyst tools were used to provide an elevation profile to be used as

a baseline for interpretive cross sections at each study site. The interpolate line tool was used to

draw a line between boreholes and the profile graph tool was used to create elevation profiles

between each of the boreholes in the study areas. The profile graph is important because it sets a

base-height for subsurface data to correlate with the real world surface. Interpretive geologic

cross sections were created using Adobe® Illustrator® and the elevation profile exported from

ArcMAP®.   Graphic logs displaying data from particle size analysis and OSL dating were hung

from the elevation profile, ensuring that the subsurface data was drawn to the correct depth.

Using this information, an interpretive cross section of the subsurface was drawn. The cross-

section shows the approximate depth to the Pleistocene-Holocene boundary, as well as surfaces

and boundaries thought to exist in the subsurface.

4 Results

A total of 15 OSL age estimates (Figure 4.4) were produced for alluvial sediments recovered in six cores drilled in the Hershey East 7.5' Quadrangle. Recovered sediments and OSL ages and varied widely with location and depth typical of braid-bar depositional systems of the North and South Platte Rivers (Smith, 1971). Results of this study will be discussed in three ways; a brief discussion of trends observed between different cores recovered from alluvial deposits, detailed results from each core in transect order (North to South) across the Platte River Valley (Figure 4.3, 4.12), and an in-depth analysis of results from each study area.

Relative ages of the upper portions of alluvial fills in the Platte River Valley can be determined by examining the morphology of surficial features and comparing the elevations and ages of older alluvial surfaces to those of the modern floodplain. The modern floodplain surface Qap_N1a has bar and swale topography readily apparent (Figure 4.1). Bar and swale topography on older alluvial surfaces have been diminished by both agricultural activities and infill of swales by fine-grained sediment deposition during flood events (Figure 4.2). Alluvial surfaces generally increase in age as distance from the current floodplain increases.

The elevation profile of the Platte River shows very little variation in slope (Figure 4.23). Very few significant nick points are apparent on the profile, likely due in part to the lack of consolidated bedrock in the shallow subsurface beneath the Platte River. The underlying older Platte River alluvium and Ogallala silts and sands are relatively soft, making it unlikely that a nick point would develop.

4.1   Hershey East Results
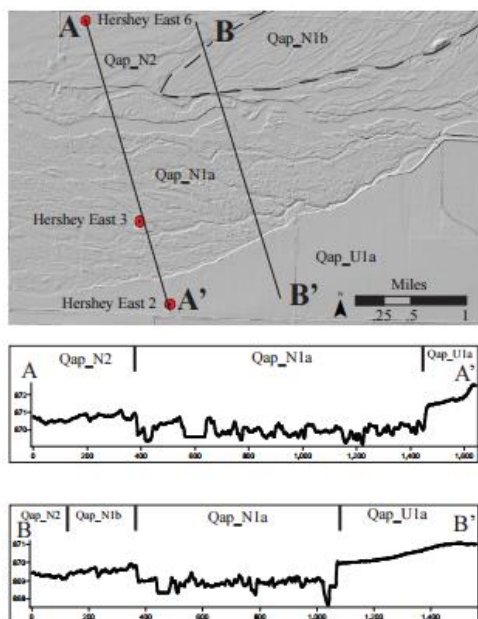
Figure 4.1 N. Platte Topo.
Bar and swale topography visible in the current N. Platte River floodplain Qap_N1a, and the abandoned floodplain Qap_N1b (Hanson et al. 2015)
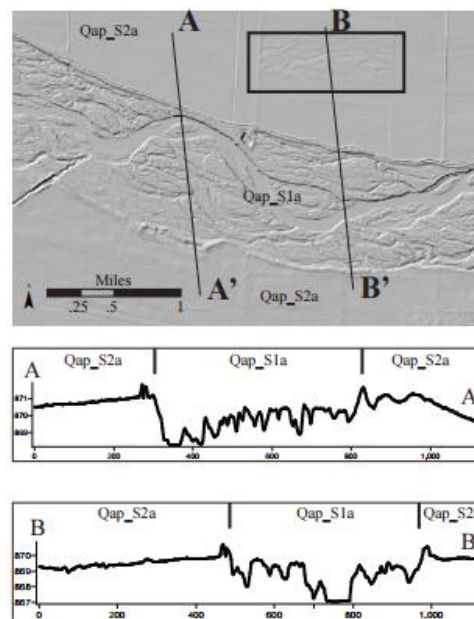
Figure 4.2 S. Platte Topo.
Bar and swale topography visible in current S. Platte River floodplain Qap_S1a, obscured in older alluvium Qap_S2a, with the exception of the black box. (Hanson et al. 2015)

The Surficial Geology of Hershey East 1:24,000 Quadrangle (Hanson et al. 2015) has a number of different alluvial surfaces of varying age and elevation. The modern floodplains of the North and South Platte Rivers, denoted Qap_N1a and Qap_S1a, have bar and swale topography typical of braided river systems present. A slightly older, abandoned floodplain surface denoted Qap_N1b is observed near the North Platte River, but is not observed at the South Platte River. Middle to late Holocene terraces deposited near the North Platte River sit 0.5 – 1 meter above the modern floodplain, and are denoted Qap_N2. A similar surface exists on either side of the South Platte River, denoted Qap_S2a and Qap_S2b. The difference between these surfaces is the presence of saline soils in Qap_S2b. The highest observed terrace of the North Platte, Qap_N3 sits 3 – 4 meters above the Qap_N1a surface, and is middle to late Holocene in age. The highest

observed terrace of the South Platte River, Qap_S3, sits only 2 – 3 meters above the Qap_S1a

surface, and is Holocene in age. Between the North and South Platte Rivers, there is alluvium

which is not directly associated with either the North or South Platte Rivers, denoted Qap_U1a-d.

Relief is greatest on the Qap_U1a surface, and smallest on the Qap_U1d surface, which follow a

west to east trend. In the northern sections of the Hershey East quadrangle, eolian dune sands,

Qes_d, with relief greater than 30 meters form the northern wall of the Platte River Valley.

Eolian sand sheets, Qes_ss, sit perched on the Qap_N3 surface, with sand sourced from the dunes

just to the north. In the very southwest corner of the map, a deposit of Peoria Loess, Qp, is

perched atop the Qap_S3 alluvium. Boreholes locations were chosen to examine the age and

elevations of different alluvial surfaces across the Platte River Valley.

Hershey East 6 was drilled into older alluvium of the North Platte River (Qap_N2) that

sits 300 meters north of the modern floodplain (Qap_N1a), and slightly higher in elevation.

Hershey East 3 was drilled directly into the modern alluvium, approximately 1 km south-

southwest of Hershey East 6. The uppermost samples from both Hershey East-3 and Hershey

East -6 were taken from approximately the same elevation, 868 meters above sea level (Figure

4.5). The OSL age from the uppermost Hershey East -6 sample (UNL-3951), 2.7 meters below

ground surface (BGS), resulted in an age of approximately 1.9 ka; the uppermost sample from

Hershey East -3 (UNL-3940), 2.9 m BGS, resulted in an age of approximately 0.9 ka. Hershey

East 6 had one deeper sample taken for OSL dating (UNL-3953); Hershey East 3 had two deeper

samples (UNL-3941, UNL-3942). All three of these samples resulted in ages too old to calculate

using blue light OSL dating techniques. Minimum OSL ages were determined for each of these

samples using the maximum beta dose (200Gy) given to the aliquots.

Hershey East cores 2, 1, and 5 were all drilled into topographically high alluvial deposits

that were mapped as undifferentiated surfaces (Qap_Q1a-d) that lie between the modern North

and South Platte River floodplains. OSL ages obtained from sediment underlying these surfaces

were similar. The uppermost sample of these cores, each located within 5 meters of the surface,

had OSL ages that calculated to be between 11,000 and 12,000 years in age (UNL-3932, UNL-3937). Hershey East 2 (Figure 4.8) had OSL ages showing a significant age inversion falling outside the error range of each age. Two samples from the Hershey East 5 core (Figure 4.10), UNL-3946 and UNL-3947 had an apparent age inversion, but the ages overlapped within their 1 σ error range. The deepest samples in each of these cores resulted in late Pleistocene ages, all of which were considerably older than the relatively young Holocene ages found in the upper sections of the core. The oldest result from these cores was in the Hershey East -5 core which was too old to date using OSL, but a minimum age of 93,100 years was calculated using the maximum D_e value used in the lab, 200 Gy.

Hershey East 4 was drilled into the older South Platte River alluvium (Qal_S2a) just north of the modern South Platte River channel. The uppermost age (UNL-3943) from this core came from approximately 7 meters depth, and resulted in an OSL age of 12,900 years, which is comparable to the ages recovered from the upper samples of the Hershey East 2, 1, and 5 cores (UNL-3937, UNL-3932, UNL-3946).   The deepest age from Hershey East -4 was again too old to calculate using OSL techniques, but a minimum age of 132,900 years was calculated using the maximum D_e value administered to the sample, 200 Gy.

In summary, sediments recovered in cores from the Hershey East 7.5' Quadrangle contain over 100,000 years of the geologic record. Relatively old sediments, late Pleistocene in age, are directly overlain by much younger sediments. The braid belts of both the North and South Platte Rivers have migrated across the entirety of the Platte River Valley in the Holocene.
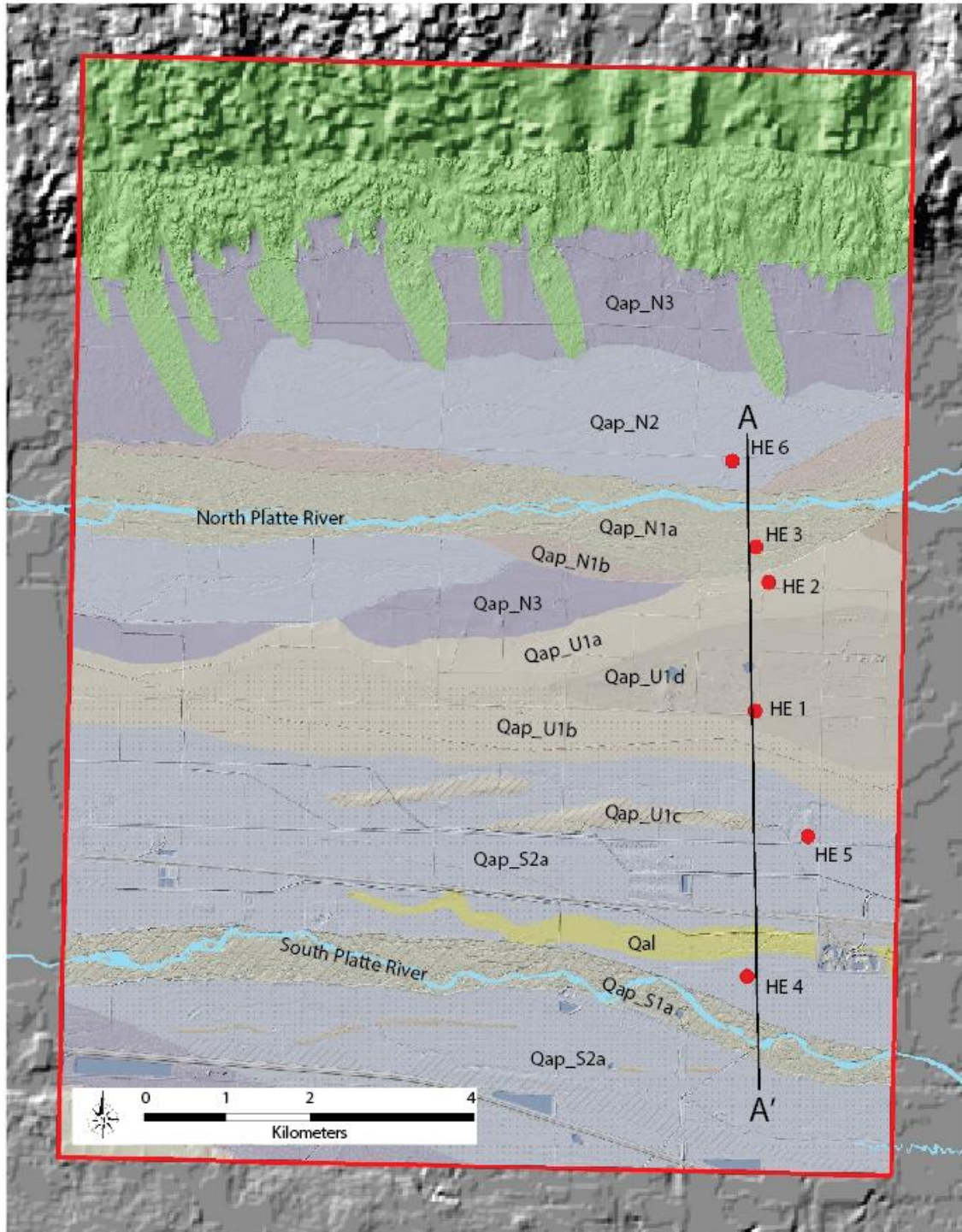
Figure 4.3 Surficial Geology of Hershey East 7.5' Quadrangle
Map adapted from Surficial Geology of Hershey East 7.5' Quad. Red dots indicate study boreholes. Landforms generally increase in age and elevation moving away from modern North and South Platte River floodplains. Map adapted from Hanson et al. (2015).

Core	Field #	UNL Lab #	Depth (m)	U (ppm)	Th (ppm)	K_2O (wt %)	In Situ H_2O (%)	Adjusted H_2O (%)[a]	Dose Rate (Gy/ka)	CAM[b] D_e (Gy) ± 1 Std. Err.	Aliquots (n)[c]	OSL Age (Ka) ± 1 σ (Ka)	O.D.[d]
HE 1	HE 1-1	3932	2.89	0.32	13.82	3.06	22.7	15.0	2.9	32.5±1.8	(44)60	11.1±1.1	36.7
	HE 1-4	3935	10.21	1.25	4.80	1.83	14.5	25.0	2.2	99.5±5.0	(49)78	55.2 ± 7.1	31.5
HE 2	HE 2-1	3937	4.57	0.91	4.78	2.88	17.2	25.0	2.5	26.1±1.4	(47)50	11.5±1.5	31.2
	HE 2-2	3938	7	1.61	7.69	4.14	11.5	25.0	3.8	25±1.4	(44)70	8.0± 1.1	37.3
	HE 2-3	3939	10.36	1.24	6.10	1.75	18.0	25.0	1.8	120±5.0	(40)92	72.9±8.8	23.1
HE 3	HE 3-1	3940	2.95	1.05	5.26	2.37	14.5	15.0	2.3	2.03±0.2	(44)79	0.9±0.1	53.1
	HE 3-2	3941	4.1	1.88	11.14	1.85	40.1	25.0	1.9	>200	--	>90.8	--
	HE 3-3	3942	7.19	1.96	9.77	2.12	27.1	25.0	2.2	>200	--	>87.7	--
HE 4	HE 4-1	3943	7.31	0.92	3.94	2.65	14.8	25.0	2.3	26.7±1.1	(46)50	12.9±1.7	23.7
	HE 4-3	3945	10.21	1.10	3.84	1.64	21.6	25.0	1.5	>200	--	>135.8	--
HE 5	HE 5-1	3946	4.1	2.58	10.83	3.05	11.3	25.0	3.5	35.3±1.8	(47)58	11.9±1.5	33.0
	HE 5-2	3947	7.14	1.15	5.82	3.57	13.2	25.0	3.1	27.5±1.6	(49)55	10.3±1.5	39.2
	HE 5-5	3950	13.25	1.55	9.16	2.14	22.6	25.0	2.2	>200	--	>93.1	--
HE 6	HE 6-1	3951	2.74	1.27	5.13	2.15	17.3	15.0	2.1	4.07±0.2	(42)79	1.9±0.2	23.3
	HE 6-3	3953	5.79	1.10	3.84	1.64	15.9	25.0	1.6	>200	--	>132.9	--

[a]Assumes 50% variability in estimated moisture content

[b]Central Age Model (Galbraith et al., 1999)

[c]Accepted disks/all disks

[d]Overdispersion

Figure 4.4 Table of OSL Results from the Hershey East 7.5' Quadrangle
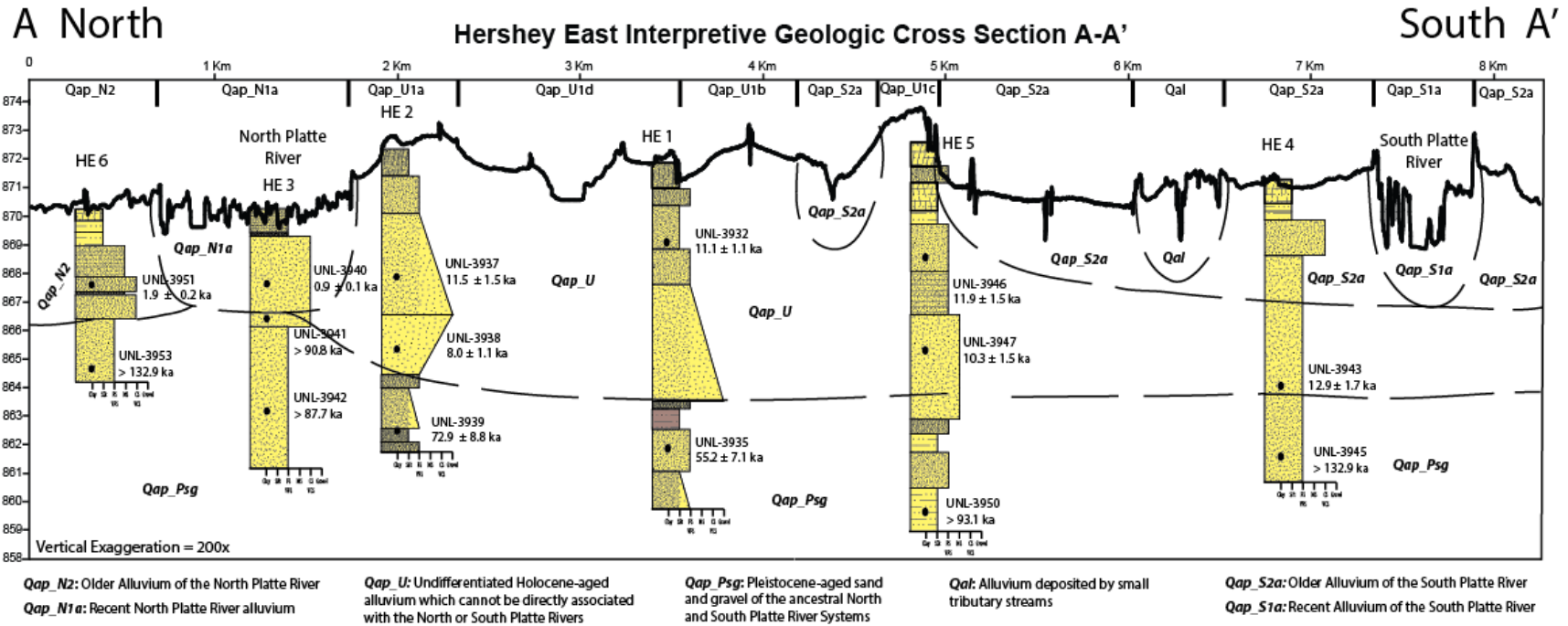
Figure 4.5 Interpretive Geologic Cross-Section of the Hershey East 7.5' Quadrangle
Graphic logs and OSL ages of Hershey East cores hanging from an elevation profile (North to South) taken from 2 meter resolution LiDAR data. Dashed lines indicate approximate boundaries between different ages of alluvium.

4.1.1 Hershey East 6 Results

Particle size analysis (PSA) from the Hershey East 6 core (Figure 4.6) results depict generally fine grained sediments, dominantly silt and fine-grained sand from the surface to a depth of approximately 1 meter. From 1 to 2 meters, PSA shows a coarsening-upwards sequence, with a slight increase in sand grain size from very fine sand to medium sand. From 2 to 4 meters, alluvium is coarser, predominately poorly-sorted sand and gravel with minimal silt. Recovered sediments from below 4 meters consist of silt and very fine sand.

The Hershey East 6 core was drilled on the most recently abandoned alluvial surface of the North Platte River, Qap_N2, approximately 300 meters north of the modern channel surface Qap_N1a (Figure 3.1). An age of 1.9 ± 0.2 ka was calculated for Hershey East 6-1 (UNL-3951) at a depth of 2.7 m BGS, in a package of medium-grained sand. Hershey East 6-2 (UNL-3953) was sampled in silty sand at a depth of 5.8m BGS, and resulted in an age too old to accurately calculate using OSL dating techniques. A minimum age of 132.9 ka was calculated for this sample, using the maximum D_e of 200 Gy (Figure 4.4). Ages calculated with OSL present an erosional disconformity occurring between modern alluvium and Pleistocene-aged alluvium within the recovered core sediments. However, no distinct boundary is present between the different-aged sediment packages in the recovered core.

Figure 4.6 Particle Size Analysis and Graphic Log for Hershey East 6 Core
In PSA chart, hollow shapes indicate data obtained from laser particle size
analysis; filled shapes indicate data obtained from sieve analysis. Silt is defined
to be < .063 mm, Sand .063 – 2mm, and Gravel is > 2 mm

4.1.2   Hershey East 3 Results

Results from particle size analysis from the Hershey East 3 show that a meter of

overbank silt and fine sand overlie coarser recent alluvial deposits. The modern alluvial fill sits

from 1 to 4 meters below the surface, consisting of poorly sorted sand and gravel with very

minimal silt. At a depth of 4 meters to 5 meters, there is an abrupt decrease in sand and gravel,

and recovered sediments are fine-grained interbedded silts and sands are. Recovered sediments

from deeper than 4.2 meters consist of silt and fine to very fine sand. (Figure 4.7)

The Hershey East 3 core was drilled in the floodplain just south of the modern North

Platte River, on the modern channel surface Qap_N1a (Figure 4.3). An OSL age of 0.9 ± 0.2 ka

was calculated for HE 3-1 (UNL-3940), buried at a depth of 2.9 meters below the modern

channel.   Buried only 1.2 meters beneath the Hershey East 3-1 (UNL-3940) sample at ~ 3.9 m

BGS, Hershey East 3-2 (UNL-3941) was too old to accurately date with OSL, and was assigned

minimum OSL age of 90.8 ka. Hershey East 3-3 (UNL-3942), the deepest sample from this core

at a depth of 7.2 meters, was also too old to date with OSL. This sample resulted in a minimum

OSL age of 87.7 ka (Figure 4.4). Samples collected from lower in these cores were too old to

date using OSL. Resulting ages again show an erosional disconformity between modern alluvium

and Pleistocene-aged alluvium, similar to that in core Hershey East 6 (Figure 4.6).
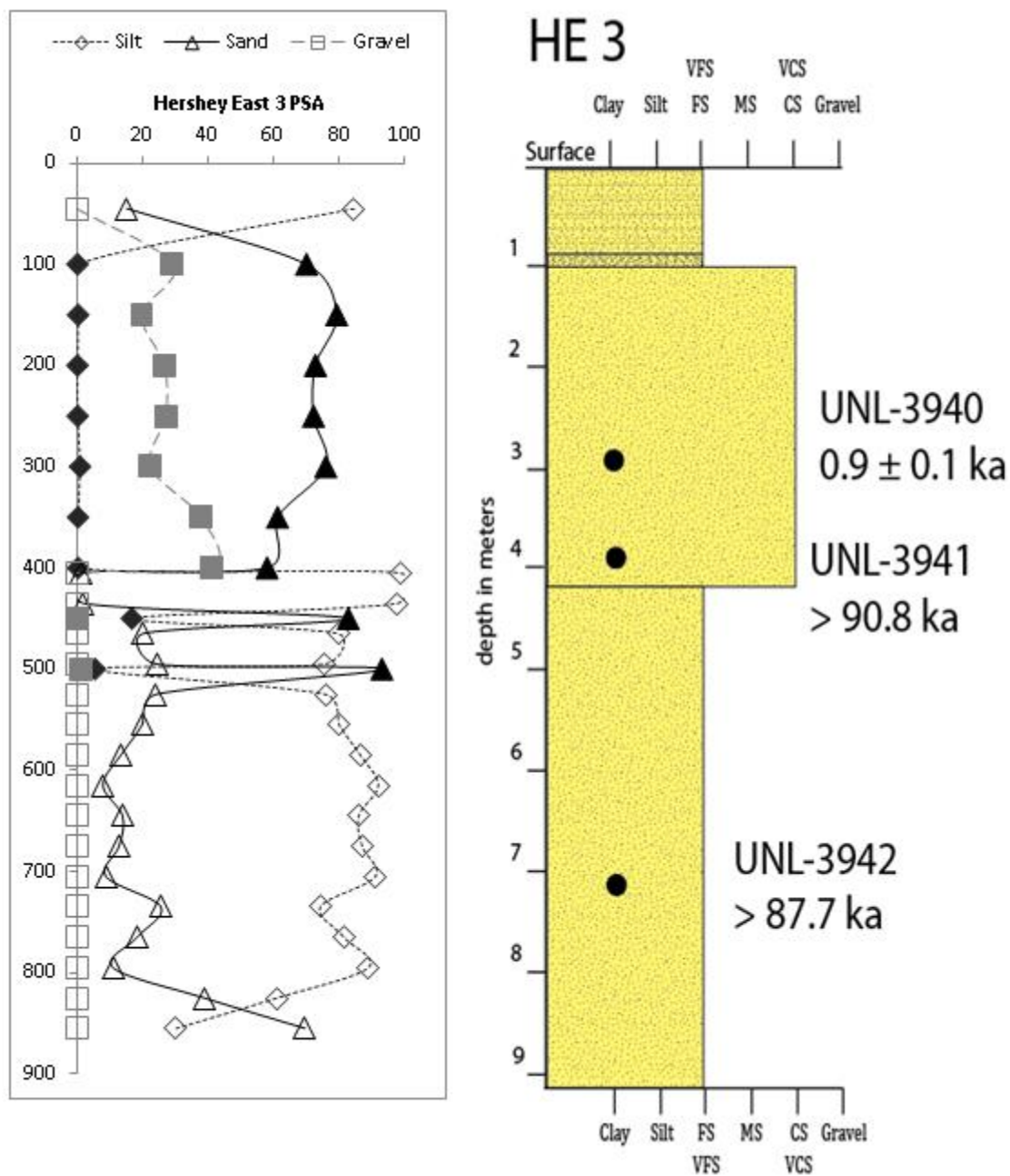
Figure 4.7 Particle Size Analysis and Graphic Log for Hershey East 3 Core
In PSA chart, hollow shapes indicate data obtained from laser particle size
analysis; filled shapes indicate data obtained from sieve analysis. Silt is defined
to be < .063 mm, Sand .063 – 2mm, and Gravel is > 2 mm

4.1.3   Hershey East 2 Results

Results from particle size analysis and core descriptions from the Hershey East 2 core

indicate soil development on the upper meter of the abandoned alluvial surface. Evidence of a

soil profile is seen due to high silt content, fine-grained sands, 10YR 3/2 color, and rootlets

present at depth. The presence of this soil indicates that the surface has not been active recently,

as is expected on a topographic high in the Platte River Valley (Figure 4.5). Below the soil profile

are fine-grained sands from 1-2.5 meters depth.   A fining upward sequence with decreasing

gravel content and increasing sand content occurs from 2 to 5 meters. From 5 to 7 meters, there

is a coarsening upward sequence with gravel content increasing and sand content decreasing.

Below 7 meters, gravel is absent, and recovered core sediments are interbedded silt and fine-

grained sand units. (Figure3.5)

The Hershey East 2 core was drilled into alluvial material that was mapped as

Undifferentiated Platte River Alluvium Qap_U1a (Figure 3.1). These sediments cannot be

directly associated with either the North or South Platte Rivers. OSL ages from the upper two

samples from this core resulted in an age inversion, potentially the result of problems associated

with partial bleaching. Hershey East 2-1 (UNL-3937) has an OSL age of 11.5 ± 1.5 ka at a depth

of 4.6 meters; Hershey East 2-2 (UNL-3938) has an OSL age of 8.0 ± 1.1 ka at a depth of 7

meters. While neither age falls within the error range of the other, they are both Holocene

alluvium of roughly the same age. An OSL age for Hershey East 2-3 (UNL-3939) was calculated

to be 72.9 ± 8.8 ka, at a depth of 10.36 meters (Figure 4.4). The age difference between early

Holocene sediments and late Pleistocene sediments is significant; it is likely that an erosional

disconformity is also present in this core.
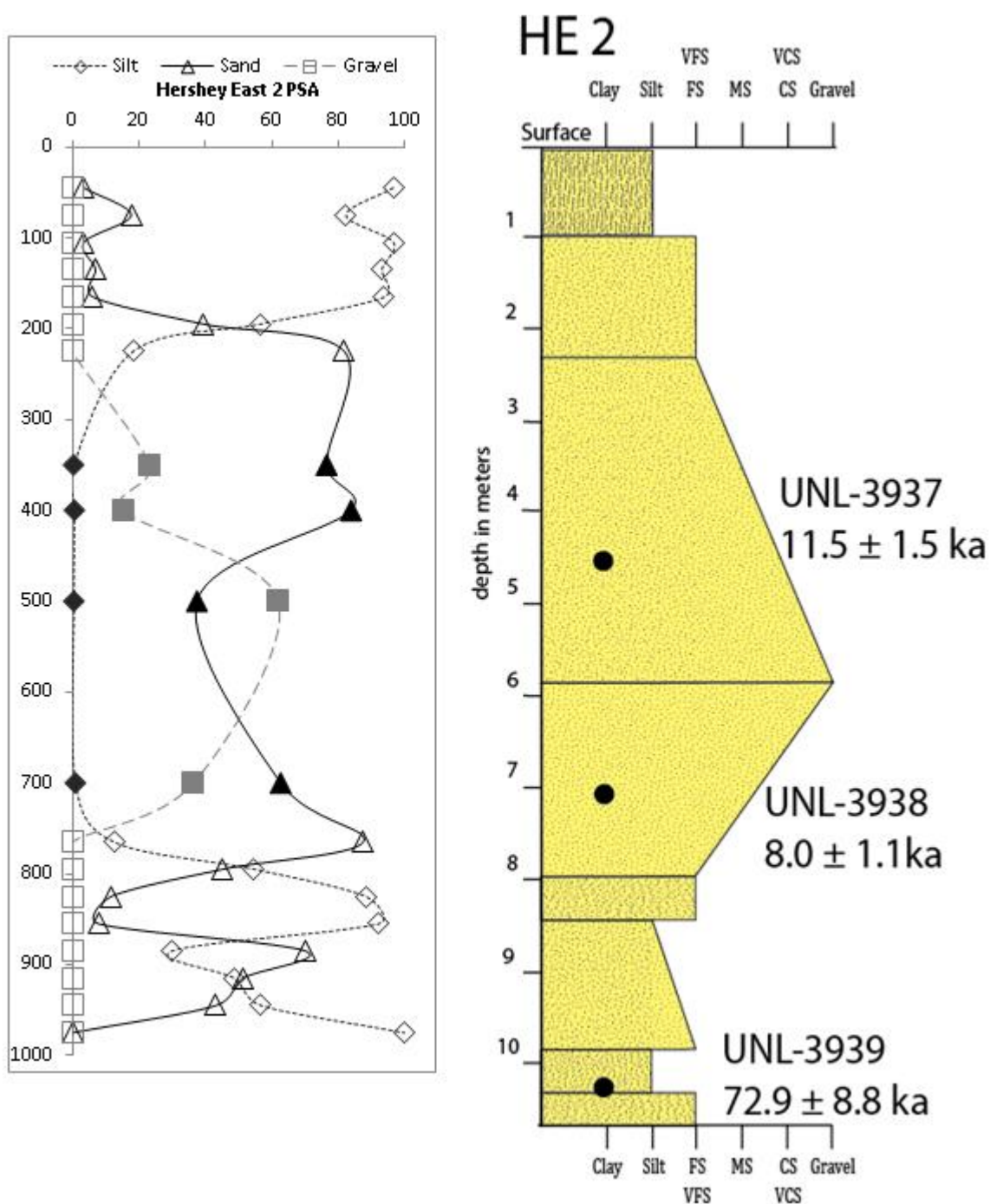
Figure 4.8 Particle Size Analysis and Graphic Log for Hershey East 2 Core
In PSA chart, hollow shapes indicate data obtained from laser particle size analysis; filled shapes indicate data obtained from sieve analysis. Silt is defined to be < .063 mm, Sand .063 – 2mm, and Gravel is > 2 mm

4.1.4 Hershey East 1 Results

Results from particle size analysis and core descriptions from Hershey East 1 indicate a soil developed in the upper meter of this abandoned alluvial surface. The soil profile is dominantly silt, with clay and very fine-grained sands. Rootlets are also present, as well as the 10YR 3/2 color typical of an A-horizon. Similar to the Hershey East -2 core, Hershey East -1 sits at a relatively high elevation in the Platte River Valley (Figure 4.5), and is not an active alluvial surface. Below the soil profile, between 3 and 5 meters depth, interbedded fine-grained sands and silts are present. From 5 to 8 meters, sediments consist of poorly sorted coarse sand and gravel, with little to no silt or clay present. There is a meter-thick package of very fine-grained overbank sediment which sits 8.5 to 9.5 meters below the surface, consisting of 30-40% clay, and 60-70% silt with no sand or gravel. Below 9.5 meters depth, the clay content decreases and sediments are predominantly silt and fine-grained sands. This sediment package fines slightly upwards, from medium sand to fine sand and silt (Figure 4.9).

The Hershey East 1 core was drilled in another alluvial deposit mapped as Undifferentiated Platte River Alluvium, Qap_U1d (Figure 3-1), which sits slightly higher topographically than the Qap_U1a unit (Figure 4.5). An OSL age from Hershey East 1-1 (UNL-3932) sampled 2.9 meters below the surface was calculated to be 11.1 ± 1.1 ka. The resulting OSL age of the next sample, Hershey East 1-4 (UNL-3935) was 55.2 ± 7.1 ka, sampled from 10.2 meters depth. Unfortunately, no OSL ages were analyzed for sediment lying between Hershey East 1-1 and 1-4 (Figure 4.4).
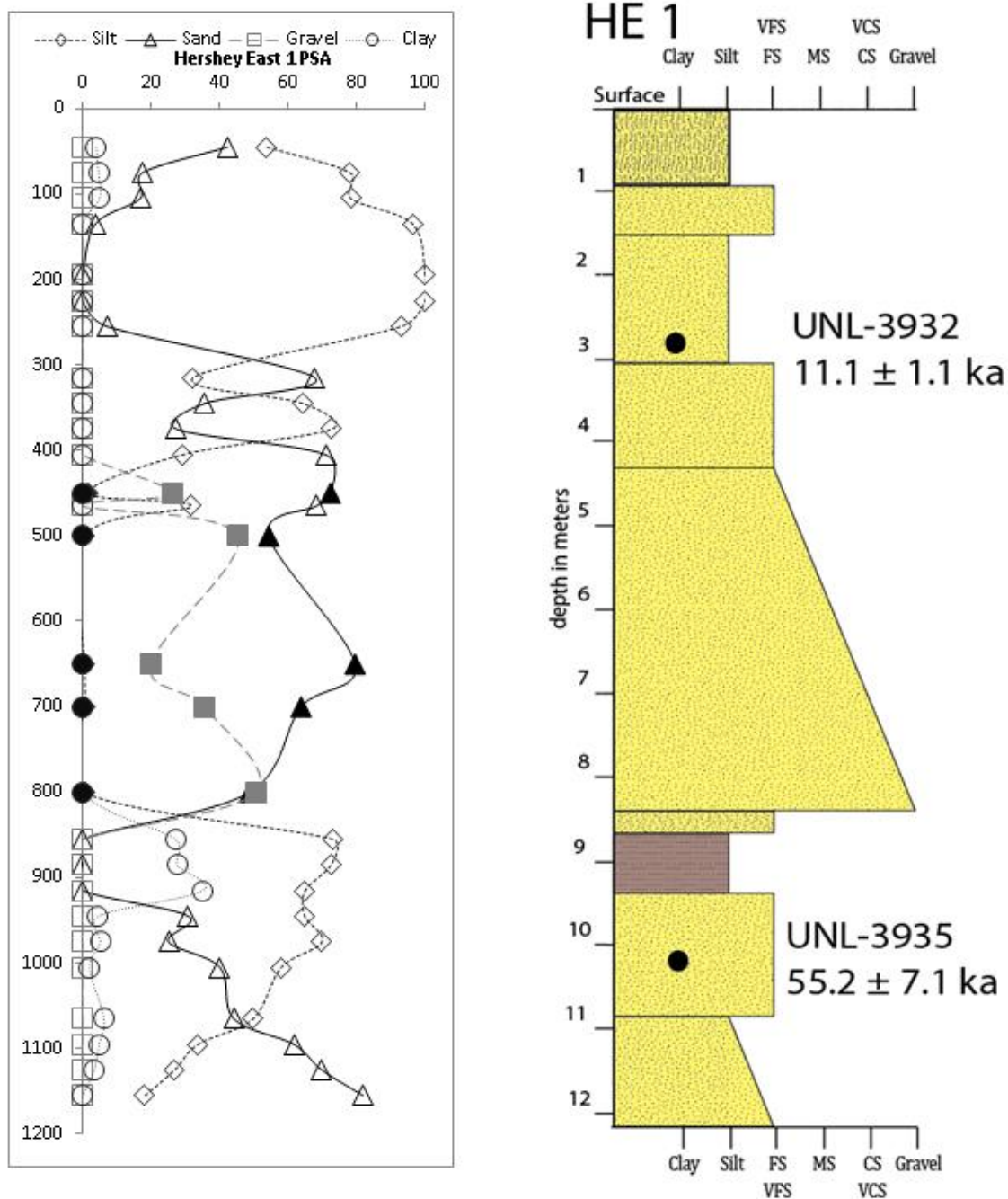
Figure 4.9 Particle Size Analysis and Graphic Log for Hershey East 1 Core
In PSA chart, hollow shapes indicate data obtained from laser particle size
analysis; filled shapes indicate data obtained from sieve analysis. Silt is defined
to be < .063 mm, Sand .063 – 2mm, and Gravel is > 2 mm

4.1.5   Hershey East 5 Results

Results from particle size analysis and core descriptions from the Hershey East 5 core indicate an A-horizon developed in the uppermost meter of the abandoned alluvial surface. Particle size analysis of this soil profile indicates high silt content, with some very fine and fine-grained sands present. The soil has a 10YR 3/2 color typical of an A horizon. From 1 to 1.5 meters, sediments are silt and fine sand and the deposit lacks evidence of soil development. An Ab-horizon is present below the silty sand unit from 1.5-2.5 meters, with high silt content with some fine-grained sand, and 10YR 3/2 color. Similarly to Hershey East -2 and Hershey East -1, Hershey East -5 sits on a topographic high within the Platte River Valley (Figure 4.5). From 2.5 meters to 6 meters, there is a slight fining upwards sand sequence, with laminated fine-grained sands from 4.5 to 6 meters. Between 6 and 10 meters depth, poorly sorted coarse-grained sands and gravel are prevalent. Below 10 meters depth, recovered sediments consist largely of silt and fine-grained sands (Figure 4.10).

The Hershey East 5 core was drilled into the South Platte River Alluvium (Qap_S2a), sitting slightly higher than the modern alluvium of the South Platte River (Figure 4.5). OSL ages from the upper two samples from this core resulted in an age inversion. Hershey East 5-1 (UNL-3946) resulted in an OSL age of 11.9 ± 1.5 ka at a depth of 4.1 meters; Hershey East 5-2 (UNL-3947) resulted in an OSL age of 10.3 ± 1.5 ka at 7.1 meters. Each of these OSL ages fall within the error range of the other, and straddle the late Pleistocene and Holocene boundary. The deepest sample taken in the Hershey East quad, Hershey East 5-5 (UNL-3950), from a depth of 13.25 meters, resulted in an age too old to date using OSL techniques. The minimum age calculated for this sample using a maximum lab D_e of 200 Gy was 93.1 ka (Figure 4.4).
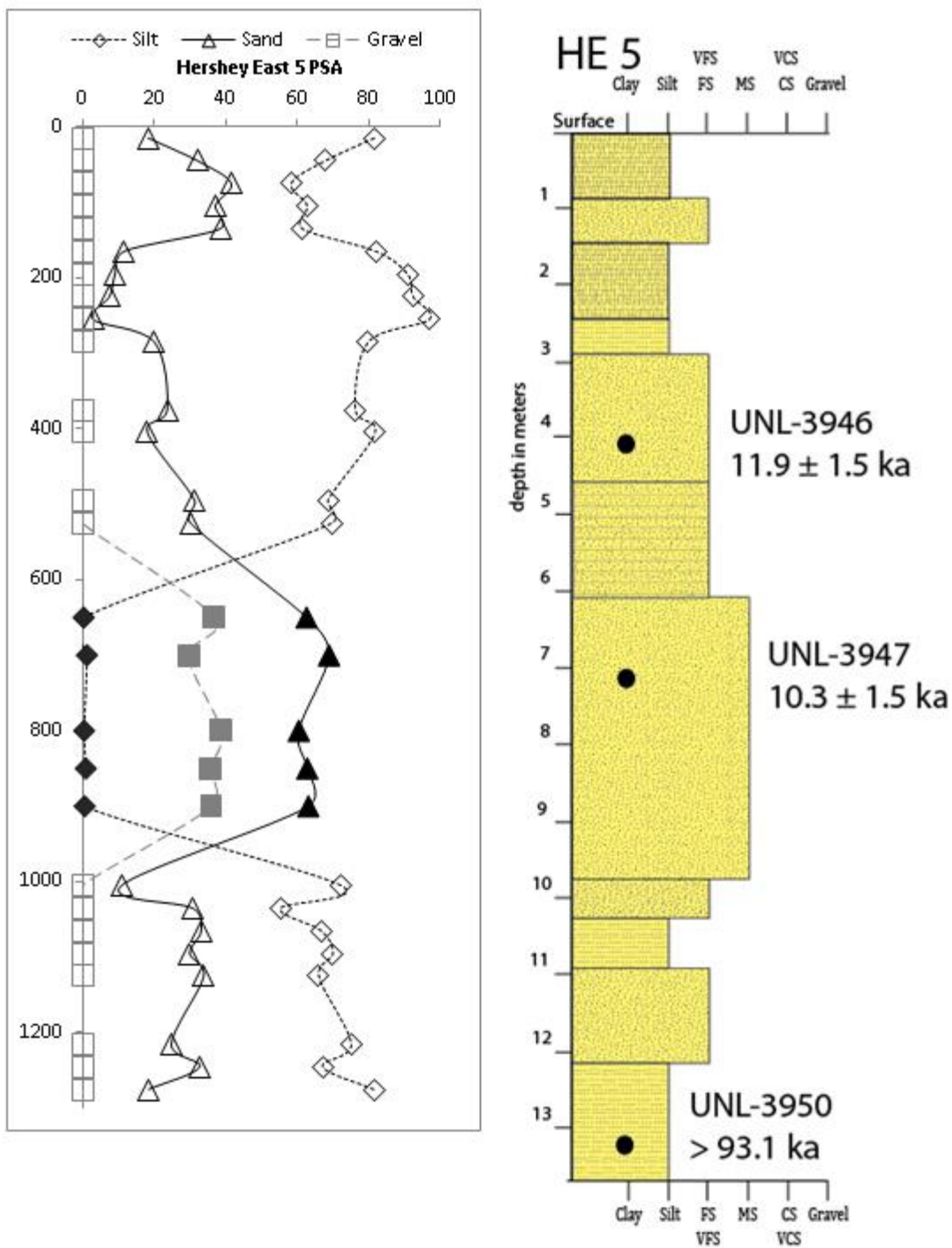
Figure 4.10 Particle Size Analysis and Graphic Log for Hershey East 5 Core
In PSA chart, hollow shapes indicate data obtained from laser particle size analysis; filled shapes indicate data obtained from sieve analysis. Silt is defined to be < .063 mm, Sand .063 – 2mm, and Gravel is > 2 mm

4.1.6   Hershey East 4 Results

Results from particle size analysis and core descriptions from the Hershey East 4 core showed evidence of soil development on the recently abandoned alluvial surface to a depth of 1 meter. Soil color was 10YR 4/2, and consisted mainly of silt, with some very fine-grained sand and rootlets. Though this core was drilled relatively low topographically (Figure 4.5), the drill site was on agricultural land, with no recent alluvial deposition. The soil horizon ends 1 meter below the surface, but the texture remains silty sand to a depth of 1.5 meters. Between 1.5 and 3 meters is a fining-upward sequence with decreasing amounts of poorly sorted sand and gravel, and an increase in silt. A coarsening-upward sequence is present from 3 to 5.5 meters with medium-grained sands changing to poorly sorted coarse sand and gravel. Sediments between 5.5 to 6.5 meters were deposited in a fining-upward sequence. Sediments from 6.5 to 7 meters are deposited in a coarsening-upwards sequence. Below 7 meters recovered sediments are fine-grained sand and silt-sized particles. Each of these fining and coarsening-upwards sequences were subtle, and didn't appear until particle size analysis results were graphed.

The Hershey East 4 core was also drilled into older alluvium of the South Platte River Qap_S2a, but is located much closer to the modern channel of the South Platte River. Though the borehole was drilled much closer to the modern South Platte channel, OSL ages calculated from samples in this core show similar characteristics to those of the Hershey East 5 core drilled two km to the northeast. Once again, there is likely an erosional unconformity between sediments straddling the Holocene-Pleistocene boundary directly overlying much older Pleistocene material. Unfortunately, no age control is available closer to the surface than 7.3 meters, where Hershey East 4-1 (UNL-3943) was sampled, which resulted in an OSL age of 12.9 ± 1.7 ka. Below the erosional disconformity, Hershey East 4-3 (UNL-3945) resulted in a minimum OSL age of 135.8 ka, at a depth of 10.2 meters (Figure 4.4).
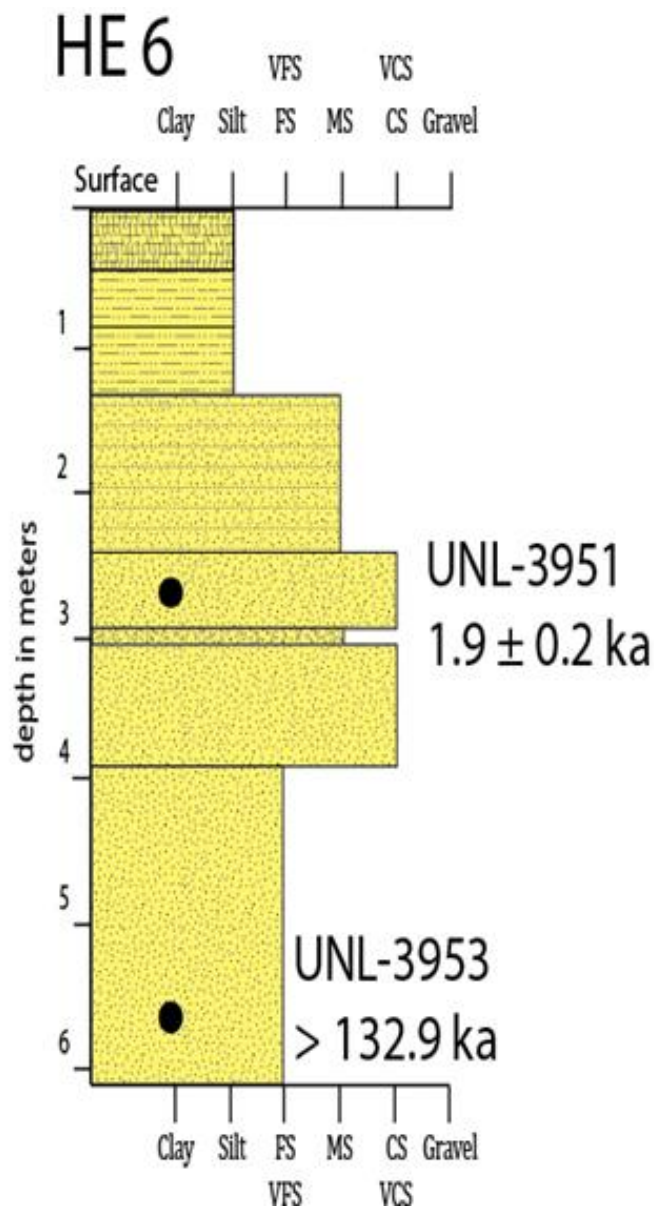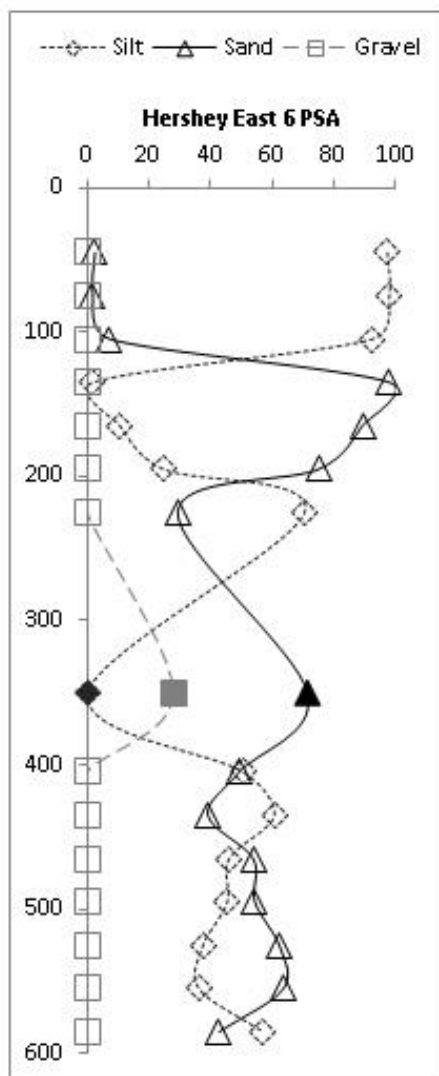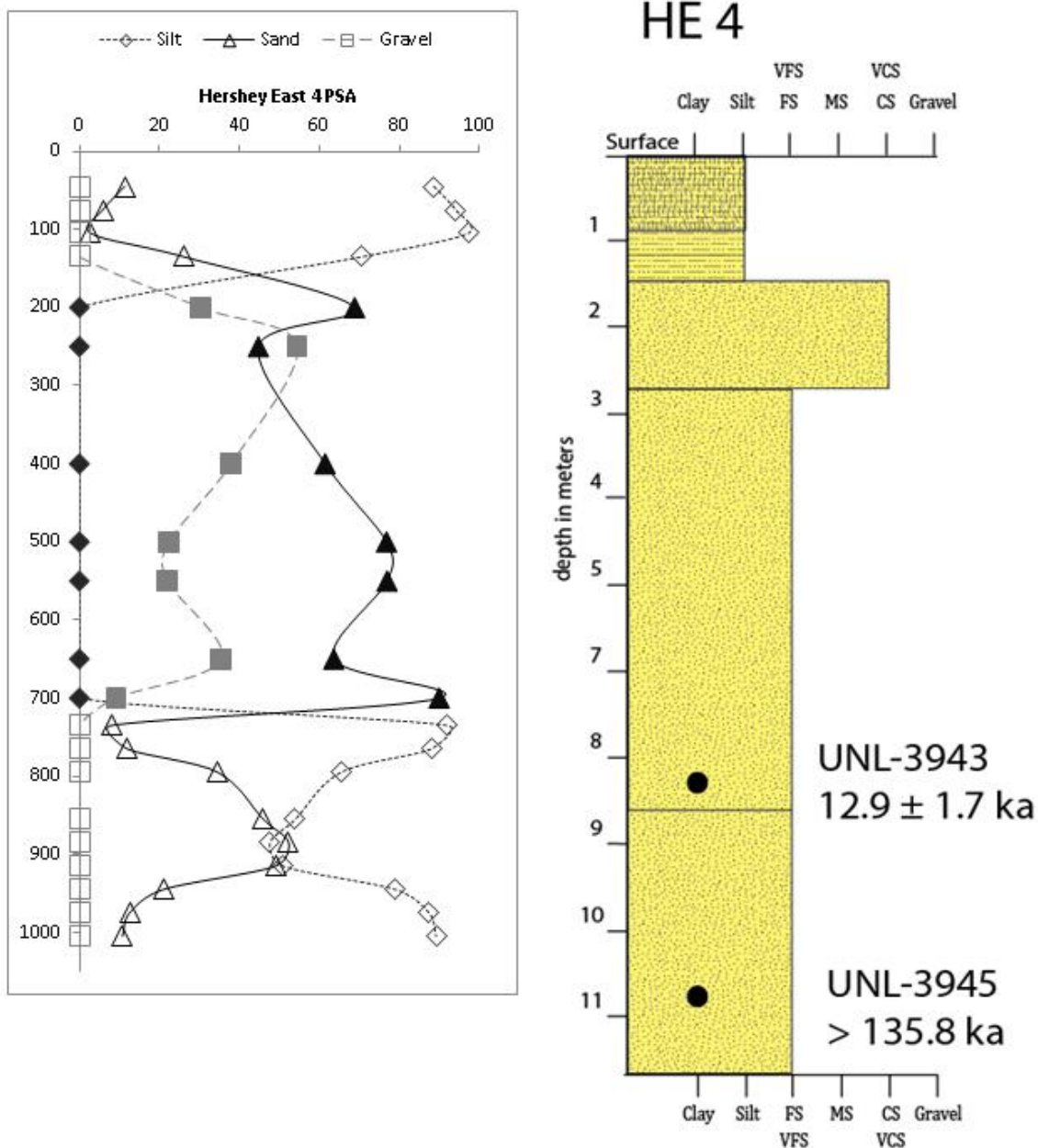
Figure 4.11 Particle Size Analysis and Graphic Log for Hershey East 4 Core
In PSA chart, hollow shapes indicate data obtained from laser particle size
analysis; filled shapes indicate data obtained from sieve analysis. Silt is defined
to be < .063 mm, Sand .063 – 2mm, and Gravel is > 2 mm

OSL ages calculated from samples taken from sediment cores drilled in the Hershey East quadrangle covered over 130,000 years of geologic history. 15 total OSL samples resulted in five late Pleistocene ages too old to calculate using OSL, two ages dated to the late Pleistocene, six Holocene ages, and two young ages from the modern North Platte River floodplain. The deepest sediments recovered all resulted in late Pleistocene or older ages. Overlying the Pleistocene sediments is an undifferentiated alluvial fill, associated with early Holocene ages. This fill is 3-10 meters thick, but has been modified by the overlying modern alluvium, which has deposited approximately 3 meters of sediment within the last 2 ka.

The deepest samples recovered from each core resulted in late Pleistocene ages; the youngest were 55.5 ± 7.1 ka and 72.9 ± 8.8 ka. The rest had saturated OSL traps and were assigned minimum OSL ages, the youngest being 87.7 ka. While samples with saturated OSL traps don't provide accurate age control, they are still useful in providing a baseline for the oldest material recovered in sediment cores. The late Pleistocene-aged sediments recovered in drill cores are a minimum of 5 meters thick. However, it is likely that the entirety of the Pleistocene fill may be considerably thicker than was recovered in drill cores.

OSL data suggest that the Pleistocene-aged surface is approximately 864 ± 2 meters above current sea level, with the error range accounting for any paleotopography that may exist. While the Pleistocene-Holocene boundary is drawn as a relatively flat line, there is almost certainly greater variation in the elevation of the boundary that cannot be resolved with the available data.

OSL ages from the undifferentiated alluvial fills were significantly younger than those of the underlying Pleistocene alluvial fill. Six ages from this fill ranged from 8 to 13 ka, and accounting for the error range all samples could fall within the Holocene. One possible exception is an age of 12.9 ± 1.7 ka, which is likely very late Pleistocene, but could fall in the Holocene using the associated error range. A few ages in this fill were stratigraphically inverted, but the overall trend in the OSL ages indicate that the majority of the alluvium was deposited in the early

Holocene. The recovered core sediments resulting in Holocene-aged sediments range in thickness from 3 to 10 ± 2 meters at the base to account for any underlying paleotopography on the Pleistocene surface. Importantly, the Holocene-aged fill is considerably thicker where it is not overlain by modern alluvial sediments; the modern rivers have likely eroded a significant volume of sediment from the undifferentiated Holocene fill.

It is likely that some of the surficial topography in the undifferentiated fill between the North and South Platte Rivers is eolian in origin, but no conclusions can be made in that regards with data collected in this study. On average, the undifferentiated Holocene alluvial fill is approximately 7 meters thick in areas undisturbed by modern erosion and deposition. Both the Holocene and late Pleistocene alluvial fills have a significantly greater thickness than observed in the modern alluvial fill.

The modern alluvial fill of the North Platte River is considerably thinner than both the Holocene and Pleistocene alluvial fills. While only two ages were recovered from these modern sediments, they were consistent with expectations based on respective alluvial surfaces. The older age, 1.9 ± 0.2 ka, was taken from the abandoned floodplain just north of the modern floodplain. The younger sample resulted in an age of 0.9 ± 0.1 ka, from just below the modern floodplain surface. Both samples were taken from approximately the same elevation, around 867 meters above sea level.

The modern alluvial fill underlying the North Platte River directly overlies the late Pleistocene fill; any previously deposited Holocene sediment has since been removed. Both the modern and late Holocene alluvial deposits in the North Platte appear to be significantly thinner than the underlying Pleistocene-aged fill and the undifferentiated Holocene alluvium to the south. Thickness of the modern alluvial fill is approximately 3 ± 2 meters, with the error accounting for any paleotopography in the Holocene fill. Unfortunately, no cores or OSL ages were obtained for the modern alluvium directly underlying the South Platte River channel. It is approximated to be roughly the same thickness as the North Platte fill, 3 ± 2 meters.

4.2   Kearney Results

The Surficial Geology of Kearney 1:24,000 Quadrangle (Hanson et al. 2014) has a number of different alluvial surfaces of varying age and elevation. The modern floodplain of the Platte River, denoted Qap1a&b, has bar and swale topography typical of braided river systems present. Older alluvium of middle to late Holocene age sits 1 – 2 meters above the modern floodplain surface, denoted Qap2, extending up to 3 km north and south of the modern floodplain. Bar and swale topography on this surface has been largely obscured by infilling, but is locally visible. Early Holocene aged deposits, denoted Qap3, sit 2 – 3 meters above the modern floodplain, beyond the Qap2 surface. In the north section of the map, a layer of Peoria Loess has been deposited on top of alluvium; the surface of the Peoria Loess sits 4 – 5 meters above the modern Platte River floodplain. A few small yazoo tributaries, which are small, entrenched streams that run in the floodplain parallel to a larger river are present in the Kearney quadrangle, and are denoted Qal. In the southwest corner of the quadrangle, eolian dunes and sand sheets enter the Quadrangle. Dunes are 5 – 7 meters in relief, and sand is on average 15 meters thick.

A total of 11 OSL age estimates (Figure 4.13) were produced for alluvial and eolian sediments recovered in four cores drilled in the Kearney 7.5' Quadrangle. Recovered sediments and OSL ages and varied with location and depth, as expected with the braid-bar depositional systems of the North and South Platte Rivers (Smith, 1971) and the younger eolian sediments overlying the older alluvium. Results of this study will be discussed in three ways; a brief discussion of trends observed between different cores recovered from alluvial deposits, detailed results from each core in transect order (North to South) across the Platte River Valley (Figure 4.3, 4.12), and an in-depth analysis of results from each study area. .

OSL samples are labelled differently than those in the Hershey East quadrangle. Many other cores were drilled in the Kearney 7.5' quadrangle as part of the Nebraska STATEMAP project, and field ID's of study cores were re-labelled with different ID numbers later in the

study. In this case, the field ID Kearney 1 became Kearney 9; 2 became 10, 3 became 11, and 4 became 12. OSL samples were taken prior to the re-numbering, and were labeled according to the field ID of the core they were taken from, in order of depth.

Kearney 8 was drilled into an upland deposit of Peoria Loess overlying alluvial sand and gravel (Qp_t1). The loess was likely deposited between approximately 25,000 and 14,000 years ago (Bettis et al., 2003; Mason et al., 2011; Muhs et al., 2013). Though no OSL age chronology is available for this core, a radiocarbon age of approximately 23,500 calendar years BP was calculated from a deposit of spruce needles buried in alluvium under the Peoria Loess (J. Dillon, personal communication). A thin layer of poorly sorted coarse sand and gravel was present at the bottom of the core, indicating that the Peoria Loess does overlie what could be either late Pleistocene aged Platte River or Wood River alluvium (Figure 4.15).

Kearney 12 was drilled in a deposit of older Platte River alluvium (Qap3) approximately 3 km north of and 2-3 meters in elevation above the modern Platte River floodplain. Three ages were calculated from the Kearney 12 core. A shallow Holocene age of 11.6 ± 1.3 ka (UNL-3823), and two late Pleistocene ages of 18.2 ± 2.4 ka and 30.2 ± 4.3 ka (UNL 3825, UNL-3827) were calculated from samples taken deeper in the core (Figure 4.13).

Kearney 11 was drilled into a deposit of slightly older Platte River alluvium (Qap2) just south of the modern floodplain. This surface sits 1-2 meters in elevation above the modern Platte River floodplain. Two ages were calculated from the Kearney 11 core. A shallow Holocene age of 7.5 ± 0.7 ka (UNL-3820), and a deeper late Pleistocene age of 37.0 ± 5.9 ka (UNL-3822) were calculated from samples taken in the core (Figure 4.17). The late Pleistocene age calculated in this core is slightly older than that of the deepest OSL age from Kearney 12, though it sits higher in elevation (Figure 4.14)

Kearney 10 was drilled into a similar deposit of older Platte River alluvium (Qap3) as Kearney 12, but to the south of the modern Platte River floodplain. Resulting ages were similar to those found in the Kearney-12 core. In this case, Holocene ages were calculated from two

samples within the upper 6 meters of recovered core. This core (Figure 4.18) had OSL results showing an age inversion falling just inside the error range of the other age. The oldest age calculated from the Kearney-10 core is the oldest OSL age calculated in the Kearney quad, from higher in elevation than the rest of the late Pleistocene OSL ages (Figure 4.13).

Kearney 9 was drilled into eolian dune (Qes) deposits in the southwest corner of the Kearney quad. An OSL age from 4.1 m BGS shows that the dune sand was deposited approximately 1.1 ± 0.1 ka ago, making it the youngest dated geologic feature in this area. The dune sand is perched on the older alluvium of the Platte River (Qap3) surface, in which the Kearney 10 and 12 cores were drilled. Late Pleistocene ages were calculated for the two OSL samples taken in the Platte River alluvium underlying the eolian deposits. An age of approximately 14.3 ± 1.4 ka was calculated at a depth of approximately 10 m BGS, and at 15 meters the resulting age was approximately 23.3 ± 2.5 ka.

In summary, sediments recovered in cores from the Kearney 7.5' quad contain approximately 50,000 years of the geologic record. As in the Hershey East quadrangle, older sediments of late Pleistocene age are directly overlain by much younger sediments. The age differences between Holocene and Pleistocene aged sediments at Kearney are much less extreme than those of the Hershey East quadrangle. The braid belt of the Platte River has migrated across the entirety of the Platte River Valley. Based on evidence from the presence of Platte River alluvium in the Kearney-12 core, and alluvium related to either the ancestral Platte River or Wood River at the bottom of the Kearney-8 core, it is likely that the Peoria Loess was deposited atop an alluvial unit- likely alluvium within the Qap3 or an older alluvial deposit. The remnant loess in the northern section of the Kearney 7.5' Quadrangle was never fully eroded, and is forms the current uplands. However, the loess deposition directly overlying the active Platte River floodplain was removed by the ancestral Platte River, leaving deposits of alluvial sand and gravel in its place. Unfortunately, no OSL age control is available from the alluvium underlying the Peoria Loess to verify radiocarbon ages. Using OSL ages and local elevations of both Holocene

and late Pleistocene ages across the Platte River valley in the Kearney Quadrangle, it seems likely that the ancestral Platte River would have been significantly wider and/or had separate channels. Channel width has decreased significantly in the historic era (Joeckel and Henebry, 2008) from study sites 120 + km downstream from Kearney, which may help explain the relatively broad valley compared to the width of the modern Platte River.
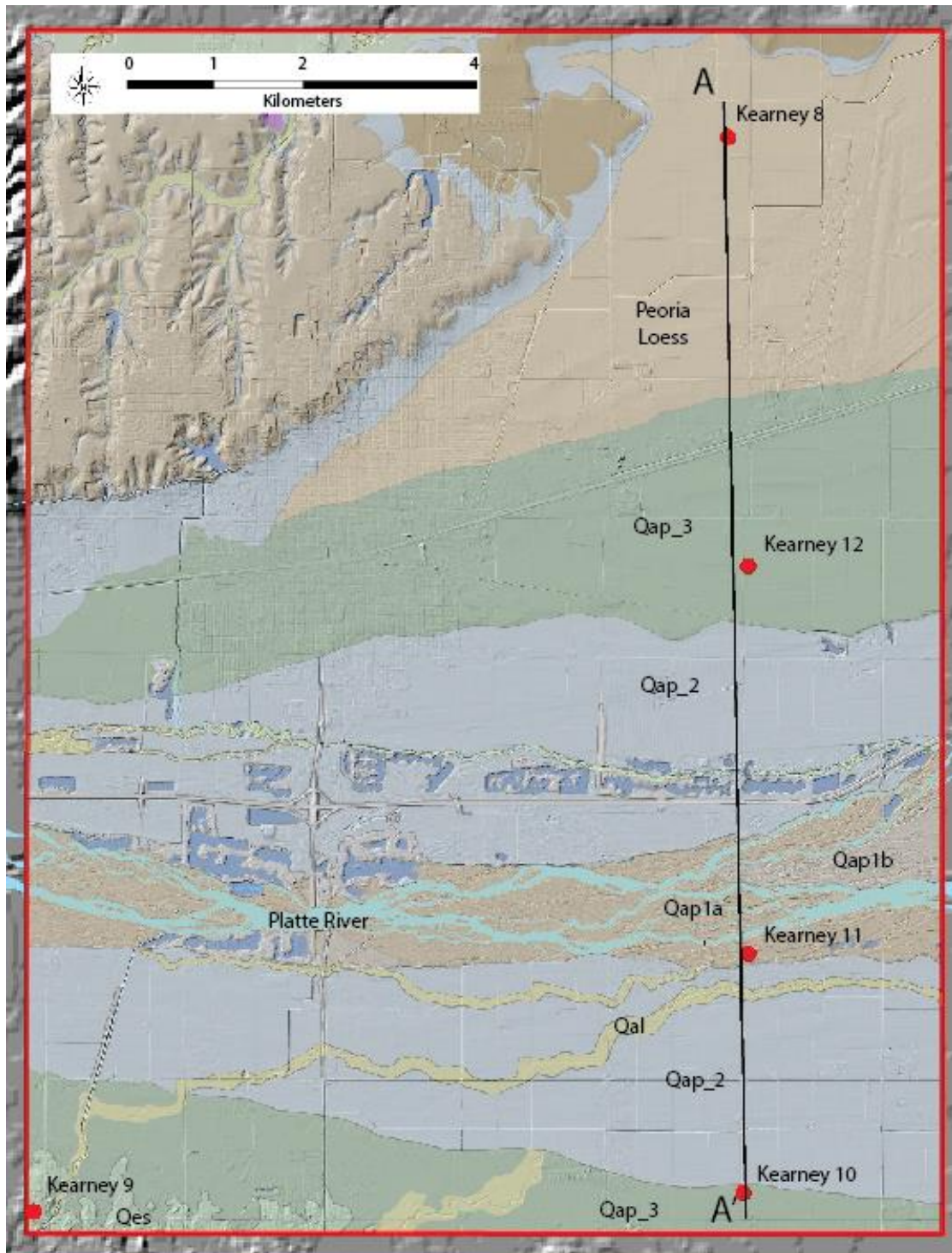
Figure 4.12 Surficial Geology of Kearney 7.5' Quadrangle
Map adapted from Surficial Geology of Kearney 7.5' Quad. Red dots
indicate study boreholes. Landforms generally increase in age and
elevation moving away from the modern Platte River floodplain. Map
adapted from Hanson et al. (2014).

Core	Field #	UNL Lab #	Depth (m)	U (ppm)	Th (ppm)	K_2O (wt %)	In Situ H_2O (%)[a]	Adjusted H_2O (%)[a]	Dose Rate (Gy/ka)	CAM[b] D_e (Gy) ± 1 Std. Err.	Aliquots (n)[c]	OSL Age (Ka) ± 1 σ (Ka)	O.D.[d]
Kearney 9	K 1-1	3811	4.1	0.98	5.53	1.95	4.6	15.0	2.0	2.1 ± 0.2	(43)69	1.1 ± 0.1	46.4
	K 1-3	3813	9.8	0.98	4.83	2.16	14.1	15.0	2.0	28.68 ± 1.1	(43)48	14.3 ± 1.4	25.7
	K 1-5	3815	15.7	0.91	6.77	3.17	13.1	15.0	2.8	64.49 ± 3.2	(40)83	23.3 ± 2.5	29.6
Kearney 10	K 2-1	3816	2.4	0.84	3.78	1.73	12.5	15.0	1.7	20.7 ± 1.2	(43)54	12.1 ± 1.3	37.6
	K 2-2	3817	5.8	0.95	4.60	2.64	11.5	25.0	2.1	20.7 ± 0.9	(46)61	9.5 ± 1.3	30.3
	K 2-4	3819	11.3	0.90	4.68	2.72	11.5	25.0	2.1	106.9 ± 4.9	(46)63	49.9 ± 6.7	28.5
Kearney 11	K 3-1	3820	2.1	2.13	6.25	2.70	10.1	15.0	2.8	20.8 ± 1.0	(50)63	7.5 ± 0.7	32.4
	K 3-3	3822	11.9	0.80	4.16	2.26	11.9	25.0	1.8	66.8 ± 6.6	(43)63	37.0 ± 5.9	55.9
Kearney 12	K 4-1	3823	2.1	1.02	7.98	1.77	2.5	15.0	2.0	23.7 ± 1.6	(42)53	11.6 ± 1.3	43.7
	K 4-3	3825	8.5	0.77	3.83	2.35	13.3	25.0	1.9	33.7 ± 1.4	(54)63	18.2 ± 2.4	30.1
	K 4-5	3827	14.5	0.84	4.36	3.37	8.3	25.0	2.5	75.2 ± 4.5	(43)73	30.2 ± 4.3	37.4

[a]Assumes 50% variability in estimated moisture content

[b]Central Age Model (Galbraith et al., 1999)

[c]Accepted disks/all disks

[d]Overdispersion

Figure 4.13 Table of OSL Results from the Kearney 7.5' Quadrangle

Figure 4.14 Interpretive Geologic Cross-Section of the Kearney 7.5' Quadrangle
Graphic logs and OSL ages of Hershey East cores hanging from an elevation profile (North to South) taken from 2 meter resolution LiDAR data. Dashed lines indicate approximate boundaries between different ages of alluvium. Note presence of Peoria Loess in the North, as well as the relatively young late Pleistocene ages at depth in the alluvial fill.

4.2.1 Kearney 8 Results

The Kearney 8 core drilled on the Qp_t1 surface (Figure 4.1), which sits high on the landscape (Figure 4.14), ~4 – 5 meters above the modern floodplain. The top 7.5 meters of recovered sediment is Peoria Loess, deposited after 23,500 calendar years BP (J. Dillon, personal communication), and likely before 14,000 years (Muhs, 2003). Below 7.5 meters is a 0.5 meter thick package of fine-grained silt, likely alluvial in origin. A radiocarbon age of approximately 23,500 calendar years BP were calculated near the bottom of the core. Below 8 meters of depth, coarse-grained alluvial sand and gravel was recovered. Unfortunately, no OSL ages or particle size data are available for this core.
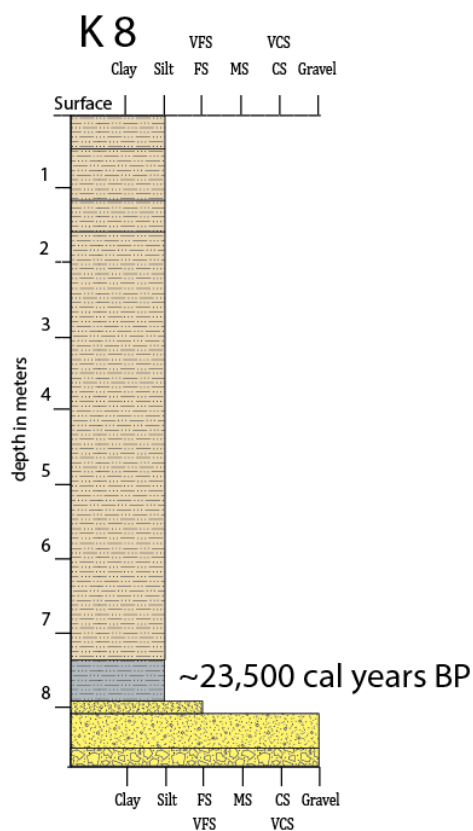
Figure 4.15 Graphic Log for Kearney 8 Core
Radiocarbon age was collected from spruce
needles (Dillon, personal communication).

4.2.2   Kearney 12 Results

Results from particle size analysis of the Kearney 12 core indicate that the first meter of recovered sediment is medium-coarse grained sand with some silt-sized particles present. Thick packages of poorly sorted coarse sands and gravel that are intermittently disrupted by thin packages of finer-grained sediments exist between 1 and 9 meters depth. Some minor coarsening and fining-upward trends appear throughout this depth within the core, but were not apparent in visual description. From 9 to 13.5 meters, a fining upwards sequence is apparent in the particle size graph, with a decreasing percentage of gravel and increasing sand. From 13.5 meters depth to the bottom of the core, recovered sediments show a coarsening-upwards sequence with an increase in gravel and decrease in sand (Figure 4.16)

The Kearney 12 core was drilled into older deposits of Platte River alluvium, Qap3, about 3 km north of the recent alluvium deposited on the modern floodplain (Figure 4.1). Kearney 4-1 (UNL-3823) resulted in an early Holocene age of 11.6 ± 1.3 ka, at a depth of 2.1 meters below the surface. The next OSL sample, Kearney 4-3 (UNL-3825) was taken from a depth of 8.5 meters, and resulted in a late Pleistocene age of 18.2 ± 2.4 ka. The deepest OSL sample from the Kearney 12 core, K 4-5 (UNL-3827) resulted in another late Pleistocene age of 30.2 ± 4.3 ka, at 14.5 meters depth (Figure 4.13). The Holocene-Pleistocene boundary lies somewhere between UNL-3823 and UNL-3825; unfortunately no obvious boundary appears in recovered core sediments and the corresponding particle size analysis data.
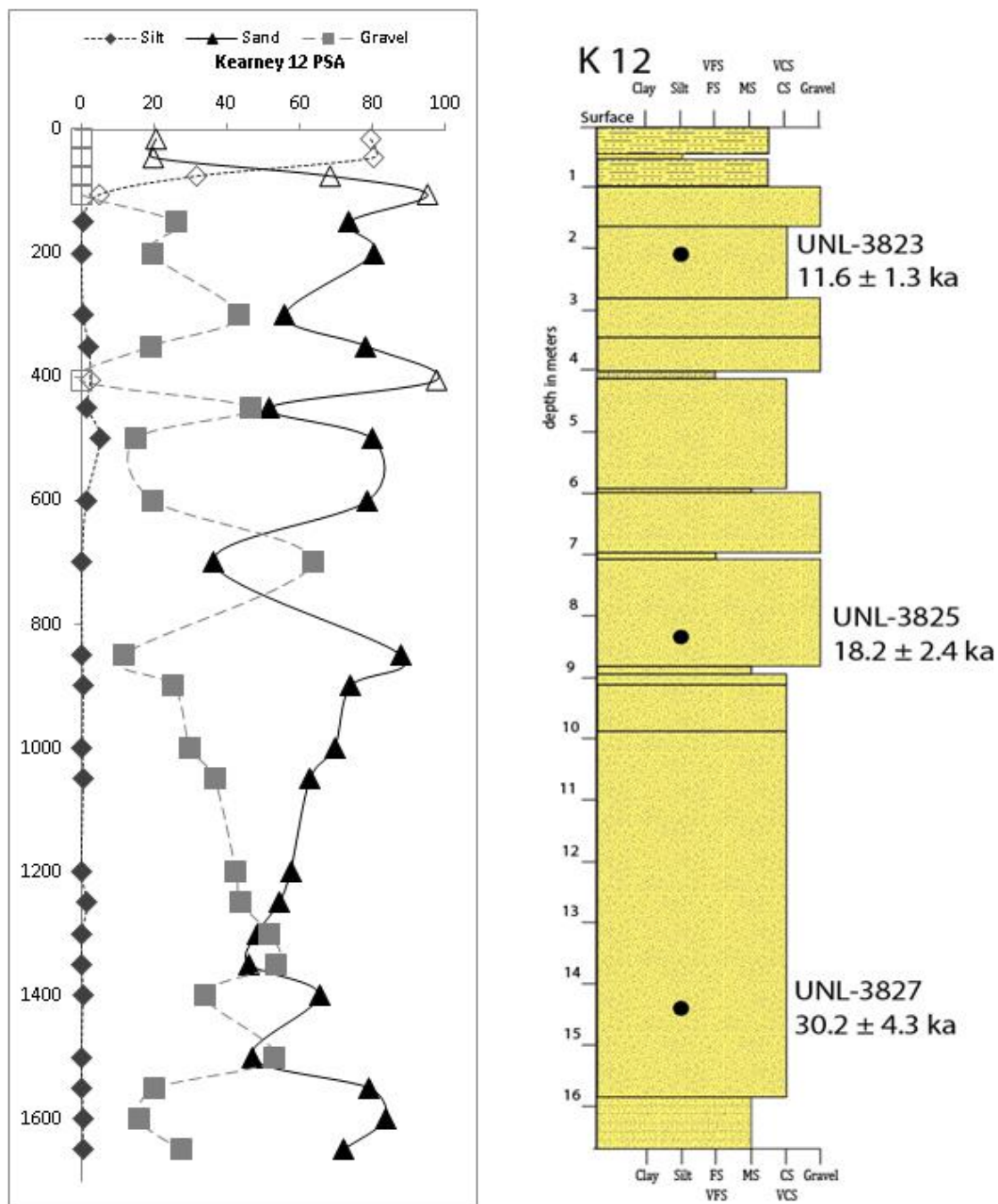
Figure 4.16 Particle Size Analysis and Graphic Log for Kearney 12 Core
In PSA chart, hollow shapes indicate data obtained from laser particle size
analysis; filled shapes indicate data obtained from sieve analysis. Silt is defined
to be < .063 mm, Sand .063 – 2mm, and Gravel is > 2 mm

4.2.3 Kearney 11 results

Results from particle size analysis of the Kearney 11 core indicate that from the surface to 1.5 meters depth, recovered sediments are silts, with a thin package (20 cm thick) of fine-grained sand interbedded between them. From 1.5 to 8.8 meters, recovered sediments consist of poorly sorted coarse sands and gravel. A fining-upwards sequence is apparent in the particle size analysis graph between 6 and 8.8 meters. A thin package (30 cm thick)of medium-grained sand is present from 8.8 to 9.1 meters. The deepest package of sediments recovered in this core, from 9.1 to 12.1 meters, consist of a fining-upwards sequence of poorly sorted coarse sand and gravel, with decreasing gravel content moving upwards in the sequence (Figure 4.17).

The Kearney 11 core was drilled into older alluvium of the Platte River Qap2, which sits 1-2 meters above the modern floodplain (Figures 4.12, 4.14). The first OSL age calculated from this core, Kearney 3-1 (UNL 3820), resulted in a mid-Holocene OSL age of $7.5 \pm .75$ ka at a depth of 2.1 meters below the surface. The second, deeper sample, Kearney 3-3 (UNL-3822), was obtained from a depth of 11.9 meters, and OSL data was used to assign a late Pleistocene age of 37.0 ± 5.9 ka (Figure 4.13). A possible boundary between the Holocene and Pleistocene occurs at 9.1 meters depth, where the fining-upwards sequence is interrupted by a bed of medium-grained sand. However this is not a distinct boundary, as overlying sediments are generally poorly sorted, and 10 meters of alluvium sits between the OSL ages. Further OSL dating in this core would be necessary to more accurately characterize the Holocene-Pleistocene boundary.
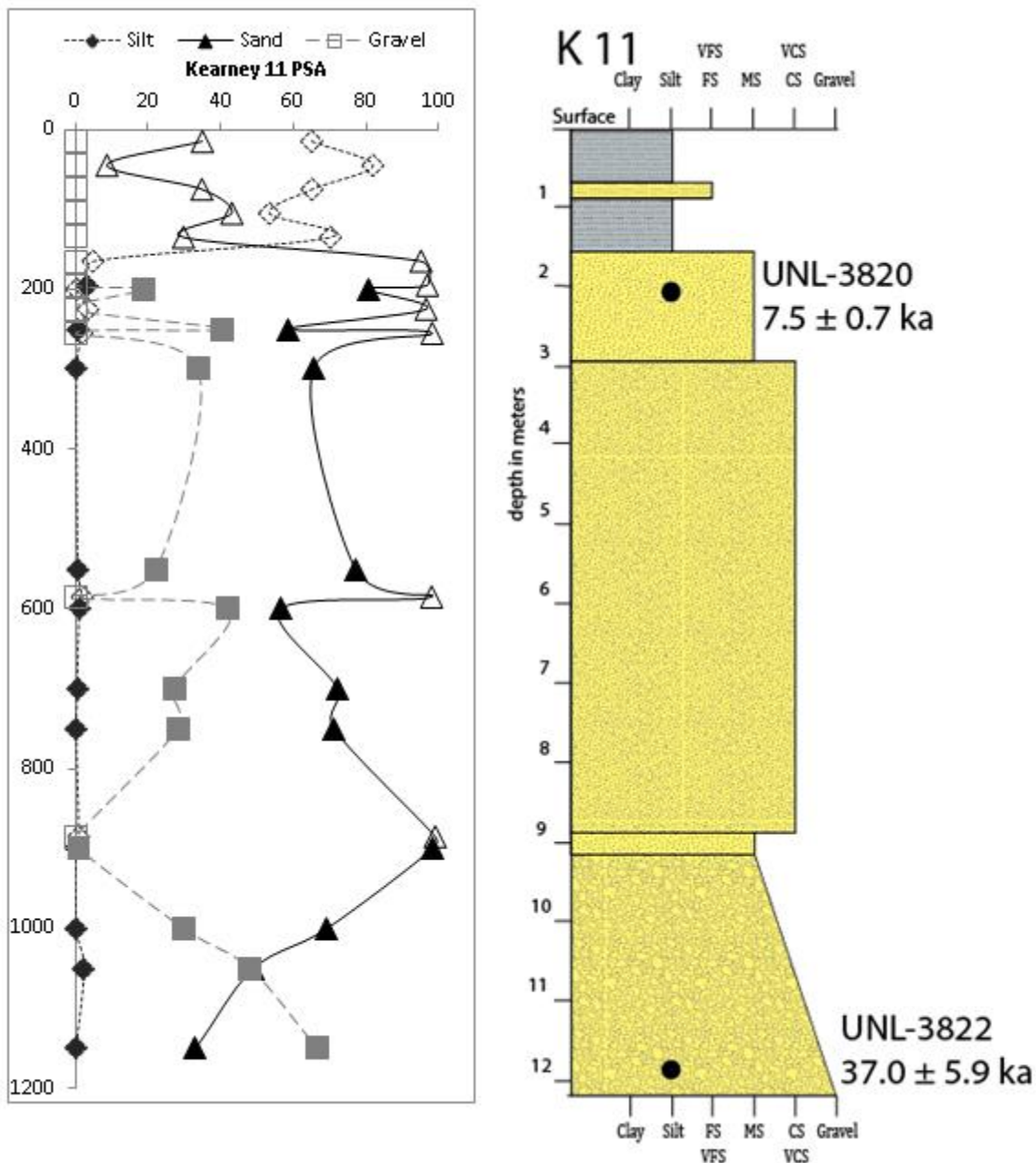
Figure 4.17 Particle Size Analysis and Graphic Log for Kearney 11 Core
In PSA chart, hollow shapes indicate data obtained from laser particle size analysis; filled shapes indicate data obtained from sieve analysis. Silt is defined to be < .063 mm, Sand .063 – 2mm, and Gravel is > 2 mm

4.2.4 Kearney 10 Results

Results from particle size analysis of the Kearney 10 core from the surface to .8 meters depth depict a fining-upwards sequence of silt and fine-grained sand. From .8 to 4 meters, a slight coarsening-upwards sequence of fine to medium-grained sands with some silt is present. Another coarsening-upwards sequence is present from 4 to 6.8 meters, though particle size data is only available at the top and bottom of this package. Between 6.8 and 7 meters, a thin package of medium-grained sand directly overlies a slightly thicker package of coarse-grained sand and gravel from 7 to 7.3 meters. A package of medium to fine sand is present from 7.3 to 10.5 meters; this package is disrupted by one thin (~ 20 cm) package of coarse sand and gravel. From 10.5 to 12 meters, a fining-upwards sequence of gravel and very coarse sand to medium and coarse sand is present. From 12 meters to the bottom of the core, a coarsening-upwards sequence of medium and coarse sand to very coarse sand and gravel exists (Figure 4.18).

The Kearney 10 core was drilled into the Qap3 surface; this is the same unit of older alluvium of the Platte River that Kearney 12 is drilled in, to south of the Platte River (Figure 4.12). OSL ages from the upper two samples from this core resulted in an age inversion. Kearney 2-1 (UNL-3816) resulted in an OSL age of 12.1 ± 1.3 ka at a depth of 2.4 meters; Kearney 2-2 (UNL-3817) resulted in an OSL age of 9.5 ± 1.3 ka at 5.8 meters. These OSL ages fall within the error range of each other, and straddle the age boundary between the late Pleistocene and the Holocene. The deepest sample from the Kearney 10 core resulted in a late Pleistocene age of 49.9 ± 6.7 ka (Table 4.13).
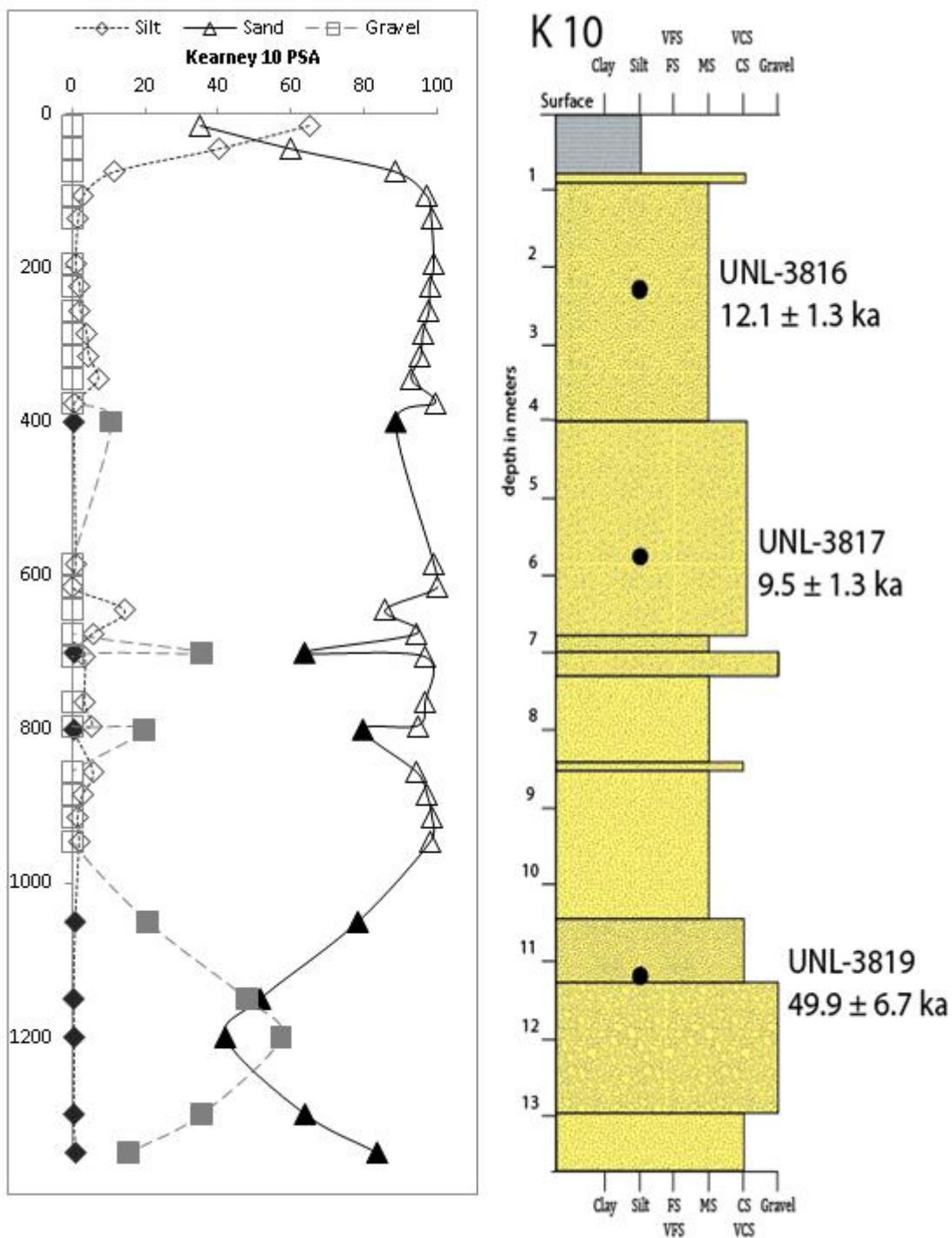
Figure 4.18 Particle Size Analysis and Graphic Log for Kearney 10 Core
In PSA chart, hollow shapes indicate data obtained from laser particle size
analysis; filled shapes indicate data obtained from sieve analysis. Silt is defined
to be < .063 mm, Sand .063 – 2mm, and Gravel is > 2 mm

4.2.5   Kearney 9 Results

Results from particle size analysis of the Kearney 9 core indicate that a package of silt and very fine-grained sand is present from the surface to .8 meters depth. Beneath the silt package, from 1 to 6 meters depth, laminated eolian dune sand is present. Grain size is quite consistent throughout the package; with the approximately 80% of the material being fine or medium-grained sands. Below 6 meters depth, sediments are alluvial in nature. Between 6 and 9 meters depth, sediments are generally coarser, but also have more variation in grain sizes than the overlying eolian sands. From 9 to 13 meters, poorly sorted coarse and very coarse sands and gravel are prevalent with some local interbedded fine-grained sands. Between 13 and 13.7 meters, there is a thick package of very coarse sand and gravel. Between 13.7 and 14.9 meters, a fining-upwards sequence occurs, with a decrease in gravel content and increasingly finer sands. Below 14.9 meters, sediments are poorly sorted coarse sand and gravel; though there is a 10 cm package of medium-grained sand at 17.2 meters depth (Figure 4.19).

The Kearney 9 core is located in the extreme southwest corner of the Kearney quad (Figure 4.1), and was drilled into the eolian sand dunes surface, Qes. The first dated sample, K 1-1 (UNL-3811) was taken at a depth of 4.1 meters, in the eolian sand deposits, and resulted in an age of 1.1 ± 0.1 ka. This is similar to results from other studies of eolian dunes in Nebraska (Miao et al., 2007, Hanson, 2009). The next dated sample, K 1-3, was taken at a depth of 9.8 meters, and resulted in a late Pleistocene age of 14.3 ± 1.4 ka. The deepest sample dated from the Kearney 9 core, K 1-5 (UNL-3815), was taken from a poorly-sorted, coarse-grained sand and gravel deposit at a depth of 15.7 meters. The OSL age was calculated to be another late Pleistocene age of 23.3 ± 2.5 ka (Figure 4.13).
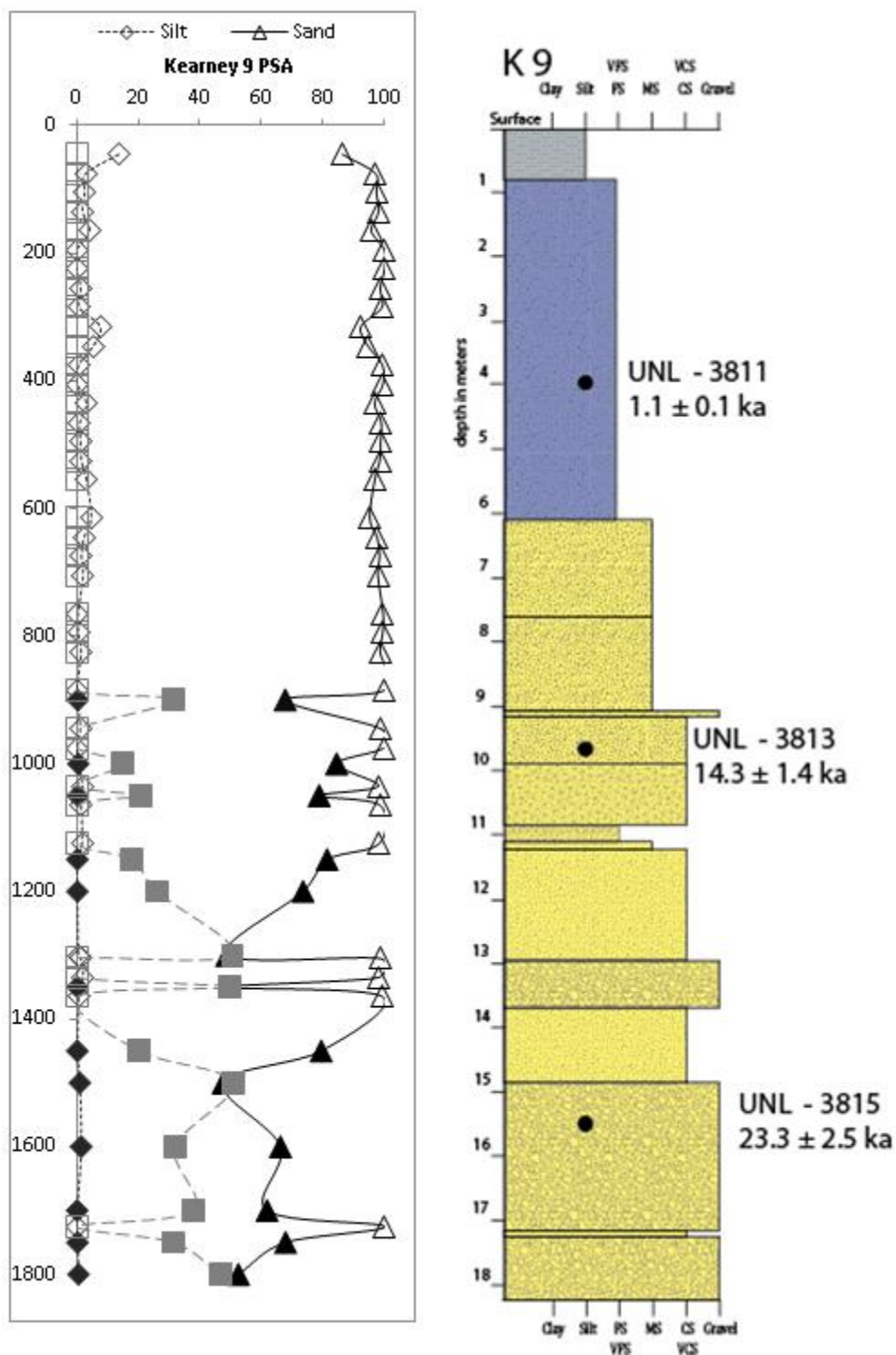
Figure 4.19 Particle Size Analysis and Graphic Log for Kearney 9 Core
In PSA chart, hollow shapes indicate data obtained from laser particle size
analysis; filled shapes indicate data obtained from sieve analysis. Silt is defined
to be < .063 mm, Sand .063 – 2mm, and Gravel is > 2 mm

OSL ages calculated from samples taken from sediment cores drilled in the Kearney quadrangle recovered approximately 50,000 years of geologic history. In general, sediments deposited at this study site are significantly younger, and the thickness of the Pleistocene alluvial fill is too great to recover very old samples using the Geoprobe® coring techniques employed in this study. A total of 11 OSL samples resulted in five datable late Pleistocene ages, five Holocene ages, and one young eolian age. In addition, one radiocarbon age of 23,400 years was recovered from alluvium buried beneath Peoria Loess.

While these OSL ages are not perfect, they allow us to approximate general ballpark age estimates for the alluvial fills encountered in the study areas. All samples were run as 2 mm aliquots, with accuracy approaching that of single-grain techniques. Over dispersion values for dated samples were generally higher than those from the Hershey East quad and ranged from the high 20's to the mid-40's, with an outlier of 55.9 (Figure 4.13).

Results from this study led to the differentiation of three major alluvial fills in the Platte River Valley, with the additional presence of loess and eolian dune sand deposits forming the valley walls at the Kearney study area. OSL ages from the deepest dated samples all resulted in late Pleistocene ages. Overlying the late Pleistocene sediments is a younger, Holocene aged alluvium, 8-10 meters thick. The Holocene alluvium has been modified by the modern alluvium, with an approximate thickness of 3 meters.

Ages from the deepest OSL samples recovered from each core resulted in late Pleistocene ages between 18 and 50 ka. The late Pleistocene-aged sediments are a minimum of 10 meters thick, and it is likely that the entirety of the Pleistocene fill is considerably thicker than the recovered sediments indicate.

OSL data suggest that the top of the Pleistocene-aged surface is approximately 635 ± 4 meters above current sea level. The estimated range accounts for paleotopography that may exist, uncertainty about the elevation of the boundary, and gaps between OSL ages. While the Pleistocene-Holocene boundary is drawn as a relatively smooth line, there is certainly some

variation in the elevation of the boundary, depending on where the ancestral Platte River eroded and deposited sediments in the late Pleistocene. It is a distinct possibility is that the alluvium underlying the Peoria Loess in the Kearney area is unrelated to the Platte River system. That material may have been deposited by the ancestral Wood River, but inconclusive evidence prevents interpretations about the origins of this alluvium.

OSL ages from the Holocene alluvial fill did not show the vast differences in age between Holocene-aged sediments and the underlying Pleistocene alluvial fill that was found at the Hershey East location. Four Holocene ages from this fill ranged from 7 to 12 ka, and accounting for the error range all samples could fall within the Holocene. One possible exception is an age of 12.1 ± 1.3 ka, which could be very late Pleistocene, but could also fall in the Holocene using the associated error range. A few ages in this fill were stratigraphically inverted, but the overall trend in the OSL ages indicate that the majority of the alluvium was deposited in the Holocene. The recovered core sediments resulting in Holocene-aged sediments range in thickness from 8 to 10 ± 4 meters at the base to account for any underlying paleotopography on the Pleistocene surface. The Holocene-aged fill is considerably thicker where it is not overlain by modern alluvial sediments; the modern rivers have likely eroded a significant volume of sediment from the undifferentiated Holocene fill. On average, the undifferentiated Holocene alluvial fill is approximately 7 meters thick in areas undisturbed by modern erosion and deposition.

The modern alluvial fill of the Platte River is considerably thinner than both the Holocene and Pleistocene alluvial fills. While no ages were recovered from the modern surface, one age of 7.5 ± 0.7 ka was calculated from a sample in the slightly older alluvium, at a depth of two meters. Using that age, modern alluvial fills are interpreted as being roughly consistent in thickness with modern alluvial fills found in the Hershey East quad, approximately 3 ± 2 meters depth, with the error range accounting for variations in topography on the Holocene surface.

4.3 Accuracy of OSL Dating Results
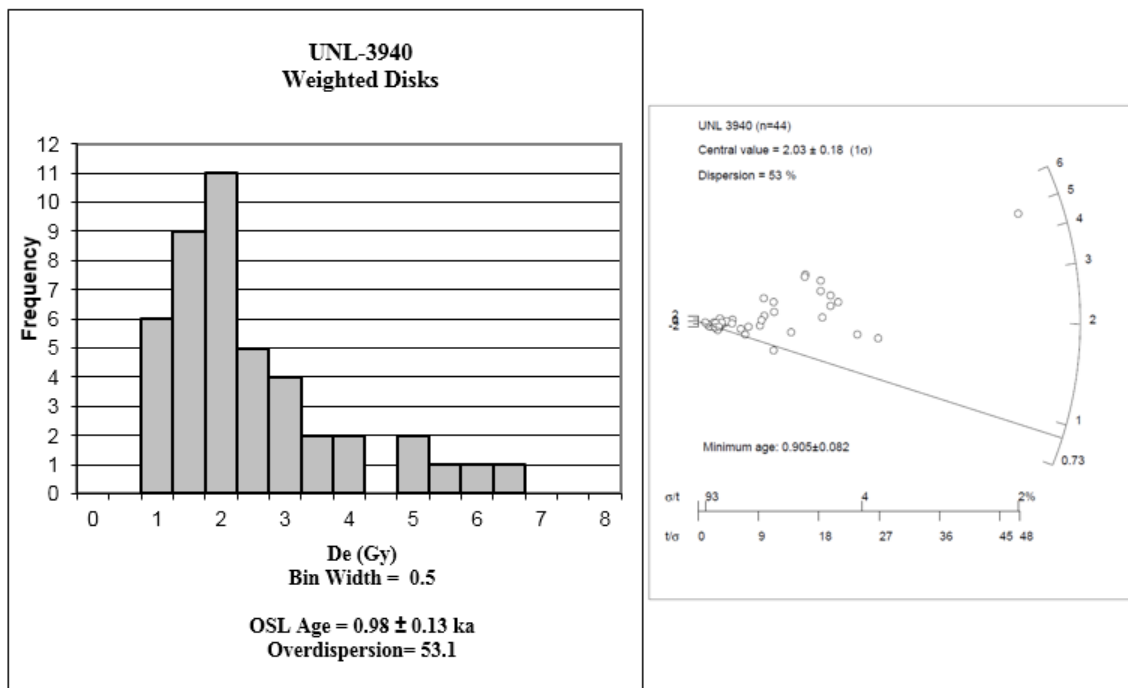
Figure 4.20 Histogram and Radial Plot of D_e Values for a young OSL sample

Figure 4.20 shows an example of a relatively young sample taken from 3 meters depth below the modern floodplain of the North Platte River. D_e values are graphed in a histogram and radial plot. Histograms for the majority of 'young' samples, with OSL ages younger than approximately 5 ka, show similar characteristics. In this case, the histogram is asymmetric with a significant tail which can be indicative of partial bleaching. The majority of the D_e values fall between 1 and 2 Gy, with larger D_e values in the tail extending to 6.5 Gy. In this example, the D_e values are relatively low, but the spread given the population size is relatively large, indicating overdispersion in this sample. This sample resulted in a relatively young age of approximately 1000 years.
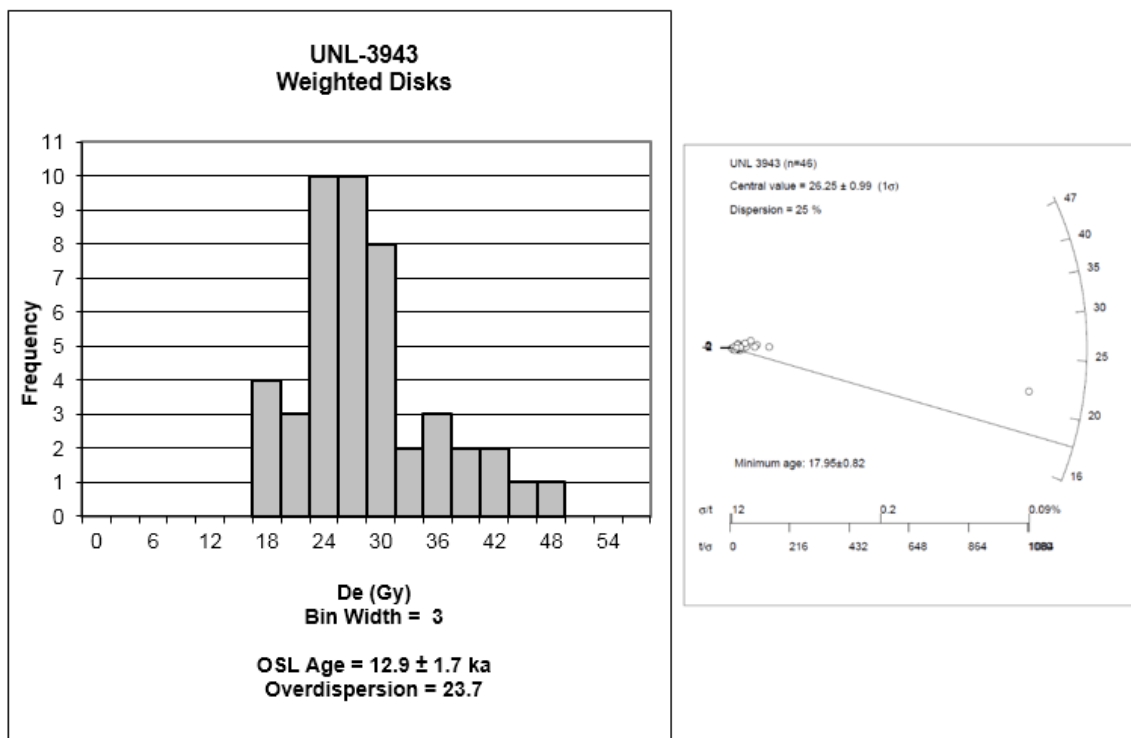
Figure 4.21 Histogram and Radial Plot of D_e values for a Holocene OSL sample

Figure 4.21 is an example of a sample with an age of approximately 12,900 years, roughly the very latest Pleistocene. For this sample and others like it, errors associated with both age and overdispersion values are typically quite low. This sample shows slight asymmetry in the histogram, possibly indicating partial bleaching and that a remnant luminescence signal may have been present prior to burial. Though problems with partial bleaching are present (and are rarely non-existent), they become less of an issue as samples increase in age. Due to the accumulation of luminescence signal over time, the effects of a luminescence signal not fully zeroed prior to deposition are diminished. The majority of D_e values in this example are centered between 24 to 30 Gy, with a tail extending to 48 Gy. In this example, the D_e values are high, but the spread compared to the population size is relatively small, resulting in a lower overdispersion value than commonly seen in younger sediments (Figure 4.20).
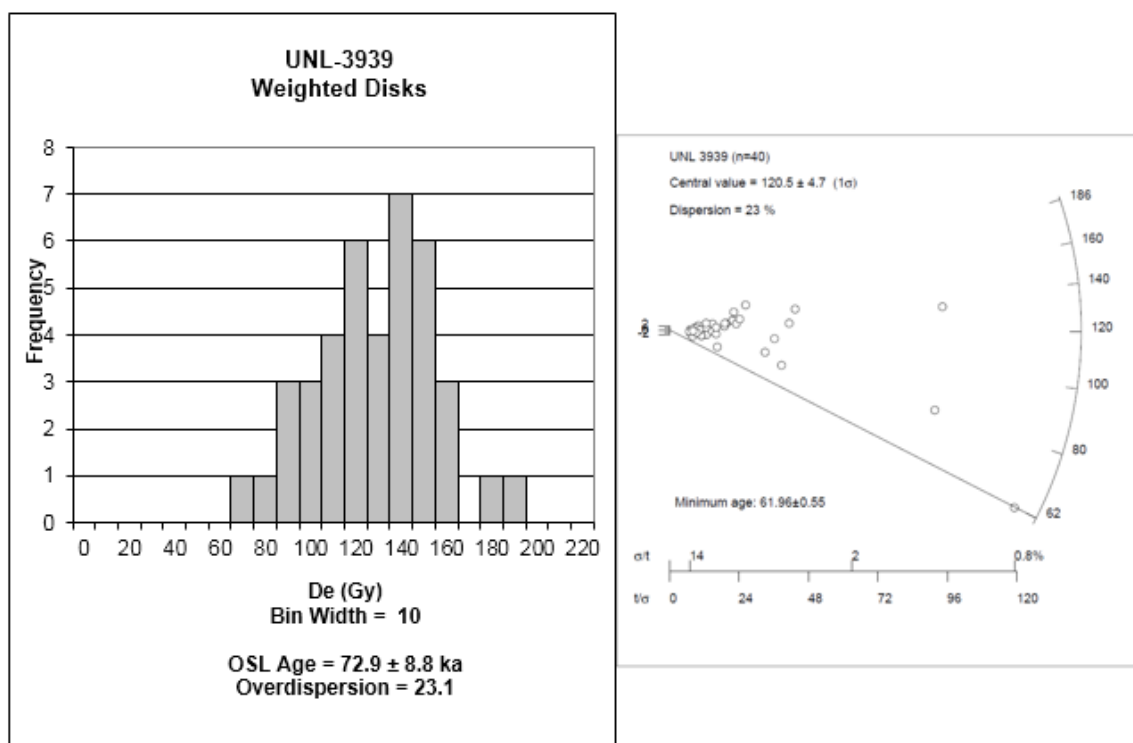
**Figure 4.22 Histogram and Radial Plot of D_e values for a late Pleistocene
OSL sample**

Figure 5.3 is an example of a relatively old sample taken from 10.3 meters depth, with a

late Pleistocene aged of approximately 72,900 ± 8,800 years. The majority of 'old' OSL samples

with ages greater than approximately 25 ka show similar characteristics. These older sediments

typically exhibit greater errors as the OSL age increases, but overdispersion values generally

remain low. Partial bleaching problems decrease with age, as the luminescence signal has built

up significantly more than that of a younger sample, limiting the observed effects of remnant

luminescence signals. The histogram in this example shows relative symmetry; the lack of a tail

suggests that partial bleaching is not a major issue.   D_e values of older samples tend to be more

variable due to the increasing uncertainty that occurs with older samples. Though the D_e values

are high in this example, the spread compared to the population size is quite small, resulting in

relatively low overdispersion values.
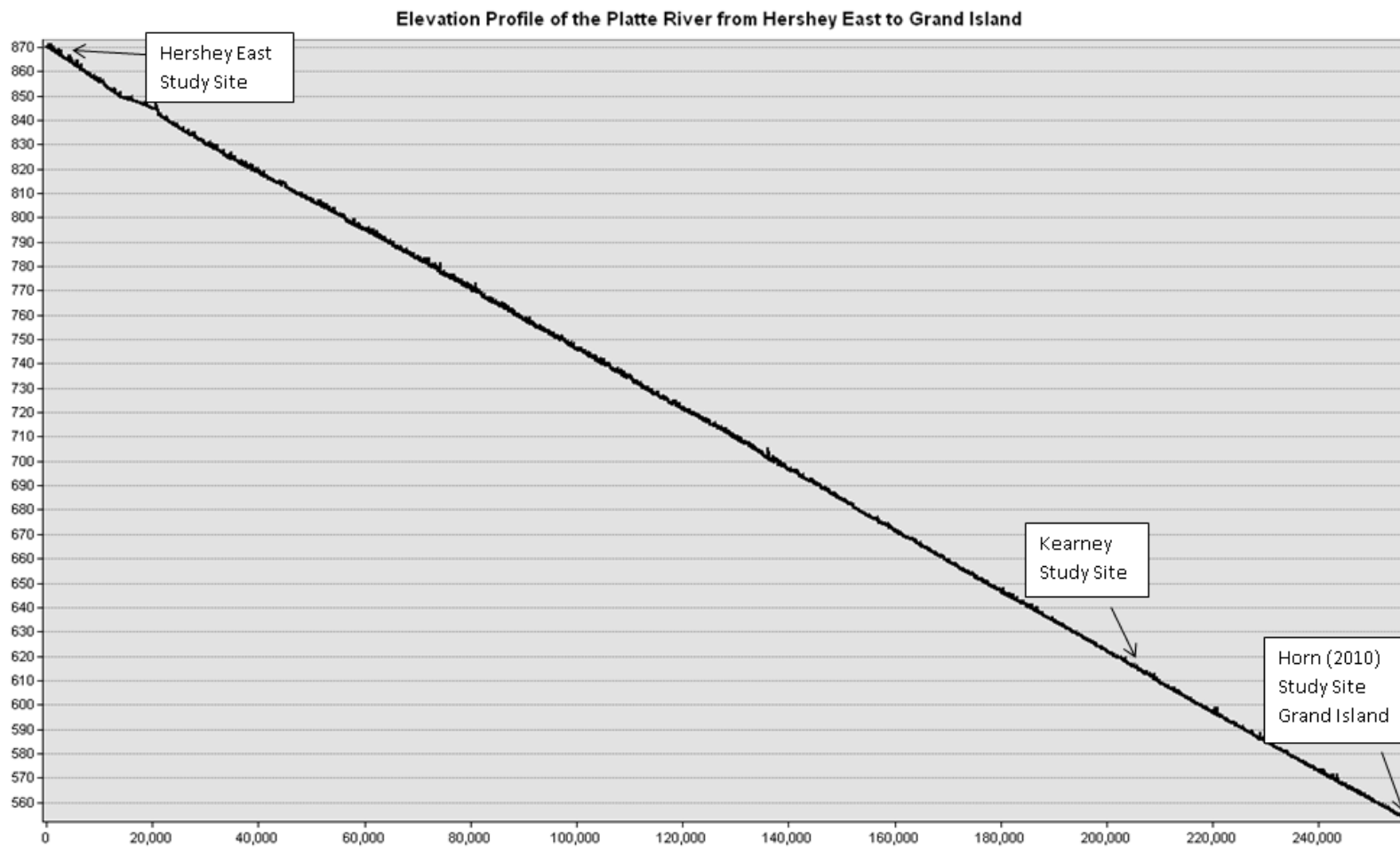
Figure 4.23 Elevation Profile of the Platte River from Hershey East to Grand Island
Note that the elevation profile is essentially straight; there is very little concavity observed.
Average gradient is 1.25 meters per kilometer

5 Discussion

The results of this study suggest that there were periods of aggradation related to climate change associated with glacial and interglacial episodes. This interpretation is made regarding the nature of the alluvial fills present in the modern Platte River Valley based on their ages and thicknesses, as well as topographic and stratigraphic relationships. The reliability of OSL ages from the Hershey East and Kearney quadrangles will be discussed prior to discussing a broader understanding of nature of the alluvial fills in the Platte River Valley. The distance between study areas allows for observations of changing river dynamics of the Platte River moving downstream. It is important to note that the Platte River alluvial history is quite complex, and results from this study and others are limited by relatively low-resolution data.

5.1 Discussion of Accuracy of OSL Dating

OSL results from this study are quite adequate, but single – grain techniques could improve dating accuracy, especially in very young and relatively old samples. The 2 mm mask used in this study is efficient and provides relatively accurate ages in significantly less time than single – grain techniques. However, the improved statistics associated with single – grain techniques could decrease errors associated with partial bleaching and over-dispersion by allowing for the identification of individually luminescing quartz sand grains.

OSL dating techniques work best on eolian sediments where grains have adequate exposure to sunlight at the time of deposition (Duller 2004; Olley et al. 1998, Rhodes 2011). In contrast, alluvial samples, particularly those younger than approximately 5 ka (Figure 4.20), and older than approximately 50 ka (Figure 4.23) often have some problems resulting from incomplete sunlight exposure prior to burial, and high over dispersion values can be used to evaluate the extent of this potential problem (Rittenour 2008, Rodnight 2006). Overdispersion

(OD) is the spread in D_e values for the aliquots analyzed for a given sample (Rodnight 2006, Galbraith et al., 1999).

Overdispersion values in this study ranged from low 20's to mid-40's, with two outliers in the low 50's (Figure 4.4, 4.13). These values indicate that there are issues with partial bleaching in certain samples. For example, UNL-3940 (Figure 4.20), a relatively young sample from the modern floodplain, with an age of 0.9 ± 0.1 ka has a high OD value of 53.1 (Figure 4.4). High OD values from relatively young samples typically indicate that partial bleaching may be an issue, presenting the possibility of age over-estimation. Another example, UNL-3943 (Figure 4.21), is a late-Pleistocene or early Holocene sample with an age of 12.9 ± 1.7 ka has an OD value of 23.7 (Figure 4.4), indicating that partial bleaching is not likely a major issue with this sample. A final example, UNL-3939 (Figure 4.22) is a late-Pleistocene sample with an age of 72.9 ± 8.8 ka. The overdispersion value for this sample is 23.1 (Figure 4.4), again indicating that partial bleaching is not likely to be a factor for this sample.

Error ranges for samples with ages falling between approximately 5 to 25 ka are typically low, usually between 5 to 10% of the total age (Figure 4.4, and 4.13). Samples with calculated ages older than approximately 25 ka are generally associated with increasing error ranges typically between 15 to 20% of the calculated age (Figure 4.4, and 4.13). A contributing factor is that older samples are generally found deeper below the ground surface, where water contents are expected to be higher than water contents at shallower depth. The increase in water content results in increasing error range for the age of the sample. However, these error ranges remain accurate enough to determine a general age for an alluvial deposit, especially with multiple samples resulting in similar ages from one deposit. OSL samples resulting in ages too old to calculate are caused by at least a portion of the grains on an aliquot having saturated OSL traps. In these cases, only minimum OSL ages can be calculated. The ages are calculated using the maximum D_e the quartz grains were exposed to in the lab, 200 Gy. Further attempts to date

quartz grains with saturated OSL traps using traditional OSL dating methods are unlikely to provide any further information about the age of the sediment in question.

5.2 Alluvial fills of the Platte River Valley

5.2.1 Late Pleistocene aged alluvial fills at Hershey East and Kearney

The thickness and relative age of the Platte River alluvial fill varies widely between the Hershey East and Kearney study areas. Significant differences are observed in the relative age and thickness of the late Pleistocene alluvial fills at each location. Ages of the late Pleistocene material in the Hershey East study area range from 55 ka to a maximum age greater than 133 ka. Late Pleistocene alluvium at Kearney resulted in ages ranging from a 19 ka to only 50 ka, with no ages too old to calculate using OSL. Unfortunately, without any saturated OSL samples, it is apparent that the recovered core does not contain any of the oldest alluvium that is likely present deeper in the alluvial fill at the Kearney study area.

The dated thickness of the late Pleistocene alluvium at Hershey East is interpreted to be less than 8 meters thick in most areas. In other areas, this unit appears to be only ~4 – 5 meters thick, buried beneath deposits of what is interpreted to be modern alluvium (Figure 5.1). At the Kearney site, the full thickness of late Pleistocene material is unknown, so depth interpretations are considered minimum depths. The dated late Pleistocene alluvium is interpreted to be more than 15 meters thick, though other areas may possibly be less thick, with approximately 8 – 10 + meters of sediment. Unfortunately, the OSL sampling density used does not allow for high resolution dating to better approximate the Pleistocene – Holocene boundary (Figure 5.2).

While the total thickness of the late Pleistocene alluvium was not recovered at either location, OSL ages allow for interpretations to be made about the depth and nature of the fill at both locations. Much older late Pleistocene sediments were recovered from the Hershey East

study area, at a relatively shallow depth in the subsurface. Late Pleistocene aged sediments from the Kearney alluvial fill resulted in younger ages than were seen at Hershey East, from sediments buried much deeper in the subsurface. This leads to the interpretation that the late Pleistocene alluvial fill at Kearney is thicker and younger than the late Pleistocene alluvial fill at Hershey East. While each of the study sites has relatively thick accumulations of late Pleistocene sediment, the Kearney alluvial fill is relatively younger and more than twice the thickness than that which was recovered at the Hershey East site. It is apparent that there was significant aggradation occurring in the Platte River Valley during the late Pleistocene, at both sites, though much more aggradation is seen at Kearney than at Hershey East.

5.2.2   Holocene aged alluvial fills at Hershey East and Kearney

The Holocene aged fills at Hershey East and Kearney study areas show significant differences in thickness, however the resulting ages are quite similar. At the Hershey East study area, the Holocene fills generally range in thickness from approximately 4 to 7 meters. There is some variation in this thickness in the subsurface, interpreted to be due to the entrenchment of the modern alluvial deposits of the North and South Platte River. Most Holocene OSL ages from Hershey East are early to middle Holocene, and range from 8 to 11.9 ka. At the Kearney study site, the Holocene alluvial deposit is slightly younger, ranging in age from 7.5 to 11.6 ka, with a thickness of approximately 8 to 12 meters (Figure 5.1, 5.2). Age inversions are observed at both locations, but each age falls within the 1 σ error range of the other.

Holocene sediments at both study areas are interpreted to be the result of aggradation occurring approximately during the transition from the late Pleistocene to the Holocene. With the exception of what is interpreted to be modern alluvium, no young Holocene ages were calculated, possibly due to a sampling bias towards older, deeper samples, resulting in the calculation of fewer samples from the shallow subsurface. It is likely that discharge rates through the Platte

increased following the transition from the relatively cold and dry glacial period to the relatively warm and wet interglacial period. This is interpreted to have caused a decrease in rates of aggradation. In the middle to late Holocene, the Platte River is interpreted to have been approximately at equilibrium, and possibly eroding a small amount of sediment out of the older Holocene alluvial fill.

5.2.3   Modern Alluvial Fills at Hershey East and Kearney

Two ages were calculated for alluvial fills that are interpreted to be relatively modern in age, less than 2 ka. These fills are thought to be slightly entrenched into the Holocene alluvium, to a depth of approximately 3 meters below the surface. Only two OSL ages were calculated for these modern fills, both of which are observed near the North Platte River floodplain in the Hershey East Quadrangle. At Hershey East, the boundary between the much younger, modern Holocene sediments and the relatively old late Pleistocene sediments is quite abrupt. The age difference between modern and late Pleistocene sediment indicates the presence of an erosional disconformity. These ages transition from sediment older than the dating capabilities of blue light OSL, to modern ages of less than 2 ka, within only a few meters of sediment. These disconformities support the interpretation that aggradation decreased sometime following the late Pleistocene – Holocene transition, and some amount of entrenchment of the modern North Platte River must have occurred (Figure 5.1).

At Kearney, the transition from late Pleistocene to Holocene aged sediments is much more gradual, with no obvious disconformities present. Unfortunately, no OSL ages were calculated from the modern alluvial fill of the Platte River at Kearney (Figure 5.2). However, the approximate entrenchment depth of the modern fill is interpreted to be roughly equivalent to that at Hershey East, with approximately 3 meters of sediment deposited in place of sediment deposited during the late Pleistocene – Holocene transition.

5.2.4   Comparison of Hershey East and Kearney to Grand Island - Doniphan

Results from Horn's (2010) study at Grand Island – Doniphan (GI-D) showed results similar to findings from the Hershey East study site, with three late Pleistocene ages too old to calculate and an oldest age greater than 78,000 years (Figure 5.3), at depths as shallow as 6 meters below the surface. This supports the interpretation that during the late Pleistocene, significant aggradation was occurring throughout the Platte River.

However, Holocene ages calculated from samples at the GI-D study area are relatively young in comparison to those at Hershey East and Kearney. Most ages were calculated to be late Holocene ages of 5 ka or younger, without any ages in the 5 – 12 ka range. The overall thickness of Holocene-aged alluvium in Horn (2010) study is minimal, ranging between 2 to 4 meters maximum thickness. This indicates that there may have been significantly different amounts of sediment being deposited in the river system at different locations. There are a few possible explanations for this lack of early Holocene alluvium observed at GI-D. It is possible that the area did not receive nearly as much sediment during the early Holocene as Hershey East and Kearney did, or sediment moving downstream did not reach GI-D. Conversely, it is also possible that some early to middle Holocene sediment may have been deposited, but has since been eroded prior to the deposition of the late Holocene alluvium. Additionally, sand sourced from the Nebraska Sand Hills dammed the Platte River system near the Hershey East study area during the late Pleistocene (Muhs et al. 2000). This event contributed an unknown volume of sediment to the river system, and may be a factor in the extensive aggradation encountered at the Kearney study area.

Significant entrenchment of the Platte River is observed at the Grand Island - Doniphan site that is not observed to such an extent at either the Hershey East or Kearney locations. In the GI-D study area, sediments of modern age were recovered 8 meters lower topographically than late Pleistocene sediments (Figure 5.3). The GI0805 core was drilled into the Qap3 alluvium, defined as a Pleistocene-aged alluvium on the north side of the modern Platte River (Horn 2010).

Samples from this core were dated to be late Pleistocene in age, ranging from 15 ka near the surface to ages of approximately 60 ka at depths of 3.5 and 7 meters. The lower surface, Qap1nc4, sits approximately 8 meters lower than the Qap3 surface, resulted in ages of 1 ka at a depth of 1 meter, and late Pleistocene ages of 13 and greater than 68 ka at depths of 6 and 10 meters, respectively. The modern Platte River channel sits approximately 12 km to the south, and 4 meters above the entrenched Qap1nc4 surface (Figure 5.3).

The modern alluvial fills at both Hershey East and Kearney are thought to be generally similar to the modern alluvial fill at Grand Island-Doniphan. The modern fills of the present Platte River appear to be entrenched between 3-4 meters into the underlying alluvium, with some possible variation due to underlying paleotopography. OSL ages from the modern alluvial fill at the Hershey East and Kearney Study sites range from 0.9 to 2 ka, which are slightly younger than modern ages of approximately 5 ka in the GI – D study area (Horn 2010).

Paleotopography that may exist in the underlying alluvial fills of the Platte River Valley are thought to be highly variable, and relatively poorly understood, due to the relatively low resolution of the study. While OSL ages from this study and Horn (2012) provide some approximate paleosurface elevation estimations, the reality is that these elevations are based on 15 boreholes at 3 study sites. Each borehole is separated by a minimum of 1 km; given the highly variable nature of braided river systems, there are likely unobserved differences in the alluvial fills between boreholes at each study site.
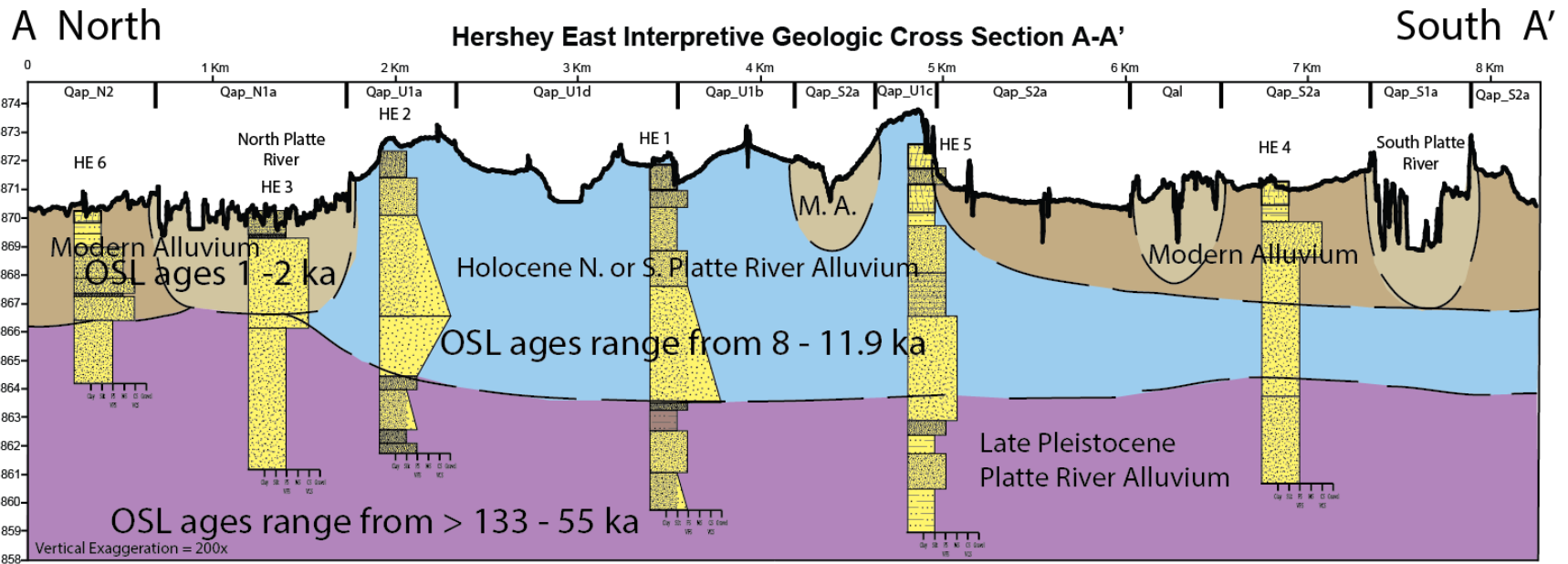
Figure 5.1 Interpretive Geologic Cross-Section of the Hershey East 7.5' Quadrangle
Note old age, depth, and thickness of late Pleistocene sediments (purple). Late Holocene alluvium (blue) is relatively thick with modern floodplain deposits beneath the North and South Platte Rivers. Erosional disconformities are present between the modern/recently abandoned floodplain sediments (tan/brown) and the late Pleistocene alluvial fill, see cores HE 3 and HE 6.
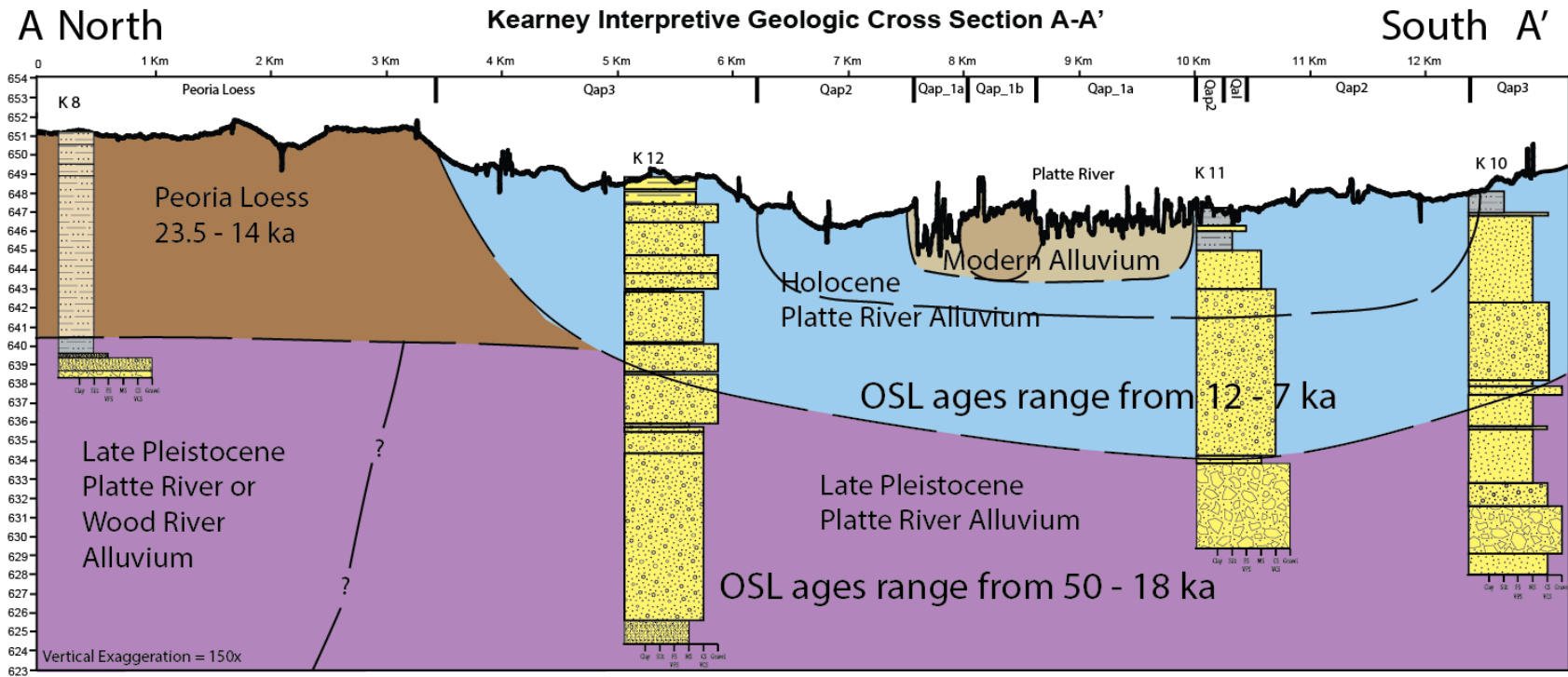
Figure 5.2 Interpretive Geologic Cross-Section of the Kearney 7.5' Quadrangle
Note young age and thickness of late Pleistocene sediments (purple). Alluvium north of dashed line (-?-?-) was deposited by either the ancestral Platte River or Wood River sometime before 23,300 cal years BP. Peoria Loess (dark brown) was deposited in northern part of cross-section between 23,500 and 14,000 cal years BP. Late Holocene aged sediments (blue) are relatively thick and are interpreted to have a nested stacking pattern. The north – south migration of the Platte is interpreted to have ended following the deposition of Peoria Loess. The Modern Alluvium (tan/brown) is interpreted to be entrenched 3 – 4 meters and be younger than ~ 1 – 2 ka
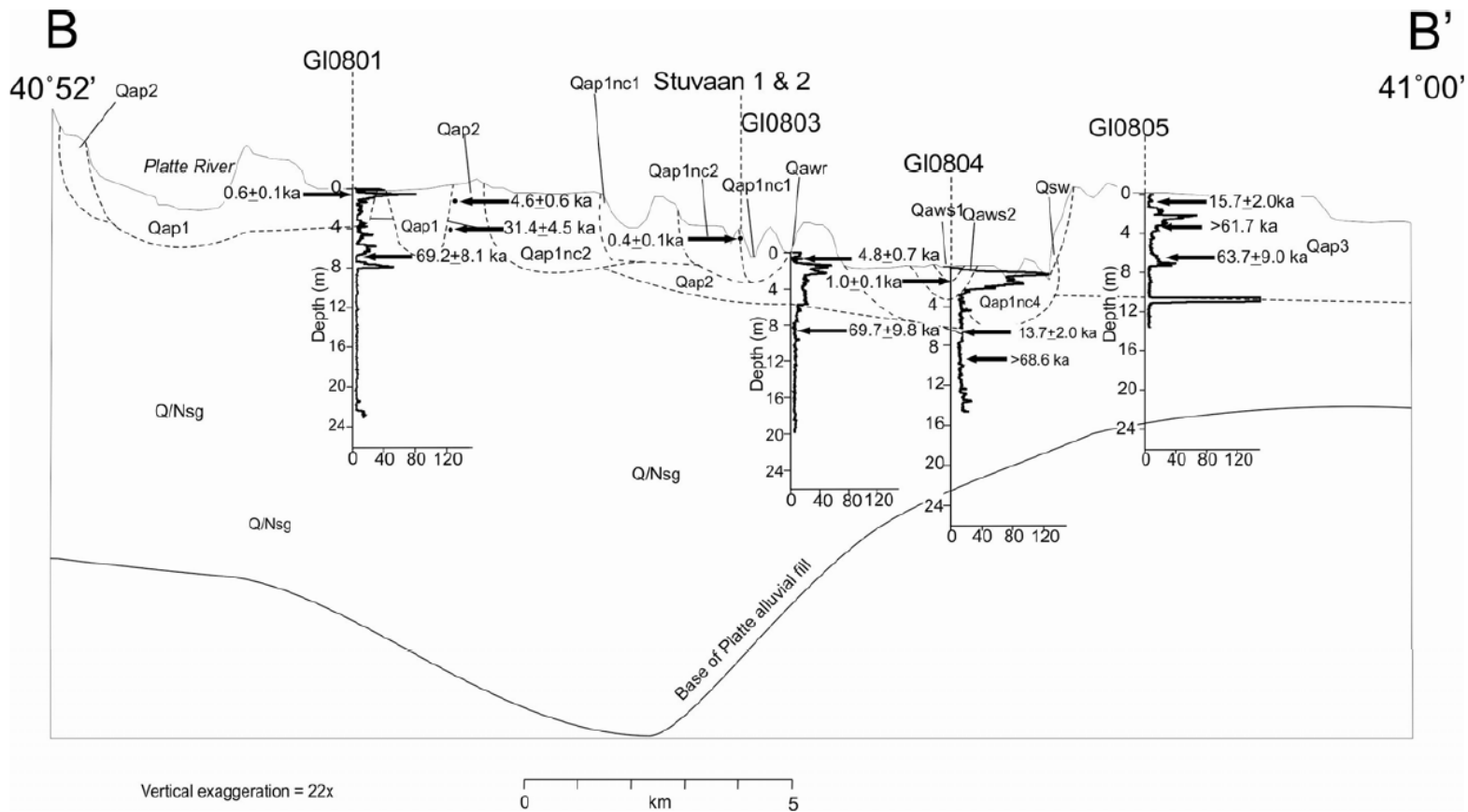
Figure 5.3 Interpretive Geologic Cross-Section near Grand Island, Nebraska
Note the significant entrenchment of the Platte River near GI0804. Late Pleistocene alluvial fill is very thick, with OSL ages too old to calculate at approximately 7 meters depth. Holocene alluvium is significantly less thick and much younger than that at Hershey East and Kearney; no early Holocene aged sediment is present. B is South, B' is North (Horn, 2010)

6 Conclusions and Future Work

The alluvial fills of the Platte River system vary considerably with location. Evidence from this study and from Horn (2010) indicate that all study sites in the Platte River system appear to have experienced periods of significant aggradation during the late Pleistocene and early Holocene. This aggradation was likely caused by large sediment loads in the late Pleistocene due to changes in sediment supply and discharge caused by climate change (Dethier 2001). Alpine glaciation may have caused changes to the flow regime through the Platte and its tributaries, as well as changes in sediment flux from hillslopes. Additionally, a significant amount of quartz sand may have entered the Platte River system in the late Pleistocene due to the eolian dunes of the Nebraska Sand Hills that may have dammed or partially dammed the Platte River (Muhs et al. 2000). More importantly, discharge through the Platte River System was likely much more variable than is currently observed in the modern Platte River system. During the late Pleistocene, evidence such as eolian activity in the Nebraska Sand Hills, eolian sand dune damming of the North and South Platte Rivers, and loess deposition suggest that the regional climate was cold and dry. This cold, dry climate may have resulted in much different snowmelt patterns, and highly variable discharge through the Platte River system than are observed today. Discharge through the Platte River was likely highly variable through different periods of the Quaternary, with short periods of extremely high discharge and longer periods with reduced discharge. The Platte River system in the late Pleistocene likely had more sediment in the system than the discharge could transport, leading to the aggradation observed in the late Pleistocene fills at both the Hershey East and Kearney study sites, as well as at GI-D (Horn 2010).

The alluvial fill at the Kearney study site is significantly thicker and younger than was observed at both the Hershey East site and Grand Island – Doniphan. There are a few potential reasons for this, the most probable being that the deposition of Peoria Loess inhibited lateral migration. This deposit would have decreased the area in which the alluvium could have been

deposited, resulting in a thicker than average late Pleistocene aged deposit. This may have caused a change in river dynamics similar to findings by Fotherby (2009), in which the planform migration pattern is limited, resulting in a narrower channel belt. However, the loess deposition model cannot account for the relatively young age of late Pleistocene sediments from below the base of the Peoria Loess in the alluvial fill, nor the abnormal thickness and young age of the deposit. Another possibility is that the gradient of the river was shallower at the Kearney study site during the Holocene; however, support for this is not found in the modern profile of the Platte River (Figure 4.23).

Hershey East and Kearney also show significantly greater volumes of Holocene aged alluvium than is observed at the Grand Island-Doniphan study area. The Holocene alluvial fill from Horn (2010) is quite thin and young, generally less than 5ka (Figure 5.3). Aggradation likely ended around the transition from late Pleistocene to the early Holocene, and there is little evidence for aggradation in the late Holocene. However, this may in part be a result of the OSL sampling technique being biased towards dating deeper, older sediments of the alluvial fill at both study sites. Results from Horn (2010) may agree with this interpretation, as there is little evidence for aggradation in the early Holocene at the Grand Island location. Differing rates of aggradation occurring at different locations could be indicative of a change in sediment supply. The possibility that eolian dune damming of the North and South Platte River Valley in the late Pleistocene may well have caused a localized shift in river dynamics, resulting in the increased aggradation seen at Kearney. Additionally, it is possible that aggradation at Kearney is due to sequestration of sediment caused by a change in equilibrium state in the area. .

There are many questions that remain unanswered about the nature of the Platte River alluvial fills. There are many gaps in the data on a variety of scales. Analysis of additional OSL samples from cores recovered in this study would improve the resolution of the age and thickness of the alluvium, especially in the shallow subsurface. Additionally, increasing the number of boreholes in each transect would significantly improve the resolution of the subsurface.

Many more studies at other locations within the Platte River Valley will be necessary to fully understand the response of the Platte River to climate change. Due to the heterogeneity of alluvial deposits at a variety of scales in braided river systems, much more data is needed to fully understand the river system. Other data sources, including geophysical data, such as wireline logs, seismic reflections, and ground penetrating radar, would provide much more detailed information about the subsurface. This study and that of Horn (2010) improve the current understanding of Platte River dynamics and geomorphology on a glacial – interglacial timescale, but there is much more work to be done!

7 References Cited

Aitken, M.J., 1998. An introduction to Optical Dating. Oxford, *Oxford University Press*.

Arbogast, A.F. & Johnson, W.C., 1994. Climatic implications of the late Quaternary alluvial record of a small drainage basin in the central Great Plains, *Quaternary Research* 41, 298-305.

Benedict, J.B., 1973. Chronology of cirque glaciation, Colorado front range. *Quaternary Research*, *3*(4), pp.584-599.

Berger, G. W. & Luternauer, J. J., 1987. Preliminary field work for thermoluminescence dating studies at the Fraser River delta, British Columbia. *Geological Survey of Canada Paper* 87/IA, 901–904.

Berger, G. W., 1990. Effectiveness of natural zeroing of the thermoluminescence in sediments. *Journal of Geophysical Research* 95, 12,375–12,397.

Bettis, E. A., Muhs, D. R., Roberts, H. M., Wintle, A. G., 2003., Last glacial loess in the conterminous USA. *Quaternary Science Reviews*, *22*(18), 1907-1946.

Blodgett, R.H. & Stanley, K.O., 1980. Stratification, bedforms and discharge relations of the Platte River system, Nebraska. *J. Sediment. Petrol*, 50, 139–148.

Blong, R. J. & Gillespie, R., 1978. Fluvially transported charcoal gives erroneous 14C ages for recent deposits. *Nature* 271, 739–741.

Blum, M. D. & Tornqvist, T. E., 2000. Fluvial response to climate and sea-level change: A review and a look forward. *Sedimentology* 47, 2–48.

Blum, M. D., Guccione, M. J., Wysocki, D. A., Robnett, P. C., Rutledge, M., 2000. Late Pleistocene evolution of the lower Mississippi Valley, Southern Missouri to Arkansas. *Geological Society of America Bulletin* 112, 221–235.

Busschers, F. S., Kasse, C., van Balen, R. T., Vandenberghe, J., Cohen, K. M.,Weerts H, . J. T., Wallinga, J., Johns, C., Cleveringa, P., Bunnick, F. P. M., 2007. Late Pleistocene evolution of the Rhine-Meuse system in the southern North Sea basin: Imprints of climate change, sea-level oscillation and glacio-isostacy. *Quaternary Science Reviews* 26, 3216–3248.

Busschers, F. S., Weerts, H. J. T., Wallinga, J., Cleveringa, P., Kasse, C., de Wolf, H., Cohen, K. M., 2005. Sedimentary architecture and optical dating of Middle and late Pleistocene Rhine–Meuse deposits – fluvial response to climate change, sea–level fluctuation and glaciation. *Netherlands Journal of Geosciences* 84, 25–41.

Busschers, F.S., Kasse, C., Van Balen, R.T., Vandenberghe, J., Cohen, K.M., Weerts, H.J.T., Wallinga, J., Johns, C., Cleveringa, P., Bunnik, F.P.M., 2007. Late Pleistocene evolution of the Rhine-Meuse system in the southern North Sea basin: imprints of climate change,

sea-level oscillation and glacio-isostacy. *Quaternary Science Reviews*, 26(25), pp.3216-3248.

Brice, J.C., 1964. Channel patterns and terraces of the Loup Rivers in Nebraska, *U.S. Geological Survey Professional Paper* 422-D.

Colls, A. E., Stokes, S., Blum, M. D., Straffin, E., 2001. Age limits on the Late Quaternary evolution of the upper Loire River. *Quaternary Science Reviews* 20, 743–750.

Condon, S. M., 2005. Geologic studies of the Platte River, South-Central Nebraska and adjacent areas—Geologic maps, subsurface study, and geologic history. *Publications of the US Geological Survey.* Paper 22

Crowley, K. D., 1983. Large-scale bedforms in the Platte River, Nebraska, *U. S.Geological Survey Professional Paper.* pp. 161.

Dethier, D. P., 2001. Pleistocene incision rates in the western United States calibrated using Lava Creek B tephra. *Geology*, 29(9), 783-786.

Duller, G. A. T., 2000. Optical dating of single sand-sized grains of quartz: Sources of variability. *Radiation Measurements* 32, 453–457.

Duller, G. A.T., 2004. Luminescence dating of Quaternary sediments: recent advances. *Journal of Quaternary Science*, *19*(2), 183-192.

Duller, G. A. T., 2008. Single-grain optical dating of Quaternary sediments: why aliquot size matters in luminescence dating. *Boreas* 37, 589–612.

Fotherby, L. M., 2009. Valley confinement as a factor of braided river pattern for the Platte River. *Geomorphology*, 103(4), 562-576.

Galbraith, R., Roberts, R., Laslett, G., Yoshida, H., Olley, J., 1999. Optical dating of single and multiple grains of quartz from jinmium rock shelter, northern Australia: Part I, experimental design and statistical models. *Archaeometry* 41, 339e364.

Gillespie, R., Prosser, I. P., Dlugokencky, E., Sparks, R. J., Wallace, G., Chappell, J. M. A., 1992. AMS dating of alluvial sediments on the southern tablelands of New South Wales Australia. *Radiocarbon* 34, 29–36.

Goble, R.J., Mason, J.A., Loope, D.B., Swinehart, J.B., 2004. Optical and radiocarbon ages of stacked paleosols and dune sands in the Nebraska Sand Hills, USA. *Quaternary Science Reviews* 23,1173-1182.

Hanson, P. R., 2006. Dating ephemeral stream and alluvial fan deposits on the central Great Plains: Comparing multiple-grain OSL, single-grain OSL, and radiocarbon ages. United *States Geological Survey Open File Report* 2006-1351, p. 14. Available at: http://pubs.usgs.gov/of/2006/1351/pdf/of06–1351_508.pdf

Hanson, P.R., Mason, J.A. and Goble, R.J., 2006. The formation of fluvial terraces along Wyoming's Laramie Range as a response to late Pleistocene flooding events. *Geomorphology* 76, 12-25

Hanson, P. R., Joeckel, R. M., Young, A. R., Horn, J., 2009. Late Holocene dune activity in the Eastern Platte River Valley, Nebraska. *Geomorphology*,103(4), 555-561.

Hanson, P. R., Korus, J. T., Divine, D. P., Larson, D. R., 2012. Three-dimensional hydrostratigraphy of the Platte River Valley near Ashland, Nebraska: Results from Helicopter Electromagnetic (HEM) mapping in the Eastern Nebraska Water Resources Assessment (ENWRA). *Conservation Bulletin*, 2.

Hanson, P.R., Dillon, J.S., Bruihler, J.C., Howard, L.M., 2014. Surficial Geology of the Kearney 7.5 Minute Quadrangle, Nebraska. http://snr.unl.edu/csd-esic/download/geologysoils/digitalgeologicmaps/Kearney_Files/Kearney_Quad.pdf

Hanson, P.R., Bruihler, J.C., Howard, L.M., 2015. Surficial Geology of the Hershey East 7.5 Minute Quadrangle, Nebraska. http://snr.unl.edu/csd-esic/download/geologysoils/digitalgeologicmaps/Hershey_East_Files/Hershey_East_Quad.pdf

Holbrook, J. M. & Schumm, S. A., 1999: Geomorphic and sedimentary response of rivers to tectonic deformation: A brief review and critique of a tool for recognizing subtle epeirogenic deformation in modern and ancient settings. *Tectonophysics* 305, 287–306.

Horn, J.D., 2010. Fluvial evolution of the central Platte River sand body near Grand Island, Nebraska. *ETD Collection for University of Nebraska-Lincoln* http://digitalcommons.unl.edu/dissertations/AAI3412919

Horn, J. D., Fielding, C. R., Joeckel, R. M., 2012a. Revision of Platte River alluvial facies model through observations of extant channels and barforms, and subsurface alluvial valley fills. *Journal of Sedimentary Research*, 82(2), 72-91.

Horn, J. D., Joeckel, R. M., Fielding, C. R., 2012b. Progressive abandonment and planform changes of the central Platte River in Nebraska, central USA, over historical timeframes. *Geomorphology*, 139, 372-383.

Jain, M. & Tandon, S. K., 2003. Fluvial response to late Quaternary climate changes, western India. Quaternary Science Reviews 22, 2223–2235.

Jain, M., Murray, A.S., Botter-Jensen, L., 2004. Optically stimulated luminescence dating: How significant is incomplete light exposure in fluvial environments? *Quaternaire* 15, 143-157.

Jain, M., Murray, A. S., Btter-Jensen, L., Wintle, A. G., 2005a. A single-aliquot regenerative-dose method based on IR (1.49 eV) bleaching of the fast OSL component in quartz. *Radiation Measurements* 39, 309–318.

Joeckel, R. M., & Henebry, G. M., 2008. Channel and island change in the lower Platte River, Eastern Nebraska, USA: 1855–2005. *Geomorphology*, 102(3), 407-418.

Joeckel, R.M.. Wooden, S.R., Korus, J.T., & Garbaisch, J.O., 2014. Architecture, heterogeneity, and origin of late Miocene fluvial deposits hosting the most important aquifer in the Great Plains, USA. *Sedimentary Geology*, 311, pp. 75 – 95.

Kammerer, J. C., 1990, Largest Rivers in the United States, USGS open file report 87-242, 2p http://pubs.usgs.gov/of/1987/ofr87-242/

Lewis, S. G., Maddy, D., Scaife, R. G., 2001: The fluvial system response to abrupt climate change during the last cold stage: The Upper Pleistocene River Thames fluvial succession at Ashton Keynes, UK. *Global and Planetary Change* 28, 341–359.

Lewis C.J., McDonald E.V., Sancho C., Pena J.L., Rhodes E.J., 2009. Climatic implications of correlated Upper Pleistocene glacial and fluvial deposits on the Cinca and G´allego Rivers, NE Spain. *Glob. Planet. Change* 67:141–52

Lu, H., Mason, J. A., Stevens, T., Zhou, Y., Yi, S., Miao, X., 2011. Response of surface processes to climatic change in the dunefields and Loess Plateau of North China during the late Quaternary. *Earth Surface Processes and Landforms*, *36*(12), 1590-1603.

Lugn, A. L., 1935. Pleistocene geology of Nebraska.

Maddy, D., Bridgland, D., Westaway, R., 2001. Uplift-driven valley incision and climate-controlled river terrace development in the Thames Valley, UK. Quaternary International, 79(1), pp.23-36.

Mason, J.A., 2001. Transport direction of Peoria Loess in Nebraska and implications for loess sources on the central Great Plains. Quaternary Research, 56(1), pp.79-86.

Mason, J.A., Miao, X., Hanson, P.R., Johnson, W.C., Jacobs, P.M., Goble, R.J., 2008. Loess record of the last Glacial-Interglacial transition on the northern and central Great Plains, *Quaternary Science Reviews* 27, 1772-1783.

Mason, J.A., Swinehart, J.B., Goble, R.J., Loope, D.B., 2004. Late Holocene dune activity linked to hydrological drought, Nebraska Sand Hills, USA. *The Holocene* 14, 209-217

May, D.W., 1989. Holocene alluvial fills in the South Loup Valley, Nebraska, *Quaternary Research* 32, 117-120.

Miall, A. D., 1977. A review of the braided-river depositional environment, *Earth-Science Reviews*, v. 13, pp.1-62.

Miall, A. D., 1978. Lithofacies types and vertical profile models in braided river deposits; a summary, *Canadian Society of Petroleum Geologists*, pp.597-604.

Miall, A. D., 1986. Facies architecture in sedimentary basins; the decline and fall of vertical profile analysis, *AAPG Bulletin*, November 1986, v. 70, pp. 1761.

Miao, X., Mason, J.A., Goble, R.J., Hanson, P.R., 2005. Loess-inferred dry climate and eolian activity in the early to mid-Holocene, central Great Plains, North America. *The Holocene* 15, 339-346.

Miao, X., Mason, J.A., Swinehart, J.B., Loope, D.B., Hanson, P.R., Goble, R.J., Liu, X., 2007. A 10,000 year record of dune activity, dust storms and severe drought in the central Great Plains. *Geology* 35, 119-122.

Mol, J., Vandenberghe, J., Kasse, C., 2000. River response to variations of periglacial climate in mid-latitude Europe. *Geomorphology,* 33(3), pp.131-148.

Muhs, D. R., & Bettis, E. A., 2000. Geochemical variations in Peoria Loess of western Iowa indicate paleowinds of midcontinental North America during last glaciation. *Quaternary Research*, 53(1), 49-61.

Muhs, D. R., Bettis, E. A., Aleinikoff, J. N., McGeehin, J. P., Beann, J., Skipp, G., ... & Benton, R., 2008. Origin and paleoclimatic significance of late Quaternary loess in Nebraska: evidence from stratigraphy, chronology, sedimentology, and geochemistry. *Geological Society of America Bulletin*, 120(11-12), 1378-1407.

Muhs, D. R., Swinehat, J.B., Loope, D.B., Been, J., Mahan, S.A., & Bush, C.A., 2000. Geochemical evidence for an eolian sand dam across the North and South Platte Rivers in Nebraska. *Quaternary Research,* 53(2). 214-222

Muhs, D. R., 2013. The geologic records of dust in the Quaternary. *Aeolian Research*, *9*, 3-48.

Murray, A. S., Olley, J. M., & Caitcheon, G. G., 1995. Measurement of equivalent doses in quartz from contemporary water-lain sediments using optically stimulated luminescence. *Quaternary Science Reviews* 14, 365–371.

Murray, A.S. & Wintle, A.G., 2000. Luminescence dating of quartz using an improved single-aliquot regenerative-dose protocol. *Radiation Measurements* 32, 57–73.

Murray, A. S. & Wintle, A. G., 2003. The single aliquot regenerative dose protocol: potential for improvements in reliability. *Radiation Measurements*, 37(4), 377-381.

Olley J., Caitcheon, G., Murray, A.S., 1998.Thedistribution of apparent dose as determined by optically stimulated luminescence in small aliquots of fluvial quartz: implications for dating young sediments. *Quat. Sci. Rev*. 17:1033–40

Olley, J., Caitcheon, G., Roberts, R., 1999. The origin of dose distributions in fluvial sediments, and the prospect of dating single grains from fluvial deposits using optically stimulated luminescence. *Radiation Measurements* 30, 207e217.

Prescott, J.R., Hutton, J.T., 1994. Cosmic ray contributions to dose rates for luminescence and ESR dating: large depths and long-term time variations. Radiation Measurements 23, 497–500.

Rhodes, E.J., 2011. Optically stimulated luminescence dating of sediments over the past 200,000 years. *Annual Review of Earth and Planetary Sciences* 39, 461-488

Rittenour, T. M., Goble, R. J., Blum, M. D., 2003. An optical age chronology of Late Pleistocene fluvial deposits in the Northern Lower Mississippi Valley. *Quaternary Science Reviews* 22,1105–1110.

Rittenour, T. M., Goble, R. J., Blum, M. D., 2005. Development of an OSL chronology for late Pleistocene channel belts in the lower Mississippi valley. *Quaternary Science Reviews* 24, 2539–2554.

Rittenour, T. M., Blum, M. D., Goble, R. J., 2007. Fluvial evolution of the lower Mississippi River valley during the last 100-kyr glacial cycle: Response to glaciation and sea-level change. *Geological Society of America Bulletin* 119, 586–608.

Rittenour TM., 2008. Luminescence dating of fluvial deposits: applications to geomorphic, palaeoseismic and archaeological research. *Boreas* 37: 613–635

Rodnight, H., Duller, G. A. T., Tooth, S., Wintle, A. G., 2005. Optical dating of scroll-bar sequence on the Klip River, South Africa, to derive the lateral migration rate of a meander bend. *The Holocene* 15, 802–811.

Rodnight, H., Duller, G. A. T., Wintle, A. G., Tooth, S., 2006. Assessing the reproducibility and accuracy of optical dating of fluvial deposits. *Quaternary Geochronology* 1, 109–120.

Roberts, H.M.; Muhs, D.R., Wintle, A.G., Duller, G.A.T., Bettis III, E. A., 2003. Unprecedented last-glacial mass accumulation rates determined by luminescence dating of loess from western Nebraska. *USGS Staff -- Published Research.* Paper 176. http://digitalcommons.unl.edu/usgsstaffpub/176

Schumm, S.A., 1993. River response to baselevel change: implications for sequence stratigraphy. *The Journal of Geology*, pp.279-294.

Skelly, R. L., Bristow, C. S., Ethridge, F. G., 2003. Architecture of channel-belt deposits in an aggrading shallow sandbed braided river: the lower Niobrara River, northeast Nebraska. *Sedimentary Geology*, 158(3), 249-270.

Smith, N. D., 1970. The braided stream depositional environment; comparison of the Platte river with some Silurian clastic rocks, north-central Appalachians, *Geological Society of America Bulletin,* v. 81, pp.2993-3013.

Smith, N. D., 1971. Transverse bars and braiding in the lower Platte River, Nebraska, *Geological Society of America Bulletin*, v. 82, pp.3407-3420.

Smith, N. D., 1972 Some sedimentological aspects of planar cross-stratification in a sandy braided river, *Journal of Sedimentary Petrology*, v. 42, pp. 624-634.

Srivastava, P., Sharma, M., Singhvi, A. K., 2003a. Luminescence chronology of incision and channel pattern changes in the River Ganga, India. *Geomorphology* 51, 259–268.

Srivastava, P., Singh, I. B., Sharma, M., Singhvi, A. K., 2003b. Luminescence chronometry and Late Quaternary geomorphic history of the Ganga Plain, India. *Palaeogeography, Palaeoclimatology, Palaeoecology* 197, 15–41.

Stanley, D. J. & Hait, A. K., 2000. Deltas, radiocarbon dating, and measurement of sediment storage and subsidence. *Geology* 28, 295–298.

Swinehart, J. B., Souders, V. L., DeGraw, H. M., Diffendal Jr, R. F., 1985. Cenozoic paleogeography of western Nebraska. *Rocky Mountain Section (SEPM)*.

Swinehart, J.B. & Diffendal Jr, R.F., 1997. Geologic map of the Scottsbluff 1 degree by 2 degrees Quadrangle, Nebraska and Colorado (No. 2545).

Tanaka, K., Hataya, R., Spooner, N. A., Questiaux, D. G., 2001: Optical dating of river terrace sediments from Kanto plains, Japan. *Quaternary Science Reviews* 20, 826–828.

Thomas, M. F., Nott, J., Murray, A. S., Price, D. M., 2007a. Fluvial response to late Quaternary climate change in NE Queensland, Australia. *Palaeogeography, Palaeoclimatology, Palaeoecology* 251, 119–136.

Tornqvist, T. E., 1998. Longitudinal profile evolution of the Rhine–-Meuse system during the last deglaciation: Interplay of climate change and glacio-eustacy? *Terra Nova* 10, 11–15.

Tornqvist, T. E., Wallinga, J., Murray, A. S., De Wolf, H., Cleveringa, P., De Gans, W., 2000. Response of the Rhine–Meuse system (west-central Netherlands) to the last Quaternary glacio-eustatic cycles: A first assessment. *Global and Planetary Change* 27, 89–111.

Vandenberghe, J. & Maddy, D., 2000. The significance of fluvial archives in geomorphology. *Geomorphology*, 33(3), pp.127-130.

Wallinga, J., 2002. Optically stimulated luminescence dating of fluvial deposits: a review. *Boreas*, 31(4), pp.303-322.

Wallinga, J., Tornqvist, T. E., Busschers, F. S., Weerts, H. J. T., 2004. Allogenic forcing of late-Quaternary Rhine–Meuse fluvial record: The interplay of climate change, sea level change, and crustal movements. Basin Research 16, 535–547.

Wintle, A. G., & Murray, A. S., 2006. A review of quartz optically stimulated luminescence characteristics and their relevance in single-aliquot regeneration dating protocols. *Radiation Measurements*, *41*(4), 369-391.

8 Appendix One: Particle Size Analysis Data

8.1 Hershey East Cores

Hershey East 1

Clay	Silt	V. Fine	Fine	Medium	Coarse	V. Coarse	>2mm	>4mm	>8mm	>16mm	Sand Total	>2mm total	Depth	%	Method
0-2µm	2-63µm	63-125µm	125-250µm	250-500µm	500µm-1mm	1mm-2mm	2mm-4mm	4mm-8mm	8mm-16mm	>16mm	V.Fine-V. Coarse	Gravel	cm		
3.95	53.76	35.42	6.87	0.00	0.00	0.00	0.00	0.00	0.00	0.00	42.28	0.00	45	100.00	Laser
4.56	77.99	16.32	1.13	0.00	0.00	0.00	0.00	0.00	0.00	0.00	17.45	0.00	75	100.00	Laser
4.92	78.18	13.68	3.00	0.22	0.00	0.00	0.00	0.00	0.00	0.00	16.90	0.00	105	100.00	Laser
0.00	96.34	3.63	0.03	0.00	0.00	0.00	0.00	0.00	0.00	0.00	3.66	0.00	135	100.00	Laser
0.00	99.95	0.05	0.00	0.00	0.00	0.00	0.00	0.00	0.00	0.00	0.05	0.00	195	100.00	Laser
0.00	100.00	0.00	0.00	0.00	0.00	0.00	0.00	0.00	0.00	0.00	0.00	0.00	225	100.00	Laser
0.00	93.00	7.00	0.00	0.00	0.00	0.00	0.00	0.00	0.00	0.00	7.00	0.00	255	100.00	Laser
0.00	32.30	35.15	29.87	2.68	0.00	0.00	0.00	0.00	0.00	0.00	67.70	0.00	315	100.00	Laser
0.00	64.29	31.84	3.87	0.00	0.00	0.00	0.00	0.00	0.00	0.00	35.71	0.00	345	100.00	Laser
0.00	72.66	19.60	6.81	0.93	0.00	0.00	0.00	0.00	0.00	0.00	27.34	0.00	375	100.00	Laser
0.00	29.11	35.97	31.71	3.20	0.00	0.00	0.00	0.00	0.00	0.00	70.89	0.00	405	100.00	Laser
0.00	1.56	3.41	10.11	22.71	20.38	15.71	13.51	9.45	3.14	0.00	72.32	26.10	450	99.98	Sieve
0.00	31.77	37.96	27.91	2.36	0.00	0.00	0.00	0.00	0.00	0.00	68.23	0.00	465	100.00	Laser
0.00	0.48	1.40	4.73	12.58	15.85	19.69	23.30	19.07	2.85	0.00	54.25	45.22	500	99.95	Sieve
0.00	0.48	2.84	10.31	23.18	26.84	16.33	11.33	6.06	2.50	0.00	79.50	19.89	650	99.87	Sieve
0.00	0.72	1.34	4.62	11.55	23.94	22.30	18.52	10.94	5.91	0.00	63.75	35.37	700	99.84	Sieve
0.00	0.61	1.57	3.83	8.40	17.37	17.57	22.31	16.96	5.22	6.11	48.74	50.60	800	99.95	Sieve
27.04	72.96	0.00	0.00	0.00	0.00	0.00	0.00	0.00	0.00	0.00	0.00	0.00	855	100.00	Laser
27.55	72.45	0.00	0.00	0.00	0.00	0.00	0.00	0.00	0.00	0.00	0.00	0.00	885	100.00	Laser
35.05	64.95	0.00	0.00	0.00	0.00	0.00	0.00	0.00	0.00	0.00	0.00	0.00	915	100.00	Laser
4.40	64.80	25.06	5.74	0.00	0.00	0.00	0.00	0.00	0.00	0.00	30.80	0.00	945	100.00	Laser
5.11	69.88	18.88	5.97	0.17	0.00	0.00	0.00	0.00	0.00	0.00	25.01	0.00	975	100.00	Laser
2.00	57.92	31.46	8.63	0.00	0.00	0.00	0.00	0.00	0.00	0.00	40.08	0.00	1005	100.00	Laser
6.19	49.76	27.37	15.71	0.97	0.00	0.00	0.00	0.00	0.00	0.00	44.05	0.00	1065	100.00	Laser
4.74	33.65	36.43	23.99	1.20	0.00	0.00	0.00	0.00	0.00	0.00	61.62	0.00	1095	100.00	Laser
3.39	26.84	43.85	24.87	1.06	0.00	0.00	0.00	0.00	0.00	0.00	69.77	0.00	1125	100.00	Laser
0.00	18.16	56.21	25.33	0.31	0.00	0.00	0.00	0.00	0.00	0.00	81.84	0.00	1155	100.00	Laser

Hershey East 2

Clay	Silt	V. Fine	Fine	Medium	Coarse	V. Coarse	>2mm	>4mm	>8mm	>16mm	Sand Total	>2mm total	Depth	%	Method
	2-	63-	125-	250-	500µm-	1mm-	2mm-	4mm-	8mm-		V. Fine-				
0-2µm	63µm	125µm	250µm	500µm	1mm	2mm	4mm	8mm	16mm	>16mm	V. Coarse	Gravel			
0.00	96.52	3.37	0.11	0.00	0.00	0.00	0.00	0.00	0.00	0.00	3.48	0.00	45	100.00	Laser
0.00	82.30	5.77	10.59	1.34	0.00	0.00	0.00	0.00	0.00	0.00	17.70	0.00	75	100.00	Laser
0.00	96.52	3.48	0.00	0.00	0.00	0.00	0.00	0.00	0.00	0.00	3.48	0.00	105	100.00	Laser
0.00	93.00	6.80	0.20	0.00	0.00	0.00	0.00	0.00	0.00	0.00	7.00	0.00	135	100.00	Laser
0.00	93.83	3.93	2.24	0.00	0.00	0.00	0.00	0.00	0.00	0.00	6.17	0.00	165	100.00	Laser
4.03	56.39	6.68	28.59	4.31	0.00	0.00	0.00	0.00	0.00	0.00	39.58	0.00	195	100.00	Laser
0.00	18.24	15.88	57.51	8.37	0.00	0.00	0.00	0.00	0.00	0.00	81.76	0.00	225	100.00	Laser
0.00	0.38	0.81	4.19	20.03	32.35	19.03	11.42	9.14	2.55	0.00	76.41	23.11	350	99.90	Sieve
0.00	0.63	1.03	4.68	25.03	41.33	11.70	7.08	5.12	3.33	0.00	83.77	15.53	400	99.93	Sieve
0.00	0.48	0.73	1.81	6.57	11.58	16.78	27.41	23.15	5.95	5.44	37.47	61.95	500	99.90	Sieve
0.00	0.92	1.88	4.13	9.47	25.04	22.11	10.65	6.18	6.72	12.86	62.63	36.41	700	99.96	Sieve
0.00	12.51	66.81	20.68	0.00	0.00	0.00	0.00	0.00	0.00	0.00	87.49	0.00	765	100.00	Laser
0.00	54.68	27.10	17.65	0.57	0.00	0.00	0.00	0.00	0.00	0.00	45.32	0.00	795	100.00	Laser
0.00	88.22	11.78	0.00	0.00	0.00	0.00	0.00	0.00	0.00	0.00	11.78	0.00	825	100.00	Laser
0.00	92.09	7.91	0.00	0.00	0.00	0.00	0.00	0.00	0.00	0.00	7.91	0.00	855	100.00	Laser
0.00	29.98	55.96	14.06	0.00	0.00	0.00	0.00	0.00	0.00	0.00	70.02	0.00	885	100.00	Laser
0.00	48.76	45.26	5.97	0.00	0.00	0.00	0.00	0.00	0.00	0.00	51.24	0.00	915	100.00	Laser
0.00	56.79	37.73	5.48	0.00	0.00	0.00	0.00	0.00	0.00	0.00	43.21	0.00	945	100.00	Laser
0.00	99.86	0.14	0.00	0.00	0.00	0.00	0.00	0.00	0.00	0.00	0.14	0.00	975	100.00	Laser

Hershey East 3

Clay	Silt	V. Fine	Fine	Medium	Coarse	V. Coarse	>2mm	>4mm	>8mm	>16mm	Sand Total	>2mm total	Depth	%	Method
	2-	63-	125-	250-	500µm-	1mm-	2mm-	4mm-	8mm-		V. Fine-				
0-2µm	63µm	125µm	250µm	500µm	1mm	2mm	4mm	8mm	16mm	>16mm	V. Coarse	Gravel	cm		
0.00	84.62	12.74	2.24	0.40	0.00	0	0	0	0	0	15.38	0	45	100.00	Laser
0.00	0.34	1.64	7.99	19.39	22.29	18.77	14.41	7.50	5.31	2.07	70.08	29.29	100	99.71	Sieve
0.00	0.52	0.71	3.50	16.62	31.59	26.85	12.79	4.92	0.32	1.90	79.27	19.93	150	99.72	Sieve
0.00	0.34	1.92	9.17	22.46	21.84	17.40	11.92	9.60	1.35	3.90	72.79	26.77	200	99.90	Sieve
0.00	0.37	1.64	12.03	21.99	18.27	18.30	14.24	8.64	4.29	0.00	72.23	27.17	250	99.77	Sieve
0.00	1.11	1.29	3.86	13.01	24.17	33.65	19.57	2.29	0.66	0.00	75.98	22.52	300	99.61	Sieve
0.00	0.48	0.68	1.39	16.22	24.38	18.58	20.03	11.71	0.71	5.46	61.25	37.91	350	99.64	Sieve
0.00	0.50	0.81	3.86	19.55	20.86	12.99	14.28	15.60	11.18	0.00	58.07	41.06	400	99.63	Sieve
0.00	98.68	1.32	0.00	0.00	0.00	0.00	0.00	0.00	0.00	0.00	1.32	0	405	100.00	Laser
0.00	97.90	2.10	0.00	0.00	0.00	0.00	0.00	0.00	0.00	0.00	2.10	0	435	100.00	Laser
0.00	16.88	41.76	20.12	16.91	3.67	0.34	0.12	0.00	0.00	0.00	82.80	0.12	450	99.80	Sieve
0.00	79.79	14.08	5.80	0.33	0.00	0.00	0.00	0.00	0.00	0.00	20.21	0	465	100.00	Laser
0.00	75.64	19.07	5.19	0.11	0.00	0.00	0.00	0.00	0.00	0.00	24.36	0	495	100.00	Laser
0.00	5.65	24.98	29.43	32.49	4.96	1.21	1.16	0.00	0.00	0.00	93.07	1.16	500	99.88	Sieve
0.00	75.82	20.16	4.02	0.00	0.00	0.00	0.00	0.00	0.00	0.00	24.18	0	525	100.00	Laser
0.00	79.97	16.95	3.09	0.00	0.00	0.00	0.00	0.00	0.00	0.00	20.03	0	555	100.00	Laser
0.00	86.46	12.23	1.31	0.00	0.00	0.00	0.00	0.00	0.00	0.00	13.54	0	585	100.00	Laser
0.00	91.94	7.73	0.33	0.00	0.00	0.00	0.00	0.00	0.00	0.00	8.06	0	615	100.00	Laser
0.00	85.94	10.94	3.03	0.09	0.00	0.00	0.00	0.00	0.00	0.00	14.06	0	645	100.00	Laser
0.00	87.01	10.18	2.54	0.26	0.00	0.00	0.00	0.00	0.00	0.00	12.99	0	675	100.00	Laser
0.00	91.04	8.60	0.36	0.00	0.00	0.00	0.00	0.00	0.00	0.00	8.96	0	705	100.00	Laser
0.00	74.25	19.60	6.08	0.08	0.00	0.00	0.00	0.00	0.00	0.00	25.75	0	735	100.00	Laser
0.00	81.49	17.87	0.64	0.00	0.00	0.00	0.00	0.00	0.00	0.00	18.51	0	765	100.00	Laser
0.00	88.85	9.69	1.36	0.09	0.00	0.00	0.00	0.00	0.00	0.00	11.15	0	795	100.00	Laser
0.00	61.05	28.04	10.89	0.02	0.00	0.00	0.00	0.00	0.00	0.00	38.95	0	825	100.00	Laser
0.00	30.33	41.43	26.86	1.38	0.00	0.00	0.00	0.00	0.00	0.00	69.67	0	855	100.00	Laser

Hershey East 4

Clay	Silt	V. Fine	Fine	Medium	Coarse	V. Coarse	>2mm	>4mm	>8mm	>16mm	Sand Total	>2mm total	Depth	%	Method
	2- 63µm	63- 125µm	125- 250µm	250- 500µm	500µm- 1mm	1mm- 2mm	2mm- 4mm	4mm- 8mm	8mm- 16mm		V. Fine- V. Coarse				
0-2µm	63µm	125µm	250µm	500µm	1mm	2mm	4mm	8mm	16mm	>16mm	V. Coarse	Gravel	cm		
0.00	88.65	10.26	1.09	0.00	0	0.00	0	0	0	0	11.35	0	45	100.00	Laser
0.00	94.11	5.71	0.18	0.00	0	0.00	0	0	0	0	5.89	0	75	100.00	Laser
0.00	97.19	2.78	0.02	0.00	0	0.00	0	0	0	0	2.81	0	105	100.00	Laser
3.23	70.76	8.10	16.02	1.89	0	0.00	0	0	0	0	26.01	0	135	100.00	Laser
0.00	0.00	0.47	3.35	15.53	27.61	21.85	14.76	9.80	5.81	0	68.81	30.37	200	99.18	Sieve
0.00	0.00	0.60	1.99	9.88	16.63	15.67	17.96	15.07	19.07	2.34	44.77	54.44	250	99.21	Sieve
0.00	0.00	1.04	4.86	15.17	23.01	17.38	14.19	9.25	7.82	6.64	61.46	37.9	400	99.36	Sieve
0.00	0.00	2.32	8.24	28.94	24.03	13.27	10.56	8.27	3.58	0.00	76.80	22.41	500	99.21	Sieve
0.00	0.00	1.87	6.82	17.48	29.45	21.32	12.46	8.77	0.84	0.00	76.94	22.07	550	99.01	Sieve
0.00	0.00	2.38	5.64	12.77	23.26	19.56	17.62	13.19	4.72	0.00	63.61	35.53	650	99.14	Sieve
0.00	0.00	1.70	4.77	25.13	38.35	20.01	5.21	2.74	1.24	0.00	89.96	9.19	700	99.15	Sieve
0.00	92.06	7.40	0.54	0.00	0.00	0.00	0.00	0.00	0.00	0.00	7.94	0	735	100.00	Laser
0.00	88.04	9.95	1.86	0.15	0.00	0.00	0.00	0.00	0.00	0.00	11.96	0	765	100.00	Laser
0.00	65.39	25.53	8.79	0.28	0.00	0.00	0.00	0.00	0.00	0.00	34.61	0	795	100.00	Laser
0.00	54.01	37.03	8.96	0.00	0.00	0.00	0.00	0.00	0.00	0.00	45.99	0	855	100.00	Laser
0.00	47.69	34.29	17.11	0.92	0.00	0.00	0.00	0.00	0.00	0.00	52.31	0	885	100.00	Laser
0.00	50.91	30.59	16.81	1.69	0.00	0.00	0.00	0.00	0.00	0.00	49.09	0	915	100.00	Laser
0.00	79.02	20.04	0.89	0.04	0.00	0.00	0.00	0.00	0.00	0.00	20.98	0	945	100.00	Laser
0.00	87.46	12.44	0.10	0.00	0.00	0.00	0.00	0.00	0.00	0.00	12.54	0	975	100.00	Laser
0.00	89.21	10.79	0.01	0.00	0.00	0.00	0.00	0.00	0.00	0.00	10.79	0	1005	100.00	Laser

Hershey East 5

Clay	Silt	V. Fine	Fine	Medium	Coarse	V. Coarse	>2mm	>4mm	>8mm	>16mm	Sand Total	>2mm total	Depth	%	Method
	2-	63-	125-	250-	500µm-	1mm-	2mm-	4mm-	8mm-		V. Fine-				
0-2µm	63µm	125µm	250µm	500µm	1mm	2mm	4mm	8mm	16mm	>16mm	V. Coarse	Gravel	cm		
0.00	81.60	18.34	0.06	0.00	0.00	0	0	0	0	0	18.40	0	15	100.00	Laser
0.00	67.87	27.50	4.63	0.00	0.00	0	0	0	0	0	32.13	0	45	100.00	Laser
0.00	58.38	30.48	10.70	0.44	0.00	0	0	0	0	0	41.62	0	75	100.00	Laser
0.00	62.88	30.82	6.31	0.00	0.00	0	0	0	0	0	37.12	0	105	100.00	Laser
0.00	61.48	28.76	9.39	0.37	0.00	0	0	0	0	0	38.52	0	135	100.00	Laser
6.25	82.03	10.65	1.01	0.07	0.00	0	0	0	0	0	11.72	0	165	100.00	Laser
0.00	90.87	8.79	0.33	0.00	0.00	0	0	0	0	0	9.13	0	195	100.00	Laser
0.00	92.43	6.98	0.59	0.00	0.00	0	0	0	0	0	7.57	0	225	100.00	Laser
0.00	97.04	2.77	0.19	0.00	0.00	0	0	0	0	0	2.96	0	255	100.00	Laser
0.00	79.89	16.35	3.58	0.18	0.00	0	0	0	0	0	20.11	0	285	100.00	Laser
0.00	76.27	20.04	3.56	0.12	0.00	0	0	0	0	0	23.73	0	375	100.00	Laser
0.00	81.81	13.11	4.60	0.49	0.00	0	0	0	0	0	18.19	0	405	100.00	Laser
0.00	68.60	28.97	2.43	0.00	0.00	0	0	0	0	0	31.40	0	495	100.00	Laser
0.00	69.75	28.85	1.40	0.00	0.00	0	0	0	0	0	30.25	0	525	100.00	Laser
0.00	0.36	0.82	3.48	16.55	23.98	17.85	16.17	17.24	3.54	0	62.68	36.95	650	99.99	Sieve
0.00	1.27	3.11	5.97	12.30	27.08	20.48	15.14	11.87	2.62	0	68.94	29.63	700	99.84	Sieve
0.00	0.52	1.36	4.07	20.03	18.76	16.26	19.28	14.32	5.13	0	60.48	38.73	800	99.73	Sieve
0.00	0.97	1.81	4.58	17.49	19.46	19.54	16.93	13.41	5.6	0	62.88	35.94	850	99.79	Sieve
0.00	0.66	1.60	5.16	12.82	9.86	33.73	27.19	6.91	1.91	0	63.17	36.01	900	99.84	Sieve
16.75	72.30	8.38	2.57	0.00	0.00	0	0	0	0	0	10.95	0	1005	100.00	Laser
13.82	55.32	25.50	5.37	0.00	0.00	0	0	0	0	0	30.86	0	1035	100.00	Laser
0.00	66.80	28.31	4.89	0.00	0.00	0	0	0	0	0	33.20	0	1065	100.00	Laser
0.00	70.02	24.71	5.16	0.11	0.00	0	0	0	0	0	29.98	0	1095	100.00	Laser
0.00	66.07	27.98	5.88	0.08	0.00	0	0	0	0	0	33.93	0	1125	100.00	Laser
0.00	75.15	19.84	4.82	0.20	0.00	0	0	0	0	0	24.85	0	1215	100.00	Laser
0.00	67.18	20.56	11.40	0.85	0.00	0	0	0	0	0	32.82	0	1245	100.00	Laser
0.00	81.45	10.66	7.22	0.67	0.00	0	0	0	0	0	18.55	0	1275	100.00	Laser

Hershey East 6

Clay	Silt	V. Fine	Fine	Medium	Coarse	V. Coarse	>2mm	>4mm	>8mm	>16mm	Sand Tota	>2mm total	Depth	%	Method
	2-	63-	125-	250-	500µm-	1mm-	2mm-	4mm-	8mm-		V.				
0-2µm	63µm	125µm	250µm	500µm	1mm	2mm	4mm	8mm	16mm	>16mm	Coarse	Gravel	cm		
0.00	97.31	2.69	0.00	0.00	0.00	0.00	0.00	0.00	0.00	0.00	2.69	0.00	45	100.00	Laser
0.00	98.03	1.97	0.00	0.00	0.00	0.00	0.00	0.00	0.00	0.00	1.97	0.00	75	100.00	Laser
0.00	92.62	6.42	0.96	0.00	0.00	0.00	0.00	0.00	0.00	0.00	7.38	0.00	105	100.00	Laser
0.00	1.98	24.47	66.02	7.53	0.00	0.00	0.00	0.00	0.00	0.00	98.02	0.00	135	100.00	Laser
0.00	10.71	42.80	43.25	3.24	0.00	0.00	0.00	0.00	0.00	0.00	89.29	0.00	165	100.00	Laser
0.00	24.62	59.45	15.93	0.00	0.00	0.00	0.00	0.00	0.00	0.00	75.38	0.00	195	100.00	Laser
0.00	70.53	23.15	6.17	0.15	0.00	0.00	0.00	0.00	0.00	0.00	29.47	0.00	225	100.00	Laser
0.00	0.35	1.23	9.12	23.08	17.55	20.47	15.96	8.36	3.70	0.00	71.45	28.02	350	99.82	Sieve
0.00	50.66	35.87	13.02	0.45	0.00	0.00	0.00	0.00	0.00	0.00	49.34	0.00	405	100.00	Laser
0.00	60.77	33.00	6.24	0.00	0.00	0.00	0.00	0.00	0.00	0.00	39.23	0.00	435	100.00	Laser
0.00	46.10	42.11	11.79	0.00	0.00	0.00	0.00	0.00	0.00	0.00	53.90	0.00	465	100.00	Laser
0.00	45.56	40.28	13.81	0.35	0.00	0.00	0.00	0.00	0.00	0.00	54.44	0.00	495	100.00	Laser
0.00	37.69	46.19	16.12	0.00	0.00	0.00	0.00	0.00	0.00	0.00	62.31	0.00	525	100.00	Laser
0.00	36.25	40.44	22.32	1.00	0.00	0.00	0.00	0.00	0.00	0.00	63.75	0.00	555	100.00	Laser
0.00	57.10	33.43	9.14	0.32	0.00	0.00	0.00	0.00	0.00	0.00	42.90	0.00	585	100.00	Laser

8.2 Kearney Cores

Kearney 9

Clay	Silt	V. Fine	Fine	Medium	Coarse	V. Coarse	>2mm	>4mm	>8mm	>16mm	Sand Total	>2mm total	Depth	%	Method
	2-	63-	125-	250-	500µm-	1mm-	2mm-	4mm-	8mm-		V. Fine-				
0-2µm	63µm	125µm	250µm	500µm	1mm	2mm	4mm	8mm	16mm	>16mm	V. Coarse	Gravel	cm		
0	13.69	12.44	39.84	31.07	2.95	0.00	0	0	0	0	86.31	0	45	100.00	Laser
0	2.97	7.42	41.56	41.14	6.91	0.00	0	0	0	0	97.03	0	75	100.00	Laser
0	2.67	9.02	47.96	37.72	2.62	0.00	0	0	0	0	97.33	0	105	100.00	Laser
0	1.94	3.16	28.90	46.73	18.56	0.71	0	0	0	0	98.06	0	135	100.00	Laser
0	4.27	6.70	34.51	42.29	12.04	0.20	0	0	0	0	95.73	0	165	100.00	Laser
0	0.00	3.16	41.65	50.18	5.00	0.00	0	0	0	0	100.00	0	195	100.00	Laser
0	0.00	7.17	49.28	41.19	2.36	0.00	0	0	0	0	100.00	0	225	100.00	Laser
0	1.42	5.10	34.63	45.58	13.18	0.09	0	0	0	0	98.58	0	255	100.00	Laser
0	0.85	5.28	38.30	45.67	9.83	0.07	0	0	0	0	99.15	0	285	100.00	Laser
0	7.68	9.47	38.74	36.21	7.70	0.20	0	0	0	0	92.32	0	315	100.00	Laser
0	5.46	10.46	44.56	35.92	3.61	0.00	0	0	0	0	94.54	0	345	100.00	Laser
0	0.70	8.19	42.47	40.34	8.16	0.15	0	0	0	0	99.30	0	375	100.00	Laser
0.26	0.23	6.76	48.43	41.11	3.22	0.00	0	0	0	0	99.51	0	405	100.00	Laser
0	3.22	5.64	33.47	42.77	14.41	0.48	0	0	0	0	96.78	0	435	100.00	Laser
0	1.08	6.30	44.88	42.92	4.81	0.00	0	0	0	0	98.92	0	465	100.00	Laser
0	1.27	10.91	50.58	35.41	1.83	0.00	0	0	0	0	98.73	0	495	100.00	Laser
0	1.57	8.16	35.34	40.31	14.07	0.55	0	0	0	0	98.43	0	525	100.00	Laser
0	3.19	14.29	45.32	34.00	3.20	0.00	0	0	0	0	96.81	0	555	100.00	Laser
0	4.81	2.76	20.47	41.82	27.67	2.46	0	0	0	0	95.19	0	615	100.00	Laser
0	2.41	2.84	36.30	48.96	9.49	0.00	0	0	0	0	97.59	0	645	100.00	Laser
0	1.59	3.17	39.39	49.66	6.19	0.00	0	0	0	0	98.41	0	675	100.00	Laser
0	2.14	0.99	22.48	48.30	24.47	1.62	0	0	0	0	97.86	0	705	100.00	Laser
0	0.46	0.03	15.85	63.55	20.08	0.03	0	0	0	0	99.54	0	765	100.00	Laser
0	0.61	0.00	13.58	48.23	34.44	3.14	0	0	0	0	99.39	0	795	100.00	Laser
0	1.47	10.40	38.23	37.84	11.60	0.46	0	0	0	0	98.53	0	825	100.00	Laser
0	0.00	0.00	8.07	45.64	42.16	4.12	0	0	0	0	100.00	0	885	100.00	Laser
0	0.39	3.51	9.07	17.68	22.37	15.13	16.21	9.24	6.2	0	67.76	31.65	900	99.80	Sieve
0	1.19	3.00	16.11	37.67	37.50	4.52	0	0	0	0	98.81	0	945	100.00	Laser
0	0.22	1.03	0.79	20.40	65.41	12.15	0	0	0	0	99.78	0	975	100.00	Laser
0	0.61	2.67	9.16	27.49	28.93	16.21	9.66	4.01	1.14	0	84.46	14.81	1000	99.88	Sieve

Kearney 9 (Continued)

Clay	Silt	V. Fine	Fine	Medium	Coarse	V. Coarse	>2mm	>4mm	>8mm	>16mm	Sand Total	>2mm total	Depth	%	Method
	2-	63-	125-	250-	500µm-	1mm-	2mm-	4mm-	8mm-		V. Fine-				
0-2µm	63µm	125µm	250µm	500µm	1mm	2mm	4mm	8mm	16mm	>16mm	V. Coarse	Gravel	cm		
0	0.61	2.67	9.16	27.49	28.93	16.21	9.66	4.01	1.14	0	84.46	14.81	1000	99.88	Sieve
0	1.96	4.11	39.80	47.16	6.98	0.00	0	0	0	0	98.04	0	1035	100.00	Laser
0	0.42	1.66	9.05	25.87	31.98	10.20	10.05	5.83	4.81	0	78.76	20.69	1050	99.87	Sieve
0	1.47	14.18	50.62	29.97	3.71	0.06	0	0	0	0	98.53	0	1065	100.00	Laser
0	1.72	0.30	2.29	29.52	57.22	8.95	0	0	0	0	98.28	0	1125	100.00	Laser
0	0.28	2.64	5.75	21.23	36.12	15.60	8.3	5.55	4.21	0	81.34	18.06	1150	99.68	Sieve
0	0.27	0.58	2.58	24.03	30.72	15.64	12.77	8.98	4.25	0	73.55	26	1200	99.82	Sieve
0	0.56	2.16	15.65	14.47	6.82	9.63	16.05	15.39	10.34	8.87	48.73	50.65	1300	99.94	Sieve
0	1.38	3.14	22.88	44.34	26.23	2.04	0	0	0	0	98.62	0	1305	100.00	Laser
0	2.18	1.05	27.39	52.02	16.92	0.43	0	0	0	0	97.82	0	1335	100.00	Laser
0	0.30	0.86	1.85	5.95	13.85	27.30	28.75	11.13	2.29	7.7	49.81	49.87	1350	99.98	Sieve
0	0.65	0.00	9.52	44.06	41.43	4.34	0	0	0	0	99.35	0	1365	100.00	Laser
0	0.26	0.69	5.17	23.92	26.55	23.09	15.77	4.51	0	0	79.42	20.28	1450	99.96	Sieve
0	1.09	1.63	3.60	7.53	16.66	18.22	19.24	18.4	13.27	0	47.64	50.91	1500	99.64	Sieve
0	1.52	1.48	3.04	12.41	28.29	21.00	18.42	12.4	1.16	0	66.22	31.98	1600	99.72	Sieve
0	0.19	0.54	5.25	35.42	10.57	10.09	11.54	7.6	2.89	15.75	61.87	37.78	1700	99.84	Sieve
0	0.00	0.00	11.58	65.67	22.58	0.16	0	0	0	0	100.00	0	1725	100.00	Laser
0	0.30	0.52	7.14	21.67	21.81	16.71	13.12	9.98	5.75	2.47	67.85	31.32	1750	99.47	Sieve
0	0.64	0.72	2.87	13.29	13.35	22.31	28.43	16.11	2.06	0	52.54	46.6	1800	99.78	Sieve

Kearney 10

Clay	Silt	V. Fine	Fine	Medium	Coarse	V. Coarse	>2mm	>4mm	>8mm	>16mm	Sand Total	>2mm total	Depth	%	Method
	2-	63-	125-	250-	500µm-	1mm-	2mm-	4mm-	8mm-		V. Fine				
0-2µm	63µm	125µm	250µm	500µm	1mm	2mm	4mm	8mm	16mm	>16mm	V. Coarse	Gravel	cm		
0	64.87	13.45	10.62	7.94	3.12	0	0	0	0	0	35.13	0	15	100.00	Laser
0	40.12	13.10	15.69	18.93	12.17	0	0	0	0	0	59.88	0	45	100.00	Laser
0	11.52	10.47	20.34	30.59	27.08	0	0	0	0	0	88.48	0	75	100.00	Laser
0	3.14	3.11	25.67	47.43	20.65	0	0	0	0	0	96.86	0	105	100.00	Laser
0	1.75	1.82	32.54	50.80	13.08	0	0	0	0	0	98.25	0	135	100.00	Laser
0	1.07	0.11	19.62	51.98	27.21	0	0	0	0	0	98.93	0	195	100.00	Laser
0	2.20	0.99	25.30	49.49	22.02	0	0	0	0	0	97.80	0	225	100.00	Laser
0	2.32	3.66	32.13	49.08	12.81	0	0	0	0	0	97.68	0	255	100.00	Laser
0	4.08	7.51	32.64	41.79	13.97	0	0	0	0	0	95.92	0	285	100.00	Laser
0	4.68	0.49	21.65	51.78	21.40	0	0	0	0	0	95.32	0	315	100.00	Laser
0	7.11	4.15	30.43	46.56	11.74	0	0	0	0	0	92.89	0	345	100.00	Laser
0	0.68	0.15	21.24	53.46	24.47	0	0	0	0	0	99.32	0	375	100.00	Laser
0	0.54	2.07	10.73	12.59	32.02	31.11	9.81	0.89	0	0	88.52	10.7	400	99.76	Sieve
0	0.99	0.40	4.60	45.78	48.23	0	0	0	0	0	99.01	0	585	100.00	Laser
0	0.00	0.00	10.41	55.21	34.38	0	0	0	0	0	100.00	0	615	100.00	Laser
0	14.36	32.01	31.14	13.34	9.16	0	0	0	0	0	85.64	0	645	100.00	Laser
0	5.71	5.09	5.83	31.85	51.52	0	0	0	0	0	94.29	0	675	100.00	Laser
0	0.69	1.45	3.45	14.68	21.75	22.26	22.72	11.54	1.2	0	63.59	35.46	700	99.74	Sieve
0	3.56	8.32	38.96	41.44	7.72	0	0	0	0	0	96.44	0	705	100.00	Laser
0	3.47	7.34	44.61	40.73	3.84	0	0	0	0	0	96.53	0	765	100.00	Laser
0	5.52	1.81	15.90	41.77	35.00	0	0	0	0	0	94.48	0	795	100.00	Laser
0	0.59	1.95	7.13	25.10	30.29	15.09	8.34	4.75	3.91	2.55	79.56	19.55	800	99.70	Sieve
0	5.76	10.33	33.94	37.31	12.66	0	0	0	0	0	94.24	0	855	100.00	Laser
0	2.86	2.05	36.07	49.65	9.37	0	0	0	0	0	97.14	0	885	100.00	Laser
0	1.51	0.11	17.99	51.61	28.78	0	0	0	0	0	98.49	0	915	100.00	Laser
0	1.93	2.38	17.61	39.88	38.19	0	0	0	0	0	98.07	0	945	100.00	Laser
0	0.90	1.87	4.42	23.02	31.52	17.35	13.14	6.64	0.96	0	78.18	20.74	1050	99.82	Sieve
0	0.47	1.13	4.01	8.37	14.97	23.01	14.06	17.58	16.12	0	51.49	47.76	1150	99.72	Sieve
0	0.65	1.08	3.02	9.51	13.61	14.70	24.16	25.51	7.52	0	41.92	57.19	1200	99.76	Sieve
0	0.56	1.24	6.01	15.57	21.46	19.45	17.95	11.23	6.34	0	63.73	35.52	1300	99.81	Sieve
0	1.04	1.85	9.01	21.78	28.35	22.45	8.8	5.48	1.12	0	83.44	15.4	1350	99.88	Sieve

Kearney 11

Clay	Silt	V. Fine	Fine	Medium	Coarse	V. Coarse	>2mm	>4mm	>8mm	>16mm	Sand Total	>2mm total	Depth	%	Method
0-2µm	2-63µm	63-125µm	125-250µm	250-500µm	500µm-1mm	1mm-2mm	2mm-4mm	4mm-8mm	8mm-16mm	>16mm	V. Fine-V. Coarse	Gravel	cm		
0	65.05	19.59	10.74	4.27	0.36	0	0	0	0	0	34.95	0	15	100.00	Laser
9.39	81.91	7.50	0.11	0.77	0.32	0	0	0	0	0	8.70	0	45	100.00	Laser
0.00	65.14	17.29	10.93	4.86	1.78	0	0	0	0	0	34.86	0	75	100.00	Laser
3.45	53.44	21.85	15.14	5.50	0.61	0	0	0	0	0	43.11	0	105	100.00	Laser
0	70.22	17.79	7.67	2.93	1.40	0	0	0	0	0	29.78	0	135	100.00	Laser
0	4.86	11.66	38.73	34.93	9.83	0	0	0	0	0	95.14	0	165	100.00	Laser
0	3.11	0.44	21.56	49.06	25.83	0	0	0	0	0	96.89	0	195	100.00	Laser
0	0.38	1.29	11.74	36.23	21.88	9.43	8.68	6.45	1.5	2.14	80.57	18.77	200	99.72	Sieve
0	3.46	1.32	19.50	43.29	32.43	0	0	0	0	0	96.54	0	225	100.00	Laser
0	0.61	1.09	5.27	19.09	21.97	11.34	9.05	7.89	5.52	18.1	58.76	40.56	250	99.93	Sieve
0	1.78	0.07	8.01	39.37	50.77	0	0	0	0	0	98.22	0	255	100.00	Laser
0	0.36	0.56	2.75	19.02	28.18	14.98	9.65	7.85	6.28	10.06	65.49	33.84	300	99.69	Sieve
0	0.72	1.45	4.33	15.12	31.32	24.89	14.21	4.38	1.54	2	77.11	22.13	550	99.96	Laser
0	1.93	0.83	18.23	49.09	29.91	0	0	0	0	0	98.07	0	585	100.00	Laser
0	1.07	3.52	9.68	25.31	10.72	7.26	9.22	11.43	4.85	16.62	56.49	42.12	600	99.68	Sieve
0	0.54	0.68	3.46	17.50	25.95	24.6	16.32	6.84	4.06	0	72.19	27.22	700	99.95	Sieve
0	0.25	0.57	4.65	13.58	24.66	27.76	14.94	6.5	3.64	3.13	71.22	28.21	750	99.68	Sieve
0	0.94	0.00	8.09	47.44	43.53	0	0	0	0	0	99.06	0	885	100.00	Laser
0	0.17	0.48	6.92	51.50	32.97	6.53	0.79	0.17	0	0	98.40	0.96	900	99.53	Sieve
0	0.35	0.59	5.06	21.12	21.05	21.43	17	9.29	2.04	1.53	69.25	29.86	1000	99.46	Sieve
0	2.41	2.30	5.03	9.14	14.73	17.85	28.03	16.38	3.74	0	49.05	48.15	1050	99.61	Sieve
0	0.19	0.35	1.54	7.35	11.27	12.63	23.4	31.41	11.8	0	33.14	66.61	1150	99.94	Sieve

Kearney 12

Clay	Silt	V. Fine	Fine	Medium	Coarse	V. Coarse	>2mm	>4mm	>8mm	>16mm	Sand Total	>2mm total	Depth	%	Method
0-2µm	2-63µm	63-125µm	125-250µm	250-500µm	500µm-1mm	1mm-2mm	2mm-4mm	4mm-8mm	8mm-16mm	>16mm	V. Fine V.Coarse	Gravel			
0	79.43	14.21	5.90	0.46	0.00	0	0	0	0	0	20.57	0	15	100.00	Laser
0	80.21	12.36	3.77	3.18	0.49	0	0	0	0	0	19.79	0	45	100.00	Laser
0	31.71	9.60	5.80	18.38	34.51	0	0	0	0	0	68.29	0	75	100.00	Laser
0	5.02	4.34	14.22	37.29	39.13	0	0	0	0	0	94.98	0	105	100.00	Laser
0	0.42	1.78	10.98	27.39	20.38	12.78	9.64	9.01	7.4	0	73.31	26.05	150	99.78	Sieve
0	0.16	0.39	3.44	37.05	25.85	13.42	9.91	4.61	1.92	2.98	80.15	19.42	200	99.73	Sieve
0	0.59	0.74	2.17	12.37	23.83	16.81	12.09	8.52	7.05	15.44	55.92	43.1	300	99.61	Sieve
0	2.24	2.24	5.74	28.06	26.82	15.29	9.76	5.71	3.85	0	78.15	19.32	350	99.71	Sieve
0	2.54	30.64	57.43	9.38	0.00	0	0	0	0	0	97.46	0	405	100.00	Laser
0	1.80	2.15	5.97	10.56	16.62	16.22	14.45	10.03	9.42	12.71	51.52	46.61	450	99.93	Sieve
0	5.20	8.93	18.78	11.89	22.99	17.17	9.47	4.88	0.44	0	79.76	14.79	500	99.75	Sieve
0	1.41	3.03	16.11	38.41	11.04	10.03	11.48	4.52	3.87	0	78.62	19.87	600	99.90	Sieve
0	0.26	0.47	1.39	4.84	11.10	18.46	26.71	23.66	10.48	2.6	36.26	63.45	700	99.97	Sieve
0	0.32	1.67	9.71	24.65	33.43	18.24	5.88	4.51	1.28	0	87.70	11.67	850	99.69	Sieve
0	0.64	1.15	4.69	27.70	24.98	15.34	12.26	3.72	1.85	7.57	73.86	25.4	900	99.90	Sieve
0	0.34	1.48	9.18	17.15	24.28	17.4	11.73	10.45	5.35	2.37	69.49	29.9	1000	99.73	Sieve
0	0.62	0.85	3.07	17.16	23.61	18.06	11.5	5.32	0.93	18.82	62.75	36.57	1050	99.94	Sieve
0	0.12	0.19	1.31	11.32	15.91	28.67	30.29	8.89	3.26	0	57.40	42.44	1200	99.96	Sieve
0	1.77	1.96	4.92	13.61	19.12	14.7	16.88	17.58	9.25	0	54.31	43.71	1250	99.79	Sieve
0	0.11	0.24	0.78	5.19	16.22	25.81	31.23	17.26	3.14	0	48.24	51.63	1300	99.98	Sieve
0	0.19	0.35	1.70	8.12	17.10	18.86	25.29	22.29	5.97	0	46.13	53.55	1350	99.87	Sieve
0	0.46	0.94	5.20	10.90	21.23	27.04	21.81	10.79	1.46	0	65.31	34.06	1400	99.83	Sieve
0	0.13	0.19	1.33	6.88	17.34	21.04	32.14	14.89	2.13	3.85	46.78	53.01	1500	99.92	Sieve
0	0.35	0.67	2.95	22.87	30.02	22.58	14.78	5	0.55	0	79.09	20.33	1550	99.77	Sieve
0	0.49	2.42	10.30	35.99	22.81	11.93	8.58	6.16	0.98	0	83.45	15.72	1600	99.66	Sieve
0	0.53	2.75	12.74	30.53	25.79	17.04	7.35	2.95	0	0	71.81	27.34	1650	99.68	Sieve

9 Appendix Two: OSL Data

9.1 Hershey East OSL Data

9.1.1 UNL - 3932
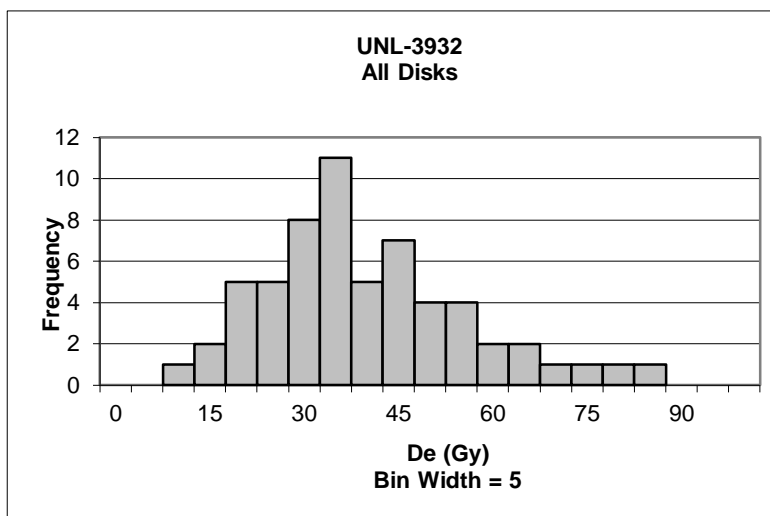
#	De	Error	Age	+/- 1 σ	#	De	Error	Age	+/- 1 σ
1	50.189	2.16	16.110	1.36	31	26.117	0.26	8.383	0.72
2	45.078	1.42	14.469	0.92	32	16.669	0.59	5.350	1.54
3	68.403	2.83	21.956	2.93	33	26.241	0.79	8.423	0.71
4	48.915	0.66	15.701	1.25	34	60.483	3.32	19.414	2.25
5	36.128	1.11	11.596	0.14	35	25.982	0.42	8.340	0.73
6	23.404	0.85	7.512	0.96	36	23.376	0.31	7.503	0.96
7	23.715	0.86	7.612	0.93	37	44.139	0.60	14.168	0.83
8	42.189	0.63	13.542	0.67	38	34.189	0.52	10.974	0.02
9	17.535	0.11	5.628	1.46	39	23.653	1.54	7.592	0.93
10	83.103	1.09	26.674	4.20	40	31.886	0.41	10.235	0.22
11	36.257	0.99	11.638	0.15	41	64.678	2.28	20.760	2.61
12	8.858	1.49	2.843	2.21	42	26.405	0.55	8.475	0.70
13	38.008	2.54	12.200	0.31	43	72.177	2.52	23.167	3.26
14	22.842	0.93	7.332	1.00	44	43.179	0.32	13.860	0.75
15	14.907	0.37	4.785	1.69	45	27.476	0.50	8.819	0.60
16	30.367	0.70	9.747	0.35	46	42.258	2.58	13.564	0.67
17	45.718	1.35	14.674	0.97	47	28.258	0.33	9.070	0.54
18	32.278	0.62	10.361	0.19	48	56.741	1.14	18.213	1.92
19	31.743	0.48	10.189	0.24	49	42.755	0.13	13.723	0.72
20	78.985	0.33	25.352	3.84	50	41.777	0.74	13.409	0.63
21	16.083	1.38	5.162	1.59	51	37.222	0.20	11.947	0.24
22	32.440	1.81	10.413	0.18	52	32.138	1.41	10.316	0.20
23	26.305	1.00	8.443	0.71	53	33.779	1.45	10.842	0.06
24	26.349	1.10	8.458	0.70	54	13.787	1.31	4.425	1.79
25	57.625	2.82	18.496	2.00	55	30.640	0.57	9.835	0.33
26	19.708	0.36	6.326	1.28	56	50.469	0.44	16.199	1.38
27	17.786	0.72	5.709	1.44	57	30.572	0.27	9.813	0.34
28	54.514	1.35	17.498	1.73	58	47.273	2.19	15.173	1.11
29	43.324	0.12	13.906	0.76	59	33.800	0.52	10.849	0.06
30	54.345	1.55	17.444	1.72	60	36.198	1.09	11.619	0.15

UNL-3932
Weighted Disks
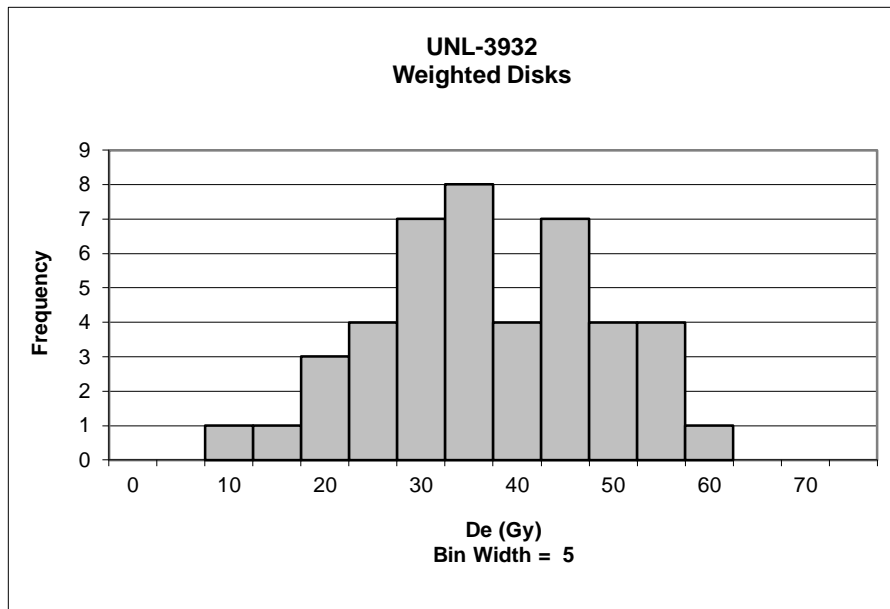
#	De	Error	Age	+/- 1 σ	#	De	Error	Age	+/- 1 σ
1	50.189	2.16	16.110	1.36	23	25.982	0.42	8.340	0.73
2	45.078	1.42	14.469	0.92	24	23.376	0.31	7.503	0.96
3	48.915	0.66	15.701	1.25	25	44.139	0.60	14.168	0.83
4	36.128	1.11	11.596	0.14	26	34.189	0.52	10.974	0.02
5	23.404	0.85	7.512	0.96	27	23.653	1.54	7.592	0.93
6	23.715	0.86	7.612	0.93	28	31.886	0.41	10.235	0.22
7	42.189	0.63	13.542	0.67	29	26.405	0.55	8.475	0.70
8	17.535	0.11	5.628	1.46	30	43.179	0.32	13.860	0.75
9	36.257	0.99	11.638	0.15	31	27.476	0.50	8.819	0.60
10	8.858	1.49	2.843	2.21	32	42.258	2.58	13.564	0.67
11	45.718	1.35	14.674	0.97	33	28.258	0.33	9.070	0.54
12	32.278	0.62	10.361	0.19	34	56.741	1.14	18.213	1.92
13	31.743	0.48	10.189	0.24	35	42.755	0.13	13.723	0.72
14	32.440	1.81	10.413	0.18	36	41.777	0.74	13.409	0.63
15	26.349	1.10	8.458	0.70	37	37.222	0.20	11.947	0.24
16	19.708	0.36	6.326	1.28	38	33.779	1.45	10.842	0.06
17	54.514	1.35	17.498	1.73	39	13.787	1.31	4.425	1.79
18	43.324	0.12	13.906	0.76	40	30.640	0.57	9.835	0.33
19	54.345	1.55	17.444	1.72	41	50.469	0.44	16.199	1.38
20	26.117	0.26	8.383	0.72	42	47.273	2.19	15.173	1.11
21	16.669	0.59	5.350	1.54	43	33.800	0.52	10.849	0.06
22	26.241	0.79	8.423	0.71	44	36.198	1.09	11.619	0.15

UNL 3932 (n=44)

Central value = 32.5 ± 1.8 (1σ)

Dispersion = 37 %

Minimum age: 17.61±0.11

9.1.2   UNL – 3935
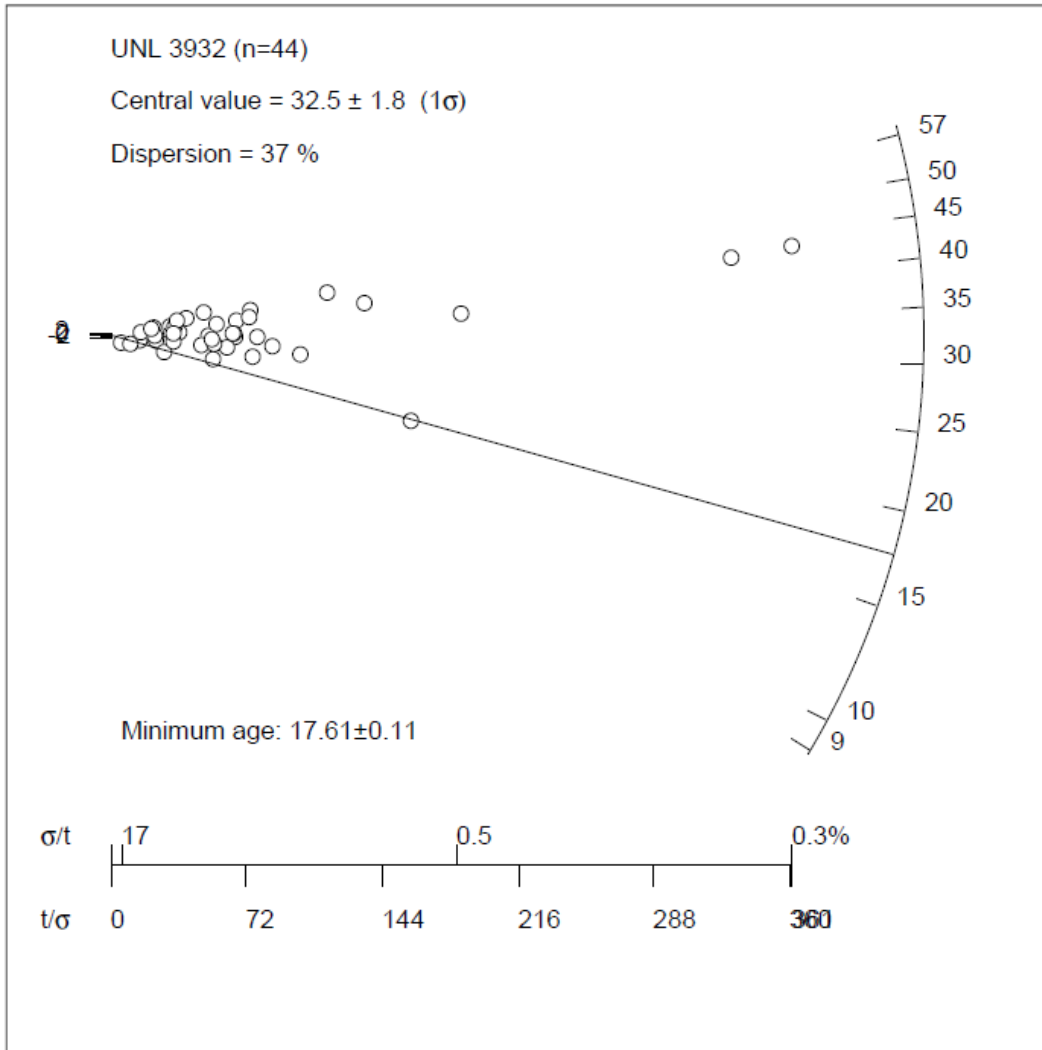
UNL-3935
All Disks
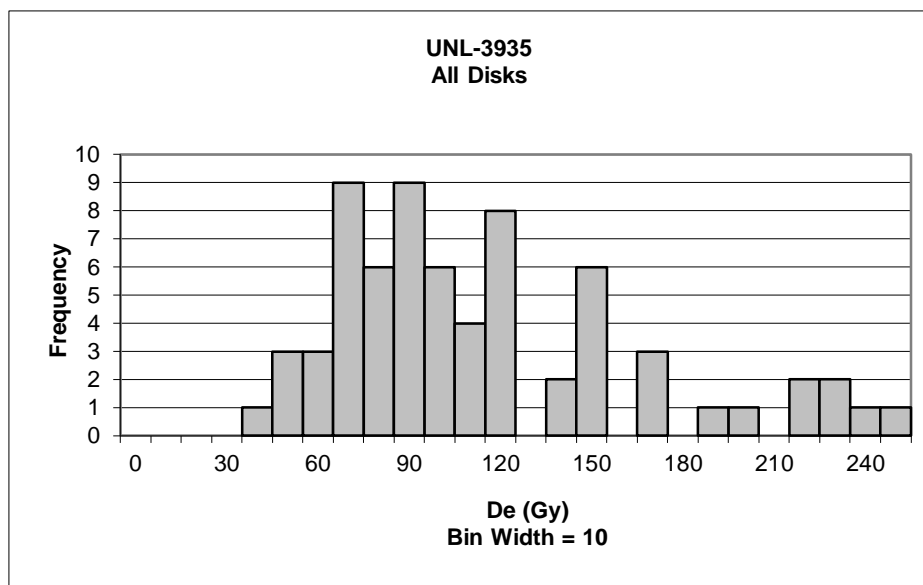
#	De	Error	Age	+/- 1 σ	#	De	Error	Age	+/- 1 σ
1	66.178	4.76	37.022	0.87	28	110.742	6.05	61.952	0.32
2	149.050	8.71	83.383	1.34	29	86.350	1.08	48.307	0.33
3	30.586	25.70	17.110	1.82	30	69.866	12.57	39.085	0.77
4	77.642	8.42	43.435	0.56	31	66.512	5.03	37.209	0.86
5	69.292	10.64	38.764	0.79	32	83.538	7.52	46.733	0.41
6	87.921	23.57	49.186	0.29	33	186.179	12.76	104.154	2.33
7	118.352	20.27	66.210	0.52	34	48.021	62.73	26.864	1.35
8	82.370	4.01	46.080	0.44	35	134.589	13.31	75.293	0.96
9	78.628	11.37	43.987	0.54	36	167.957	3.69	93.960	1.85
10	101.148	23.58	56.585	0.06	37	211.648	7.89	118.402	3.01
11	61.451	25.99	34.378	0.99	38	95.376	11.33	53.356	0.09
12	111.748	22.28	62.515	0.35	39	54.405	35.42	30.436	1.18
13	194.482	15.21	108.799	2.55	40	140.484	5.63	78.591	1.11
14	101.051	1.66	56.531	0.06	41	217.107	5.42	121.456	3.16
15	224.291	18.86	125.475	3.35	42	105.548	9.03	59.047	0.18
16	56.687	29.22	31.712	1.12	43	77.913	18.14	43.587	0.56
17	106.751	26.20	59.719	0.21	44	727.368	49.28	406.910	16.77
18	1170.238	53.91	654.665	28.58	45	131.332	5.69	73.471	0.87
19	111.643	42.34	62.456	0.34	46	81.883	13.38	45.808	0.45
20	141.030	13.68	78.896	1.13	47	45.052	9.82	25.203	1.43
21	2170.988	36.20	1214.513	55.28	48	232.899	8.48	130.290	3.58
22	67.111	12.23	37.544	0.84	49	43.604	0.25	24.393	1.47
23	98.073	9.42	54.865	0.02	50	242.587	114.60	135.710	3.84
24	1482.296	100.54	829.239	36.91	51	167.741	10.50	93.839	1.84
25	257.387	6.77	143.990	4.23	52	54.887	16.84	30.706	1.17
26	2751.598	62.57	1539.322	70.77	53	298.153	14.97	166.796	5.32
27	145.560	7.63	81.430	1.25	54	141.601	10.80	79.215	1.14

UNL-3935
Weighted Disks

De (Gy)
Bin Width = 10
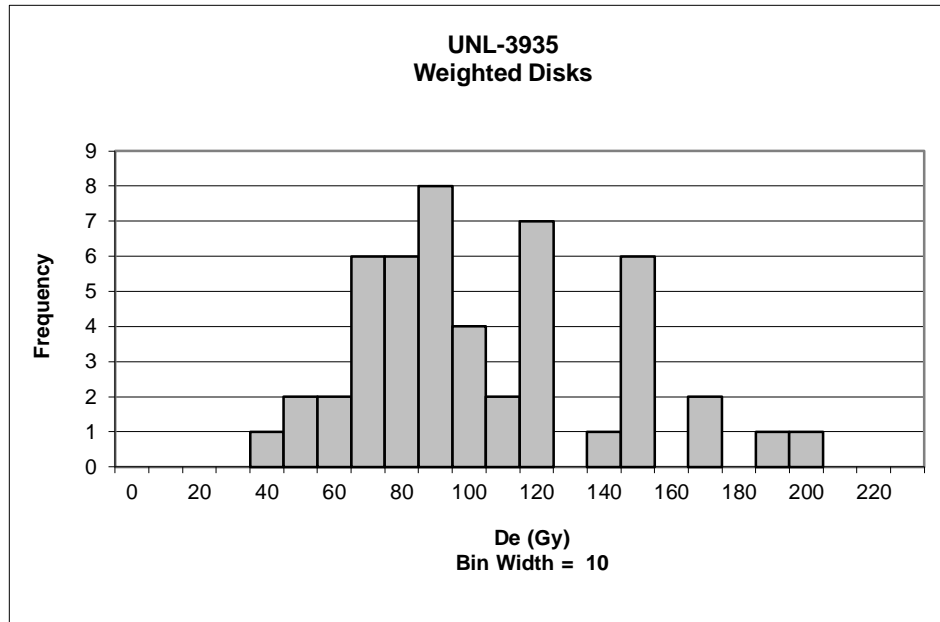
#	De	Error	Age	+/- 1 σ	#	De	Error	Age	+/- 1 σ
1	66.178	4.76	37.022	0.87	25	54.405	35.42	30.436	1.18
2	149.050	8.71	83.383	1.34	26	140.484	5.63	78.591	1.11
3	30.586	25.70	17.110	1.82	27	105.548	9.03	59.047	0.18
4	77.642	8.42	43.435	0.56	28	77.913	18.14	43.587	0.56
5	118.352	20.27	66.210	0.52	29	131.332	5.69	73.471	0.87
6	82.370	4.01	46.080	0.44	30	81.883	13.38	45.808	0.45
7	78.628	11.37	43.987	0.54	31	43.604	0.25	24.393	1.47
8	61.451	25.99	34.378	0.99	32	167.741	10.50	93.839	1.84
9	111.748	22.28	62.515	0.35	33	141.601	10.80	79.215	1.14
10	194.482	15.21	108.799	2.55	34	110.371	4.51	61.745	0.31
11	101.051	1.66	56.531	0.06	35	76.211	2.50	42.635	0.60
12	56.687	29.22	31.712	1.12	36	72.923	12.58	40.795	0.69
13	111.643	42.34	62.456	0.34	37	80.885	4.00	45.249	0.48
14	141.030	13.68	78.896	1.13	38	147.948	13.36	82.766	1.31
15	67.111	12.23	37.544	0.84	39	111.805	14.32	62.547	0.35
16	145.560	7.63	81.430	1.25	40	95.766	5.88	53.574	0.08
17	110.742	6.05	61.952	0.32	41	116.915	4.43	65.406	0.48
18	86.350	1.08	48.307	0.33	42	67.463	39.56	37.741	0.83
19	66.512	5.03	37.209	0.86	43	91.267	1.85	51.057	0.20
20	83.538	7.52	46.733	0.41	44	83.235	3.85	46.564	0.41
21	186.179	12.76	104.154	2.33	45	81.386	3.00	45.530	0.46
22	48.021	62.73	26.864	1.35	46	96.507	1.97	53.989	0.06
23	167.957	3.69	93.960	1.85	47	70.156	30.97	39.248	0.76
24	95.376	11.33	53.356	0.09	48	89.725	20.30	50.195	0.24
					49	63.226	23.25	35.370	0.95

UNL 3935 (n=49)

Central value = 99.5 ± 5 (1σ)

Dispersion = 31 %

Minimum age: 43.47±0.29

9.1.3 UNL – 3937

UNL-3937
All Disks

De (Gy)
Bin Width = 3 Gy
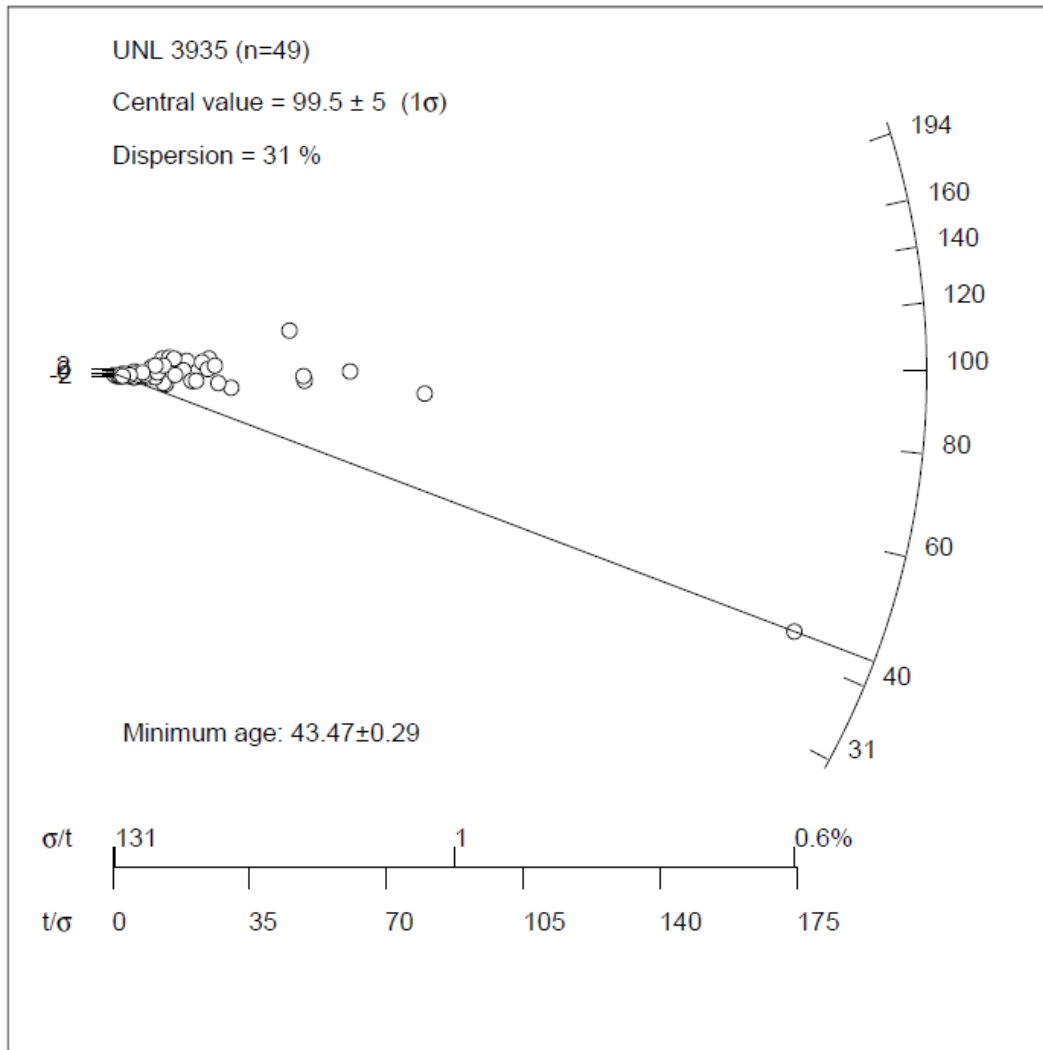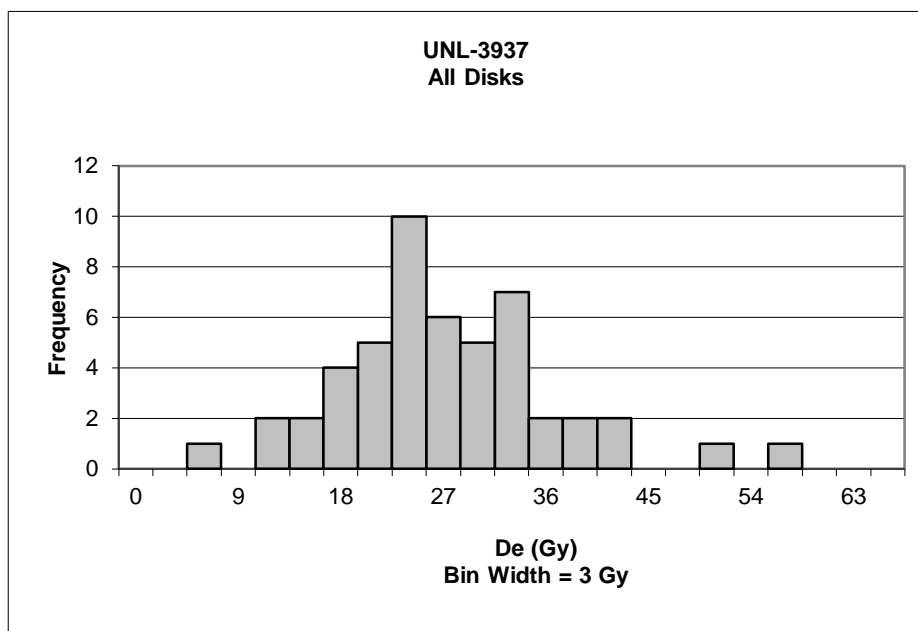
#	De	Error	Age	+/- 1 σ	#	De	Error	Age	+/- 1 σ
1	11.181	2.27	4.877	1.69	26	30.880	0.65	13.470	0.50
2	18.074	1.87	7.884	0.92	27	29.024	0.72	12.661	0.29
3	22.969	4.27	10.020	0.38	28	30.317	0.21	13.225	0.43
4	15.605	2.83	6.807	1.20	29	12.154	0.44	5.302	1.58
5	31.464	5.72	13.726	0.56	30	14.178	0.66	6.185	1.36
6	29.158	0.12	12.719	0.31	31	41.664	0.44	18.175	1.69
7	17.922	3.08	7.818	0.94	32	23.647	0.51	10.315	0.31
8	5.784	2.13	2.523	2.29	33	30.110	1.33	13.135	0.41
9	23.442	0.92	10.226	0.33	34	55.063	0.88	24.020	3.18
10	16.486	0.55	7.191	1.10	35	24.668	0.97	10.761	0.19
11	20.032	0.62	8.738	0.71	36	30.437	0.58	13.277	0.45
12	26.088	0.57	11.380	0.04	37	37.125	0.71	16.195	1.19
13	32.050	0.21	13.981	0.63	38	21.878	0.60	9.544	0.50
14	23.164	0.46	10.105	0.36	39	21.800	0.87	9.510	0.51
15	24.138	0.09	10.529	0.25	40	30.085	0.76	13.124	0.41
16	21.577	0.81	9.412	0.54	41	20.722	0.55	9.040	0.63
17	36.961	1.03	16.123	1.17	42	28.553	1.84	12.455	0.24
18	20.624	0.21	8.997	0.64	43	11.449	0.39	4.994	1.66
19	40.254	0.67	17.560	1.54	44	23.659	1.34	10.321	0.30
20	33.724	0.47	14.711	0.81	45	25.938	0.35	11.315	0.05
21	20.478	1.90	8.933	0.66	46	24.913	1.18	10.868	0.17
22	24.697	0.74	10.773	0.19	47	16.031	0.41	6.993	1.15
23	50.557	0.01	22.055	2.68	48	21.277	0.35	9.281	0.57
24	29.568	0.37	12.898	0.35	49	27.183	48.18	11.858	0.09
25	21.852	0.40	9.532	0.50	50	35.556	0.68	15.510	1.01

UNL-3937
Weighted Disks

Frequency vs De (Gy), Bin Width = 3 Gy
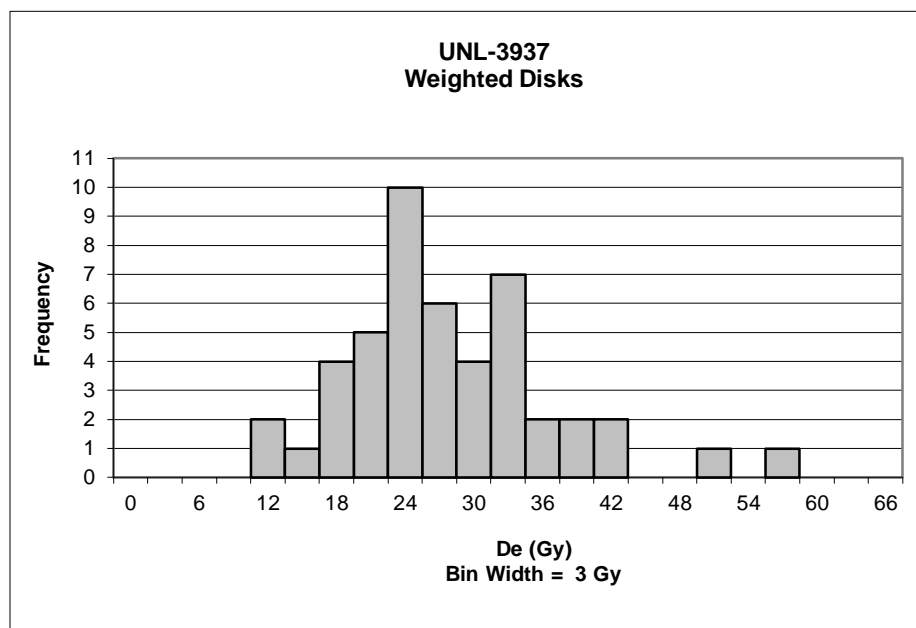
#	De	Error	Age	+/- 1 σ	#	De	Error	Age	+/- 1 σ
1	11.181	2.27	4.877	1.69	25	30.880	0.65	13.470	0.50
2	18.074	1.87	7.884	0.92	26	29.024	0.72	12.661	0.29
3	22.969	4.27	10.020	0.38	27	30.317	0.21	13.225	0.43
4	15.605	2.83	6.807	1.20	28	14.178	0.66	6.185	1.36
5	31.464	5.72	13.726	0.56	29	41.664	0.44	18.175	1.69
6	29.158	0.12	12.719	0.31	30	23.647	0.51	10.315	0.31
7	17.922	3.08	7.818	0.94	31	30.110	1.33	13.135	0.41
8	23.442	0.92	10.226	0.33	32	55.063	0.88	24.020	3.18
9	16.486	0.55	7.191	1.10	33	24.668	0.97	10.761	0.19
10	20.032	0.62	8.738	0.71	34	30.437	0.58	13.277	0.45
11	26.088	0.57	11.380	0.04	35	37.125	0.71	16.195	1.19
12	32.050	0.21	13.981	0.63	36	21.878	0.60	9.544	0.50
13	23.164	0.46	10.105	0.36	37	21.800	0.87	9.510	0.51
14	24.138	0.09	10.529	0.25	38	30.085	0.76	13.124	0.41
15	21.577	0.81	9.412	0.54	39	20.722	0.55	9.040	0.63
16	36.961	1.03	16.123	1.17	40	28.553	1.84	12.455	0.24
17	20.624	0.21	8.997	0.64	41	11.449	0.39	4.994	1.66
18	40.254	0.67	17.560	1.54	42	23.659	1.34	10.321	0.30
19	33.724	0.47	14.711	0.81	43	25.938	0.35	11.315	0.05
20	20.478	1.90	8.933	0.66	44	24.913	1.18	10.868	0.17
21	24.697	0.74	10.773	0.19	45	16.031	0.41	6.993	1.15
22	50.557	0.01	22.055	2.68	46	21.277	0.35	9.281	0.57
23	29.568	0.37	12.898	0.35	47	35.556	0.68	15.510	1.01
24	21.852	0.40	9.532	0.50					

UNL 3937 (n=47)

Central value = 25.2 ± 1.2 (1σ)

Dispersion = 32 %

Minimum age: 12.11±0.43

σ/t   20   0.04   0.02%

t/σ   0   1011   2022   3033   4044   5056

9.1.4   UNL – 3938
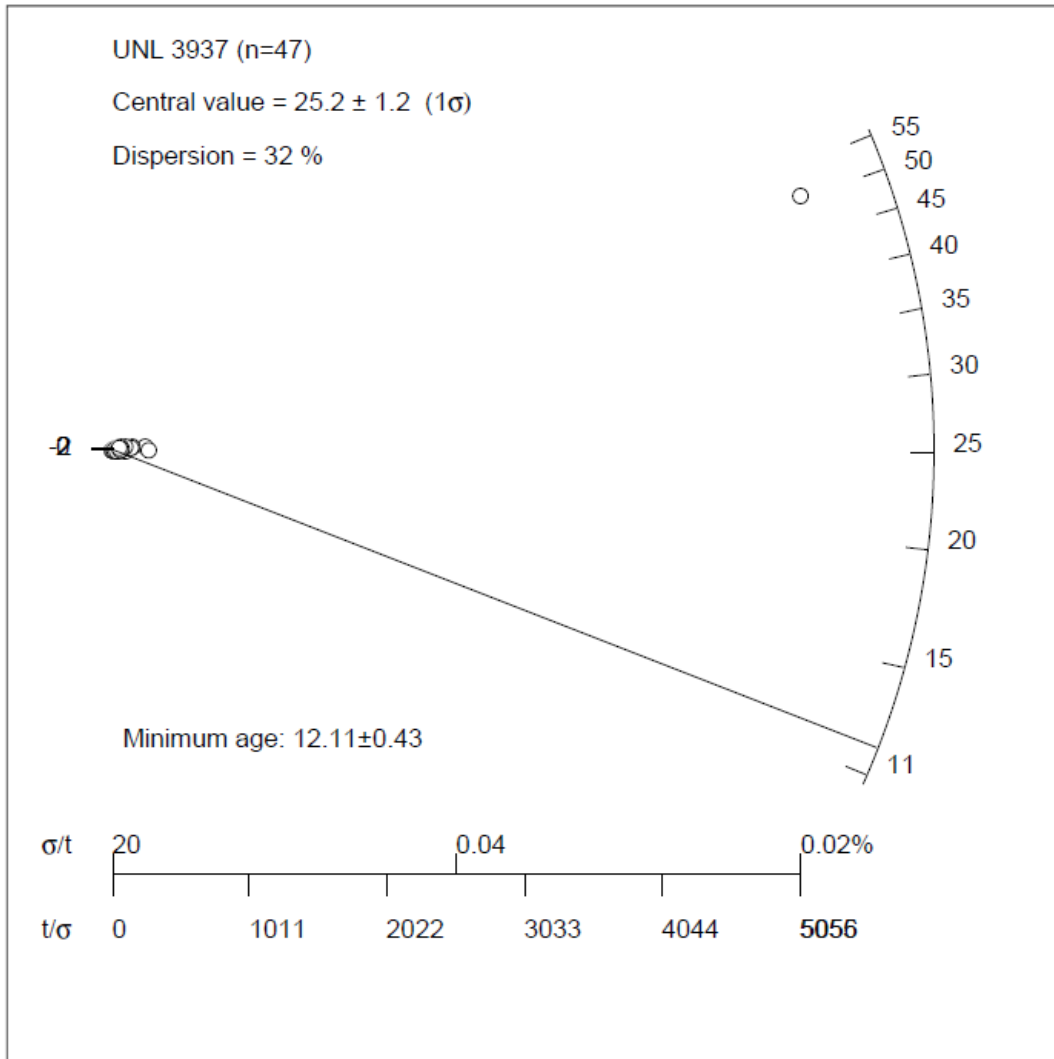
**UNL-3938
All Disks**
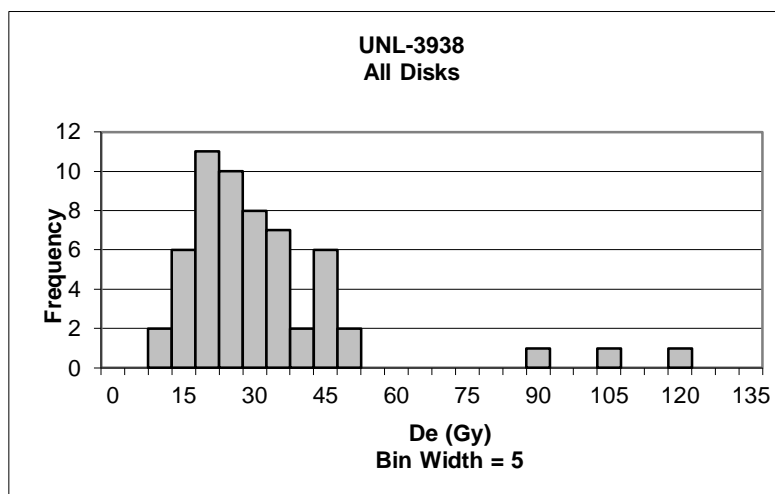
#	De	Error	Age	+/- 1 σ	#	De	Error	Age	+/- 1 σ
1	18.679	0.51	5.604	0.78	36	20.190	1.78	6.058	0.63
2	9.093	5.69	2.728	1.71	37	20.039	1.35	6.012	0.65
3	14.866	1.34	4.460	1.15	38	25.352	1.28	7.606	0.13
4	12.727	1.00	3.819	1.35	39	18.020	1.20	5.407	0.84
5	87.132	1.88	26.142	5.85	40	20.001	4.08	6.001	0.65
6	14.712	1.39	4.414	1.16	41	17.925	0.44	5.378	0.85
7	19.840	0.80	5.953	0.66	42	28.778	0.74	8.634	0.20
8	26.227	1.31	7.869	0.05	43	13.398	1.45	4.020	1.29
9	38.354	1.30	11.507	1.13	44	14.140	2.01	4.242	1.22
10	44.648	0.65	13.396	1.74	45	21.456	1.20	6.437	0.51
11	42.692	0.65	12.809	1.55	46	15.769	0.65	4.731	1.06
12	44.017	1.15	13.206	1.68	47	17.413	0.66	5.224	0.90
13	17.468	0.61	5.241	0.89	48	19.612	1.86	5.884	0.69
14	24.584	0.58	7.376	0.21	49	19.205	0.43	5.762	0.73
15	44.763	0.90	13.430	1.75	50	21.277	0.86	6.384	0.53
16	19.044	0.63	5.714	0.74	51	23.506	1.07	7.052	0.31
17	25.625	0.38	7.688	0.10	52	14.970	0.78	4.491	1.14
18	100.726	4.56	30.220	7.17	53	34.486	1.65	10.347	0.75
19	32.614	1.90	9.785	0.57	54	33.580	0.28	10.075	0.67
20	42.536	1.99	12.762	1.53	55	37.438	1.49	11.233	1.04
21	30.972	0.33	9.292	0.41	56	257.035	2.71	77.117	22.31
22	24.284	0.51	7.286	0.23	57	684.170	14.34	205.270	63.67
23	30.442	1.31	9.134	0.36	58	1512.071	18.54	453.663	143.85
24	45.784	0.80	13.737	1.85	59	947.636	24.01	284.317	89.19
25	32.972	1.02	9.892	0.61	60	1225.968	24.67	367.824	116.15
26	20.154	1.41	6.047	0.63	61	763.946	15.66	229.205	71.40
27	26.860	0.85	8.059	0.02	62	49.300	1.93	14.791	2.19
28	17.238	0.62	5.172	0.92	63	402.520	7.15	120.767	36.40
29	26.230	2.84	7.870	0.05	64	200.027	3.42	60.014	16.79
30	27.217	0.14	8.166	0.05	65	1158.566	12.93	347.602	109.62
31	20.403	0.59	6.121	0.61	66	194.389	0.90	58.322	16.24
32	42.666	2.49	12.801	1.55	67	209.717	17.90	62.921	17.72
33	30.945	0.27	9.284	0.41	68	118.380	5.85	35.517	8.88
34	28.689	1.13	8.608	0.19	69	779.222	24.06	233.788	72.88
35	6.849	0.99	2.055	1.92	70	411.641	23.35	123.504	37.28

UNL-3938
Weighted Disks

De (Gy)
Bin Width = 3
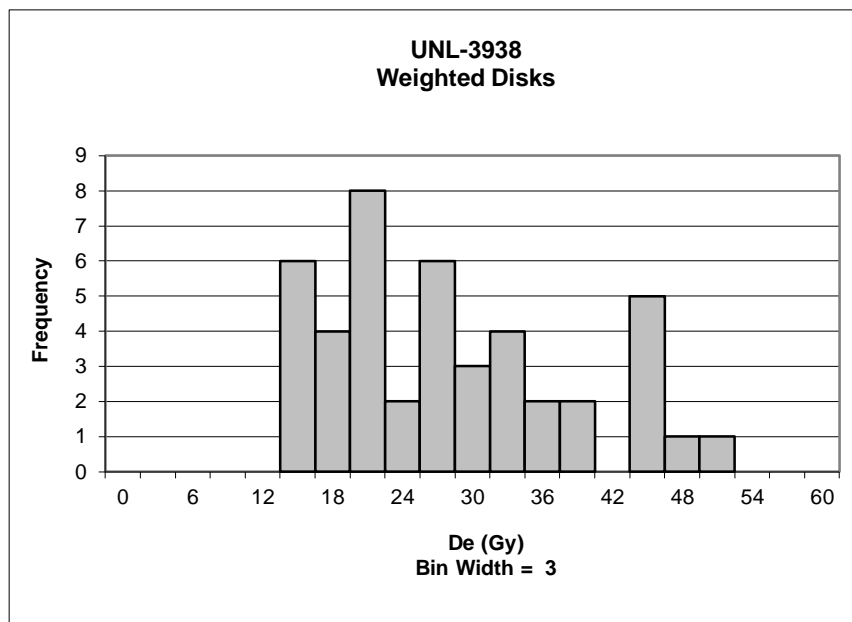
#	De	Error	Age	+/- 1 σ	#	De	Error	Age	+/- 1 σ
1	14.866	1.34	4.460	1.15	23	20.403	0.59	6.121	0.61
2	12.727	1.00	3.819	1.35	24	42.666	2.49	12.801	1.55
3	14.712	1.39	4.414	1.16	25	30.945	0.27	9.284	0.41
4	19.840	0.80	5.953	0.66	26	28.689	1.13	8.608	0.19
5	38.354	1.30	11.507	1.13	27	20.190	1.78	6.058	0.63
6	44.648	0.65	13.396	1.74	28	20.039	1.35	6.012	0.65
7	42.692	0.65	12.809	1.55	29	25.352	1.28	7.606	0.13
8	44.017	1.15	13.206	1.68	30	18.020	1.20	5.407	0.84
9	17.468	0.61	5.241	0.89	31	20.001	4.08	6.001	0.65
10	24.584	0.58	7.376	0.21	32	28.778	0.74	8.634	0.20
11	44.763	0.90	13.430	1.75	33	13.398	1.45	4.020	1.29
12	19.044	0.63	5.714	0.74	34	14.140	2.01	4.242	1.22
13	25.625	0.38	7.688	0.10	35	15.769	0.65	4.731	1.06
14	30.972	0.33	9.292	0.41	36	17.413	0.66	5.224	0.90
15	24.284	0.51	7.286	0.23	37	19.205	0.43	5.762	0.73
16	30.442	1.31	9.134	0.36	38	21.277	0.86	6.384	0.53
17	45.784	0.80	13.737	1.85	39	23.506	1.07	7.052	0.31
18	32.972	1.02	9.892	0.61	40	14.970	0.78	4.491	1.14
19	26.860	0.85	8.059	0.02	41	34.486	1.65	10.347	0.75
20	17.238	0.62	5.172	0.92	42	33.580	0.28	10.075	0.67
21	26.230	2.84	7.870	0.05	43	37.438	1.49	11.233	1.04
22	27.217	0.14	8.166	0.05	44	49.300	1.93	14.791	2.19

UNL 3938 (n=44)

Central value = 25 ± 1.4 (1σ)

Dispersion = 37 %

Minimum age: 14.77±0.83

9.1.5 UNL – 3939
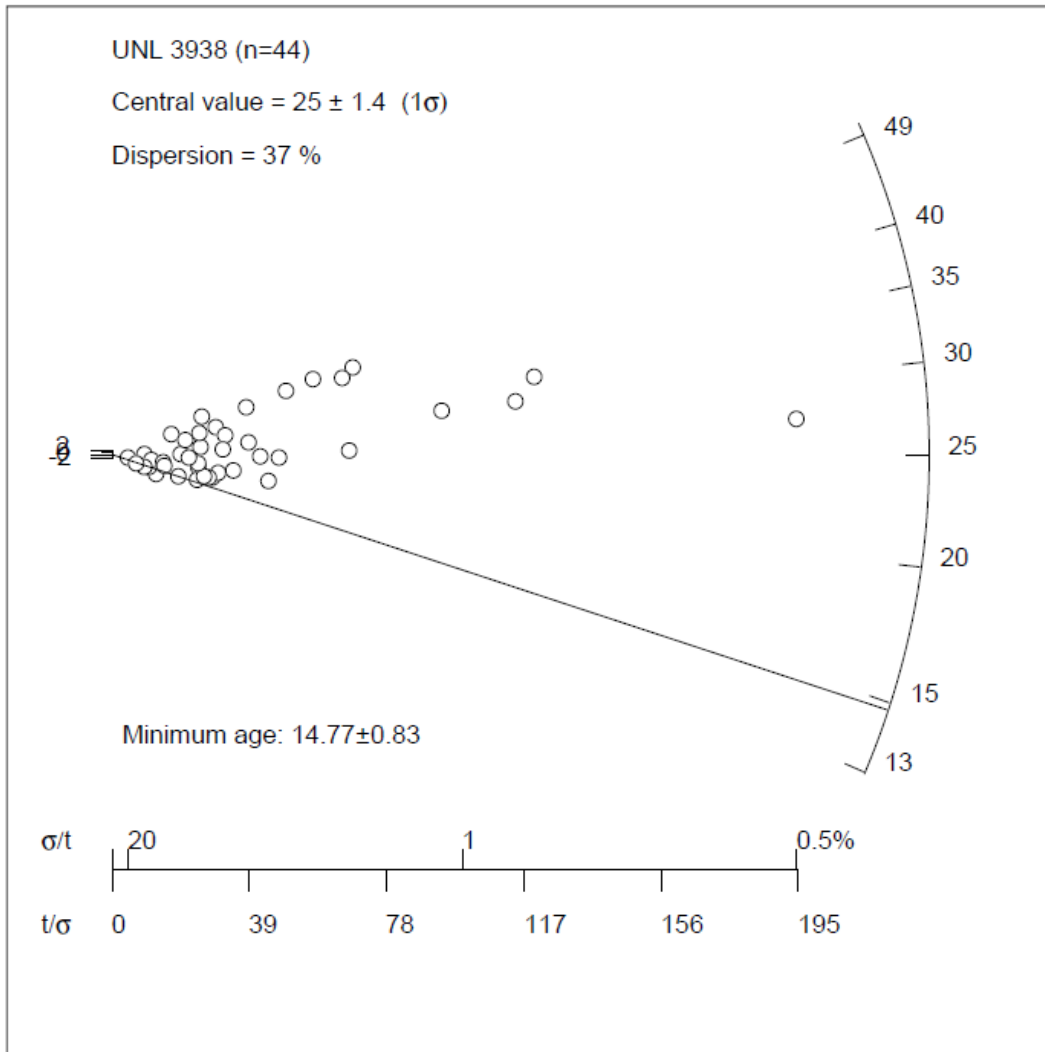
UNL-3939
All Disks
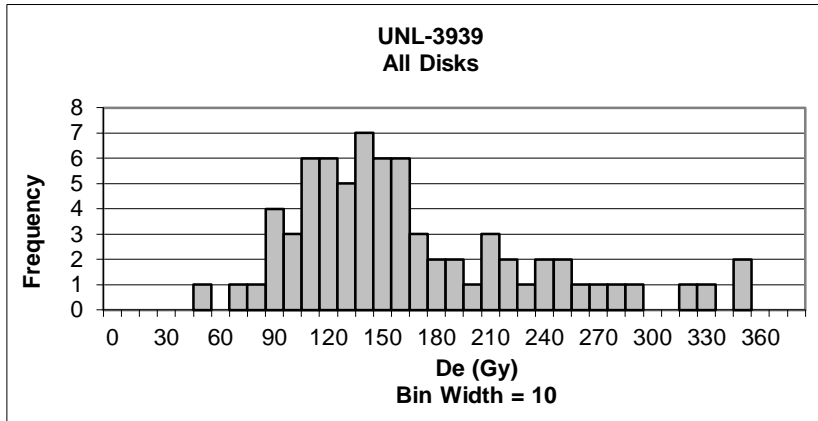
#	De	Error	Age	+/- 1 σ	#	De	Error	Age	+/- 1 σ
1	127.597	18.00	75.323	0.15	47	1808.681	27.18	1067.701	62.80
2	61.956	0.52	36.574	2.29	48	385.748	15.62	227.715	9.77
3	90.011	2.72	53.135	1.25	49	186.322	7.08	109.990	2.34
4	140.867	15.76	83.157	0.65	50	168.165	6.84	99.271	1.66
5	103.814	14.59	61.284	0.73	51	129.919	16.33	76.694	0.24
6	687.012	0.12	405.557	21.00	52	77.282	4.65	45.621	1.72
7	105.198	8.14	62.100	0.68	53	228.364	4.28	134.808	3.91
8	186.579	8.89	110.141	2.35	54	137.218	14.32	81.002	0.51
9	110.165	11.18	65.033	0.50	55	1678.988	89.22	991.140	57.97
10	81.638	0.89	48.193	1.56	56	194.273	4.91	114.684	2.64
11	216.226	2.50	127.643	3.46	57	148.515	6.11	87.671	0.93
12	1068.499	11.02	630.757	35.22	58	131.346	8.16	77.536	0.29
13	98.756	8.88	58.298	0.92	59	135.324	10.75	79.884	0.44
14	103.191	2.39	60.916	0.76	60	165.091	4.31	97.411	1.55
15	314.696	4.10	185.771	7.13	61	243.559	18.64	143.778	4.47
16	519.633	10.65	306.750	14.76	62	157.241	12.45	92.823	1.26
17	152.308	15.17	89.910	1.07	63	109.078	3.01	64.391	0.54
18	142.045	7.25	83.852	0.69	64	42.862	4.29	25.302	3.01
19	201.597	3.97	119.007	2.91	65	157.521	5.96	92.988	1.27
20	155.475	8.97	91.780	1.19	66	109.297	9.17	64.520	0.53
21	1398.000	34.50	825.268	47.50	67	124.857	11.96	73.705	0.05
22	119.350	8.12	70.454	0.15	68	342.556	14.62	202.218	8.16
23	110.666	6.85	65.328	0.48	69	241.353	8.17	142.476	4.39
24	80.618	2.08	47.590	1.60	70	143.974	7.53	84.991	0.76
25	89.205	11.18	52.660	1.28	71	121.553	10.44	71.755	0.07
26	169.816	0.33	100.246	1.73	72	109.771	11.73	64.800	0.51
27	126.422	12.83	74.629	0.11	73	203.086	6.35	119.886	2.97
28	326.906	3.68	192.979	7.58	74	1804.799	39.73	1065.410	62.66
29	348.791	17.84	205.898	8.40	75	232.354	8.33	137.163	4.06
30	150.796	3.47	89.018	1.02	76	1244.500	23.45	734.653	41.78
31	149.601	6.85	88.312	0.97	77	135.028	1.43	79.710	0.43
32	176.135	3.83	103.976	1.96	78	287.448	22.71	169.687	6.11
33	117.561	16.37	69.398	0.22	79	175.468	7.87	103.582	1.94
34	204.305	5.50	120.605	3.01	80	1063.133	6.75	627.589	35.02
35	112.025	15.97	66.131	0.43	81	157.371	5.98	92.899	1.26
36	234.837	6.38	138.629	4.15	82	681.313	10.71	402.193	20.79
37	97.862	8.81	57.770	0.96	83	1782.071	56.92	1051.992	61.81
38	82.214	0.74	48.532	1.54	84	261.038	4.64	154.096	5.13
39	137.972	5.97	81.448	0.54	85	670.879	10.13	396.033	20.40
40	130.645	3.16	77.122	0.27	86	257.500	11.04	152.007	4.99
41	1272.209	23.99	751.011	42.81	87	114.859	1.94	67.804	0.32
42	1246.062	21.95	735.576	41.84	88	197.343	7.00	116.495	2.75
43	148.483	10.00	87.653	0.93	89	118.547	14.33	69.981	0.18
44	278.526	2.67	164.419	5.78	90	85.423	17.08	50.427	1.42
45	134.445	7.09	79.365	0.41	91	123.928	8.29	73.157	0.02
46	215.048	8.48	126.947	3.41	92	387.352	22.35	228.662	9.83

UNL-3939
Weighted Disks

De (Gy)
Bin Width = 10
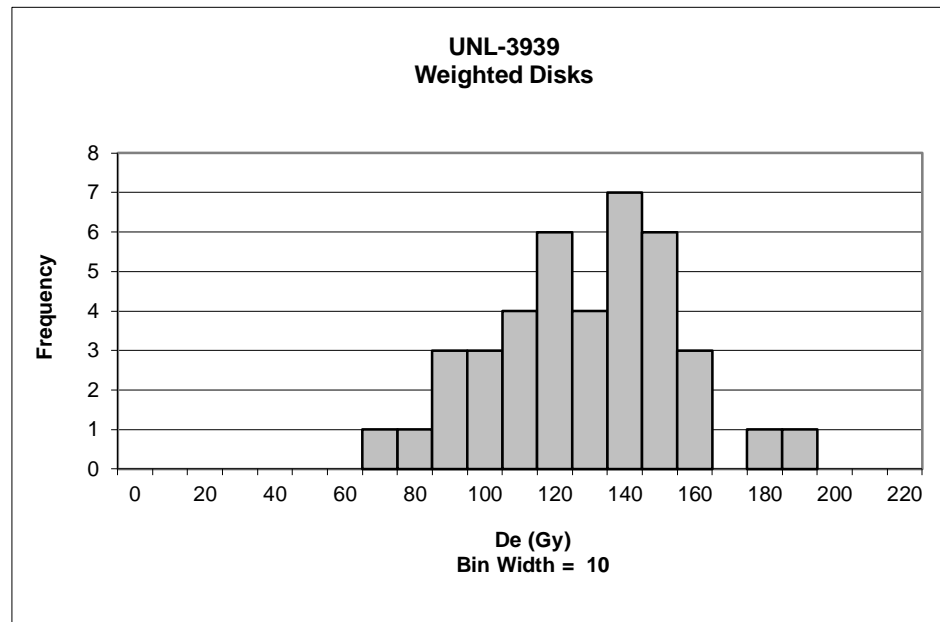
#	De	Error	Age	+/- 1 σ	#	De	Error	Age	+/- 1 σ
1	127.597	18.00	75.323	0.15	21	97.862	8.81	57.770	0.96
2	61.956	0.52	36.574	2.29	22	137.972	5.97	81.448	0.54
3	90.011	2.72	53.135	1.25	23	130.645	3.16	77.122	0.27
4	140.867	15.76	83.157	0.65	24	148.483	10.00	87.653	0.93
5	103.814	14.59	61.284	0.73	25	134.445	7.09	79.365	0.41
6	105.198	8.14	62.100	0.68	26	186.322	7.08	109.990	2.34
7	110.165	11.18	65.033	0.50	27	129.919	16.33	76.694	0.24
8	81.638	0.89	48.193	1.56	28	77.282	4.65	45.621	1.72
9	98.756	8.88	58.298	0.92	29	137.218	14.32	81.002	0.51
10	152.308	15.17	89.910	1.07	30	148.515	6.11	87.671	0.93
11	142.045	7.25	83.852	0.69	31	131.346	8.16	77.536	0.29
12	119.350	8.12	70.454	0.15	32	135.324	10.75	79.884	0.44
13	110.666	6.85	65.328	0.48	33	157.241	12.45	92.823	1.26
14	80.618	2.08	47.590	1.60	34	109.078	3.01	64.391	0.54
15	89.205	11.18	52.660	1.28	35	124.857	11.96	73.705	0.05
16	126.422	12.83	74.629	0.11	36	143.974	7.53	84.991	0.76
17	150.796	3.47	89.018	1.02	37	109.771	11.73	64.800	0.51
18	149.601	6.85	88.312	0.97	38	135.028	1.43	79.710	0.43
19	117.561	16.37	69.398	0.22	39	175.468	7.87	103.582	1.94
20	112.025	15.97	66.131	0.43	40	118.547	14.33	69.981	0.18

UNL 3939 (n=40)

Central value = 120.5 ± 4.7 (1σ)

Dispersion = 23 %

Minimum age: 61.96±0.55

9.1.6 UNL – 3940
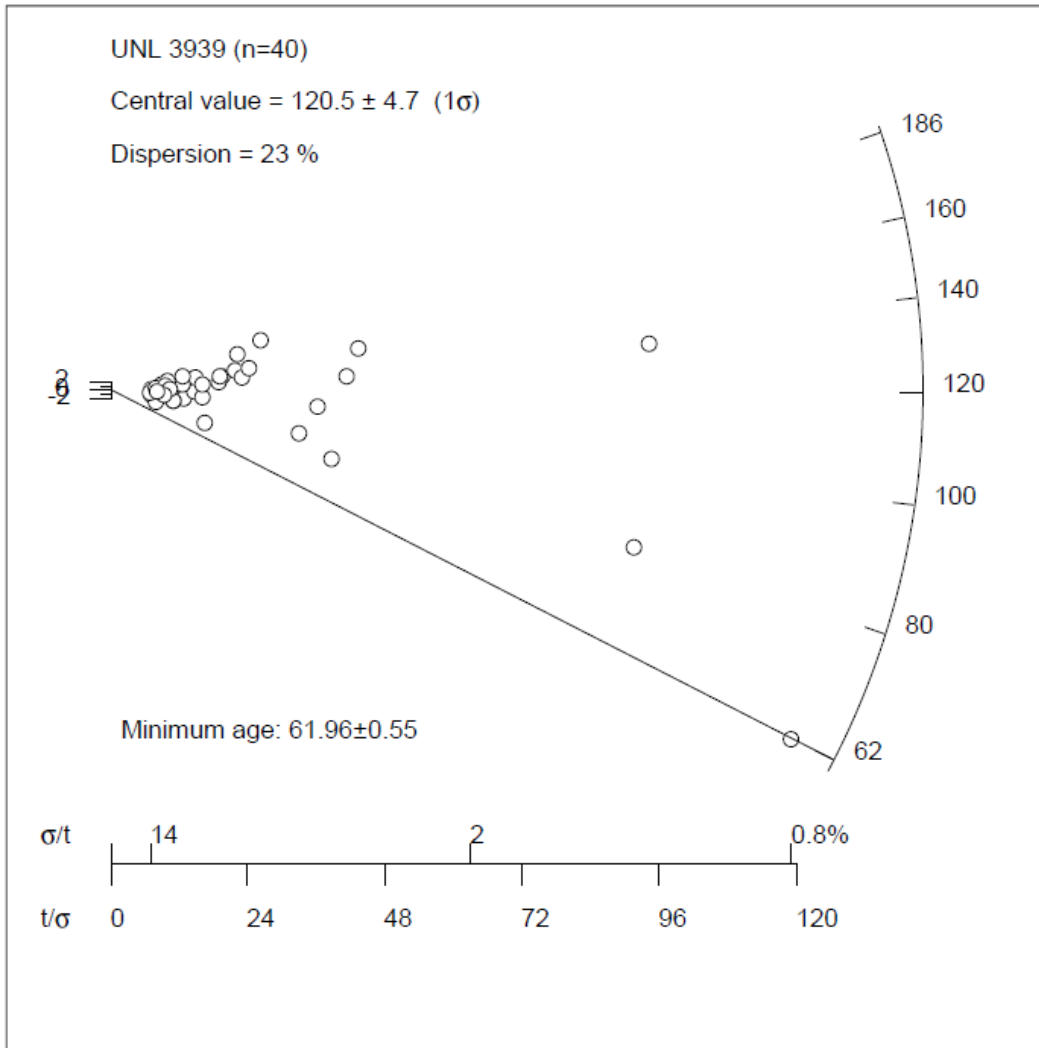
UNL-3940
All Disks
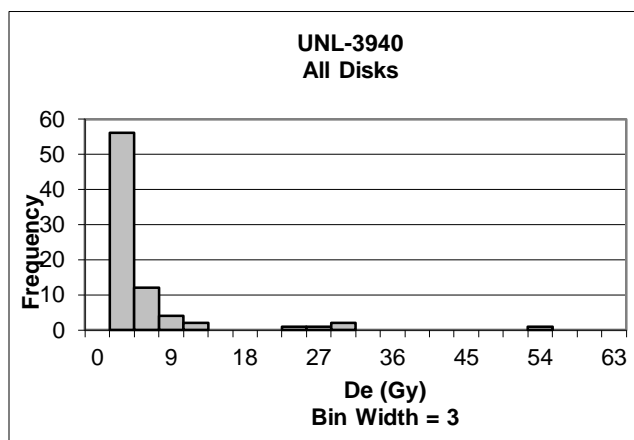
#	De	Error	Age	+/- 1 σ	#	De	Error	Age	+/- 1 σ
1	24.347	0.52	10.728	15.82	40	3.951	0.35	1.741	1.23
2	1.584	0.21	0.698	0.46	41	0.986	0.97	0.435	0.89
3	1.163	0.68	0.513	0.76	42	0.950	0.95	0.418	0.91
4	2.218	0.12	0.977	0.01	43	23.221	0.61	10.232	15.01
5	2.509	0.27	1.106	0.20	44	1.345	0.52	0.593	0.63
6	2.865	0.28	1.262	0.46	45	1.845	0.77	0.813	0.27
7	6.228	0.39	2.744	2.86	46	0.728	0.45	0.321	1.07
8	6.296	0.73	2.774	2.91	47	1.210	1.11	0.533	0.73
9	2.584	0.26	1.138	0.25	48	4.766	0.10	2.100	1.82
10	5.752	0.78	2.535	2.52	49	0.214	0.55	0.094	1.44
11	3.835	0.21	1.690	1.15	50	7.658	0.70	3.374	3.88
12	0.792	0.07	0.349	1.03	51	4.015	0.62	1.769	1.28
13	2.317	0.78	1.021	0.06	52	52.206	5.17	23.003	35.74
14	3.170	0.33	1.397	0.67	53	0.848	0.32	0.374	0.99
15	0.690	0.33	0.304	1.10	54	1.183	0.85	0.521	0.75
16	1.854	0.46	0.817	0.27	55	11.593	0.28	5.108	6.70
17	9.506	0.17	4.188	5.21	56	0.100	0.87	0.044	1.52
18	3.361	0.17	1.481	0.81	57	28.115	0.53	12.388	18.51
19	2.383	0.91	1.050	0.11	58	1.608	0.06	0.709	0.44
20	1.763	0.19	0.777	0.33	59	2.182	0.51	0.962	0.03
21	3.031	0.93	1.336	0.58	60	1.126	0.52	0.496	0.79
22	2.268	0.45	0.999	0.03	61	1.003	0.36	0.442	0.88
23	1.681	0.40	0.740	0.39	62	1.762	1.64	0.776	0.33
24	1.353	0.51	0.596	0.63	63	1.922	0.54	0.847	0.22
25	4.155	0.57	1.831	1.38	64	6.646	0.55	2.928	3.16
26	2.832	0.25	1.248	0.43	65	1.052	0.15	0.464	0.84
27	1.451	0.76	0.639	0.56	66	1.344	0.21	0.592	0.63
28	1.144	0.54	0.504	0.77	67	0.740	0.25	0.326	1.06
29	1.490	0.42	0.657	0.53	68	1.528	0.11	0.673	0.50
30	1.484	0.36	0.654	0.53	69	1.752	0.66	0.772	0.34
31	5.092	0.52	2.244	2.05	70	2.923	0.14	1.288	0.50
32	0.791	0.42	0.349	1.03	71	5.898	0.37	2.599	2.63
33	1.714	0.92	0.755	0.37	72	1.843	0.36	0.812	0.28
34	2.179	0.23	0.960	0.03	73	0.000	55.72	0.000	1.59
35	1.846	0.34	0.813	0.27	74	0.954	0.36	0.421	0.91
36	29.751	3.53	13.109	19.68	75	4.762	0.26	2.098	1.81
37	1.656	0.07	0.730	0.41	76	2.762	0.14	1.217	0.38
38	1.019	0.32	0.449	0.86	77	1.499	0.22	0.660	0.52
39	2.411	0.47	1.062	0.13	78	2.130	0.65	0.939	0.07
					79	1.147	0.37	0.505	0.77

UNL-3940
Weighted Disks

De (Gy)
Bin Width = 0.5
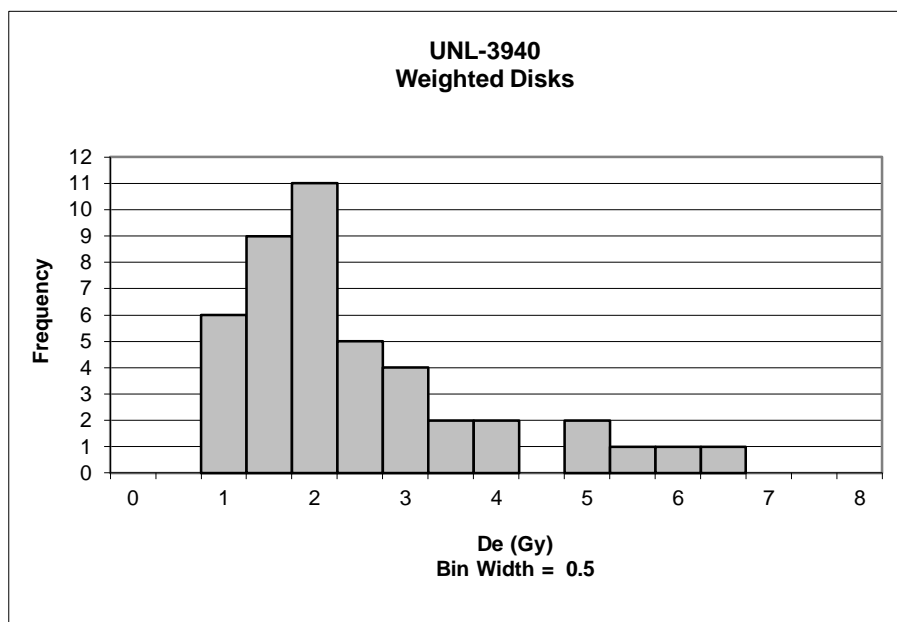
#	De	Error	Age	+/- 1 σ	#	De	Error	Age	+/- 1 σ
1	1.584	0.21	0.698	0.46	23	1.845	0.77	0.813	0.27
2	1.163	0.68	0.513	0.76	24	0.728	0.45	0.321	1.07
3	2.218	0.12	0.977	0.01	25	4.766	0.10	2.100	1.82
4	6.228	0.39	2.744	2.86	26	0.848	0.32	0.374	0.99
5	2.584	0.26	1.138	0.25	27	1.183	0.85	0.521	0.75
6	3.835	0.21	1.690	1.15	28	1.608	0.06	0.709	0.44
7	0.792	0.07	0.349	1.03	29	2.182	0.51	0.962	0.03
8	1.854	0.46	0.817	0.27	30	1.003	0.36	0.442	0.88
9	3.361	0.17	1.481	0.81	31	1.762	1.64	0.776	0.33
10	1.763	0.19	0.777	0.33	32	1.922	0.54	0.847	0.22
11	3.031	0.93	1.336	0.58	33	1.052	0.15	0.464	0.84
12	2.268	0.45	0.999	0.03	34	1.344	0.21	0.592	0.63
13	2.832	0.25	1.248	0.43	35	0.740	0.25	0.326	1.06
14	1.490	0.42	0.657	0.53	36	1.528	0.11	0.673	0.50
15	5.092	0.52	2.244	2.05	37	1.752	0.66	0.772	0.34
16	0.791	0.42	0.349	1.03	38	2.923	0.14	1.288	0.50
17	2.179	0.23	0.960	0.03	39	5.898	0.37	2.599	2.63
18	1.656	0.07	0.730	0.41	40	1.843	0.36	0.812	0.28
19	1.019	0.32	0.449	0.86	41	0.954	0.36	0.421	0.91
20	2.411	0.47	1.062	0.13	42	4.762	0.26	2.098	1.81
21	3.951	0.35	1.741	1.23	43	2.762	0.14	1.217	0.38
22	1.345	0.52	0.593	0.63	44	1.147	0.37	0.505	0.77

UNL 3940 (n=44)

Central value = 2.03 ± 0.18 (1σ)

Dispersion = 53 %

Minimum age: 0.905±0.082

σ/t   93   4   2%

t/σ   0   9   18   27   36   45 48

9.1.7 UNL – 3943

UNL-3943
All Disks

De (Gy)
Bin Width = 3
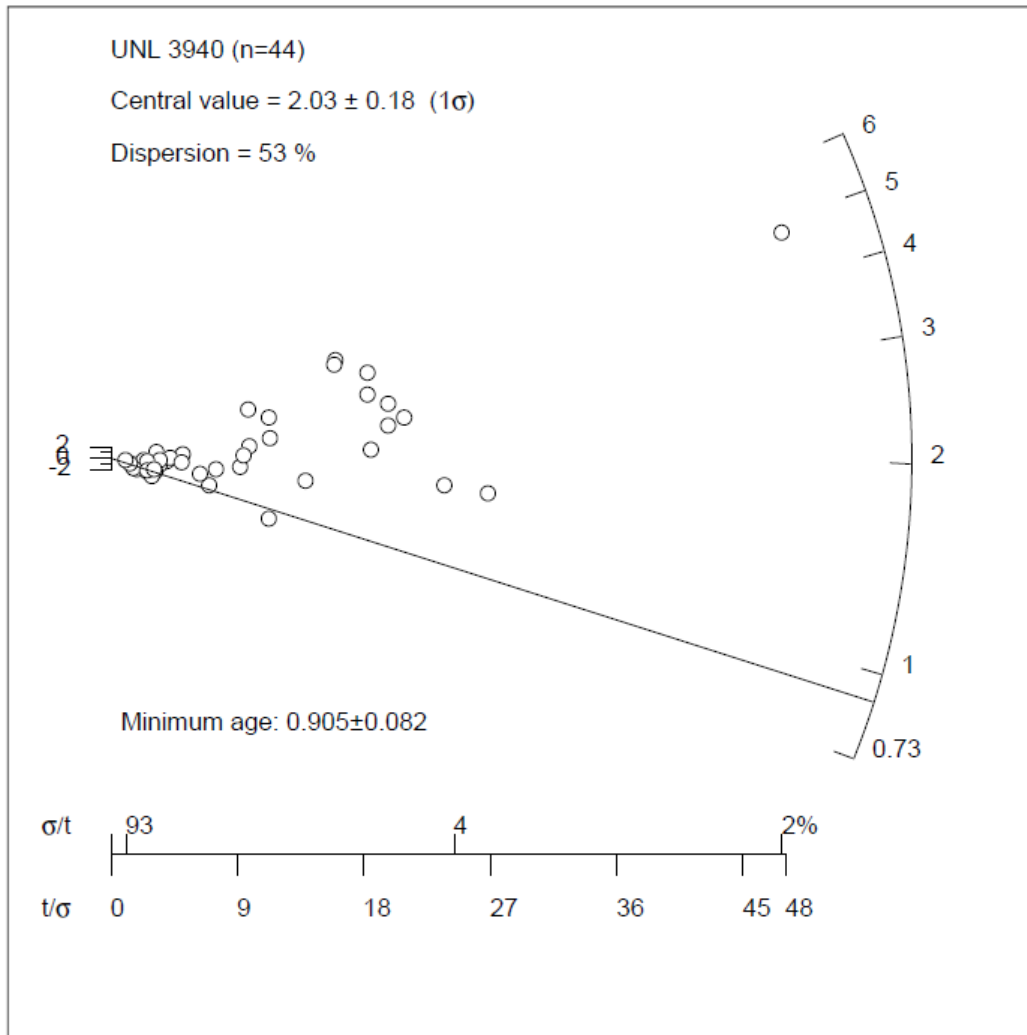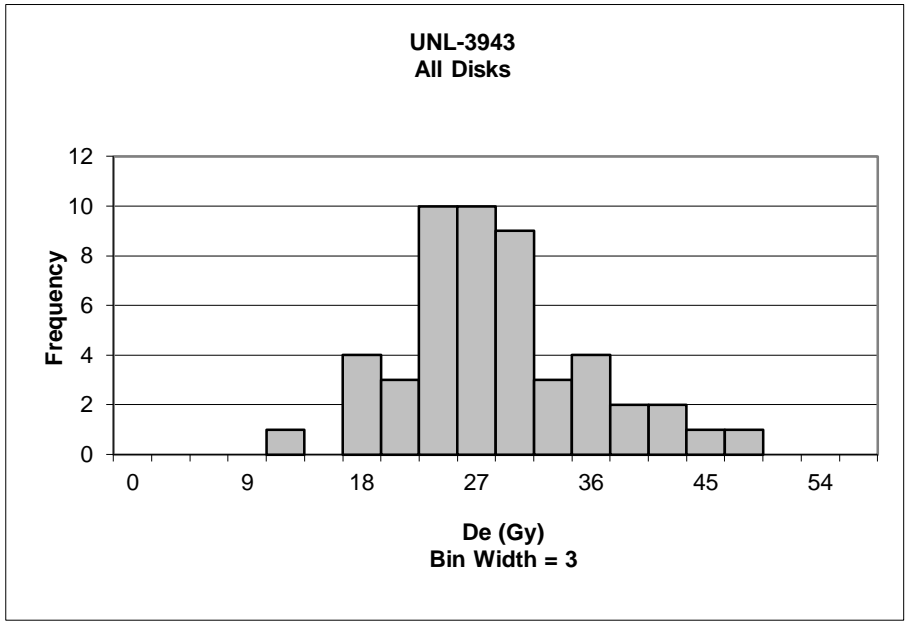
#	De	Error	Age	+/- 1 σ	#	De	Error	Age	+/- 1 σ
1	23.558	2.17	11.347	0.47	26	27.834	0.46	13.407	0.12
2	24.213	1.14	11.663	0.38	27	31.382	2.26	15.116	0.61
3	17.176	1.23	8.273	1.36	28	25.786	0.73	12.421	0.17
4	29.981	1.10	14.441	0.42	29	26.470	2.36	12.750	0.07
5	40.150	0.52	19.339	1.83	30	11.429	1.76	5.505	2.16
6	22.244	2.09	10.715	0.66	31	33.910	0.95	16.334	0.96
7	25.427	2.53	12.247	0.22	32	22.571	0.69	10.872	0.61
8	32.930	2.61	15.862	0.83	33	24.468	0.79	11.786	0.35
9	22.789	0.57	10.977	0.58	34	38.518	0.69	18.553	1.60
10	25.520	3.10	12.293	0.20	35	20.560	1.78	9.903	0.89
11	22.695	0.63	10.931	0.59	36	27.717	0.96	13.351	0.10
12	17.889	1.85	8.617	1.26	37	36.974	1.65	17.809	1.39
13	19.574	1.00	9.429	1.03	38	47.214	1.57	22.742	2.81
14	33.974	1.55	16.364	0.97	39	21.675	0.02	10.440	0.74
15	22.080	1.87	10.636	0.68	40	30.490	0.31	14.686	0.49
16	18.485	0.52	8.904	1.18	41	24.325	2.75	11.717	0.37
17	35.215	1.00	16.962	1.14	42	22.804	1.58	10.984	0.58
18	40.798	1.49	19.652	1.92	43	27.368	0.30	13.182	0.05
19	27.206	0.19	13.105	0.03	44	15.525	1.55	7.478	1.59
20	29.145	0.74	14.038	0.30	45	27.857	1.37	13.418	0.12
21	22.691	2.11	10.930	0.60	46	43.549	1.58	20.977	2.30
22	24.676	0.48	11.886	0.32	47	27.339	0.70	13.169	0.05
23	34.741	2.01	16.734	1.08	48	27.617	1.81	13.303	0.09
24	25.668	1.17	12.364	0.18	49	15.566	0.82	7.498	1.58
25	25.344	1.36	12.207	0.23	50	23.996	0.95	11.558	0.41

UNL-3943
Weighted Disks

Frequency vs De (Gy), Bin Width = 3
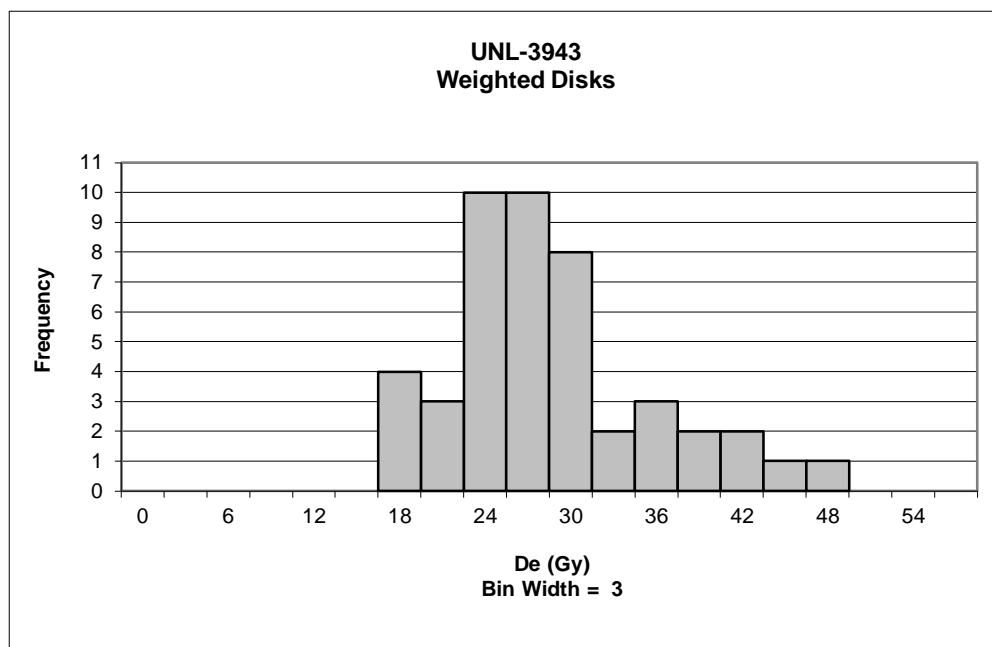
#	De	Error	Age	+/- 1 σ	#	De	Error	Age	+/- 1 σ
1	23.558	2.17	11.347	0.47	24	25.344	1.36	12.207	0.23
2	24.213	1.14	11.663	0.38	25	27.834	0.46	13.407	0.12
3	17.176	1.23	8.273	1.36	26	31.382	2.26	15.116	0.61
4	29.981	1.10	14.441	0.42	27	25.786	0.73	12.421	0.17
5	40.150	0.52	19.339	1.83	28	26.470	2.36	12.750	0.07
6	22.244	2.09	10.715	0.66	29	22.571	0.69	10.872	0.61
7	25.427	2.53	12.247	0.22	30	24.468	0.79	11.786	0.35
8	22.789	0.57	10.977	0.58	31	38.518	0.69	18.553	1.60
9	25.520	3.10	12.293	0.20	32	20.560	1.78	9.903	0.89
10	22.695	0.63	10.931	0.59	33	36.974	1.65	17.809	1.39
11	17.889	1.85	8.617	1.26	34	47.214	1.57	22.742	2.81
12	19.574	1.00	9.429	1.03	35	21.675	0.02	10.440	0.74
13	33.974	1.55	16.364	0.97	36	30.490	0.31	14.686	0.49
14	22.080	1.87	10.636	0.68	37	24.325	2.75	11.717	0.37
15	18.485	0.52	8.904	1.18	38	22.804	1.58	10.984	0.58
16	35.215	1.00	16.962	1.14	39	27.368	0.30	13.182	0.05
17	40.798	1.49	19.652	1.92	40	15.525	1.55	7.478	1.59
18	27.206	0.19	13.105	0.03	41	27.857	1.37	13.418	0.12
19	29.145	0.74	14.038	0.30	42	43.549	1.58	20.977	2.30
20	22.691	2.11	10.930	0.60	43	27.339	0.70	13.169	0.05
21	24.676	0.48	11.886	0.32	44	27.617	1.81	13.303	0.09
22	34.741	2.01	16.734	1.08	45	15.566	0.82	7.498	1.58
23	25.668	1.17	12.364	0.18	46	23.996	0.95	11.558	0.41

UNL 3943 (n=46)

Central value = 26.25 ± 0.99 (1σ)

Dispersion = 25 %

47

40

35

30

25

20

16

Minimum age: 17.95±0.82

σ/t   12   0.2   0.09%

t/σ   0   216   432   648   864   1084
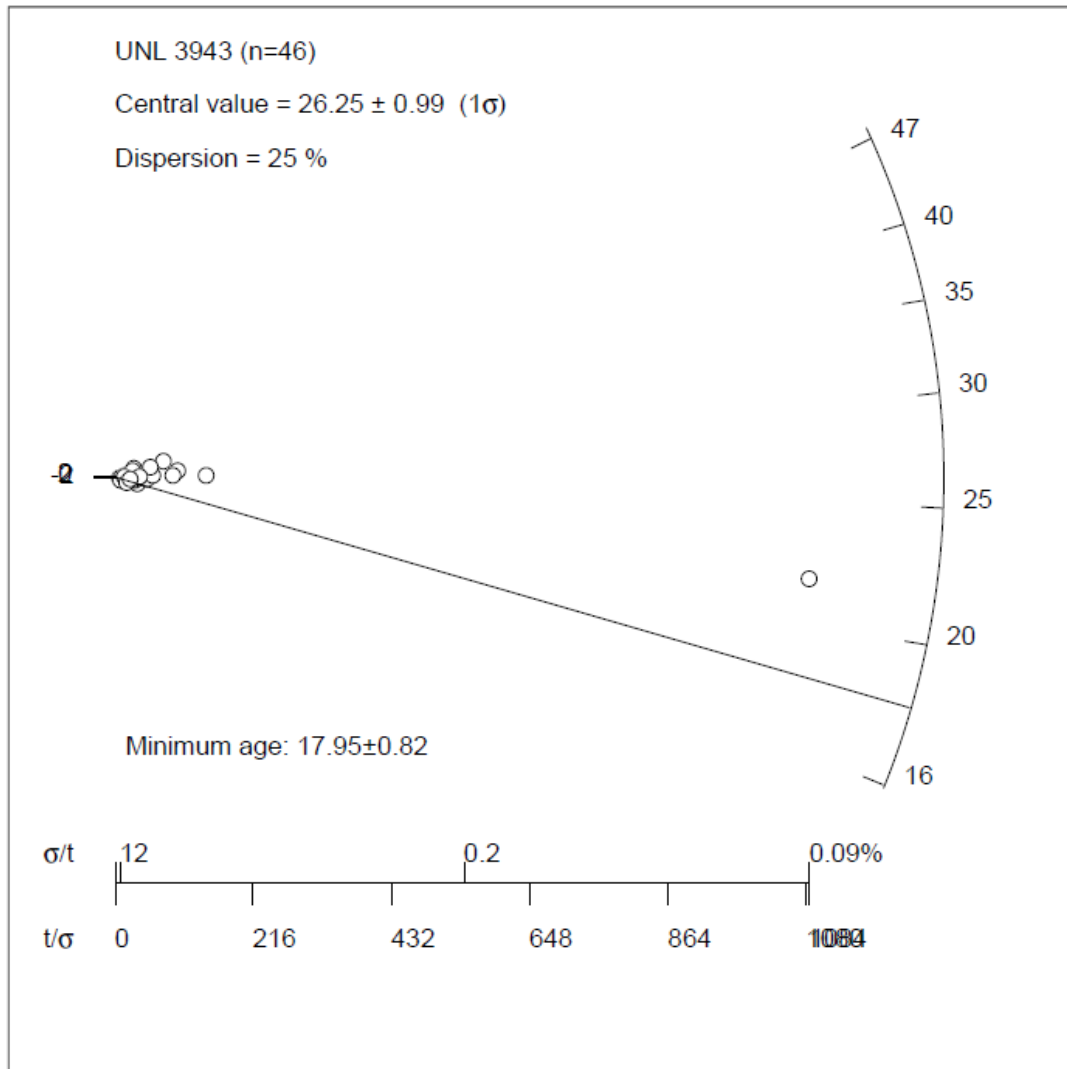
9.1.8   UNL – 3946
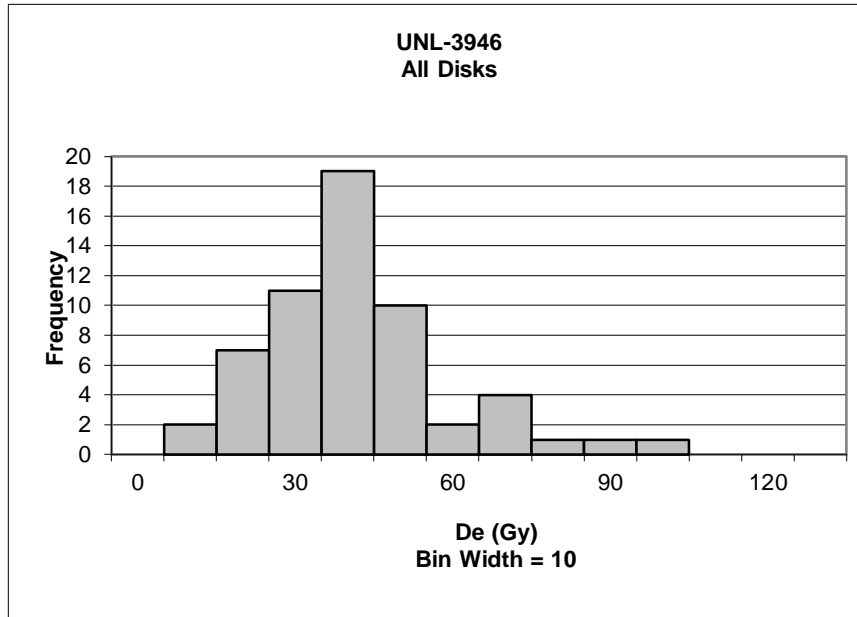
#	De	Error	Age	+/- 1 σ	#	De	Error	Age	+/- 1 σ
1	30.669	0.57	10.048	0.43	28	30.688	6.13	10.054	0.43
2	27.175	3.20	8.903	0.69	29	30.441	1.89	9.974	0.44
3	38.887	3.82	12.740	0.19	30	34.068	7.10	11.162	0.17
4	22.039	0.93	7.221	1.07	31	26.232	0.49	8.595	0.76
5	18.997	2.49	6.224	1.30	32	9.833	2.32	3.221	1.98
6	63.230	4.96	20.716	2.00	33	35.651	2.64	11.680	0.06
7	30.905	4.36	10.125	0.41	34	28.652	2.83	9.387	0.58
8	41.698	7.41	13.662	0.40	35	30.923	1.55	10.131	0.41
9	25.202	4.31	8.257	0.84	36	15.784	8.72	5.171	1.54
10	9.488	13.41	3.109	2.01	37	41.198	2.79	13.498	0.36
11	49.172	2.43	16.110	0.95	38	70.021	5.75	22.941	2.51
12	24.073	5.44	7.887	0.92	39	22.620	2.00	7.411	1.03
13	41.564	3.17	13.618	0.39	40	91.270	5.61	29.903	4.10
14	13.415	4.39	4.395	1.72	41	80.996	1.29	26.537	3.33
15	29.983	1.94	9.823	0.48	42	45.258	4.95	14.828	0.66
16	42.041	7.25	13.774	0.42	43	32.513	5.91	10.652	0.29
17	19.250	3.37	6.307	1.28	44	30.465	5.02	9.981	0.44
18	43.126	2.79	14.129	0.50	45	66.591	8.11	21.817	2.26
19	69.849	1.59	22.885	2.50	46	47.549	1.90	15.579	0.83
20	35.950	5.27	11.778	0.03	47	33.088	5.28	10.841	0.25
21	12.382	11.09	4.057	1.79	48	34.044	3.32	11.154	0.18
22	34.958	2.26	11.453	0.11	49	66.885	1.32	21.914	2.28
23	56.612	0.40	18.548	1.51	50	45.392	0.66	14.872	0.67
24	24.044	3.12	7.878	0.92	51	27.739	2.35	9.088	0.65
25	37.014	11.79	12.127	0.05	52	13.737	1.38	4.501	1.69
26	34.716	2.16	11.374	0.12	53	41.722	0.38	13.669	0.40
27	15.112	7.86	4.951	1.59	54	39.462	2.34	12.929	0.23

UNL-3946
Weighted Disks

De (Gy)
Bin Width = 5
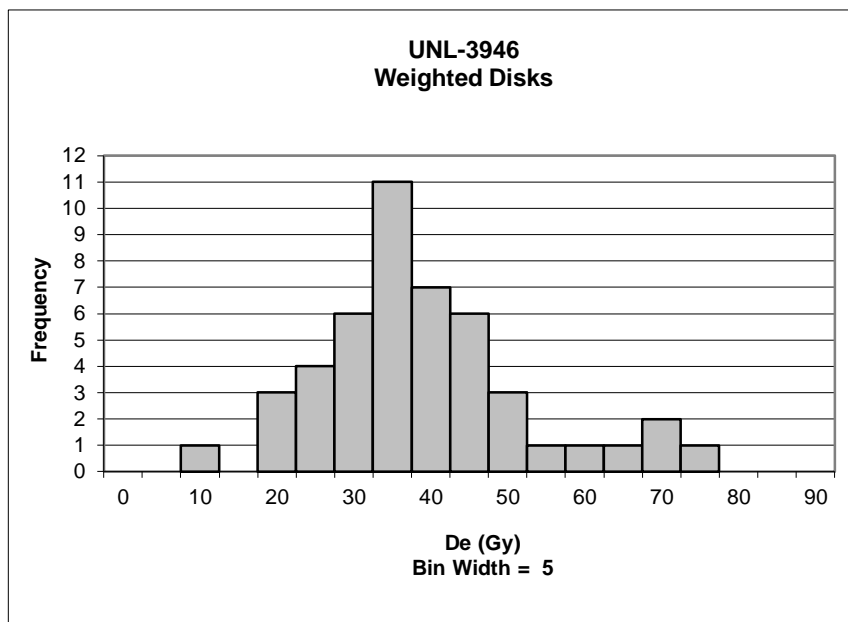
#	De	Error	Age	+/- 1 σ	#	De	Error	Age	+/- 1 σ
1	30.669	0.57	10.048	0.43	25	30.441	1.89	9.974	0.44
2	27.175	3.20	8.903	0.69	26	34.068	7.10	11.162	0.17
3	38.887	3.82	12.740	0.19	27	26.232	0.49	8.595	0.76
4	22.039	0.93	7.221	1.07	28	9.833	2.32	3.221	1.98
5	18.997	2.49	6.224	1.30	29	35.651	2.64	11.680	0.06
6	63.230	4.96	20.716	2.00	30	28.652	2.83	9.387	0.58
7	30.905	4.36	10.125	0.41	31	30.923	1.55	10.131	0.41
8	41.698	7.41	13.662	0.40	32	41.198	2.79	13.498	0.36
9	25.202	4.31	8.257	0.84	33	70.021	5.75	22.941	2.51
10	49.172	2.43	16.110	0.95	34	22.620	2.00	7.411	1.03
11	24.073	5.44	7.887	0.92	35	32.513	5.91	10.652	0.29
12	41.564	3.17	13.618	0.39	36	66.591	8.11	21.817	2.26
13	29.983	1.94	9.823	0.48	37	47.549	1.90	15.579	0.83
14	42.041	7.25	13.774	0.42	38	33.088	5.28	10.841	0.25
15	19.250	3.37	6.307	1.28	39	34.044	3.32	11.154	0.18
16	43.126	2.79	14.129	0.50	40	45.392	0.66	14.872	0.67
17	69.849	1.59	22.885	2.50	41	27.739	2.35	9.088	0.65
18	35.950	5.27	11.778	0.03	42	41.722	0.38	13.669	0.40
19	34.958	2.26	11.453	0.11	43	39.462	2.34	12.929	0.23
20	56.612	0.40	18.548	1.51	44	36.416	1.34	11.931	0.00
21	37.014	11.79	12.127	0.05	45	39.746	1.55	13.022	0.25
22	34.716	2.16	11.374	0.12	46	22.976	25.19	7.528	1.00
23	15.112	7.86	4.951	1.59	47	50.495	0.33	16.544	1.05
24	30.688	6.13	10.054	0.43					

UNL 3946 (n=47)

Central value = 35.3 ± 1.8 (1σ)

Dispersion = 33 %

Minimum age: 22.42±0.99

9.1.9   UNL – 3947
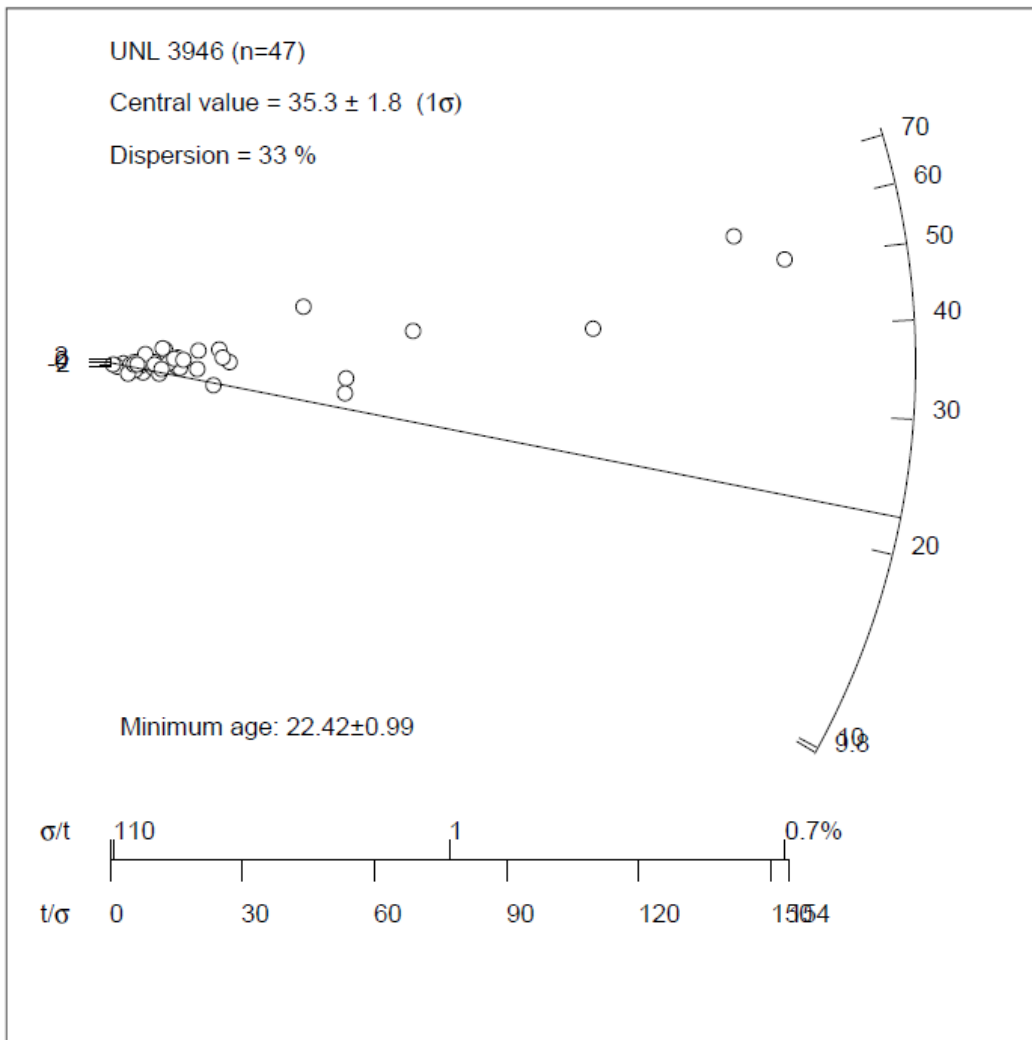
UNL-3947
All Disks
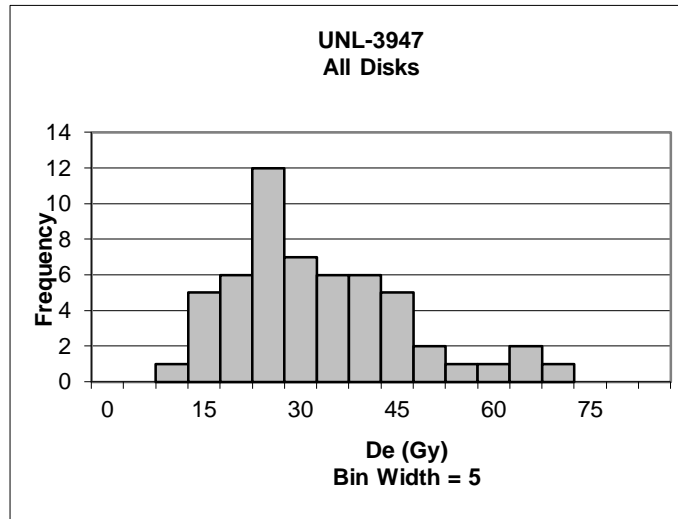
#	De	Error	Age	+/- 1 σ	#	De	Error	Age	+/- 1 σ
1	62.388	5.05	22.334	2.67	28	45.269	0.86	16.206	1.31
2	42.589	1.17	15.246	1.10	29	48.839	0.81	17.484	1.60
3	54.509	1.42	19.513	2.05	30	21.855	0.90	7.824	0.55
4	36.453	2.75	13.050	0.61	31	12.720	2.90	4.554	1.27
5	28.392	2.94	10.164	0.03	32	14.770	9.28	5.287	1.11
6	26.066	2.21	9.331	0.21	33	16.329	1.79	5.845	0.99
7	30.107	0.24	10.778	0.11	34	21.049	1.72	7.535	0.61
8	19.465	2.76	6.968	0.74	35	25.357	0.23	9.077	0.27
9	6.159	13.71	2.205	1.80	36	27.583	7.93	9.874	0.09
10	41.314	0.54	14.790	1.00	37	19.620	1.97	7.024	0.73
11	27.419	3.41	9.815	0.11	38	30.888	0.72	11.058	0.17
12	31.194	2.61	11.167	0.19	39	40.256	1.00	14.411	0.91
13	20.351	4.23	7.286	0.67	40	38.715	0.20	13.859	0.79
14	20.166	1.19	7.219	0.68	41	14.054	1.56	5.031	1.17
15	63.612	1.13	22.772	2.77	42	26.889	0.68	9.626	0.15
16	34.271	0.97	12.269	0.44	43	26.318	0.87	9.421	0.19
17	12.100	2.53	4.332	1.32	44	40.756	0.94	14.590	0.95
18	38.767	1.43	13.878	0.80	45	13.148	0.18	4.707	1.24
19	20.077	2.77	7.187	0.69	46	23.726	2.14	8.494	0.40
20	16.898	4.15	6.049	0.94	47	69.732	0.86	24.963	3.26
21	37.617	1.74	13.466	0.70	48	24.590	0.14	8.803	0.33
22	20.267	1.10	7.255	0.67	49	39.677	0.30	14.204	0.87
23	20.268	1.84	7.256	0.67	50	30.644	0.41	10.970	0.15
24	58.640	1.00	20.992	2.38	51	21.086	1.27	7.548	0.61
25	40.889	2.17	14.638	0.96	52	30.833	0.05	11.038	0.16
26	16.431	0.81	5.882	0.98	53	24.820	0.34	8.885	0.31
27	39.188	2.43	14.029	0.83	54	24.617	0.13	8.813	0.33

UNL-3947
Weighted Disks

De (Gy)
Bin Width = 5
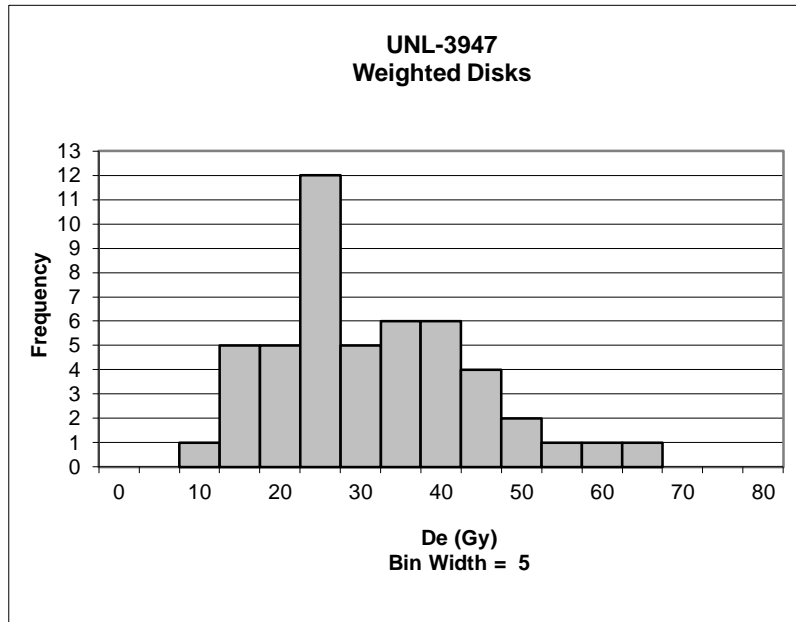
#	De	Error	Age	+/- 1 σ	#	De	Error	Age	+/- 1 σ
1	54.509	1.42	19.513	2.05	26	12.720	2.90	4.554	1.27
2	36.453	2.75	13.050	0.61	27	14.770	9.28	5.287	1.11
3	26.066	2.21	9.331	0.21	28	16.329	1.79	5.845	0.99
4	30.107	0.24	10.778	0.11	29	21.049	1.72	7.535	0.61
5	19.465	2.76	6.968	0.74	30	25.357	0.23	9.077	0.27
6	6.159	13.71	2.205	1.80	31	27.583	7.93	9.874	0.09
7	41.314	0.54	14.790	1.00	32	19.620	1.97	7.024	0.73
8	31.194	2.61	11.167	0.19	33	30.888	0.72	11.058	0.17
9	20.351	4.23	7.286	0.67	34	40.256	1.00	14.411	0.91
10	20.166	1.19	7.219	0.68	35	38.715	0.20	13.859	0.79
11	63.612	1.13	22.772	2.77	36	14.054	1.56	5.031	1.17
12	34.271	0.97	12.269	0.44	37	26.889	0.68	9.626	0.15
13	12.100	2.53	4.332	1.32	38	26.318	0.87	9.421	0.19
14	38.767	1.43	13.878	0.80	39	40.756	0.94	14.590	0.95
15	20.077	2.77	7.187	0.69	40	13.148	0.18	4.707	1.24
16	37.617	1.74	13.466	0.70	41	23.726	2.14	8.494	0.40
17	20.267	1.10	7.255	0.67	42	24.590	0.14	8.803	0.33
18	20.268	1.84	7.256	0.67	43	39.677	0.30	14.204	0.87
19	58.640	1.00	20.992	2.38	44	30.644	0.41	10.970	0.15
20	40.889	2.17	14.638	0.96	45	21.086	1.27	7.548	0.61
21	16.431	0.81	5.882	0.98	46	30.833	0.05	11.038	0.16
22	39.188	2.43	14.029	0.83	47	24.820	0.34	8.885	0.31
23	45.269	0.86	16.206	1.31	48	24.617	0.13	8.813	0.33
24	48.839	0.81	17.484	1.60	49	16.793	0.47	6.012	0.95
25	21.855	0.90	7.824	0.55					

UNL 3947 (n=49)

Central value = 27.5 ± 1.6 (1σ)

Dispersion = 39 %

Minimum age: 13.31±0.19

9.1.10   UNL – 3951
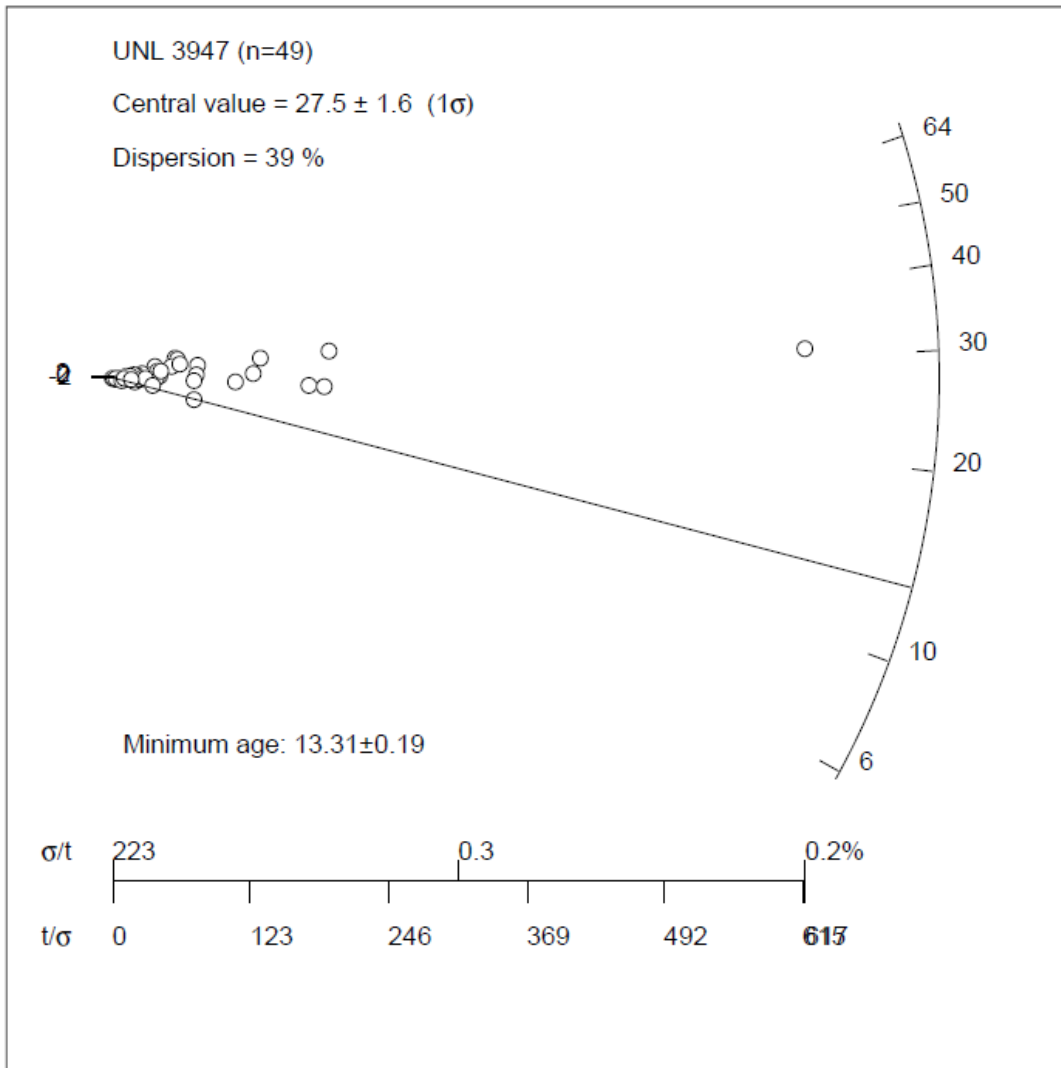
UNL-3951
All Disks
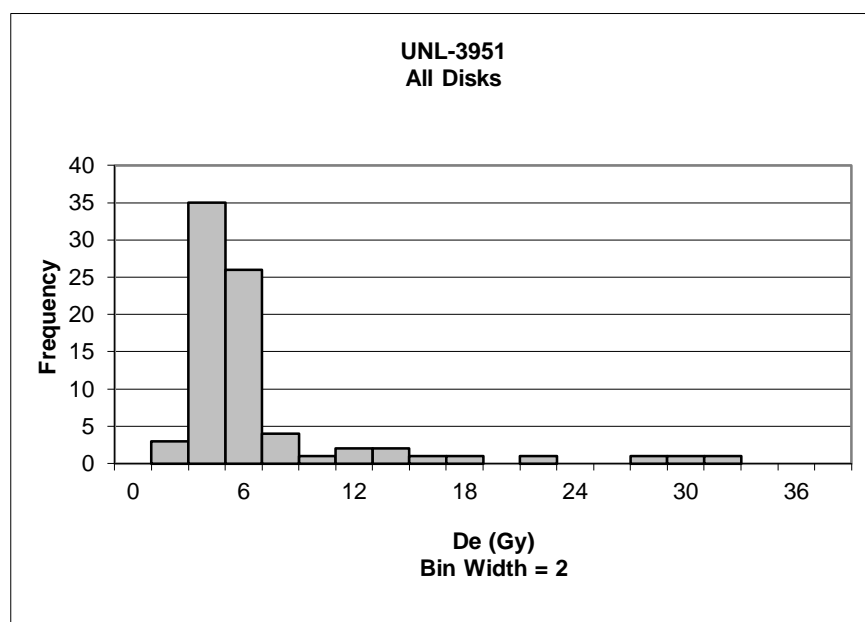
#	De	Error	Age	+/- 1 σ	#	De	Error	Age	+/- 1 σ
1	3.207	0.23	1.487	0.85	28	4.644	0.18	2.153	0.46
2	12.907	0.19	5.983	7.97	29	7.391	0.27	3.426	2.96
3	31.288	8.05	14.505	24.70	30	29.241	1.82	13.555	22.83
4	9.933	0.59	4.605	5.27	31	3.188	0.55	1.478	0.87
5	11.734	0.38	5.440	6.91	32	17.378	0.36	8.056	12.04
6	4.388	0.10	2.034	0.22	33	5.248	0.34	2.433	1.01
7	15.335	1.25	7.109	10.18	34	2.745	0.23	1.273	1.27
8	3.897	0.23	1.807	0.22	35	3.211	0.13	1.489	0.85
9	3.393	0.22	1.573	0.68	36	2.987	0.46	1.385	1.05
10	2.570	0.34	1.191	1.43	37	3.500	0.11	1.622	0.59
11	7.089	0.19	3.286	2.68	38	4.142	0.45	1.920	0.00
12	4.776	0.24	2.214	0.58	39	5.278	0.27	2.447	1.03
13	4.488	0.20	2.080	0.31	40	3.102	0.12	1.438	0.95
14	3.549	0.33	1.645	0.54	41	4.774	0.70	2.213	0.57
15	3.177	0.49	1.473	0.88	42	3.784	0.52	1.754	0.33
16	4.046	0.33	1.876	0.09	43	4.434	0.66	2.056	0.27
17	1.283	0.39	0.595	2.60	44	3.556	0.61	1.649	0.53
18	3.448	0.38	1.598	0.63	45	3.042	0.31	1.410	1.00
19	4.203	0.35	1.948	0.05	46	4.940	0.54	2.290	0.73
20	27.536	0.48	12.765	21.28	47	7.788	0.50	3.610	3.32
21	3.982	0.63	1.846	0.15	48	3.881	0.17	1.799	0.24
22	3.101	0.36	1.437	0.95	49	3.985	0.64	1.847	0.14
23	4.712	0.45	2.184	0.52	50	4.626	0.12	2.144	0.44
24	3.838	0.02	1.779	0.28	51	3.010	0.40	1.395	1.03
25	5.758	0.42	2.669	1.47	52	3.545	0.29	1.643	0.54
26	3.458	0.18	1.603	0.62	53	4.058	0.12	1.881	0.08
27	12.094	0.22	5.607	7.23	54	4.112	0.34	1.906	0.03

UNL-3951
Weighted Disks

De (Gy)
Bin Width = 0.5
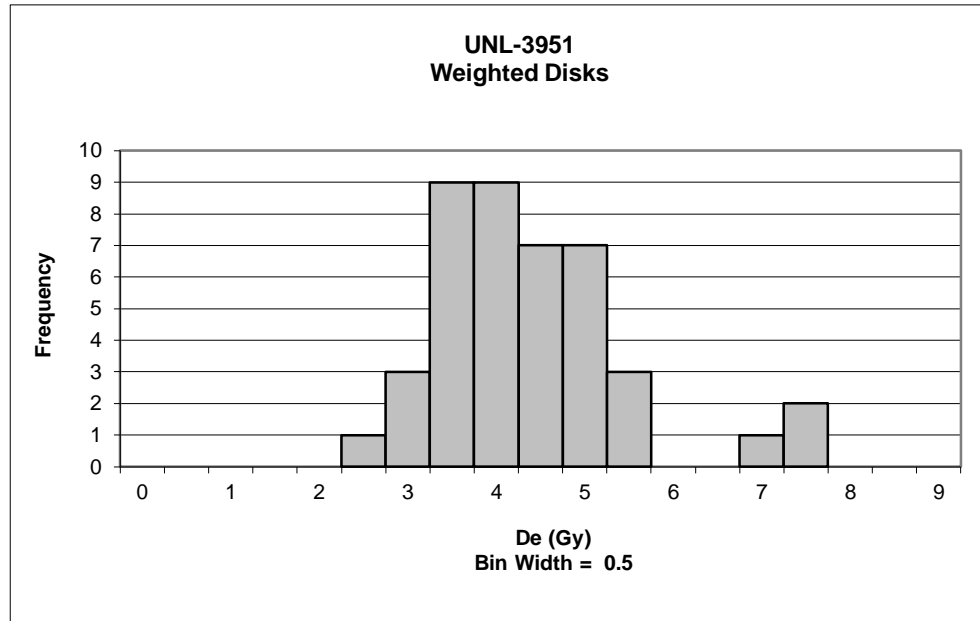
#	De	Error	Age	+/- 1 σ	#	De	Error	Age	+/- 1 σ
1	3.207	0.23	1.487	0.85	22	3.784	0.52	1.754	0.33
2	4.388	0.10	2.034	0.22	23	4.434	0.66	2.056	0.27
3	3.897	0.23	1.807	0.22	24	3.042	0.31	1.410	1.00
4	3.393	0.22	1.573	0.68	25	3.881	0.17	1.799	0.24
5	2.570	0.34	1.191	1.43	26	4.626	0.12	2.144	0.44
6	7.089	0.19	3.286	2.68	27	4.058	0.12	1.881	0.08
7	4.776	0.24	2.214	0.58	28	4.834	0.26	2.241	0.63
8	4.488	0.20	2.080	0.31	29	4.509	0.23	2.090	0.33
9	4.203	0.35	1.948	0.05	30	3.536	0.11	1.639	0.55
10	3.101	0.36	1.437	0.95	31	4.609	0.48	2.137	0.42
11	3.838	0.02	1.779	0.28	32	6.514	0.22	3.020	2.16
12	3.458	0.18	1.603	0.62	33	2.914	0.95	1.351	1.12
13	4.644	0.18	2.153	0.46	34	4.366	0.29	2.024	0.20
14	7.391	0.27	3.426	2.96	35	4.937	0.07	2.289	0.72
15	5.248	0.34	2.433	1.01	36	3.192	0.30	1.480	0.86
16	2.745	0.23	1.273	1.27	37	2.388	0.33	1.107	1.60
17	3.211	0.13	1.489	0.85	38	5.478	0.15	2.539	1.21
18	3.500	0.11	1.622	0.59	39	3.803	0.24	1.763	0.31
19	4.142	0.45	1.920	0.00	40	3.711	0.11	1.720	0.39
20	5.278	0.27	2.447	1.03	41	3.712	0.18	1.721	0.39
21	3.102	0.12	1.438	0.95	42	3.999	0.25	1.854	0.13

UNL 3951 (n=42)

Central value = 4.07 ± 0.15 (1σ)

Dispersion = 23 %

Minimum age: 3.1±0.14
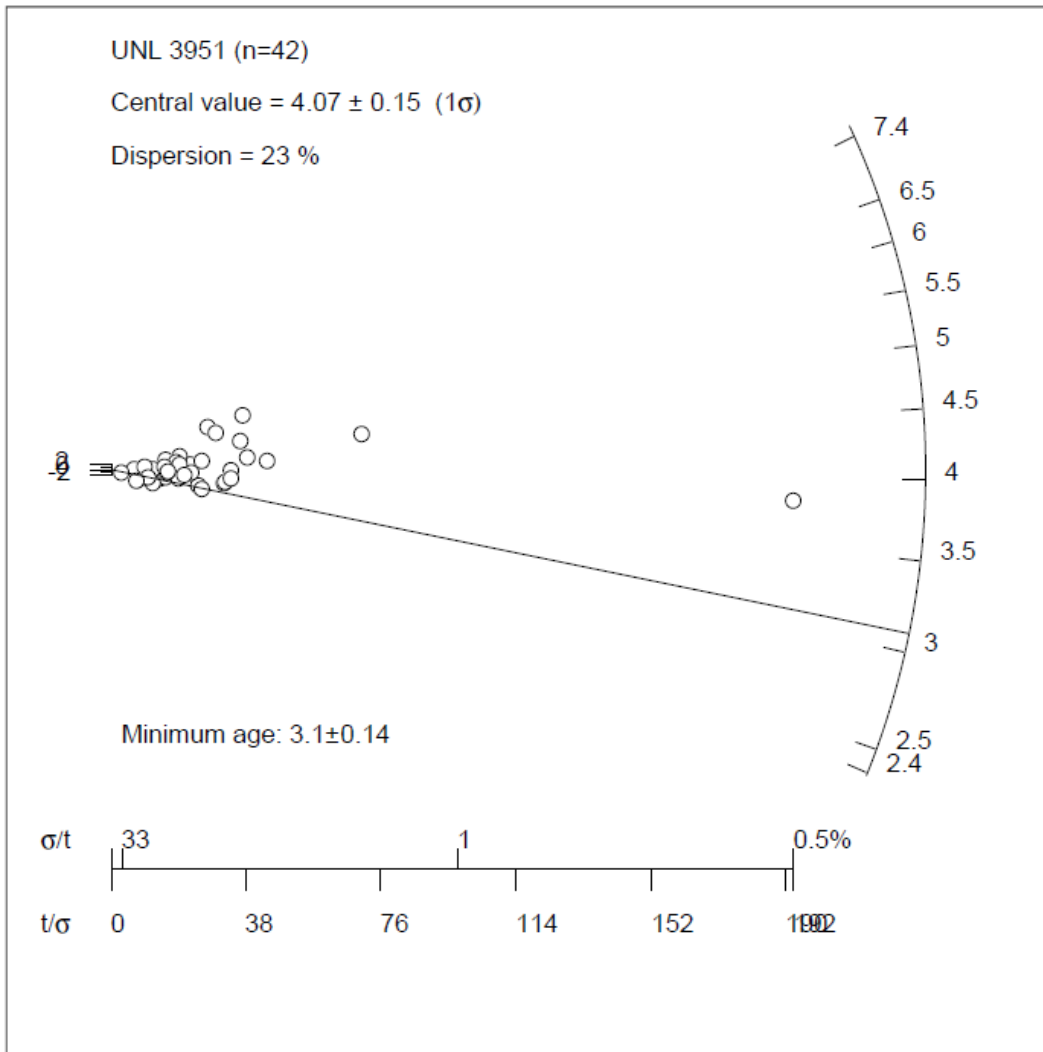
9.2 Kearney OSL Data

9.2.1 UNL – 3811

UNL-3811
All Disks
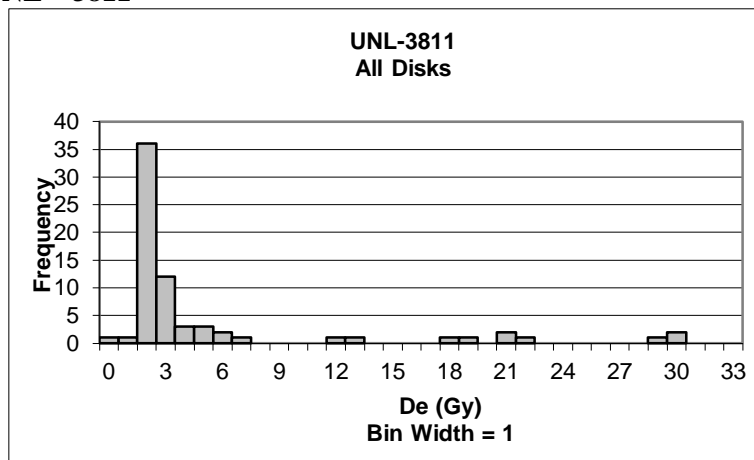
#	De	Error	Age	+/- 1 σ	#	De	Error	Age	+/- 1 σ
1	2.128	0.91	1.080	0.07	35	1.887	0.60	0.958	0.18
2	1.129	0.78	0.573	0.95	36	1.614	0.31	0.819	0.46
3	1.848	0.62	0.938	0.22	37	1.967	0.36	0.998	0.10
4	1.247	0.64	0.633	0.83	38	1.254	0.74	0.637	0.83
5	1.664	0.99	0.844	0.41	39	20.421	0.43	10.365	18.84
6	1.875	0.10	0.952	0.19	40	1.136	0.43	0.577	0.95
7	29.466	0.80	14.956	28.12	41	4.718	0.41	2.395	2.73
8	1.105	0.95	0.561	0.98	42	6.795	0.16	3.449	4.86
9	1.098	0.75	0.558	0.99	43	17.921	0.18	9.096	16.27
10	1.181	0.44	0.599	0.90	44	11.312	2.09	5.742	9.49
11	1.432	0.69	0.727	0.64	45	2.212	0.64	1.123	0.16
12	1.886	0.67	0.957	0.18	46	1.292	0.10	0.656	0.79
13	1.425	0.52	0.723	0.65	47	2.846	0.76	1.445	0.81
14	1.854	0.29	0.941	0.21	48	5.387	0.54	2.734	3.41
15	1.293	0.33	0.656	0.79	49	12.676	0.35	6.434	10.89
16	1.941	0.76	0.985	0.12	50	2.410	0.48	1.223	0.36
17	1.003	0.22	0.509	1.08	51	2.920	0.39	1.482	0.88
18	1.037	1.26	0.527	1.05	52	1.729	0.13	0.878	0.34
19	1.023	1.21	0.519	1.06	53	1.865	0.48	0.947	0.20
20	1.947	0.47	0.988	0.12	54	4.532	0.43	2.300	2.54
21	3.496	0.23	1.775	1.47	55	1.432	0.14	0.727	0.64
22	2.482	1.21	1.260	0.43	56	2.892	0.27	1.468	0.85
23	1.719	0.68	0.873	0.35	57	1.024	0.21	0.520	1.06
24	18.990	0.54	9.639	17.37	58	1.711	0.23	0.868	0.36
25	5.674	0.39	2.880	3.71	59	-1.288	1.79	-0.654	3.43
26	21.593	1.04	10.960	20.04	60	1.670	0.22	0.848	0.40
27	29.778	0.30	15.115	28.44	61	1.340	0.59	0.680	0.74
28	1.701	0.30	0.864	0.37	62	2.550	0.61	1.294	0.50
29	28.248	1.73	14.338	26.87	63	3.210	0.25	1.629	1.18
30	3.314	0.12	1.682	1.29	64	20.110	2.27	10.208	18.52
31	1.534	0.38	0.779	0.54	65	2.530	0.17	1.284	0.48
32	2.201	0.08	1.117	0.15	66	2.580	0.08	1.310	0.53
33	4.594	0.30	2.332	2.60	67	2.190	0.08	1.112	0.13
34	1.142	0.33	0.580	0.94	68	1.270	0.29	0.645	0.81
					69	0.740	0.19	0.376	1.35

UNL-3811
Weighted Disks

De (Gy)
Bin Width = 0.5
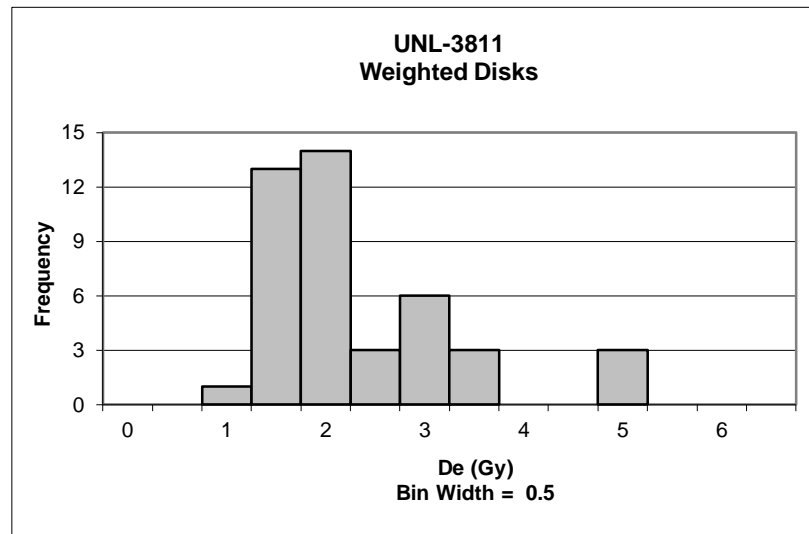
#	De	Error	Age	+/- 1 σ		#	De	Error	Age	+/- 1 σ
1	1.848	0.62	0.938	0.22		22	1.254	0.74	0.637	0.83
2	1.875	0.10	0.952	0.19		23	1.136	0.43	0.577	0.95
3	1.181	0.44	0.599	0.90		24	4.718	0.41	2.395	2.73
4	1.432	0.69	0.727	0.64		25	1.292	0.10	0.656	0.79
5	1.425	0.52	0.723	0.65		26	2.846	0.76	1.445	0.81
6	1.854	0.29	0.941	0.21		27	2.410	0.48	1.223	0.36
7	1.293	0.33	0.656	0.79		28	2.920	0.39	1.482	0.88
8	1.003	0.22	0.509	1.08		29	1.729	0.13	0.878	0.34
9	1.037	1.26	0.527	1.05		30	1.865	0.48	0.947	0.20
10	1.947	0.47	0.988	0.12		31	4.532	0.43	2.300	2.54
11	3.496	0.23	1.775	1.47		32	1.432	0.14	0.727	0.64
12	1.719	0.68	0.873	0.35		33	2.892	0.27	1.468	0.85
13	1.701	0.30	0.864	0.37		34	1.024	0.21	0.520	1.06
14	3.314	0.12	1.682	1.29		35	1.711	0.23	0.868	0.36
15	1.534	0.38	0.779	0.54		36	1.670	0.22	0.848	0.40
16	2.201	0.08	1.117	0.15		37	2.550	0.61	1.294	0.50
17	4.594	0.30	2.332	2.60		38	3.210	0.25	1.629	1.18
18	1.142	0.33	0.580	0.94		39	2.530	0.17	1.284	0.48
19	1.887	0.60	0.958	0.18		40	2.580	0.08	1.310	0.53
20	1.614	0.31	0.819	0.46		41	2.190	0.08	1.112	0.13
21	1.967	0.36	0.998	0.10		42	1.270	0.29	0.645	0.81
						43	0.740	0.19	0.376	1.35

3811 (n=43)

Central value = 1.99 ± 0.14 (1σ)

Dispersion = 40 %

Minimum age: 1.27±0.18

9.2.2   UNL – 3813
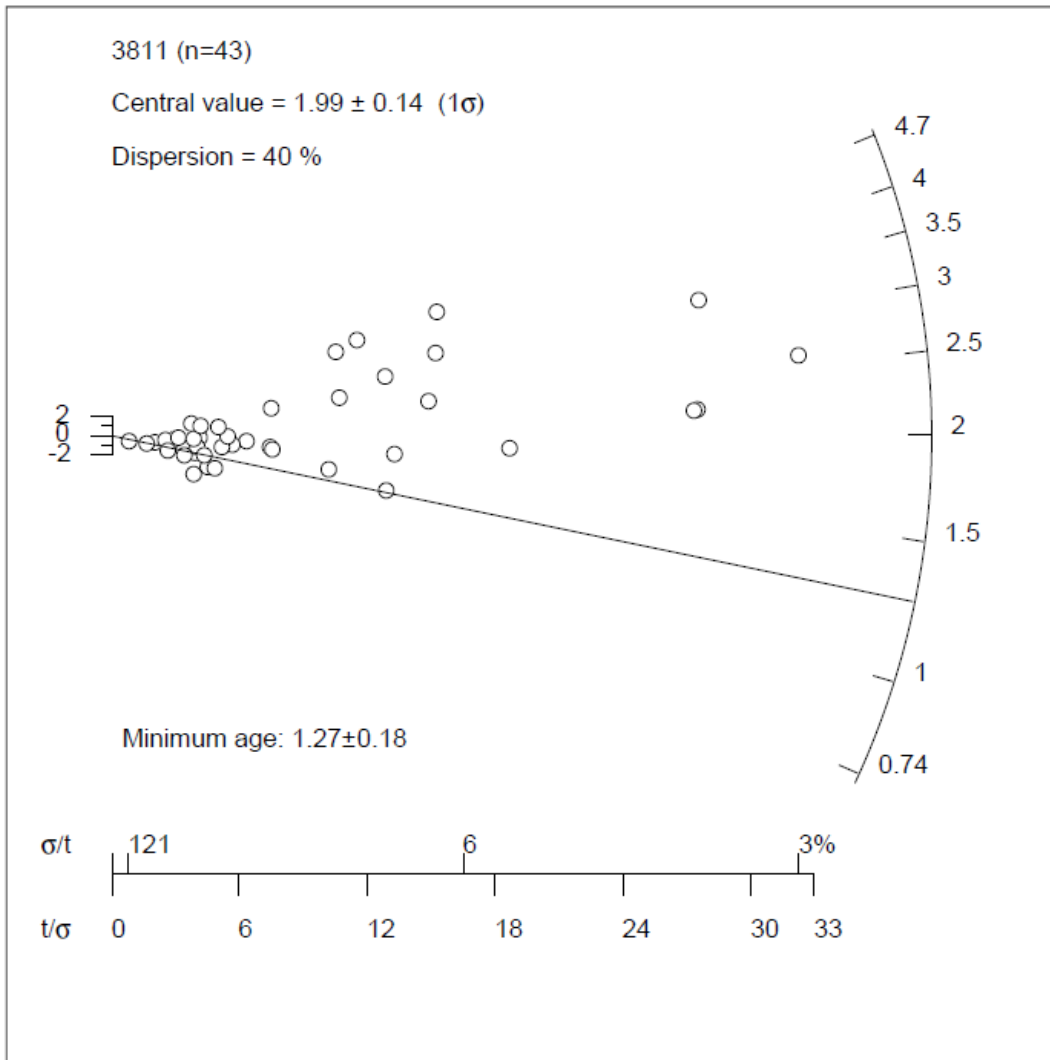
UNL-3813
All Disks
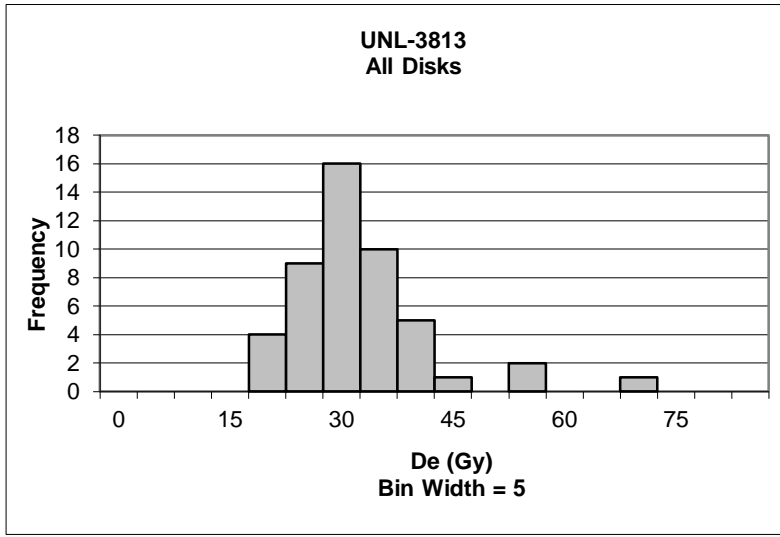
#	De	Error	Age	+/- 1 σ	#	De	Error	Age	+/- 1 σ
1	20.596	0.33	10.248	1.14	25	29.086	0.81	14.472	0.07
2	31.539	0.45	15.693	0.24	26	50.321	1.26	25.039	2.62
3	31.471	0.06	15.659	0.24	27	25.513	1.90	12.695	0.52
4	66.200	2.64	32.940	4.63	28	39.367	1.42	19.588	1.23
5	28.490	0.25	14.176	0.14	29	22.101	0.43	10.997	0.95
6	35.303	0.63	17.566	0.72	30	18.115	0.59	9.014	1.45
7	22.056	0.22	10.975	0.96	31	20.263	0.41	10.082	1.18
8	26.593	1.69	13.232	0.38	32	20.765	0.81	10.332	1.12
9	33.396	0.92	16.617	0.48	33	42.340	0.54	21.067	1.61
10	32.256	0.13	16.050	0.34	34	29.560	1.05	14.709	0.01
11	34.482	0.33	17.157	0.62	35	15.278	0.88	7.602	1.81
12	24.538	0.98	12.209	0.64	36	25.736	0.72	12.806	0.49
13	33.577	1.68	16.707	0.50	37	28.205	0.15	14.034	0.18
14	36.473	0.20	18.148	0.87	38	24.615	0.77	12.248	0.63
15	23.173	0.89	11.530	0.81	39	52.253	2.00	26.000	2.86
16	25.236	0.32	12.557	0.55	40	33.355	1.27	16.597	0.47
17	25.884	1.08	12.879	0.47	41	28.574	0.44	14.218	0.13
18	34.592	0.47	17.212	0.63	42	29.108	0.52	14.483	0.06
19	28.394	0.69	14.128	0.15	43	25.777	1.97	12.826	0.48
20	33.986	1.46	16.911	0.55	44	29.457	0.36	14.657	0.02
21	23.352	1.81	11.620	0.79	45	38.476	0.08	19.145	1.12
22	19.837	0.37	9.871	1.24	46	17.750	1.90	8.832	1.50
23	37.421	1.96	18.620	0.99	47	28.374	0.62	14.119	0.16
24	34.543	0.53	17.188	0.62	48	26.935	0.34	13.402	0.34

UNL-3813
Weighted Disks
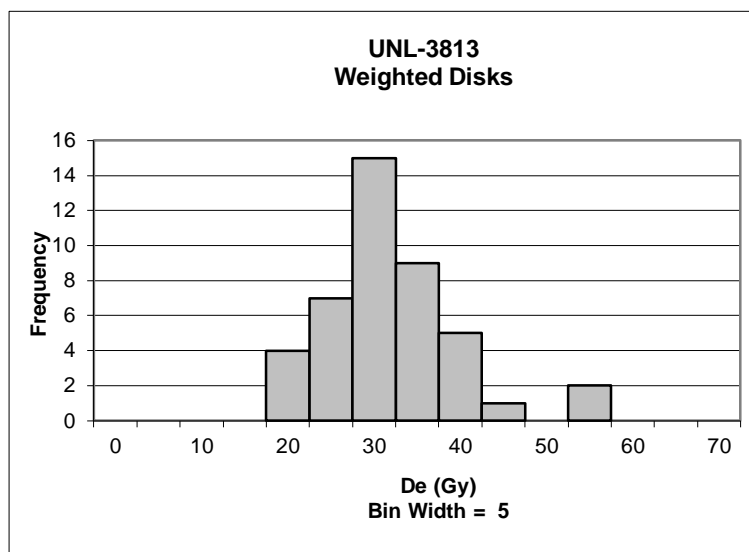
#	De	Error	Age	+/- 1 σ	#	De	Error	Age	+/- 1 σ
1	20.596	0.33	10.248	1.14	22	29.086	0.81	14.472	0.07
2	31.539	0.45	15.693	0.24	23	50.321	1.26	25.039	2.62
3	31.471	0.06	15.659	0.24	24	39.367	1.42	19.588	1.23
4	28.490	0.25	14.176	0.14	25	22.101	0.43	10.997	0.95
5	35.303	0.63	17.566	0.72	26	18.115	0.59	9.014	1.45
6	22.056	0.22	10.975	0.96	27	20.263	0.41	10.082	1.18
7	26.593	1.69	13.232	0.38	28	20.765	0.81	10.332	1.12
8	33.396	0.92	16.617	0.48	29	42.340	0.54	21.067	1.61
9	32.256	0.13	16.050	0.34	30	29.560	1.05	14.709	0.01
10	34.482	0.33	17.157	0.62	31	15.278	0.88	7.602	1.81
11	24.538	0.98	12.209	0.64	32	25.736	0.72	12.806	0.49
12	33.577	1.68	16.707	0.50	33	28.205	0.15	14.034	0.18
13	36.473	0.20	18.148	0.87	34	24.615	0.77	12.248	0.63
14	25.236	0.32	12.557	0.55	35	52.253	2.00	26.000	2.86
15	25.884	1.08	12.879	0.47	36	28.574	0.44	14.218	0.13
16	34.592	0.47	17.212	0.63	37	29.108	0.52	14.483	0.06
17	28.394	0.69	14.128	0.15	38	25.777	1.97	12.826	0.48
18	33.986	1.46	16.911	0.55	39	29.457	0.36	14.657	0.02
19	19.837	0.37	9.871	1.24	40	38.476	0.08	19.145	1.12
20	37.421	1.96	18.620	0.99	41	17.750	1.90	8.832	1.50
21	34.543	0.53	17.188	0.62	42	28.374	0.62	14.119	0.16
					43	26.935	0.34	13.402	0.34

3813 (n=43)

Central value = 28.7 ± 1.1 (1σ)

Dispersion = 26 %

Minimum age: 18.15±0.6

9.2.3   UNL – 3815

UNL-3815
All Disks

(Histogram: x-axis "De (Gy)", Bin Width = 10; y-axis "Frequency")
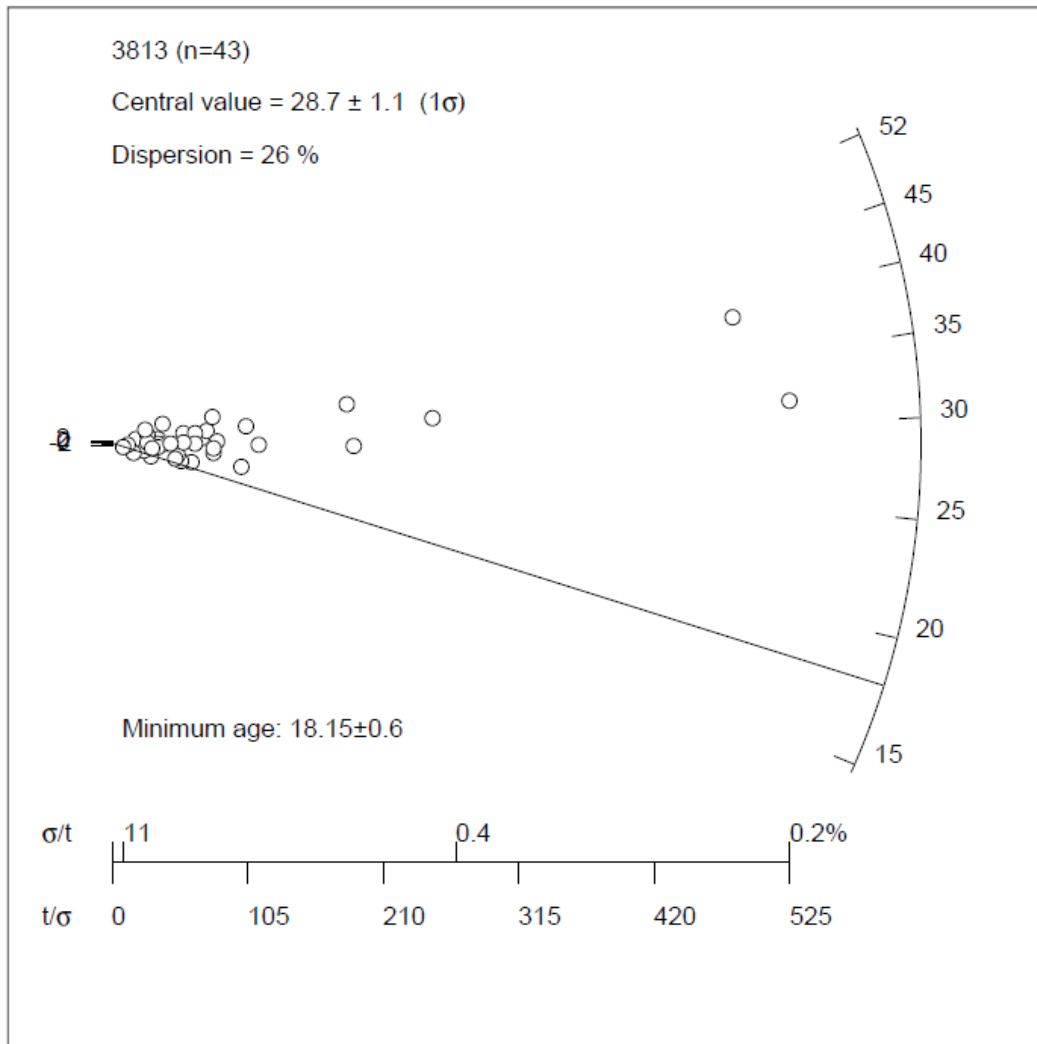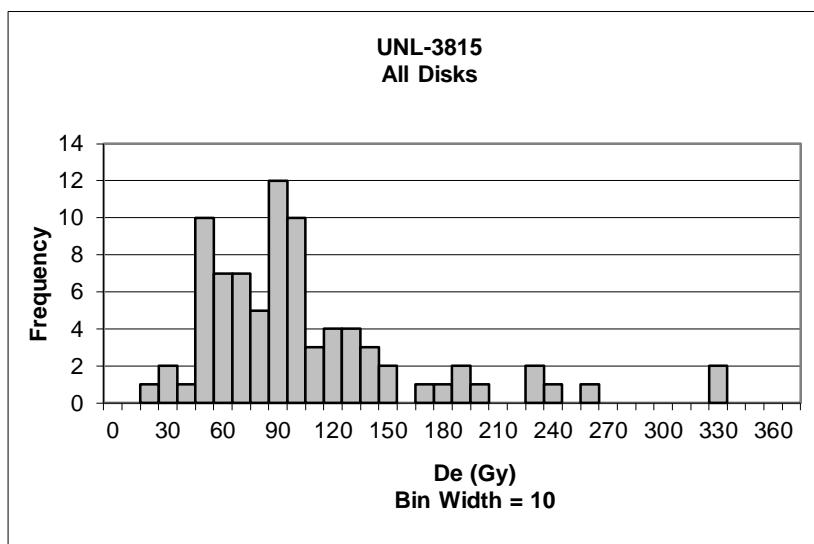
#	De	Error	Age	+/- 1 σ	#	De	Error	Age	+/- 1 σ
1	45.197	1.12	16.306	1.15	28	190.259	6.59	68.642	6.66
2	36.143	4.55	13.040	1.64	29	220.231	4.83	79.455	8.28
3	87.877	2.55	31.705	1.15	30	88.629	0.45	31.976	1.19
4	57.447	1.74	20.726	0.49	31	113.108	13.62	40.807	2.51
5	126.994	8.21	45.817	3.26	32	47.146	7.98	17.009	1.05
6	60.333	3.73	21.767	0.34	33	85.670	0.63	30.908	1.03
7	237.669	3.94	85.746	9.22	34	20.655	2.72	7.452	2.48
8	97.379	21.35	35.133	1.66	35	83.392	3.73	30.086	0.91
9	491.939	5.61	177.483	22.92	36	86.515	4.70	31.213	1.07
10	54.165	4.91	19.542	0.67	37	253.343	3.21	91.401	10.06
11	136.020	3.61	49.073	3.74	38	53.639	18.97	19.352	0.70
12	90.271	15.22	32.568	1.28	39	141.816	20.68	51.165	4.05
13	80.540	4.45	29.057	0.75	40	63.733	2.02	22.994	0.15
14	47.533	4.45	17.149	1.03	41	322.331	2.96	116.291	13.78
15	83.546	5.91	30.142	0.91	42	86.427	9.20	31.181	1.07
16	83.095	2.34	29.979	0.89	43	165.687	7.71	59.777	5.34
17	132.947	0.05	47.965	3.58	44	96.932	0.72	34.971	1.64
18	112.564	2.90	40.611	2.48	45	101.119	7.46	36.482	1.86
19	27.838	15.58	10.043	2.09	46	67.440	9.15	24.331	0.05
20	125.226	3.22	45.179	3.16	47	112.175	4.39	40.471	2.46
21	82.633	10.32	29.813	0.86	48	82.334	1.93	29.704	0.85
22	124.877	4.19	45.053	3.14	49	95.489	2.06	34.451	1.56
23	182.516	1.51	65.848	6.25	50	172.029	3.65	62.065	5.68
24	148.035	4.21	53.408	4.39	51	56.225	7.21	20.285	0.56
25	98.138	1.66	35.406	1.70	52	95.195	12.31	34.345	1.54
26	92.162	2.03	33.251	1.38	53	83.803	2.37	30.234	0.93
27	229.205	6.42	82.693	8.76	54	58.118	3.43	20.968	0.46

UNL-3815
Weighted Disks

De (Gy)
Bin Width = 5
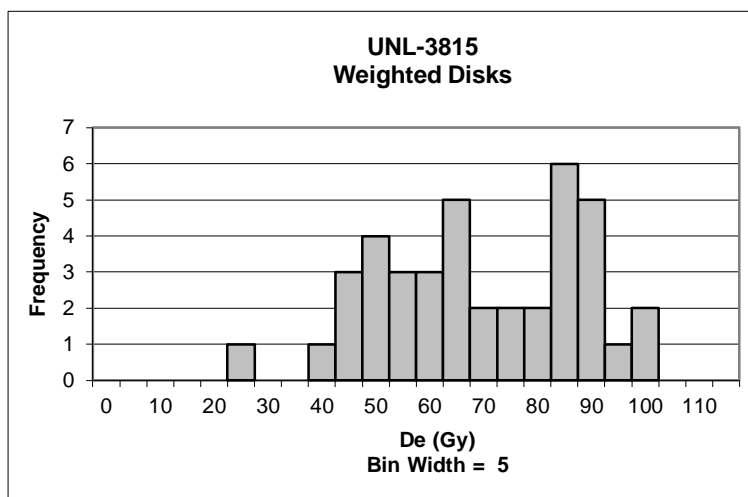
#	De	Error	Age	+/- 1 σ	#	De	Error	Age	+/- 1 σ
1	45.197	1.12	16.306	1.15	21	82.334	1.93	29.704	0.85
2	36.143	4.55	13.040	1.64	22	95.489	2.06	34.451	1.56
3	87.877	2.55	31.705	1.15	23	56.225	7.21	20.285	0.56
4	57.447	1.74	20.726	0.49	24	95.195	12.31	34.345	1.54
5	60.333	3.73	21.767	0.34	25	58.118	3.43	20.968	0.46
6	54.165	4.91	19.542	0.67	26	74.214	6.60	26.775	0.41
7	80.540	4.45	29.057	0.75	27	90.260	0.73	32.564	1.28
8	83.546	5.91	30.142	0.91	28	77.625	8.62	28.006	0.59
9	83.095	2.34	29.979	0.89	29	64.116	6.90	23.132	0.13
10	82.633	10.32	29.813	0.86	30	71.769	3.84	25.893	0.28
11	88.629	0.45	31.976	1.19	31	46.288	1.94	16.700	1.09
12	47.146	7.98	17.009	1.05	32	65.078	1.17	23.479	0.08
13	85.670	0.63	30.908	1.03	33	42.222	12.28	15.233	1.31
14	20.655	2.72	7.452	2.48	34	54.875	2.50	19.798	0.63
15	83.392	3.73	30.086	0.91	35	41.559	2.05	14.994	1.35
16	86.515	4.70	31.213	1.07	36	47.610	4.06	17.177	1.02
17	53.639	18.97	19.352	0.70	37	60.096	1.67	21.681	0.35
18	63.733	2.02	22.994	0.15	38	63.452	0.99	22.892	0.17
19	86.427	9.20	31.181	1.07	39	43.761	1.07	15.788	1.23
20	67.440	9.15	24.331	0.05	40	79.062	5.53	28.524	0.67

3815 (n=40)

Central value = 64.5 ± 3.2 (1σ)

Dispersion = 30 %

Minimum age: 43.1±4.6

95
80
70
60
50
40
30
21

σ/t   35   1   0.5%

t/σ   0   39   78   117   156   195 197

9.2.4   UNL – 3816

UNL-3816
All Disks

De (Gy)
Bin Width = 5
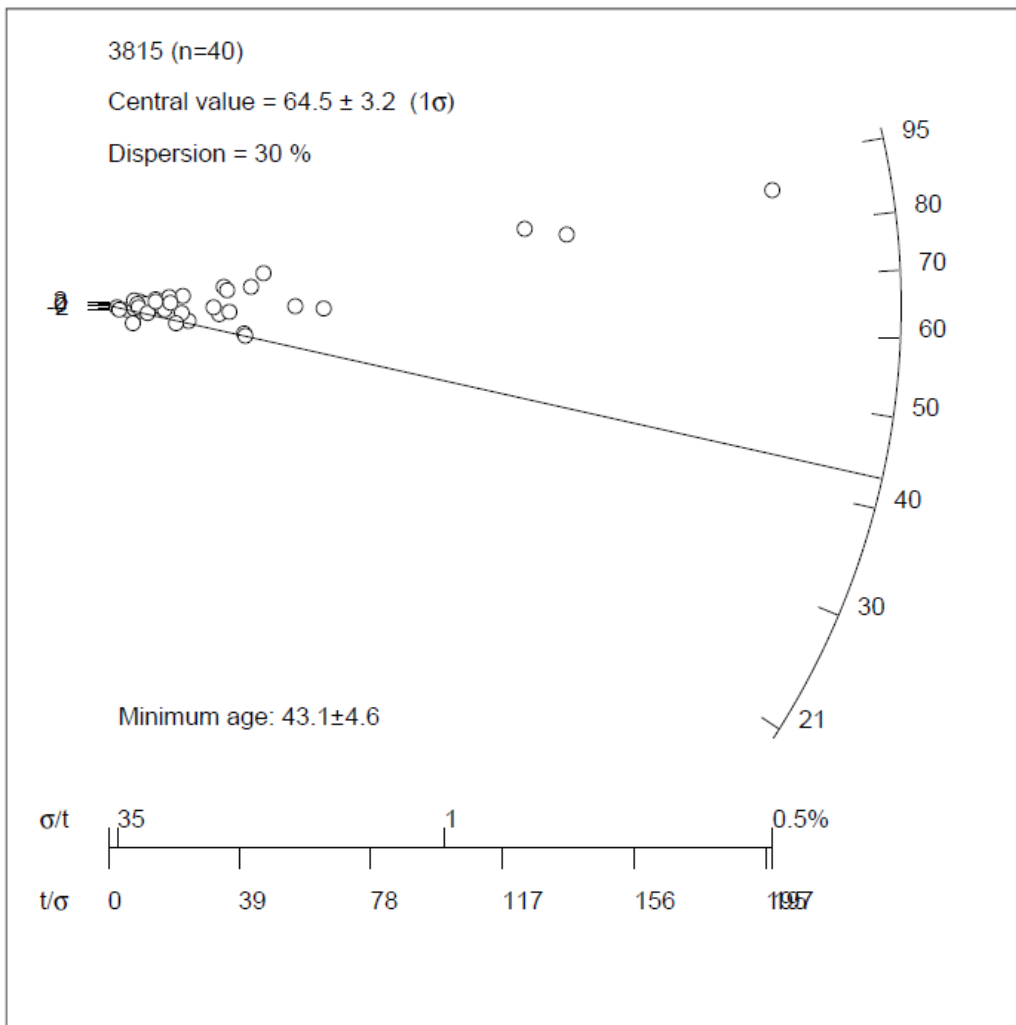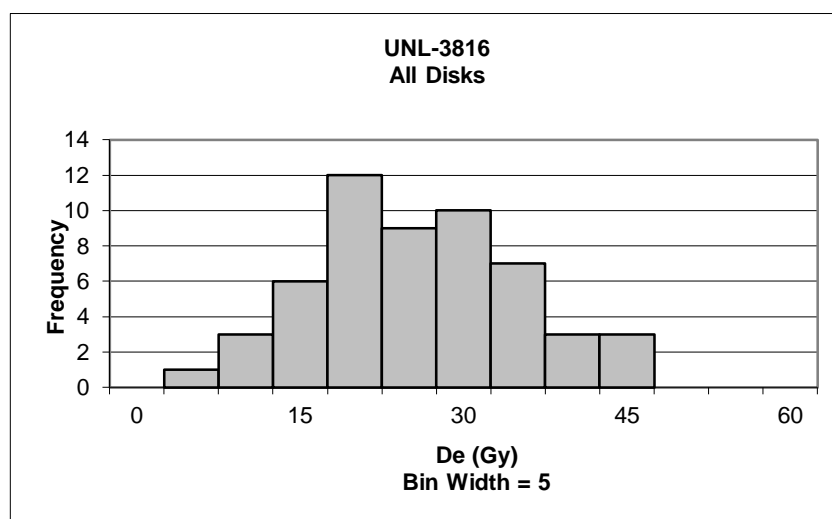
#	De	Error	Age	+/- 1 σ	#	De	Error	Age	+/- 1 σ
1	21.429	0.59	12.524	0.06	28	22.758	0.35	13.301	0.11
2	25.607	1.17	14.966	0.47	29	16.718	1.06	9.771	0.66
3	12.406	0.44	7.251	1.21	30	39.325	0.08	22.983	2.22
4	18.073	0.24	10.563	0.49	31	27.450	1.33	16.043	0.71
5	18.131	0.49	10.596	0.48	32	37.158	1.32	21.716	1.94
6	29.063	0.14	16.985	0.91	33	15.510	0.21	9.065	0.81
7	29.258	0.77	17.099	0.94	34	14.639	0.65	8.556	0.93
8	30.028	0.69	17.549	1.04	35	16.108	0.58	9.414	0.74
9	27.887	0.30	16.298	0.76	36	19.917	0.36	11.640	0.25
10	42.201	0.80	24.663	2.59	37	23.835	0.64	13.930	0.25
11	38.551	0.49	22.530	2.12	38	17.768	0.53	10.384	0.53
12	25.500	0.89	14.903	0.46	39	24.859	0.64	14.528	0.38
13	32.312	0.15	18.884	1.33	40	32.543	0.17	19.019	1.36
14	32.414	0.53	18.944	1.34	41	28.866	0.21	16.870	0.89
15	31.443	0.14	18.376	1.22	42	10.493	2.01	6.132	1.45
16	19.237	0.49	11.243	0.34	43	18.880	0.36	11.034	0.39
17	34.496	0.30	20.160	1.60	44	14.571	0.32	8.516	0.93
18	18.690	0.12	10.923	0.41	45	4.287	2.09	2.506	2.25
19	20.438	1.27	11.944	0.19	46	27.862	0.21	16.283	0.76
20	42.896	0.14	25.070	2.68	47	14.808	0.70	8.654	0.90
21	21.151	0.28	12.361	0.10	48	26.173	0.38	15.296	0.54
22	21.297	0.38	12.447	0.08	49	9.187	0.40	5.369	1.62
23	19.269	0.54	11.261	0.34	50	12.434	0.37	7.267	1.21
24	23.543	0.80	13.759	0.21	51	8.286	0.55	4.842	1.74
25	30.477	0.37	17.811	1.09	52	25.471	0.61	14.886	0.45
26	9.421	0.17	5.506	1.59	53	17.881	0.70	10.450	0.51
27	20.094	1.22	11.743	0.23	54	40.965	0.30	23.941	2.43

UNL-3816
Weighted Disks
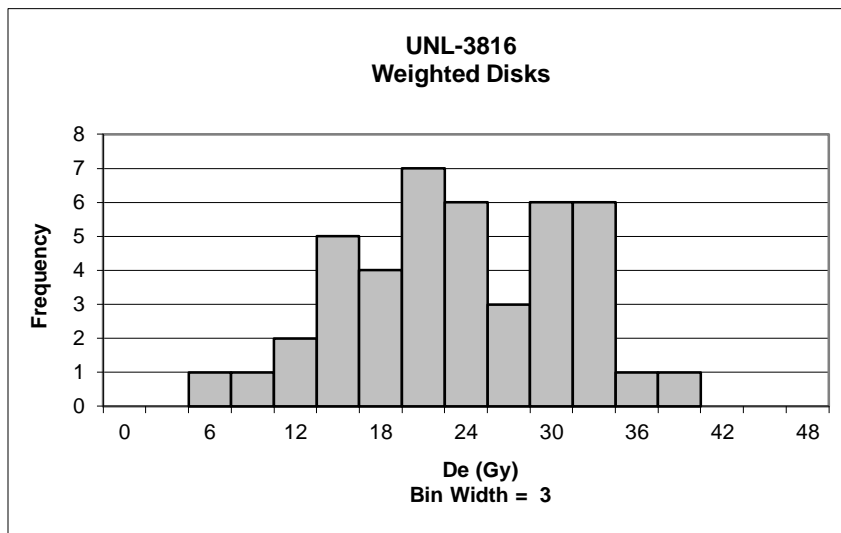
#	De	Error	Age	+/- 1 σ	#	De	Error	Age	+/- 1 σ
1	21.429	0.59	12.524	0.06	23	27.450	1.33	16.043	0.71
2	12.406	0.44	7.251	1.21	24	37.158	1.32	21.716	1.94
3	18.073	0.24	10.563	0.49	25	15.510	0.21	9.065	0.81
4	18.131	0.49	10.596	0.48	26	14.639	0.65	8.556	0.93
5	29.063	0.14	16.985	0.91	27	16.108	0.58	9.414	0.74
6	29.258	0.77	17.099	0.94	28	19.917	0.36	11.640	0.25
7	30.028	0.69	17.549	1.04	29	23.835	0.64	13.930	0.25
8	27.887	0.30	16.298	0.76	30	17.768	0.53	10.384	0.53
9	25.500	0.89	14.903	0.46	31	32.543	0.17	19.019	1.36
10	32.312	0.15	18.884	1.33	32	28.866	0.21	16.870	0.89
11	32.414	0.53	18.944	1.34	33	18.880	0.36	11.034	0.39
12	31.443	0.14	18.376	1.22	34	14.571	0.32	8.516	0.93
13	19.237	0.49	11.243	0.34	35	4.287	2.09	2.506	2.25
14	34.496	0.30	20.160	1.60	36	27.862	0.21	16.283	0.76
15	18.690	0.12	10.923	0.41	37	14.808	0.70	8.654	0.90
16	21.151	0.28	12.361	0.10	38	26.173	0.38	15.296	0.54
17	21.297	0.38	12.447	0.08	39	9.187	0.40	5.369	1.62
18	19.269	0.54	11.261	0.34	40	12.434	0.37	7.267	1.21
19	23.543	0.80	13.759	0.21	41	8.286	0.55	4.842	1.74
20	30.477	0.37	17.811	1.09	42	25.471	0.61	14.886	0.45
21	9.421	0.17	5.506	1.59	43	17.881	0.70	10.450	0.51
22	22.758	0.35	13.301	0.11					

3816 (n=43)

Central value = 20.7 ± 1.2 (1σ)

Dispersion = 38 %

Minimum age: 9.33±0.18

9.2.5   UNL – 3817
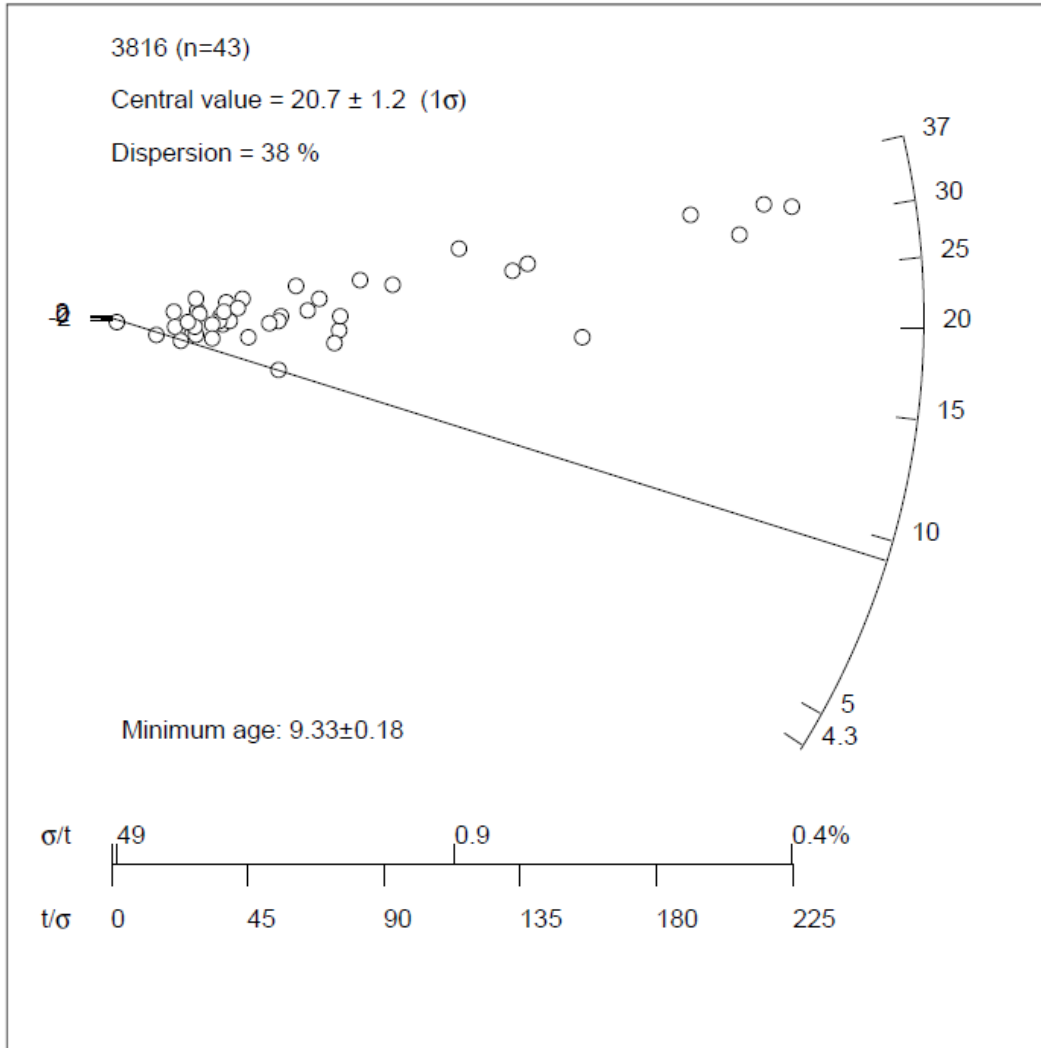
UNL-3817
All Disks
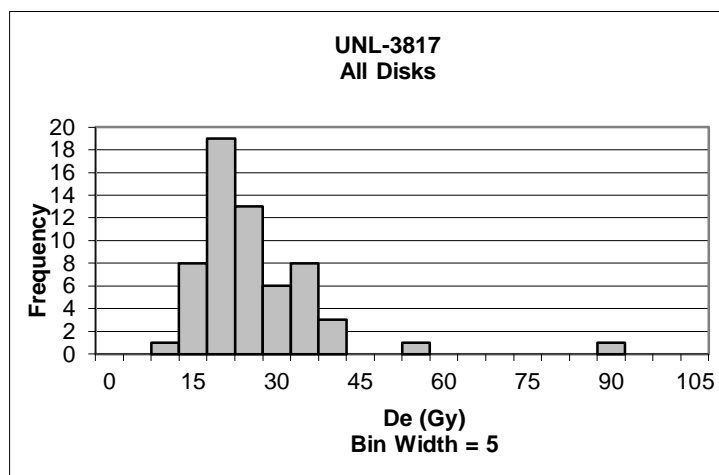
#	De	Error	Age	+/- 1 σ	#	De	Error	Age	+/- 1 σ
1	12.527	0.83	5.892	1.32	31	18.972	0.36	8.923	0.33
2	30.292	1.71	14.246	1.43	32	33.858	1.15	15.923	1.98
3	32.756	2.19	15.405	1.81	33	31.296	1.17	14.719	1.58
4	39.152	0.42	18.413	2.80	34	18.610	0.20	8.752	0.38
5	23.232	1.00	10.926	0.33	35	20.815	0.86	9.790	0.04
6	11.365	0.93	5.345	1.50	36	12.370	0.18	5.818	1.35
7	23.127	0.56	10.877	0.32	37	25.648	1.63	12.062	0.71
8	15.738	0.90	7.401	0.83	38	19.296	0.40	9.075	0.28
9	18.829	0.59	8.855	0.35	39	39.057	1.15	18.369	2.78
10	14.445	0.82	6.794	1.03	40	28.605	0.46	13.453	1.17
11	18.899	0.77	8.888	0.34	41	29.843	0.75	14.036	1.36
12	18.404	0.52	8.656	0.41	42	16.574	0.62	7.795	0.70
13	19.688	0.64	9.259	0.21	43	13.128	0.23	6.174	1.23
14	18.183	0.44	8.552	0.45	44	21.357	0.91	10.044	0.04
15	21.652	0.40	10.183	0.09	45	34.643	0.06	16.293	2.10
16	21.613	0.32	10.165	0.08	46	28.911	0.98	13.597	1.21
17	19.202	0.67	9.031	0.29	47	31.838	0.89	14.973	1.67
18	24.897	0.35	11.709	0.59	48	20.972	0.45	9.863	0.02
19	26.722	1.00	12.567	0.87	49	85.930	0.29	40.413	10.04
20	53.136	1.02	24.990	4.96	50	22.826	0.16	10.735	0.27
21	18.372	0.65	8.641	0.42	51	22.617	0.62	10.637	0.24
22	17.783	0.37	8.363	0.51	52	12.645	1.12	5.947	1.30
23	19.164	0.66	9.013	0.30	53	14.294	1.09	6.722	1.05
24	38.590	0.94	18.149	2.71	54	30.640	0.12	14.410	1.48
25	20.524	0.57	9.652	0.09	55	32.924	1.86	15.484	1.83
26	4609.525	2.00	2167.881	710.06	56	7.982	0.89	3.754	2.03
27	16.882	0.33	7.940	0.65	57	16.525	0.37	7.772	0.70
28	19.424	0.90	9.135	0.26	58	15.177	0.19	7.138	0.91
29	19.288	0.99	9.071	0.28	59	25.373	1.17	11.933	0.67
30	21.592	0.32	10.155	0.08	60	22.977	0.36	10.806	0.29
					61	13.282	0.76	6.247	1.21

UNL-3817
Weighted Disks

De (Gy)
Bin Width = 2
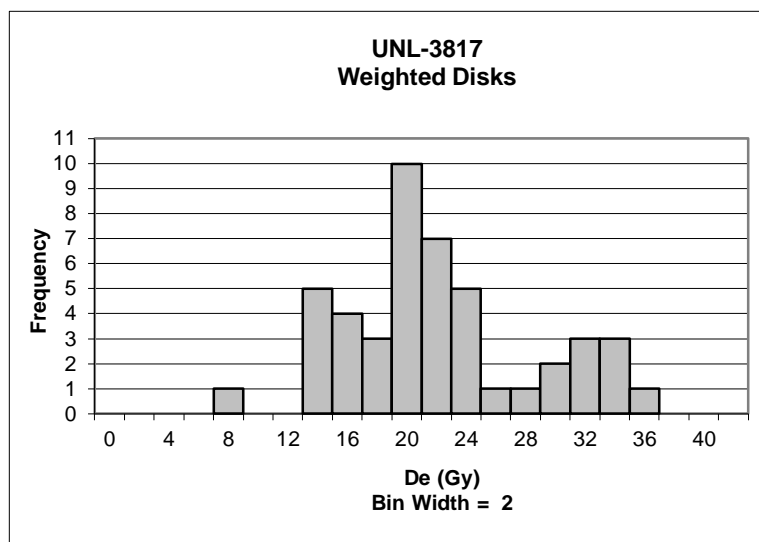
#	De	Error	Age	+/- 1 σ	#	De	Error	Age	+/- 1 σ
1	12.527	0.83	5.892	1.32	24	18.610	0.20	8.752	0.38
2	30.292	1.71	14.246	1.43	25	20.815	0.86	9.790	0.04
3	32.756	2.19	15.405	1.81	26	12.370	0.18	5.818	1.35
4	23.232	1.00	10.926	0.33	27	19.296	0.40	9.075	0.28
5	23.127	0.56	10.877	0.32	28	28.605	0.46	13.453	1.17
6	15.738	0.90	7.401	0.83	29	16.574	0.62	7.795	0.70
7	18.829	0.59	8.855	0.35	30	13.128	0.23	6.174	1.23
8	14.445	0.82	6.794	1.03	31	21.357	0.91	10.044	0.04
9	18.899	0.77	8.888	0.34	32	34.643	0.06	16.293	2.10
10	18.404	0.52	8.656	0.41	33	28.911	0.98	13.597	1.21
11	19.688	0.64	9.259	0.21	34	31.838	0.89	14.973	1.67
12	18.183	0.44	8.552	0.45	35	20.972	0.45	9.863	0.02
13	21.652	0.40	10.183	0.09	36	22.826	0.16	10.735	0.27
14	21.613	0.32	10.165	0.08	37	22.617	0.62	10.637	0.24
15	19.202	0.67	9.031	0.29	38	12.645	1.12	5.947	1.30
16	24.897	0.35	11.709	0.59	39	14.294	1.09	6.722	1.05
17	26.722	1.00	12.567	0.87	40	30.640	0.12	14.410	1.48
18	18.372	0.65	8.641	0.42	41	32.924	1.86	15.484	1.83
19	20.524	0.57	9.652	0.09	42	7.982	0.89	3.754	2.03
20	16.882	0.33	7.940	0.65	43	16.525	0.37	7.772	0.70
21	21.592	0.32	10.155	0.08	44	15.177	0.19	7.138	0.91
22	18.972	0.36	8.923	0.33	45	22.977	0.36	10.806	0.29
23	33.858	1.15	15.923	1.98	46	13.282	0.76	6.247	1.21

3817 (n=46)

Central value = 20.17 ± 0.91 (1σ)

Dispersion = 30 %

Minimum age: 12.4±0.2

9.2.6   UNL – 3819
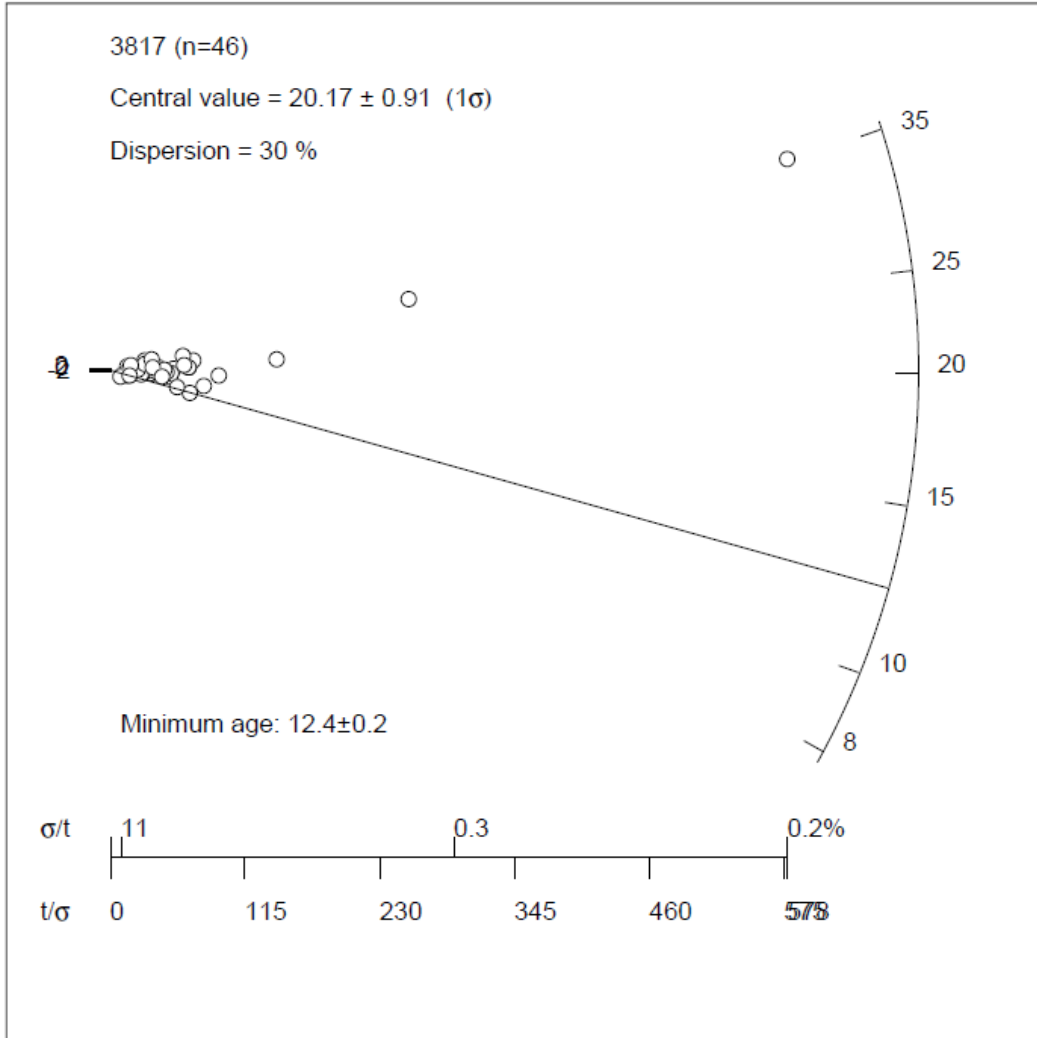
UNL-3819
All Disks
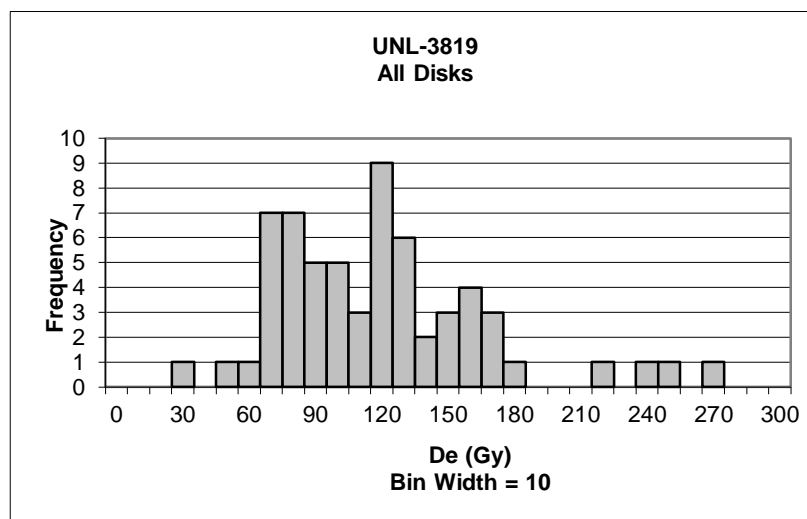
#	De	Error	Age	+/- 1 σ	#	De	Error	Age	+/- 1 σ
1	751.562	7.57	351.468	18.40	33	80.453	34.52	37.624	0.81
2	83.508	1.00	39.052	0.72	34	84.614	4.05	39.570	0.69
3	231.476	14.35	108.250	3.51	35	94.325	1.94	44.111	0.42
4	128.165	4.72	59.936	0.55	36	27.559	7.60	12.888	2.33
5	140.202	9.72	65.565	0.90	37	113.380	0.83	53.022	0.13
6	74.541	4.58	34.859	0.98	38	75.447	6.89	35.283	0.96
7	144.748	2.59	67.691	1.03	39	112.847	11.30	52.773	0.12
8	49.913	4.94	23.342	1.69	40	78.252	9.80	36.595	0.88
9	158.882	1.32	74.301	1.43	41	69.958	7.11	32.716	1.11
10	103.913	3.71	48.595	0.14	42	165.534	8.48	77.412	1.62
11	159.432	9.93	74.558	1.45	43	72.016	12.07	33.678	1.05
12	123.488	4.55	57.749	0.42	44	78.339	21.93	36.635	0.87
13	117.953	5.85	55.161	0.26	45	61.635	6.09	28.824	1.35
14	69.867	8.02	32.673	1.12	46	100.791	3.04	47.135	0.23
15	158.070	7.76	73.922	1.41	47	61.268	8.08	28.652	1.36
16	216.523	15.11	101.257	3.08	48	102.604	1.82	47.983	0.18
17	248.270	23.73	116.103	3.99	49	130.182	12.33	60.880	0.61
18	173.921	25.28	81.334	1.86	50	94.963	1.21	44.409	0.40
19	81.220	5.86	37.982	0.79	51	118.955	4.09	55.629	0.29
20	57.480	25.93	26.881	1.47	52	260.890	10.05	122.005	4.35
21	114.254	12.24	53.431	0.16	53	63.036	33.91	29.479	1.31
22	112.760	5.19	52.732	0.11	54	61.579	9.26	28.797	1.35
23	96.838	13.38	45.286	0.34	55	118.939	14.62	55.622	0.29
24	82.933	16.54	38.783	0.74	56	167.316	39.90	78.245	1.67
25	79.340	4.55	37.104	0.84	57	125.517	1.05	58.698	0.48
26	117.787	15.96	55.083	0.26	58	165.029	11.67	77.176	1.61
27	129.849	134.18	60.724	0.60	59	129.399	8.40	60.513	0.59
28	120.004	18.52	56.120	0.32	60	95.195	7.90	44.518	0.39
29	132.591	6.49	62.006	0.68	61	141.010	7.80	65.943	0.92
30	119.289	7.66	55.785	0.30	62	73.551	15.51	34.396	1.01
31	96.033	8.26	44.910	0.37	63	61.073	13.80	28.561	1.37
32	158.733	6.36	74.231	1.43					

UNL-3819
Weighted Disks

De (Gy)
Bin Width = 10
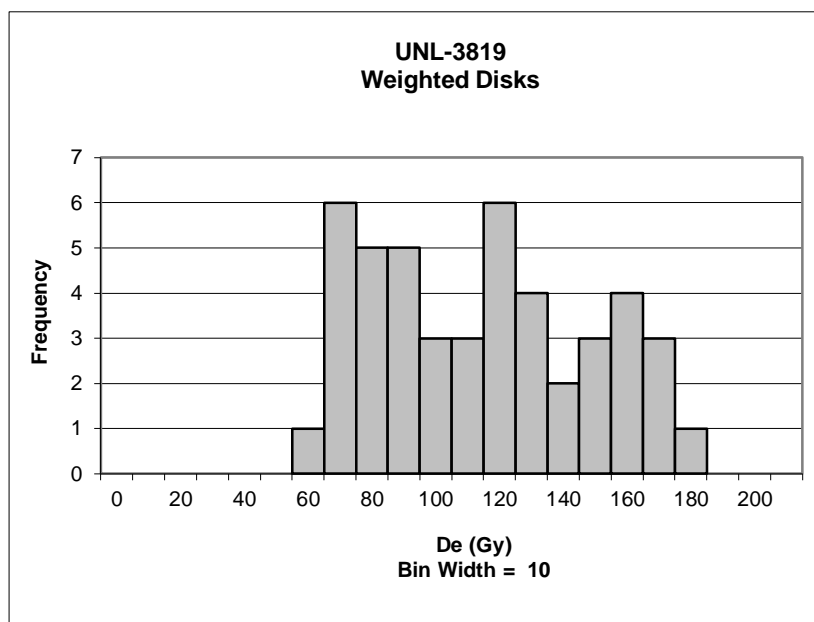
#	De	Error	Age	+/- 1 σ	#	De	Error	Age	+/- 1 σ
1	83.508	1.00	39.052	0.72	24	113.380	0.83	53.022	0.13
2	140.202	9.72	65.565	0.90	25	75.447	6.89	35.283	0.96
3	74.541	4.58	34.859	0.98	26	112.847	11.30	52.773	0.12
4	144.748	2.59	67.691	1.03	27	78.252	9.80	36.595	0.88
5	158.882	1.32	74.301	1.43	28	165.534	8.48	77.412	1.62
6	103.913	3.71	48.595	0.14	29	72.016	12.07	33.678	1.05
7	159.432	9.93	74.558	1.45	30	61.635	6.09	28.824	1.35
8	123.488	4.55	57.749	0.42	31	100.791	3.04	47.135	0.23
9	117.953	5.85	55.161	0.26	32	61.268	8.08	28.652	1.36
10	69.867	8.02	32.673	1.12	33	102.604	1.82	47.983	0.18
11	158.070	7.76	73.922	1.41	34	130.182	12.33	60.880	0.61
12	173.921	25.28	81.334	1.86	35	94.963	1.21	44.409	0.40
13	81.220	5.86	37.982	0.79	36	63.036	33.91	29.479	1.31
14	57.480	25.93	26.881	1.47	37	61.579	9.26	28.797	1.35
15	112.760	5.19	52.732	0.11	38	118.939	14.62	55.622	0.29
16	96.838	13.38	45.286	0.34	39	167.316	39.90	78.245	1.67
17	82.933	16.54	38.783	0.74	40	125.517	1.05	58.698	0.48
18	120.004	18.52	56.120	0.32	41	165.029	11.67	77.176	1.61
19	132.591	6.49	62.006	0.68	42	129.399	8.40	60.513	0.59
20	119.289	7.66	55.785	0.30	43	95.195	7.90	44.518	0.39
21	158.733	6.36	74.231	1.43	44	141.010	7.80	65.943	0.92
22	80.453	34.52	37.624	0.81	45	73.551	15.51	34.396	1.01
23	84.614	4.05	39.570	0.69	46	61.073	13.80	28.561	1.37

3819 (n=46)

Central value = 106.9 ± 4.9 (1σ)

Dispersion = 29 %

174

140

120

100

80

60
57

Minimum age: 71.7±4.7

σ/t   54   1   0.7%

t/σ   0   27   54   81   108   135   57

9.2.7   UNL – 3820

UNL-3820
All Disks

Frequency vs De (Gy), Bin Width = 5
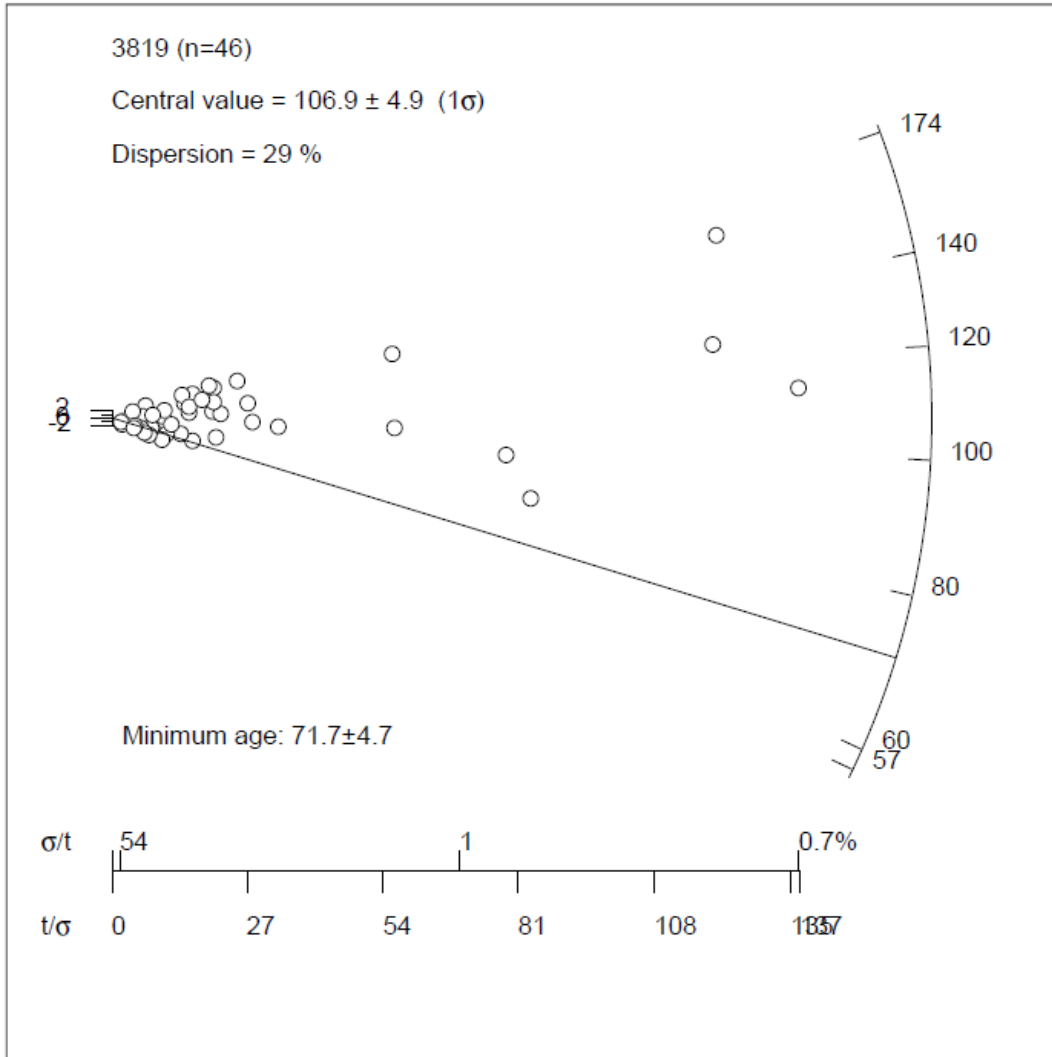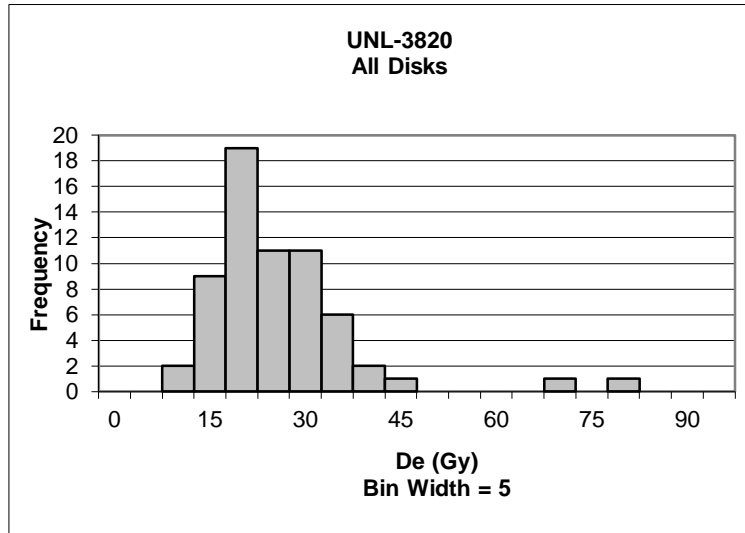
#	De	Error	Age	+/- 1 σ	#	De	Error	Age	+/- 1 σ
1	44.126	1.31	15.841	3.16	33	12.716	1.09	4.565	1.29
2	37.523	1.35	13.470	2.22	34	13.507	1.10	4.849	1.18
3	12.584	0.56	4.517	1.31	35	33.676	0.09	12.089	1.68
4	77.538	2.95	27.835	7.90	36	18.931	0.67	6.796	0.41
5	20.235	0.63	7.264	0.23	37	9.440	0.74	3.389	1.76
6	28.806	0.77	10.341	0.99	38	30.165	0.76	10.829	1.18
7	16.794	0.62	6.029	0.72	39	26.560	0.78	9.535	0.67
8	34.685	1.22	12.452	1.82	40	28.532	1.09	10.243	0.95
9	15.266	1.37	5.480	0.93	41	16.281	0.87	5.845	0.79
10	15.775	0.87	5.663	0.86	42	22.747	0.92	8.166	0.13
11	22.576	0.31	8.105	0.10	43	11.761	0.88	4.222	1.43
12	11.980	0.64	4.301	1.40	44	12.266	0.17	4.404	1.36
13	19.469	0.70	6.989	0.34	45	17.218	0.28	6.181	0.66
14	17.153	0.78	6.158	0.67	46	34.842	0.66	12.508	1.84
15	24.573	0.19	8.822	0.39	47	18.267	0.35	6.558	0.51
16	24.327	1.03	8.733	0.35	48	15.553	0.25	5.583	0.89
17	17.109	0.54	6.142	0.67	49	66.447	3.29	23.854	6.33
18	29.624	0.96	10.635	1.10	50	24.497	0.44	8.794	0.38
19	10.924	0.43	3.922	1.55	51	28.975	0.62	10.402	1.01
20	26.772	0.76	9.611	0.70	52	37.154	0.14	13.338	2.17
21	24.046	0.82	8.632	0.31	53	15.264	0.63	5.480	0.93
22	21.059	0.81	7.560	0.11	54	21.458	0.85	7.703	0.05
23	28.402	0.69	10.196	0.93	55	5.724	1.12	2.055	2.29
24	18.822	0.27	6.757	0.43	56	20.780	2.34	7.460	0.15
25	26.432	0.70	9.489	0.65	57	20.542	0.90	7.374	0.18
26	17.286	0.76	6.206	0.65	58	16.541	0.97	5.938	0.75
27	12.485	0.59	4.482	1.33	59	17.167	0.94	6.163	0.66
28	14.544	0.31	5.221	1.04	60	28.141	0.97	10.102	0.89
29	27.277	0.69	9.792	0.77	61	17.254	1.97	6.194	0.65
30	31.743	0.07	11.396	1.40	62	29.797	0.58	10.697	1.13
31	19.659	0.34	7.057	0.31	63	18.605	1.74	6.679	0.46
32	30.939	0.19	11.107	1.29					

UNL-3820
Weighted Disks

De (Gy)
Bin Width = 2
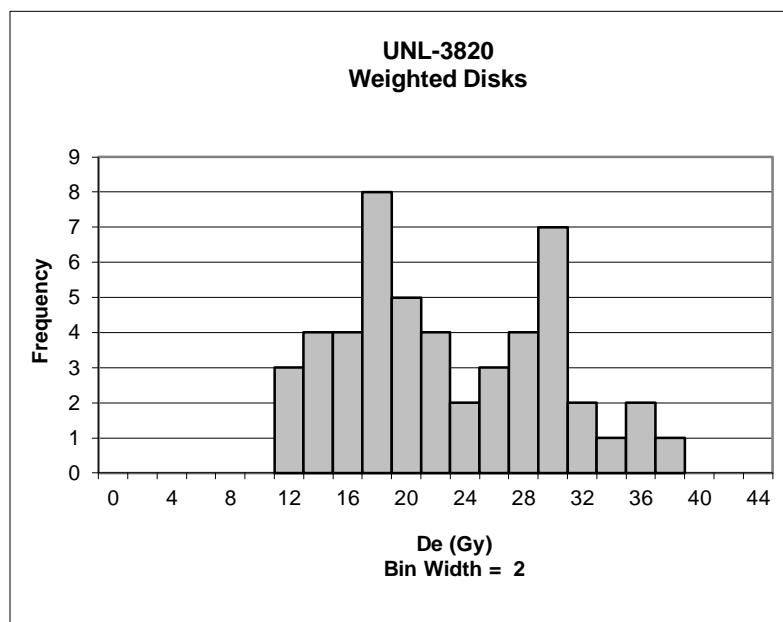
#	De	Error	Age	+/- 1 σ	#	De	Error	Age	+/- 1 σ
1	37.523	1.35	13.470	2.22	26	19.659	0.34	7.057	0.31
2	12.584	0.56	4.517	1.31	27	30.939	0.19	11.107	1.29
3	20.235	0.63	7.264	0.23	28	13.507	1.10	4.849	1.18
4	28.806	0.77	10.341	0.99	29	33.676	0.09	12.089	1.68
5	16.794	0.62	6.029	0.72	30	18.931	0.67	6.796	0.41
6	34.685	1.22	12.452	1.82	31	26.560	0.78	9.535	0.67
7	15.775	0.87	5.663	0.86	32	28.532	1.09	10.243	0.95
8	22.576	0.31	8.105	0.10	33	16.281	0.87	5.845	0.79
9	11.980	0.64	4.301	1.40	34	22.747	0.92	8.166	0.13
10	19.469	0.70	6.989	0.34	35	11.761	0.88	4.222	1.43
11	17.153	0.78	6.158	0.67	36	12.266	0.17	4.404	1.36
12	24.573	0.19	8.822	0.39	37	17.218	0.28	6.181	0.66
13	24.327	1.03	8.733	0.35	38	34.842	0.66	12.508	1.84
14	17.109	0.54	6.142	0.67	39	18.267	0.35	6.558	0.51
15	29.624	0.96	10.635	1.10	40	15.553	0.25	5.583	0.89
16	10.924	0.43	3.922	1.55	41	24.497	0.44	8.794	0.38
17	26.772	0.76	9.611	0.70	42	28.975	0.62	10.402	1.01
18	21.059	0.81	7.560	0.11	43	15.264	0.63	5.480	0.93
19	28.402	0.69	10.196	0.93	44	21.458	0.85	7.703	0.05
20	18.822	0.27	6.757	0.43	45	20.542	0.90	7.374	0.18
21	26.432	0.70	9.489	0.65	46	16.541	0.97	5.938	0.75
22	12.485	0.59	4.482	1.33	47	17.167	0.94	6.163	0.66
23	14.544	0.31	5.221	1.04	48	28.141	0.97	10.102	0.89
24	27.277	0.69	9.792	0.77	49	17.254	1.97	6.194	0.65
25	31.743	0.07	11.396	1.40	50	29.797	0.58	10.697	1.13

3820 (n=50)

Central value = 20.78 ± 0.96 (1σ)

Dispersion = 32 %

38

30

25

20

15

11

Minimum age: 12.2±0.18

σ/t   11   0.4   0.2%

t/σ   0   90   180   270   360   450

9.2.8   UNL – 3822
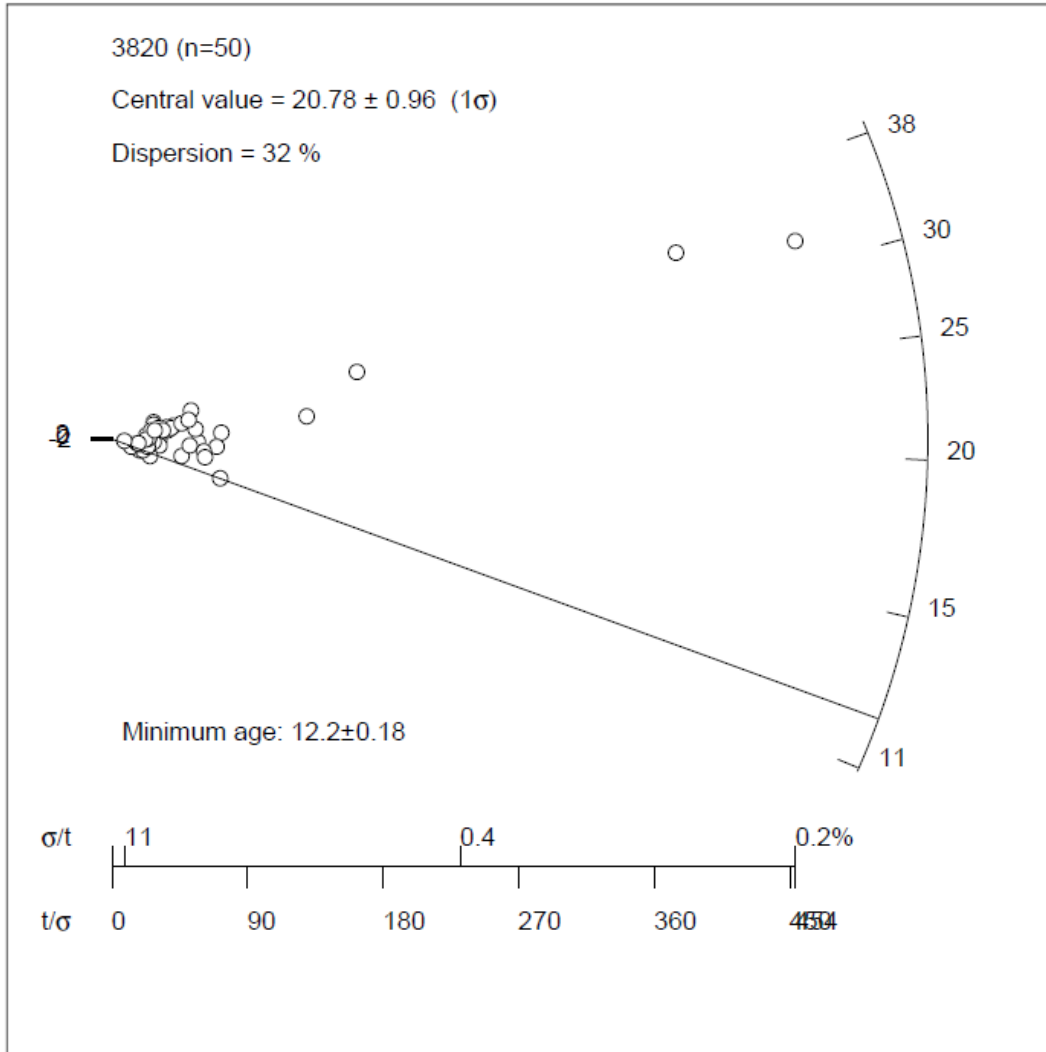
UNL-3822
All Disks
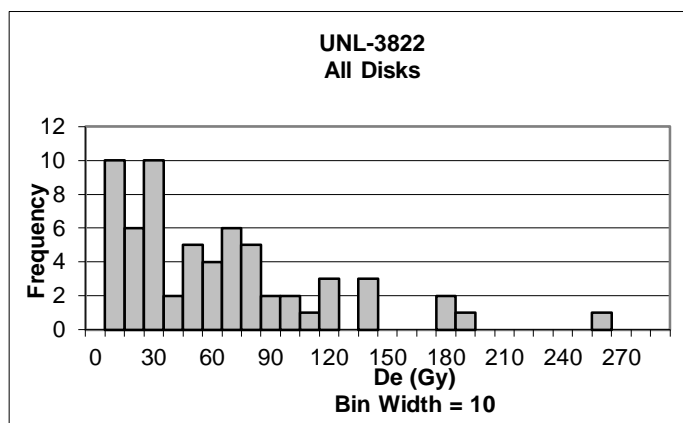
#	De	Error	Age	+/- 1 σ	#	De	Error	Age	+/- 1 σ
1	65.428	1.84	36.312	0.00	32	75.561	20.35	41.935	0.21
2	9.081	24.76	5.040	1.16	33	26.326	28.12	14.611	0.80
3	7.908	78.74	4.389	1.18	34	28.538	10.11	15.838	0.76
4	7.089	56.38	3.934	1.20	35	84.953	4.89	47.148	0.41
5	24.980	4.72	13.864	0.83	36	134.000	9.88	74.368	1.42
6	184.004	3.36	102.120	2.45	37	11.634	8.27	6.457	1.11
7	28.219	16.58	15.661	0.77	38	38.122	13.54	21.157	0.56
8	21.344	17.25	11.846	0.91	39	8.679	17.74	4.817	1.17
9	43.549	17.99	24.169	0.45	40	10.830	9.07	6.010	1.12
10	62.288	5.62	34.569	0.06	41	28.839	18.00	16.005	0.75
11	9.225	34.03	5.120	1.16	42	0.140	28.50	0.078	1.35
12	98.583	1.18	54.712	0.69	43	3.663	17.45	2.033	1.27
13	88.566	6.63	49.153	0.48	44	64.335	5.25	35.705	0.02
14	66.873	18.21	37.114	0.03	45	4.672	128.61	2.593	1.25
15	59.277	13.21	32.898	0.12	46	29.514	3.76	16.380	0.74
16	114.867	15.64	63.750	1.02	47	171.019	10.96	94.913	2.18
17	107.796	14.04	59.826	0.88	48	51.495	7.79	28.579	0.28
18	46.600	3.62	25.863	0.39	49	28.285	37.19	15.698	0.76
19	40.150	17.97	22.283	0.52	50	68.155	11.02	37.825	0.06
20	3.946	48.11	2.190	1.27	51	73.483	7.95	40.782	0.17
21	19.813	9.02	10.996	0.94	52	59.894	10.64	33.240	0.11
22	74.818	7.15	41.523	0.20	53	132.878	4.58	73.746	1.40
23	0.001	63.80	0.000	1.35	54	173.661	4.15	96.380	2.24
24	23.398	8.54	12.985	0.86	55	139.868	7.77	77.625	1.54
25	117.767	5.25	65.359	1.08	56	25.252	44.18	14.015	0.83
26	55.199	5.56	30.635	0.21	57	13.213	28.97	7.333	1.08
27	13.748	54.01	7.630	1.06	58	60.665	12.83	33.668	0.10
28	76.856	11.64	42.654	0.24	59	34.201	27.61	18.981	0.64
29	40.379	11.91	22.410	0.51	60	258.590	12.94	143.514	3.99
30	96.146	21.71	53.360	0.64	61	43.662	5.35	24.232	0.45
31	114.951	17.12	63.797	1.03	62	74.291	18.52	41.231	0.19
					63	17.844	75.38	9.903	0.98

UNL-3822
Weighted Disks

De (Gy)
Bin Width = 10
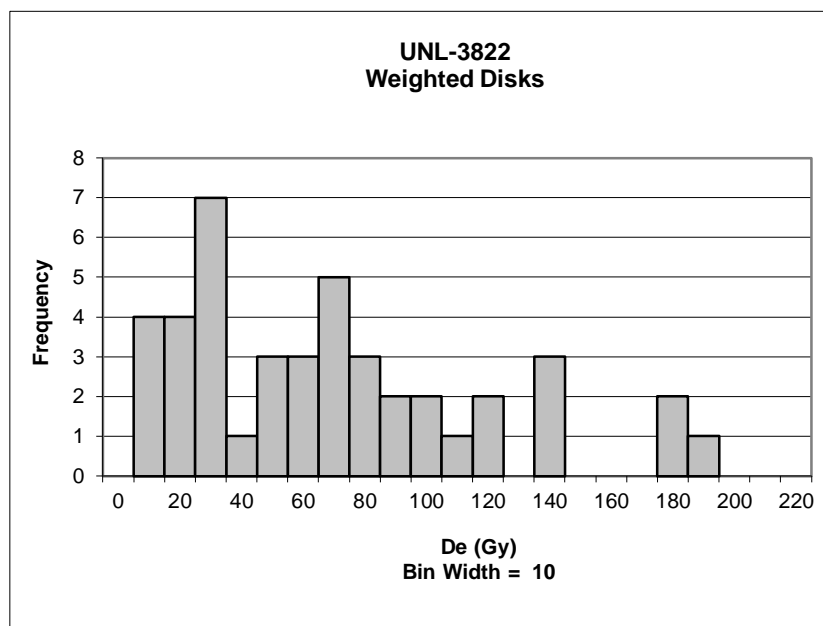
#	De	Error	Age	+/- 1 σ	#	De	Error	Age	+/- 1 σ
1	65.428	1.84	36.312	0.00	22	28.538	10.11	15.838	0.76
2	7.908	78.74	4.389	1.18	23	84.953	4.89	47.148	0.41
3	7.089	56.38	3.934	1.20	24	134.000	9.88	74.368	1.42
4	24.980	4.72	13.864	0.83	25	11.634	8.27	6.457	1.11
5	184.004	3.36	102.120	2.45	26	38.122	13.54	21.157	0.56
6	28.219	16.58	15.661	0.77	27	8.679	17.74	4.817	1.17
7	62.288	5.62	34.569	0.06	28	10.830	9.07	6.010	1.12
8	9.225	34.03	5.120	1.16	29	64.335	5.25	35.705	0.02
9	98.583	1.18	54.712	0.69	30	29.514	3.76	16.380	0.74
10	88.566	6.63	49.153	0.48	31	171.019	10.96	94.913	2.18
11	59.277	13.21	32.898	0.12	32	28.285	37.19	15.698	0.76
12	114.867	15.64	63.750	1.02	33	68.155	11.02	37.825	0.06
13	107.796	14.04	59.826	0.88	34	73.483	7.95	40.782	0.17
14	46.600	3.62	25.863	0.39	35	59.894	10.64	33.240	0.11
15	19.813	9.02	10.996	0.94	36	132.878	4.58	73.746	1.40
16	74.818	7.15	41.523	0.20	37	173.661	4.15	96.380	2.24
17	23.398	8.54	12.985	0.86	38	139.868	7.77	77.625	1.54
18	117.767	5.25	65.359	1.08	39	25.252	44.18	14.015	0.83
19	55.199	5.56	30.635	0.21	40	13.213	28.97	7.333	1.08
20	40.379	11.91	22.410	0.51	41	60.665	12.83	33.668	0.10
21	96.146	21.71	53.360	0.64	42	43.662	5.35	24.232	0.45
					43	74.291	18.52	41.231	0.19

3822 (n=43)

Central value = 66.8 ± 6.6 (1σ)

Dispersion = 56 %

Minimum age: 30.7±3.8

9.2.9 UNL – 3823
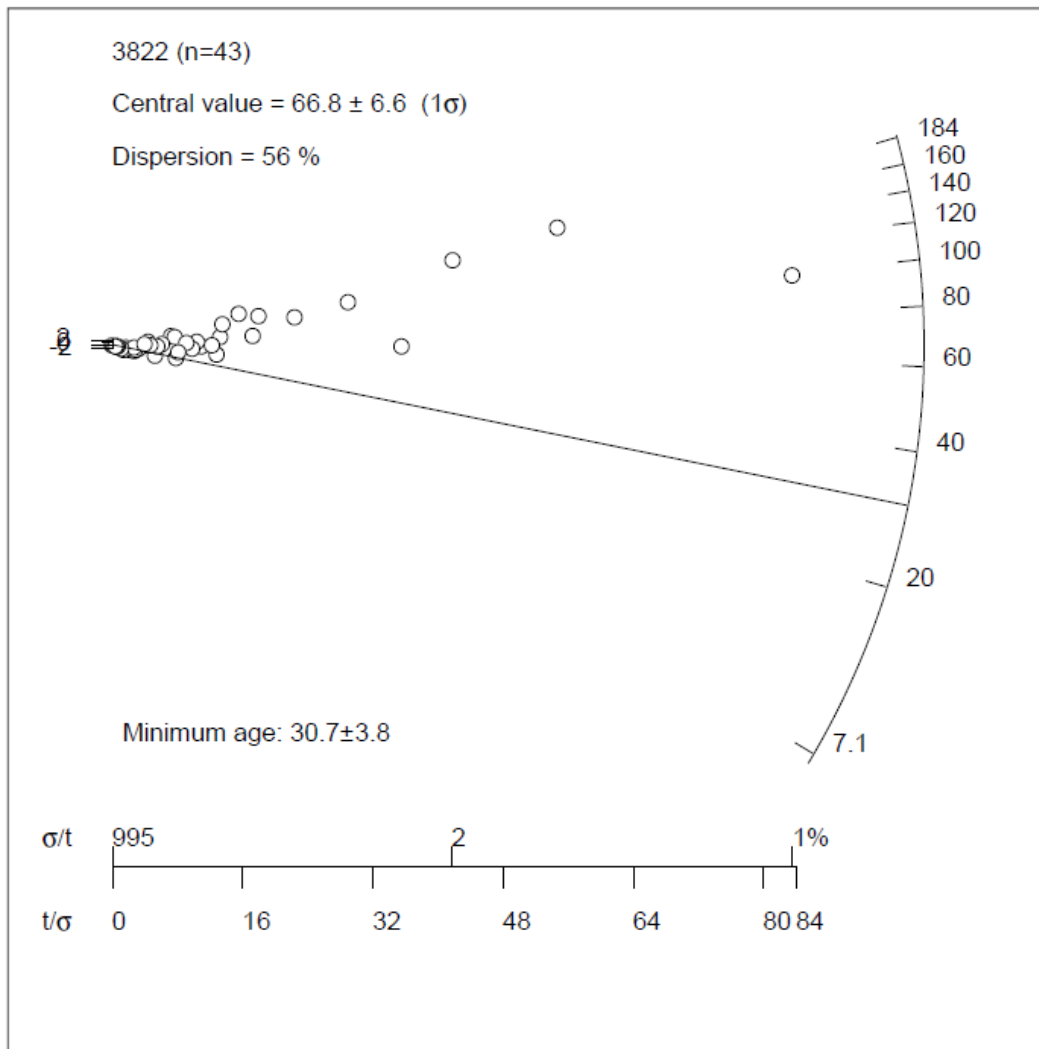
UNL-3823
All Disks
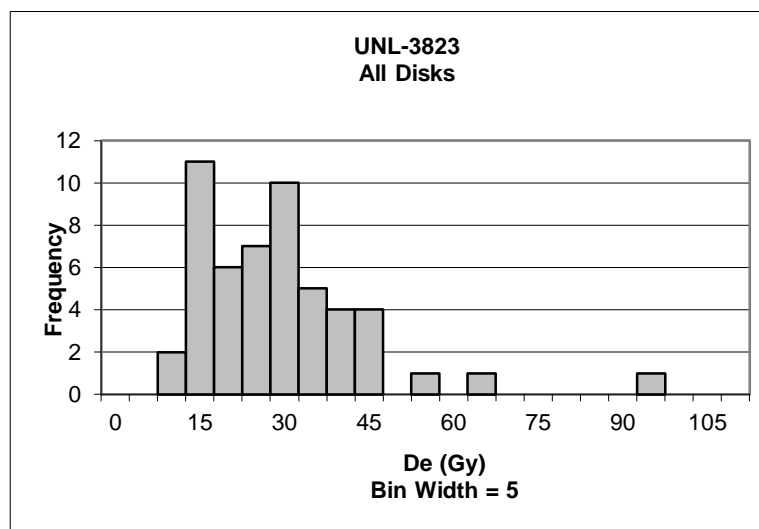
#	De	Error	Age	+/- 1 σ	#	De	Error	Age	+/- 1 σ
1	1843.271	12.58	903.876	165.64	27	14.443	3.80	7.082	1.03
2	14.646	1.83	7.182	1.01	28	17.830	0.73	8.743	0.72
3	29.082	0.25	14.261	0.31	29	26.156	0.11	12.826	0.04
4	35.887	0.61	17.598	0.93	30	31.313	0.67	15.355	0.51
5	23.205	1.41	11.379	0.23	31	34.382	1.20	16.860	0.79
6	22.981	1.72	11.269	0.25	32	43.899	0.51	21.526	1.66
7	26.832	0.40	13.157	0.10	33	13.469	0.78	6.605	1.11
8	44.797	0.82	21.967	1.74	34	28.683	2.85	14.065	0.27
9	26.896	0.73	13.189	0.11	35	33.101	0.44	16.231	0.67
10	36.562	0.58	17.929	0.99	36	8.015	0.99	3.930	1.61
11	14.355	1.01	7.039	1.03	37	53.645	0.14	26.306	2.55
12	13.432	1.90	6.587	1.12	38	64.540	2.57	31.648	3.54
13	23.437	0.15	11.493	0.21	39	23.030	1.95	11.293	0.24
14	31.520	1.13	15.456	0.53	40	24.878	1.61	12.199	0.08
15	30.035	2.73	14.728	0.39	41	42.446	0.38	20.814	1.53
16	17.011	0.19	8.342	0.79	42	14.847	0.42	7.280	0.99
17	13.805	1.36	6.769	1.08	43	9.736	2.02	4.774	1.45
18	25.972	3.06	12.736	0.02	44	18.666	2.45	9.153	0.64
19	12.974	2.45	6.362	1.16	45	26.661	0.79	13.074	0.09
20	11.780	1.69	5.777	1.27	46	40.276	2.87	19.750	1.33
21	38.153	0.33	18.709	1.13	47	20.011	1.74	9.813	0.52
22	91.636	0.76	44.935	6.01	48	27.322	7.82	13.398	0.15
23	28.955	0.52	14.199	0.30	49	37.888	0.71	18.579	1.11
24	29.816	0.63	14.621	0.37	50	17.072	1.54	8.371	0.79
25	13.960	3.28	6.846	1.07	51	15.022	1.41	7.366	0.97
26	19.993	2.50	9.804	0.52	52	23.135	1.69	11.344	0.23
					53	11.530	3.54	5.654	1.29

UNL-3823
Weighted Disks
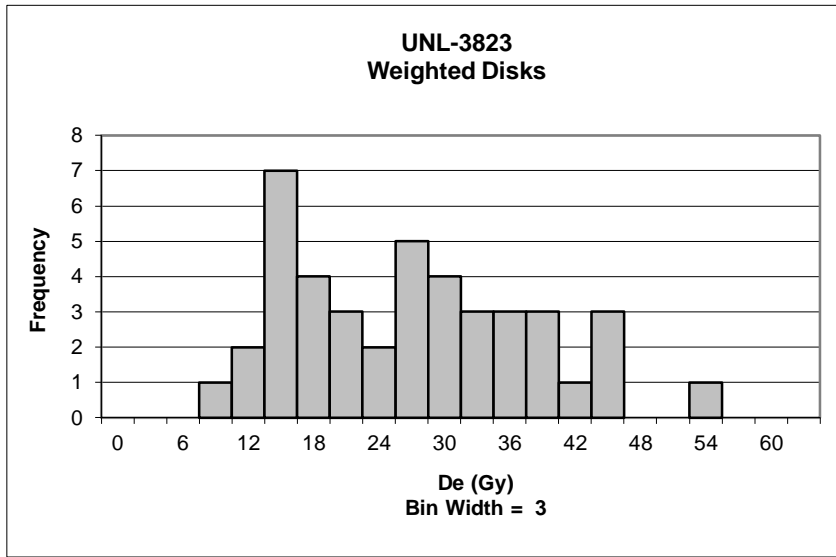
#	De	Error	Age	+/- 1 σ	#	De	Error	Age	+/- 1 σ
1	14.646	1.83	7.182	1.01	22	26.156	0.11	12.826	0.04
2	29.082	0.25	14.261	0.31	23	31.313	0.67	15.355	0.51
3	35.887	0.61	17.598	0.93	24	34.382	1.20	16.860	0.79
4	22.981	1.72	11.269	0.25	25	43.899	0.51	21.526	1.66
5	26.832	0.40	13.157	0.10	26	13.469	0.78	6.605	1.11
6	44.797	0.82	21.967	1.74	27	28.683	2.85	14.065	0.27
7	26.896	0.73	13.189	0.11	28	33.101	0.44	16.231	0.67
8	36.562	0.58	17.929	0.99	29	8.015	0.99	3.930	1.61
9	14.355	1.01	7.039	1.03	30	53.645	0.14	26.306	2.55
10	13.432	1.90	6.587	1.12	31	24.878	1.61	12.199	0.08
11	23.437	0.15	11.493	0.21	32	42.446	0.38	20.814	1.53
12	31.520	1.13	15.456	0.53	33	14.847	0.42	7.280	0.99
13	30.035	2.73	14.728	0.39	34	9.736	2.02	4.774	1.45
14	17.011	0.19	8.342	0.79	35	18.666	2.45	9.153	0.64
15	12.974	2.45	6.362	1.16	36	26.661	0.79	13.074	0.09
16	11.780	1.69	5.777	1.27	37	40.276	2.87	19.750	1.33
17	38.153	0.33	18.709	1.13	38	20.011	1.74	9.813	0.52
18	29.816	0.63	14.621	0.37	39	27.322	7.82	13.398	0.15
19	13.960	3.28	6.846	1.07	40	37.888	0.71	18.579	1.11
20	19.993	2.50	9.804	0.52	41	17.072	1.54	8.371	0.79
21	17.830	0.73	8.743	0.72	42	15.022	1.41	7.366	0.97

3823 (n=42)

Central value = 23.7 ± 1.6 (1σ)

Dispersion = 44 %

Minimum age: 8.01±0.99

9.2.10   UNL – 3825
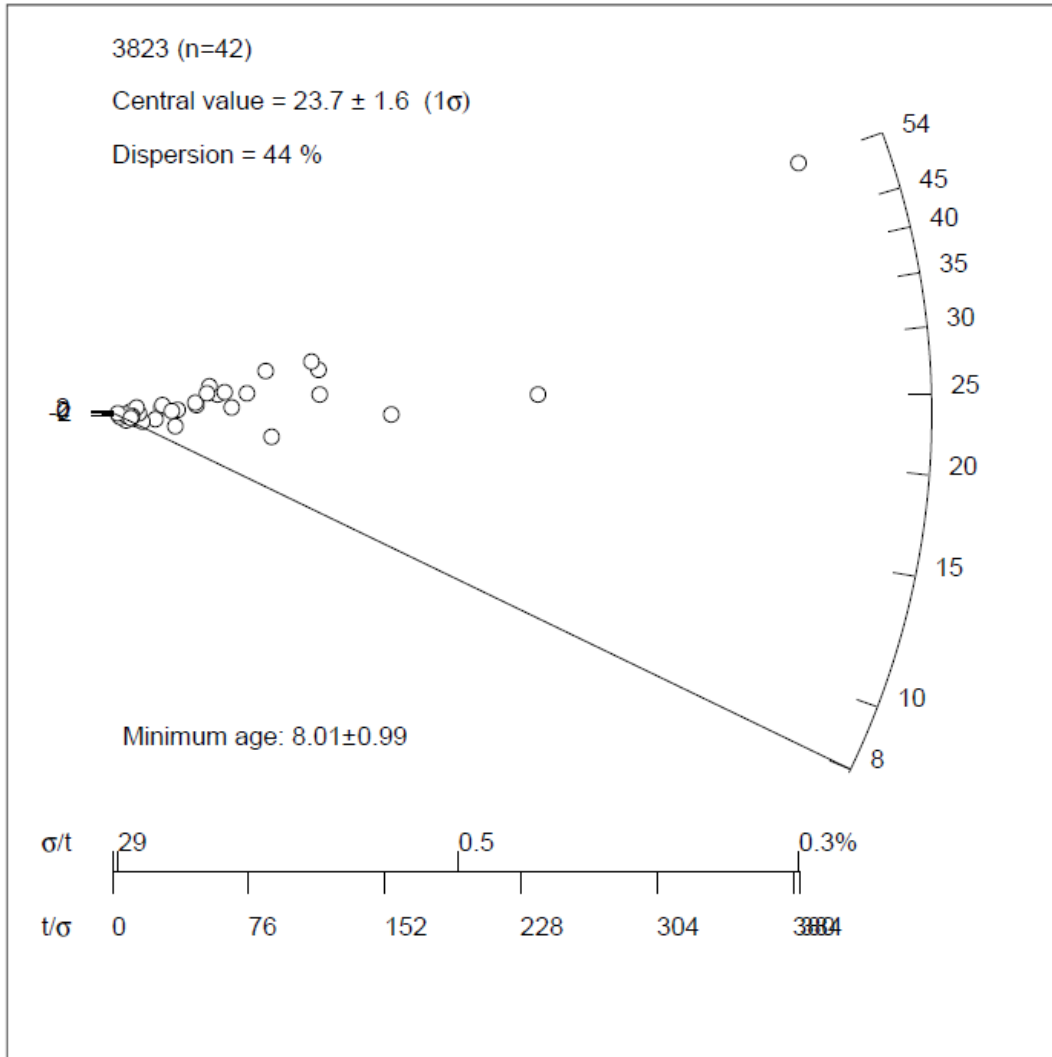
UNL-3825
All Disks
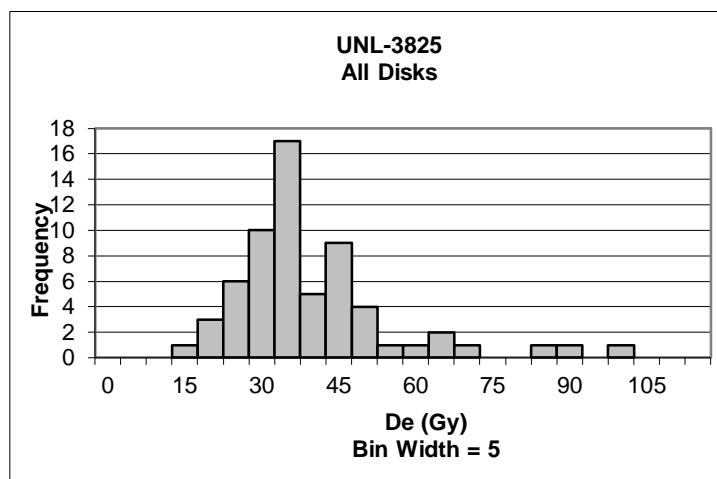
#	De	Error	Age	+/- 1 σ	#	De	Error	Age	+/- 1 σ
1	33.646	1.19	18.150	0.04	32	21.863	1.72	11.793	1.28
2	32.998	1.24	17.800	0.04	33	30.028	1.36	16.198	0.37
3	12.240	3.61	6.603	2.36	34	26.675	2.09	14.389	0.74
4	29.309	0.33	15.810	0.45	35	40.483	0.63	21.838	0.80
5	44.436	1.58	23.970	1.24	36	34.795	0.56	18.770	0.16
6	34.497	0.22	18.609	0.13	37	37.756	0.85	20.367	0.50
7	46.436	0.40	25.049	1.47	38	22.143	1.13	11.944	1.25
8	34.810	24.29	18.777	0.17	39	33.164	1.75	17.890	0.02
9	24.613	0.82	13.277	0.97	40	38.080	1.79	20.542	0.53
10	25.128	0.36	13.555	0.92	41	46.752	5.97	25.219	1.50
11	27.854	0.84	15.025	0.61	42	32.104	1.45	17.318	0.14
12	45.095	1.42	24.326	1.32	43	29.120	1.06	15.708	0.47
13	45.154	0.64	24.358	1.32	44	29.006	2.03	15.647	0.48
14	24.884	0.36	13.423	0.94	45	19.535	0.81	10.538	1.54
15	34.084	1.90	18.386	0.09	46	80.759	1.34	43.564	5.30
16	52.023	0.94	28.063	2.09	47	29.574	0.23	15.953	0.42
17	40.282	0.12	21.730	0.78	48	33.936	1.06	18.306	0.07
18	39.900	0.64	21.523	0.74	49	33.032	2.87	17.819	0.03
19	33.052	1.35	17.829	0.03	50	18.174	1.30	9.803	1.69
20	41.035	1.42	22.135	0.86	51	25.157	0.20	13.571	0.91
21	16.057	0.99	8.662	1.93	52	32.178	1.35	17.358	0.13
22	24.068	16.70	12.983	1.03	53	41.216	3.17	22.233	0.88
23	31.132	0.38	16.794	0.24	54	95.255	0.97	51.383	6.92
24	32.313	0.10	17.431	0.11	55	67.149	1.77	36.222	3.78
25	35.633	0.20	19.221	0.26	56	62.413	1.07	33.667	3.25
26	61.628	0.11	33.244	3.17	57	33.484	2.98	18.062	0.02
27	24.686	1.66	13.316	0.97	58	85.989	1.11	46.385	5.89
28	42.697	1.77	23.032	1.05	59	28.033	1.84	15.122	0.59
29	43.766	0.75	23.609	1.17	60	27.607	2.63	14.892	0.64
30	33.137	0.75	17.875	0.02	61	40.833	0.59	22.027	0.84
31	43.962	1.94	23.714	1.19	62	37.772	2.73	20.375	0.50
					63	55.210	1.57	29.782	2.45

UNL-3825
Weighted Disks
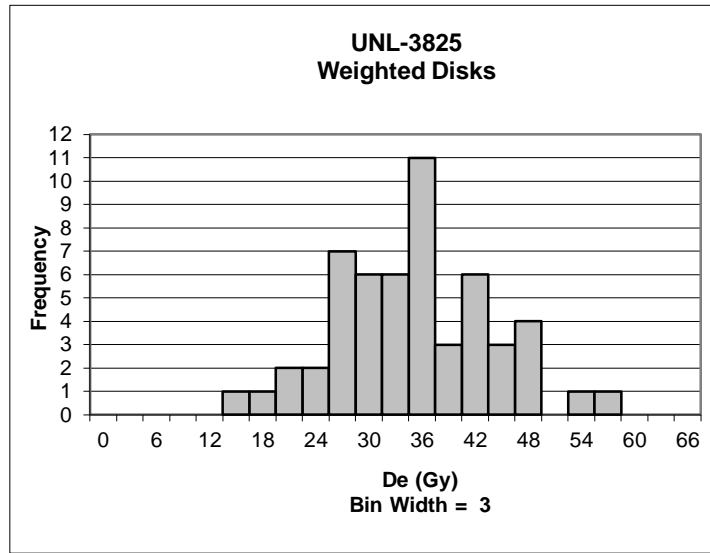
#	De	Error	Age	+/- 1 σ	#	De	Error	Age	+/- 1 σ
1	33.646	1.19	18.150	0.04	28	21.863	1.72	11.793	1.28
2	32.998	1.24	17.800	0.04	29	30.028	1.36	16.198	0.37
3	12.240	3.61	6.603	2.36	30	26.675	2.09	14.389	0.74
4	44.436	1.58	23.970	1.24	31	40.483	0.63	21.838	0.80
5	34.497	0.22	18.609	0.13	32	34.795	0.56	18.770	0.16
6	46.436	0.40	25.049	1.47	33	37.756	0.85	20.367	0.50
7	34.810	24.29	18.777	0.17	34	22.143	1.13	11.944	1.25
8	24.613	0.82	13.277	0.97	35	33.164	1.75	17.890	0.02
9	25.128	0.36	13.555	0.92	36	38.080	1.79	20.542	0.53
10	27.854	0.84	15.025	0.61	37	46.752	5.97	25.219	1.50
11	45.095	1.42	24.326	1.32	38	32.104	1.45	17.318	0.14
12	45.154	0.64	24.358	1.32	39	29.120	1.06	15.708	0.47
13	24.884	0.36	13.423	0.94	40	29.006	2.03	15.647	0.48
14	52.023	0.94	28.063	2.09	41	19.535	0.81	10.538	1.54
15	40.282	0.12	21.730	0.78	42	29.574	0.23	15.953	0.42
16	39.900	0.64	21.523	0.74	43	33.936	1.06	18.306	0.07
17	33.052	1.35	17.829	0.03	44	33.032	2.87	17.819	0.03
18	41.035	1.42	22.135	0.86	45	18.174	1.30	9.803	1.69
19	16.057	0.99	8.662	1.93	46	25.157	0.20	13.571	0.91
20	24.068	16.70	12.983	1.03	47	32.178	1.35	17.358	0.13
21	31.132	0.38	16.794	0.24	48	41.216	3.17	22.233	0.88
22	32.313	0.10	17.431	0.11	49	33.484	2.98	18.062	0.02
23	35.633	0.20	19.221	0.26	50	28.033	1.84	15.122	0.59
24	24.686	1.66	13.316	0.97	51	27.607	2.63	14.892	0.64
25	42.697	1.77	23.032	1.05	52	40.833	0.59	22.027	0.84
26	43.766	0.75	23.609	1.17	53	37.772	2.73	20.375	0.50
27	33.137	0.75	17.875	0.02	54	55.210	1.57	29.782	2.45

3825 (n=54)

Central value = 32.5 ± 1.2 (1σ)

Dispersion = 26 %

Minimum age: 19.23±0.8

9.2.11   UNL – 3827
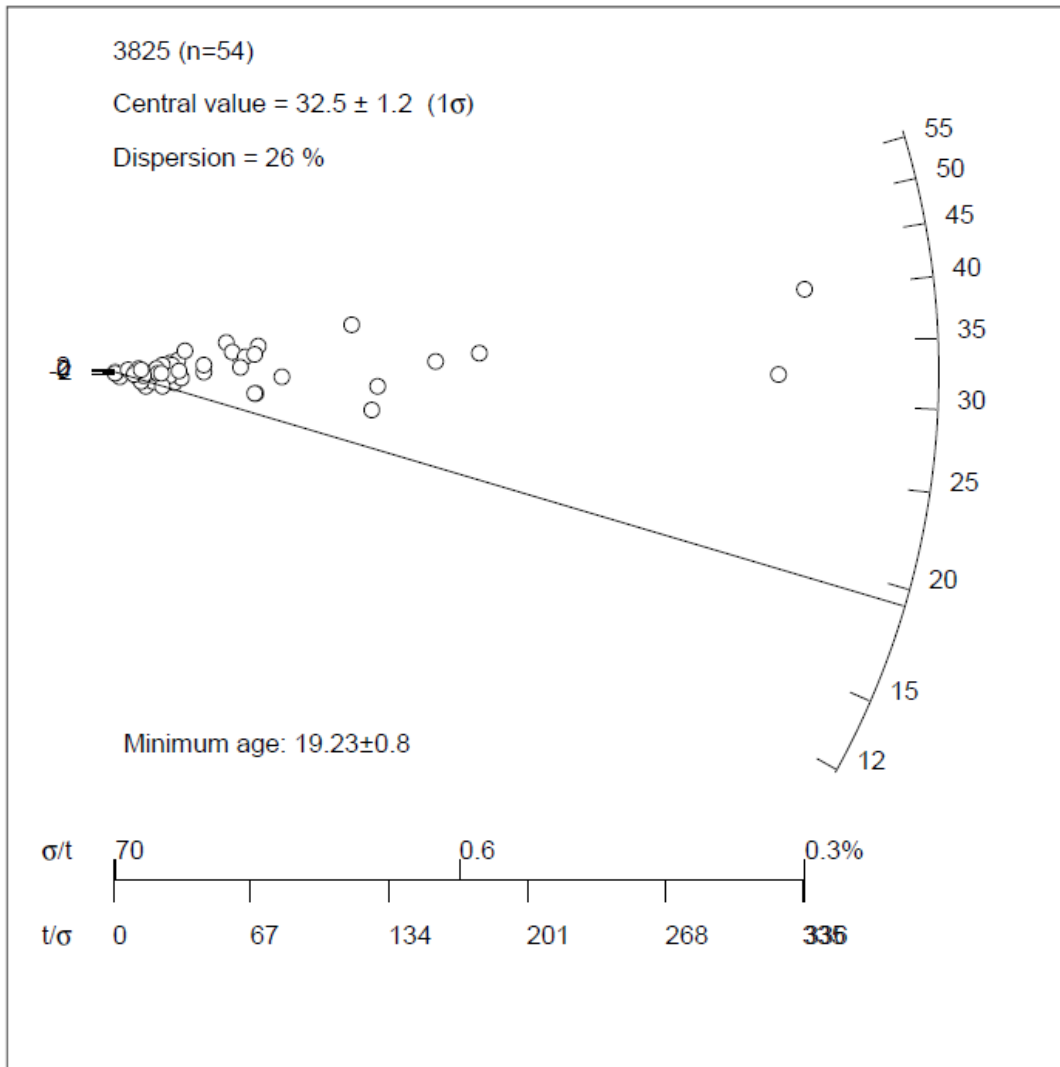
UNL-3827
All Disks
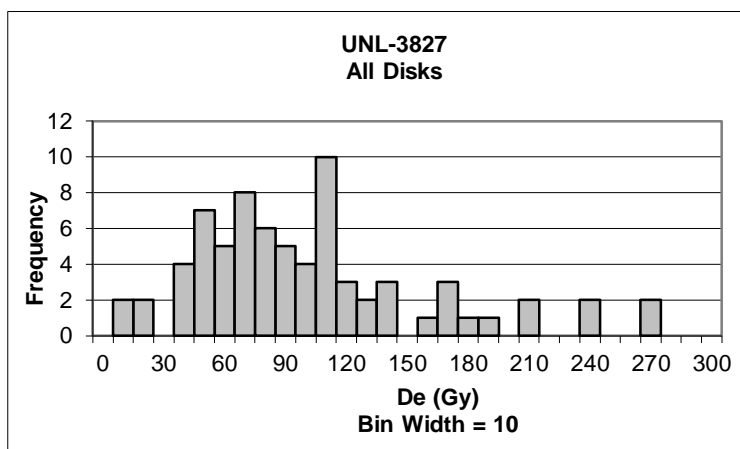
#	De	Error	Age	+/- 1 σ	#	De	Error	Age	+/- 1 σ
1	65.747	4.98	26.367	0.33	37	97.824	11.75	39.231	0.85
2	85.460	5.69	34.273	0.39	38	48.685	9.83	19.524	0.95
3	52.492	1.85	21.051	0.82	39	164.649	5.31	66.031	3.29
4	167.349	9.10	67.114	3.39	40	53.180	3.24	21.327	0.79
5	116.844	2.61	46.859	1.54	41	230.588	8.05	92.475	5.71
6	104.503	0.28	41.910	1.09	42	74.012	1.43	29.682	0.03
7	38.537	5.74	15.455	1.33	43	0.013	36.55	0.005	2.74
8	102.983	2.49	41.300	1.03	44	35.276	8.95	14.147	1.45
9	182.128	5.71	73.041	3.93	45	261.493	24.92	104.869	6.84
10	102.497	1.60	41.105	1.02	46	234.582	9.33	94.077	5.85
11	35.133	4.10	14.090	1.45	47	2.288	20.24	0.918	2.65
12	100.486	2.07	40.299	0.94	48	46.543	20.68	18.666	1.03
13	75.742	13.28	30.376	0.04	49	130.528	6.19	52.347	2.04
14	85.806	8.94	34.411	0.41	50	93.970	12.67	37.686	0.70
15	47.913	0.98	19.215	0.98	51	47.223	17.11	18.938	1.01
16	102.130	1.21	40.958	1.00	52	65.420	4.81	26.236	0.34
17	102.579	3.08	41.138	1.02	53	121.517	9.82	48.733	1.71
18	78.399	2.06	31.441	0.13	54	178.777	11.01	71.697	3.81
19	87.460	1.06	35.075	0.47	55	68.417	1.27	27.438	0.23
20	158.354	3.58	63.506	3.06	56	16.431	63.35	6.590	2.14
21	75.729	21.72	30.370	0.04	57	45.403	13.22	18.208	1.07
22	106.704	2.92	42.793	1.17	58	65.423	8.64	26.237	0.34
23	109.916	4.66	44.081	1.29	59	79.379	4.98	31.834	0.17
24	61.332	10.72	24.596	0.49	60	200.687	13.91	80.483	4.61
25	89.482	7.93	35.886	0.54	61	71.667	7.98	28.742	0.11
26	91.196	16.28	36.573	0.60	62	83.217	4.86	33.373	0.31
27	139.590	3.23	55.981	2.37	63	38.223	10.85	15.329	1.34
28	109.823	4.34	44.043	1.28	64	47.165	11.87	18.915	1.01
29	100.084	11.60	40.138	0.93	65	58.161	10.70	23.325	0.61
30	165.690	3.92	66.448	3.33	66	135.649	9.19	54.401	2.23
31	264.008	5.06	105.878	6.93	67	61.791	2.61	24.781	0.47
32	90.880	3.25	36.447	0.59	68	48.519	2.73	19.458	0.96
33	200.636	32.83	80.463	4.61	69	110.720	9.25	44.403	1.32
34	51.711	9.64	20.738	0.84	70	111.247	11.22	44.615	1.34
35	14.550	230.42	5.835	2.20	71	65.465	7.19	26.254	0.34
36	68.168	26.05	27.338	0.24	72	129.053	4.86	51.756	1.99
					73	54.455	47.88	21.838	0.74

UNL-3827
Weighted Disks

De (Gy)
Bin Width = 10
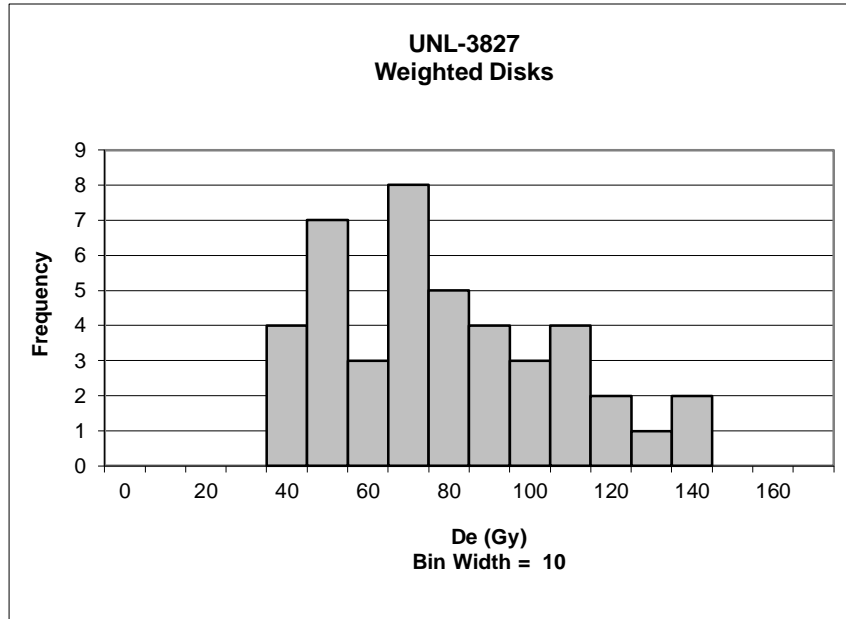
#	De	Error	Age	+/- 1 σ	#	De	Error	Age	+/- 1 σ
1	65.747	4.98	26.367	0.33	22	35.276	8.95	14.147	1.45
2	85.460	5.69	34.273	0.39	23	46.543	20.68	18.666	1.03
3	52.492	1.85	21.051	0.82	24	130.528	6.19	52.347	2.04
4	38.537	5.74	15.455	1.33	25	93.970	12.67	37.686	0.70
5	35.133	4.10	14.090	1.45	26	47.223	17.11	18.938	1.01
6	75.742	13.28	30.376	0.04	27	65.420	4.81	26.236	0.34
7	85.806	8.94	34.411	0.41	28	68.417	1.27	27.438	0.23
8	47.913	0.98	19.215	0.98	29	45.403	13.22	18.208	1.07
9	78.399	2.06	31.441	0.13	30	65.423	8.64	26.237	0.34
10	106.704	2.92	42.793	1.17	31	79.379	4.98	31.834	0.17
11	109.916	4.66	44.081	1.29	32	71.667	7.98	28.742	0.11
12	61.332	10.72	24.596	0.49	33	83.217	4.86	33.373	0.31
13	89.482	7.93	35.886	0.54	34	38.223	10.85	15.329	1.34
14	91.196	16.28	36.573	0.60	35	47.165	11.87	18.915	1.01
15	109.823	4.34	44.043	1.28	36	58.161	10.70	23.325	0.61
16	100.084	11.60	40.138	0.93	37	135.649	9.19	54.401	2.23
17	68.168	26.05	27.338	0.24	38	61.791	2.61	24.781	0.47
18	97.824	11.75	39.231	0.85	39	48.519	2.73	19.458	0.96
19	48.685	9.83	19.524	0.95	40	110.720	9.25	44.403	1.32
20	53.180	3.24	21.327	0.79	41	111.247	11.22	44.615	1.34
21	74.012	1.43	29.682	0.03	42	65.465	7.19	26.254	0.34
					43	129.053	4.86	51.756	1.99

3827 (n=43)

Central value = 72.5 ± 4 (1σ)

Dispersion = 33 %

136

100

80

60

40

35

Minimum age: 47.3±1.5

σ/t   44   4   2%

t/σ   0   10   20   30   40   50 54